iScience

CellPress
OPEN ACCESS

Article

Desaturation via Redox-Neutral Hydrogen Transfer Process: Synthesis of 2-Allyl Anilines, Mechanism and Applications

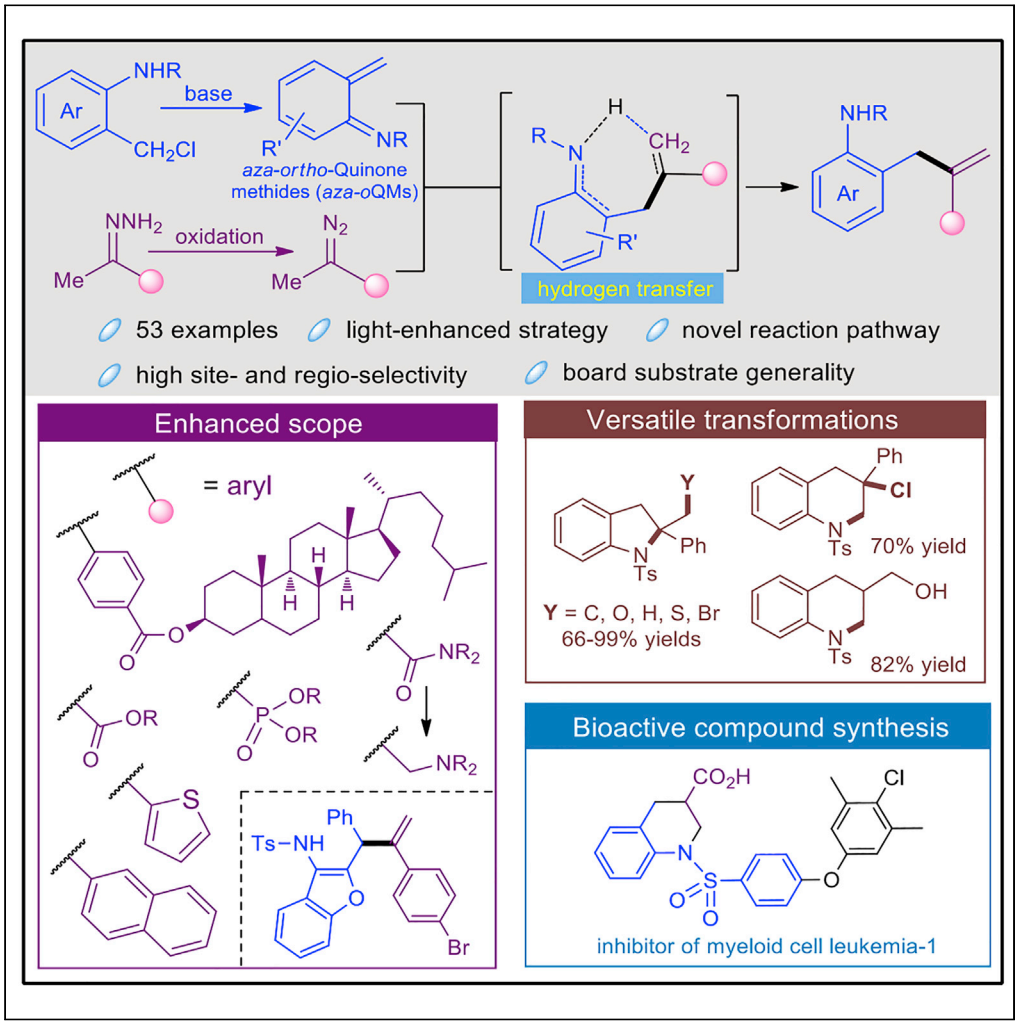

Yang Zheng, Ping Dai, Dafang Gao, ..., Wenhao Hu, Xiaoguang Bao, Xinfang Xu

huwh9@mail.sysu.edu.cn (W.H.)
xgbao@suda.edu.cn (X.B.)
xinfangxu@suda.edu.cn (X.X.)

HIGHLIGHTS

Highly site and regioselective synthesis enabled by ancillary group

Desaturation via redox-neutral inert hydrogen transfer process

Missing link in the synthesis of 2-allyl anilines with board substrate scope

Methodology development and diversity synthesis based on 2-allyl anilines

Zheng et al., iScience *23*, 101168
June 26, 2020
https://doi.org/10.1016/j.isci.2020.101168

iScience

CellPress
OPEN ACCESS

Article

Desaturation via Redox-Neutral Hydrogen Transfer Process: Synthesis of 2-Allyl Anilines, Mechanism and Applications

Yang Zheng,[1,3] Ping Dai,[1,3] Dafang Gao,[1] Kemiao Hong,[2] Luyao Kou,[1] Shanliang Dong,[2] Jundie Hu,[1,3] Lihua Qiu,[1] Wenhao Hu,[2,*] Xiaoguang Bao,[1,*] and Xinfang Xu[1,2,4,*]

SUMMARY

An unprecedented desaturation method via redox-neutral hydrogen transfer process has been disclosed under mild conditions for the selective formation of terminal alkene with alkyl diazo compounds and *aza-o*-QMs. The control experiments and DFT calculations suggest that the visible light was introduced as a key parameter to enhance the reactivity via a radical process in the formation of closed-shell cyclopropane intermediate, followed by a ring opening and redox-neutral hydrogen transfer process to give the desaturated product. The high regioselectivity in this transformation is enabled by the internal amino species as an ancillary group (AG) in the final olefin formation step. This method provides a missing link in the expeditious preparation of synthetically useful 2-allyl anilines with broad substrate generality. Further applications of these generated products in *N*-heterocycle construction, including 5- and 6-membered rings with structural diversity, have been tactfully explored, which highlight the potential in methodology development and drug discovery.

INTRODUCTION

Alkene is one of the common and key chemical stocks, which is prevalent in natural (Moosophon et al., 2009; Rukachaisirikul et al., 2012) and synthetic molecules (Kolb et al., 1994; Singh et al., 2012; Poplata et al., 2016) with a wide spectrum of applications. Its practical and selective synthesis has drawn broad attentions in synthetic chemistry (Negishi et al., 2008). In this context, carbonyl olefination, alkene metathesis, and coupling reactions constitute the most general and widely used methods for the selective construction of C=C bonds (Blakemore, 2002; Seechurn et al., 2012). Mechanistically, in the formation of alkenes via reactive intermediates, such as metal carbenes (Doyle et al., 1998; Zheng et al., 2015), organometal species (Bras and Muzart, 2011; Barluenga et al., 2007; Barluenga and Valdés, 2011; Xia et al., 2017), and cationic and radical intermediates (Mohrig, 2013), the β-*H* elimination step is regarded as the key process for the selectivity control (Figure 1A) (Seechurn et al., 2012). However, selective β-*H* elimination for the generation of terminal alkenes is still a great challenge in this content. Arguably, the formation of internal alkenes is usually favored via these conventional intermediates (see Note S1 for extended bibliography).

Recently, methods for the site-controlled desaturation via activating the inert C(sp^3)-H bonds with the assistance of the embedded directing group (DG) or the tethered radical initiator (RI) have achieved great breakthrough (Figure 1B) (Cekovic et al., 1979; Bigi et al., 2011; Voica et al., 2012; Chen and Baran, 2009; Chuentragool et al., 2018; Parasram et al., 2017; Chen and Dong, 2019; Cheng et al., 2018a, 2018b). Representative advances have been reported by Cekovic (Cekovic et al., 1979), White (Bigi et al., 2011), Baran (Voica et al., 2012; Chen and Baran, 2009), Gevorgyan (Chuentragool et al., 2018; Parasram et al., 2017), and others (Chen and Dong, 2019; Cheng et al., 2018a, 2018b). Nevertheless, the selectivity control in the following β-*H* elimination step is still a big challenge in some cases, although the initial radical intermediate formation step has been enabled selectively. Inspired by these advances, we reasoned that, if the intermediate could be temporarily stabilized before the *H*-elimination, thus, by avoiding the general β-*H*-elimination process, an alternative pathway, a delayed and selective β′-H elimination, might be enabled to form the terminal alkenes with the assistance of a neighboring functional group (or named as ancillary group, AG) (Figure 1C).

[1]Key Laboratory of Organic Synthesis of Jiangsu Province, College of Chemistry, Chemical Engineering and Materials Science Soochow University, Suzhou 215123, China

[2]Guangdong Key Laboratory of Chiral Molecule and Drug Discovery, School of Pharmaceutical Sciences, Sun Yat-sen University, Guangzhou 510006, China

[3]Institute of Materials Science and Devices, Suzhou University of Science and Technology, Suzhou 215003, China

[3]These authors contributed equally

[4]Lead Contact

*Correspondence: huwh9@mail.sysu.edu.cn (W.H.), xgbao@suda.edu.cn (X.B.), xinfangxu@suda.edu.cn (X.X.)

https://doi.org/10.1016/j.isci.2020.101168

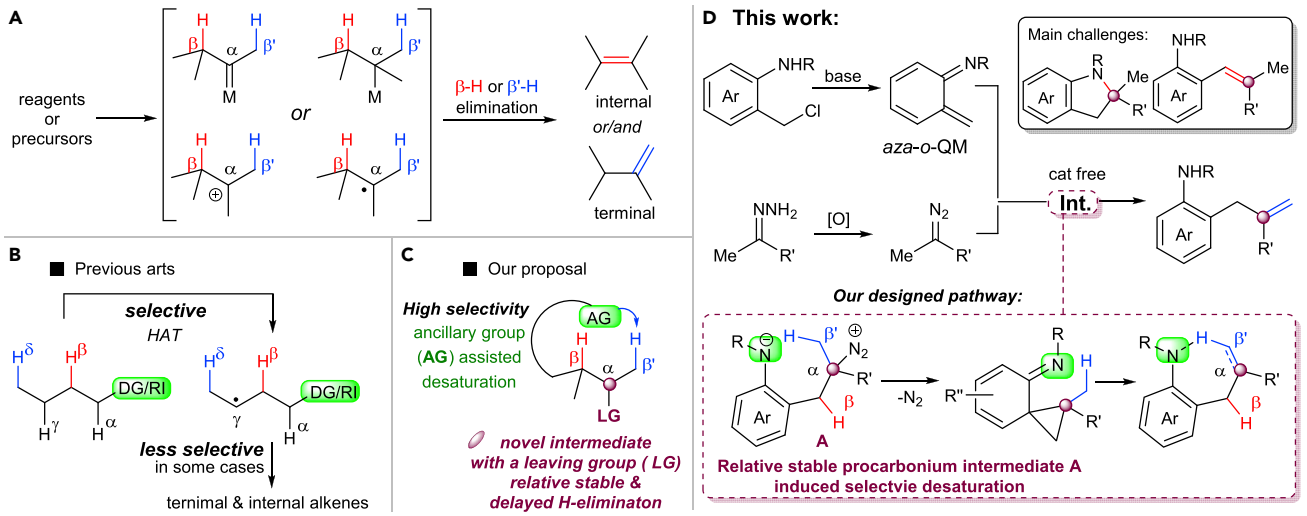

Figure 1. Strategies for the Desaturation

(A) General approaches to alkenes via β-*H* elimination/shift.

(B) Site-controlled desaturation.

(C) Our proposal: ancillary group (AG)-assisted desaturation via novel and relative stable intermediate.

(D) This work: formation of terminal alkenes via selective hydrogen transfer with the assistance of AG.

As a continuation of our interest in the transformations of diazo compounds (Kang et al., 2019; Zeng et al., 2019; Zhang et al., 2019a), we envisioned that intermediate **A** (Figure 1D in dashed box), which is formed via the electrophilic addition of diazo compound to *aza-o*-QM (Lee et al., 2014; Yang et al., 2012; Wang et al., 2016; Yang and Gao, 2018), is relatively stable and herein could act as a proper candidate for delaying the followed *H*-elimination based on previous observations (Ma et al., 2016; Dong et al., 2016; Zheng et al., 2017). In this protocol, the amino group was designed as the AG for the selective desaturation (Figure 1D in dashed box). At the stage, challenges are initially evaluated (Figure 1D in black box): (1) side reactions could take place from the *in situ* generated alkyl diazocompounds and the *aza-o*-QMs individually or in combination, which would disturb the formation of the intermediate **A**; (2) the formation of energetically favorable internal alkene; (3) the AG acts as the nucleophile, thus leading to the 5-membered *N*-heterocycle via intramolecular addition.

RESULTS AND DISCUSSION

We began our investigation by using hydrazone **2a** and *N*-(*ortho*-chloromethyl)arylamide **3a** as the model substrates. After the reaction mixture was stirred under natural light at 0°C to room temperature (rt) in 1,2-dichloromethane (DCE) for 10 h, all **2a** and **3a** were consumed. To our delight, the desired product **4a** was isolated in 43% yield together with the annulation product **13** in 15% yield (Table 1, entry 1). To indentify the internal alkene **4a′**, the crude reaction mixture was submitted to the proton NMR analysis and only trace of the internal alkene was observed (terminal:internal >20:1, see Figure S110). Besides, other observed side products may come from the decomposition of diazocompound **1a** and the dimerization of **3a** via *N*-alkylation reaction (Zhan et al., 2015). Then the reaction was conducted in the dark to decrease the decomposition of **1a**. However, the 2-allyl aniline **4a** was only yielded in 35% (entry 2), which indicates that the light might have a positive effect on this reaction, and the annulation product **13** was isolated in 18% yield. To verify the assumption, compact fluorescent light (CFL) was introduced, and the yield of **4a** was improved to 59%. Meanwhile, the yield of annulation product **13** was 13%, which is not significantly different under natural light or in the dark (entries 1 to 3). After that, we tried to reduce the reaction's temperature (from −20°C or −40°C to rt) to avoid the side reactions of **3a** (entries 4 to 5). Much to our delight, the by-product **13** was inhibited obviously (i.e., 8% yield in entry 4, and <5% yield in entries 5–8), and the best results have been obtained in terms of yield when the reaction was conducted under CFL at −40°C to rt (entry 5, 80% yield, see also Method A in SI). Investigation of different inorganic bases could not enhance the yields (entries 6 and 7). To simplify the operation, we also conducted a one-pot method, using iodosobenzene as the oxidant instead of manganese dioxide, and the desired product **4a** could be isolated in 66% yield (entry 8, see also Method B in SI).

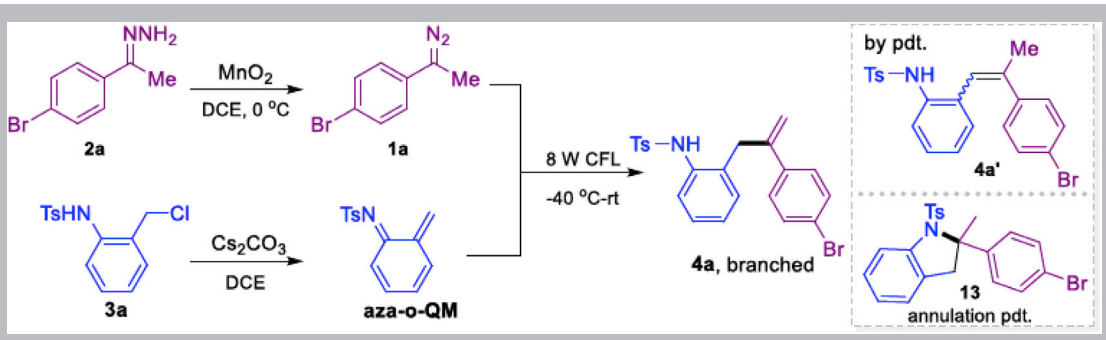

Entry	Variation from the Standard Conditions[a]	Yield (%)[b]	
		4a	13
1	Under natural light, 0°C to rt	43	15
2	In the dark, 0°C to rt	35	18
3	Under CFL, 0°C to rt	59	13
4	Under CFL, −20°C to rt	70	8
5	Under CFL, −40°C to rt	80	<5
6	Na_2CO_3 as the base, under CFL, −40°C to rt	73	<5
7	*t*-BuOLi as the base, under CFL, −40°C to rt	54	<5
8[c]	PhIO instead of MnO_2, Na_2CO_3 as the base, in one pot	66	<5

Table 1. Reaction Optimization

[a]Reaction conditions: **2a** (0.45 mmol), MnO_2 (8.0 equiv. based on **2a**), $MgSO_4$ (60.0 mg), and DCE (3.0 mL) was pre-stirred for 45 min, then the reaction mixture was filtered and injected to the oven-dried tube, which was equipped with **3a** (0.15 mmol), Cs_2CO_3 (2.0 equiv.), and the mixture was carried out at −40°C to room temperature under argon atmosphere for 10 h with the irradiation of visible light (8 W CFL).

[b]Isolated yield based on **3a**.

[c]Reaction conditions: **2a** (0.30 mmol), PhIO (0.30 mmol), **3a** (0.15 mmol), Na_2CO_3 (0.30 mmol), 4Å MS (50 mg), and DCE (2.0 mL) was carried out in one pot at −40°C to rt. under argon atmosphere for 10 h with the irradiation of visible light (8 W CFL).

With the optimized reaction conditions in hand (see also Method A in SI), we turned our attention to exploration of the scope of applicable hydrazones, and the results have been listed in Scheme 1. Hydrazones containing both electron-donating and electron-withdrawing groups on the aryl ring gave the desired products in high yields (**4a-4i**). Notably, the iodide substituent is tolerated well, which usually would not survive in the transition-metal-catalyzed transformations, generating the desired product **4g** in 76% yield. Moreover, both the alkynyl and alkenyl hydrazones are tolerated under current reaction conditions and produced the terminal-alkene products in >80% yield (**4j** and **4k**). The 2-naphthyl and 2-thienyl hydrazones worked well, leading to the corresponding products **4l** and **4m** in 76% and 78% yields, respectively. The desaturated products **4n** and **4o** were generated smoothly in 83% and 78% yields from ethyl and cyclic hydrazones, and two isomers were detected in the case with **4n** (see Figures S111 and 112). Furthermore, the representative examples of L-menthol, 1,2,3,4-diacetone galactose, and cholesterol derivatives (**4p-4r**) smoothly delivered the corresponding products in good yield, which highlighted the applicability of this method for the late-stage modification of complex molecules. In addition, the reaction performed well on a gram scale (5.0 mmol) with synthetic useful yields (note c, 60% yield). We also demonstrated the results with the fungible one-pot method in a few examples. Generally, the reactions went smoothly albeit in slightly lower yields compared with the optimal method (note b, see also Method B in SI). The structure of product **4f** was confirmed by X-ray analysis (see Table S1).

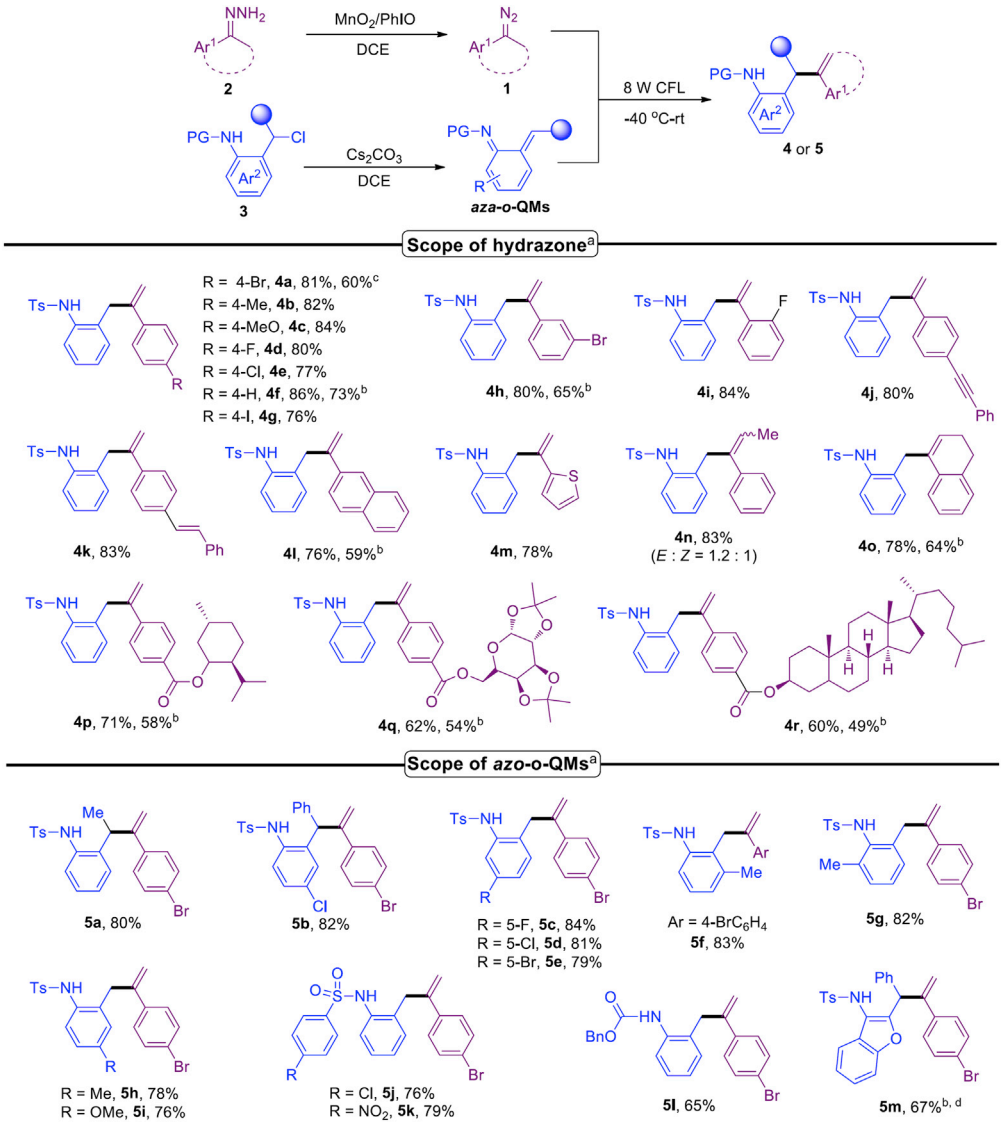

Scheme 1. Reaction Scope

[a]Reaction conditions: **2** (0.45 mmol), MnO_2 (8.0 equiv. based on **2**), $MgSO_4$ (60.0 mg), and DCE (3.0 mL) was pre-stirred for 45 min, then the reaction mixture was filtered and the filtrate was injected to the oven-dried tube containing a magnetic stirring bar, **3** (0.15 mmol), and Cs_2CO_3 (2.0 equiv.) at −40°C under argon atmosphere. Then the reaction mixture was stirred under these conditions with the irradiation of visible light (8 W CFL) for 10 h, and the reaction temperature warmed up to rt slowly in this period of time. Yields are given in isolated yields.

[b]Reaction conditions: conditions in Table 1, entry 8 was used. **2** (0.30 mmol), PhIO (0.30 mmol), **3** (0.15 mmol), Na_2CO_3 (0.30 mmol), and 4Å MS (50 mg) in DCE (2.0 mL). Yields are given in isolated yields.

[c]The reaction was conducted on a 5.0-mmol scale.

[d]The reaction was conducted in the absence of base.

Subsequently, a series of *N*-(*ortho*-chloromethyl) aryl amides **3** were explored. Arylamides with substituent at the benzylic position, including methyl and phenyl groups, underwent the transformation smoothly to give the corresponding products in high yields (**5a** and **5b**). Good tolerance for both electron-donating and electron-withdrawing groups on the different position of phenyl ring of **3** was observed, and the desired products were afforded in 76%–84% yields (**5c–5i**). Substituents on the sulfonyl part had little impact on the reaction, and corresponding products were isolated in high yields (**5j** and **5k**). In addition, substrate with *N*-CO_2Bn group instead of *N*-Ts was examined, and the reaction proceeded smoothly to give **5l** in 65% yield. Moreover, the azadiene was also tolerated well in the transformation in the absence

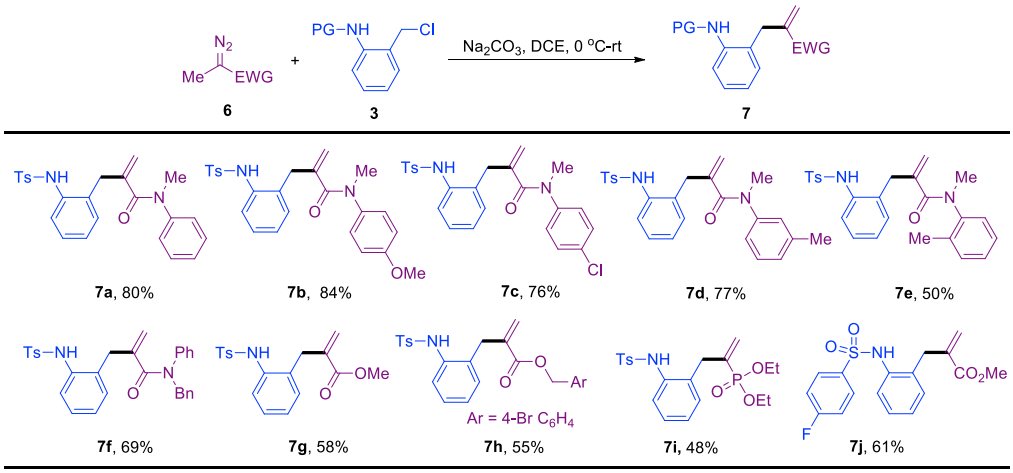

Scheme 2. Scope of α-Methyl Diazo Compounds 6

Reaction conditions: **6** (0.15 mmol), **3** (0.20 mmol), Na_2CO_3 (1.2 equiv., 25.4 mg) in DCE (2.0 mL) at 0°C under argon atmosphere for 8 h, and the reaction temperature warmed up to room temperature in this period of time.

of the base, affording the product **5m** in 67% yield. Notably, the by-products (internal alkenes or annulation product) were not detected in all above cases.

Encouraged by the above results, we further explored this formal coupling reaction with carbonyl diazo compounds **6**, which are readily available and stable, as the starting materials in the absence of oxidant (Scheme 2, see also Method C in SI). Herein, minor optimization with Na_2CO_3 as the base rather than Cs_2CO_3 was applied in the absence of visible light (8 W CFL), and no obvious difference was observed when the reactions were conducted under the visible light or dark. A variety of diazoamides were first investigated, and both electron-donating and electron-withdrawing groups on the aryl ring of **6** generally gave the desired 2-allyl aniline products **7a–7d** in good yields (76%–84%). The sterically hindered *ortho*-methyl-substituted substrate **6e** afforded the product **7e** in moderate yield. The *N*-benzyl-protected diazoamide (**6f**) performed well and gave **7f** in 69% yield. In addition, the α-methyl diazoacetates and diazophosphonate were also tolerated under these conditions, and the corresponding alkenes were isolated in moderate to high yields (**7g–7j**).

Next, we turned our attention to other types of diazo compounds that do not have the α-methyl group, and the cyclized products **9** were obtained (Figure 2, see also Method D in SI). The α-phenyl diazoacetate **8a** generated the formal [4 + 1] product **9a** in 55% yield, and the residual of unreacted diazoacetate **8a** was recovered in 40% (Figure 2A). We also examined the ethyl diazoacetate **8b** (EDA) and diazoacetamide **8c**, and both delivered the isomerized products **9b** (see Figure S113) and **9c** in 62% and 70% yields, respectively (Figure 2B). Besides, when diphenyl diazo compound **8d** was subjected to the optimized conditions, the annulation product **9d** was isolated in 45% yield contaminated with the internal olefin **9d′** in 50% yield (Figure 2C). Both the structures of **9a** and **9d′** were confirmed by X-ray (Figure 2D, see also Table S2).

Control experiments were subsequently conducted to verify the proposed reaction mechanism (see also Methods for mechanistic studies in SI). First, the intramolecular isotope labeling experiments show that the reaction undergoes a hydrogen transfer process (see Figures S114 and S115). The intermolecular kinetic isotope effect (KIE) experiment (*k*H/*k*D = 1.4:1) shows that the hydrogen transfer process is not the rate-limiting step (Figure 3A, see also Figure S114). Then **2a** was exposed under the 8-W CFL, and the hydrazine product was generated in 80% yield, which suggested the possibility of the existence of free carbene (Figure 3B) (Sha and Wei, 2013). The parallel reactions were conducted, and the results are shown in Figure 3C. Variable from optimized conditions in Table 1, we carried out the template reaction in the dark, and the bishomoallylic amine **4f** was given in 55% yield (Figure 3C, condition A), whereas **4f** was obtained in 80% yield under optimal conditions in the presence of visible light (Figure 3C, condition B). Then preliminary radical-inhibition test was conducted. Partial inhibition was observed when TEMPO was added, and the yield of **4f** dropped to 40% yield (Figure 3C, condition C), which might be contributed via the non-radical pathway. Meanwhile, 70% yield of acetophenone (yield based on **1a**) was observed after the reaction, due to the oxidization of the free carbene by TEMPO. In addition, electron paramagnetic

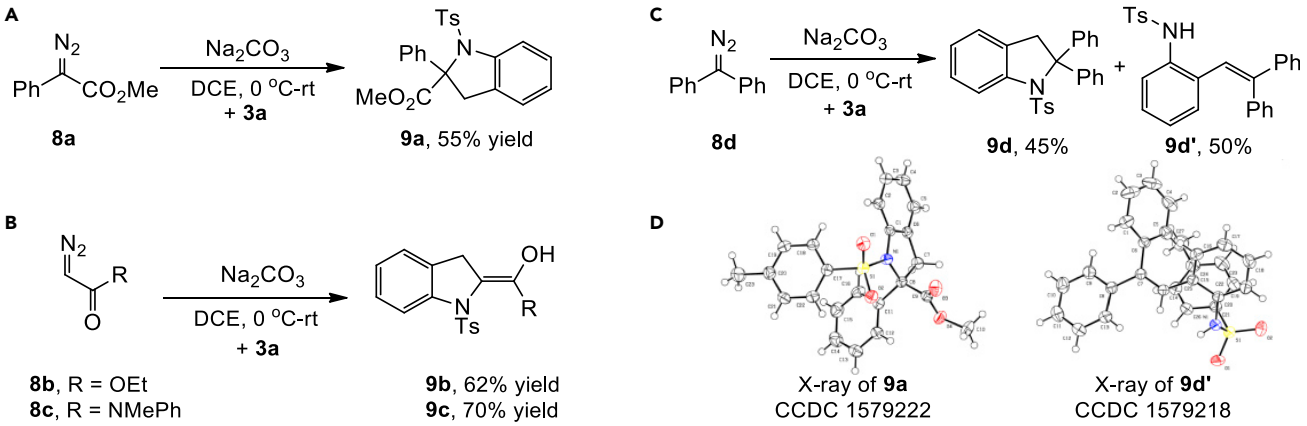

Figure 2. Cyclization Transformations of 3a with Other Types of Diazo Compounds without the α-Methyl Group (A) With α-phenyl diazoacetate. (B) With ethyl diazoacetate (EDA) and diazoacetamide. (C) With diphenyl diazo compound. (D) X-ray diffraction of compounds 9a and 9d′.

resonance (EPR) experiments were carried out (Figure 3D, see also Figure S116). No obvious signal of the diradical spin adduct was observed when diazo compound (**1a**) was treated with **3a** in the presence of 5,5-dimethyl-1-pyrroline *N*-oxide (DMPO) at room temperature in dark. On the other hand, the EPR signal of the carbon-diradical spin adduct emerged after the reaction mixture was irradiated by 8-W CFL lamps for 5 min, which obviously strengthened in the following 20 min (Figure 3D, blue line). These experiments indicated that the visible light facilitates the reaction pathway via the radical process. On basis of the literature reports (Boratyński et al., 2010; Gallagher et al., 2019; Hommelsheim et al., 2019; Jurberg and Davies, 2018; Snyder and Dougherty, 1989; Zhang et al., 2019b) and the EPR signal, we deduced that the radical process may be involved under the visible light conditions.

Computational studies were carried out to gain a mechanistic insight on this selective formation of the 2-allyl aniline **4f** (see also Computational Methods in SI). The diazo substrate **2f** could undergo intermolecular electrophilic attack to the terminal alkenyl carbon of the *in situ* generated intermediate **3a′** to form an adduct ^{1}**INT1** (Figure 4, the red line, path a). The optimized transition state (**TS**) of this step is shown as ^{1}**TS1**. The predicted energy barrier is 11.5 kcal/mol relative to separated **2f** and **3a′**. The formed ^{1}**INT1** is very ready to release N_2 via ^{1}**TS2** to yield the corresponding cyclopropane derivative **INT2**. Computational study results indicate that it is very facile for **INT1** to convert to **INT2** via ^{1}**TS2** along with the extrusion of N_2 in a concerted manner. The direct N_2 dissociation from **2f** (via ^{1}**TS3**) to afford a free carbene intermediate (path a′), however, has a much higher energy barrier, which is unlikely to occur compared with the competitive intermolecular electrophilic addition process. Alternatively, a possible reaction route leading to **INT2** in the presence of visible light was also considered (Figure 4, the blue line, path b). Irradiated by visible light, the diazo compound **2f** might be excited to triplet state (^{3}**2f**). Subsequently, the dissociation of N_2 via ^{3}**TS1b** could follow to yield the triplet carbene intermediate ^{3}**INT1b**. Afterward, the formed ^{3}**INT1b** could attack to the terminal alkenyl carbon of the *in situ*-generated intermediate **3a′** to form the intermediate **INT2** via ^{3}**TS2b**. The predicted energy barrier of this step is only 7.3 kcal/mol. Thus, it is also feasible for the formation of **INT2** in the presence of light.

It should be noted that the formed **INT2** might not be stable under the driving force of the aromatization and the ring strain release of the three-membered ring. Next, we evaluated two competitive processes, desaturation *versus* ring expansion, which were observed above. The hydrogen transfer from the methyl group attached to the three-membered ring to the *N* atom of the imine moiety can generate the unsaturated amine product **4f** (path a, Figure 5) and the [1,3] C-migration can lead to the cyclized product **9** (path b, Figure 5). The located **TS** for *path a* is shown as **TS4**, in which the C^3 … H bond distance is lengthened to 1.22 Å, whereas the H … N distance is shortened to 1.52 Å. Meanwhile, the C^1 … C^2 distance is lengthened to 2.29 Å (Figure 5A). The calculated $\Delta G^{\ddagger}$ of the hydrogen transfer step is 8.0 kcal/mol relative to **INT2**, and the formed product **4f** is exothermic by 19.2 kcal/mol. The optimized **TS** of the [1,3] C-migration to form product **9** is shown as **TS5**, in which the C^1 … C^2 distance is lengthened to 2.44 Å, whereas the C^2 … N distance is shortened to 2.80 Å (Figure 5B). The predicted energy barrier of *path b* is 11.4 kcal/mol, which is 3.4 kcal/mol higher in energy than that of *path a*. Therefore, computational results suggest that it is more feasible for **INT2** to form product **4f** via the redox-neutral hydrogen transfer pathway (it is consistent with

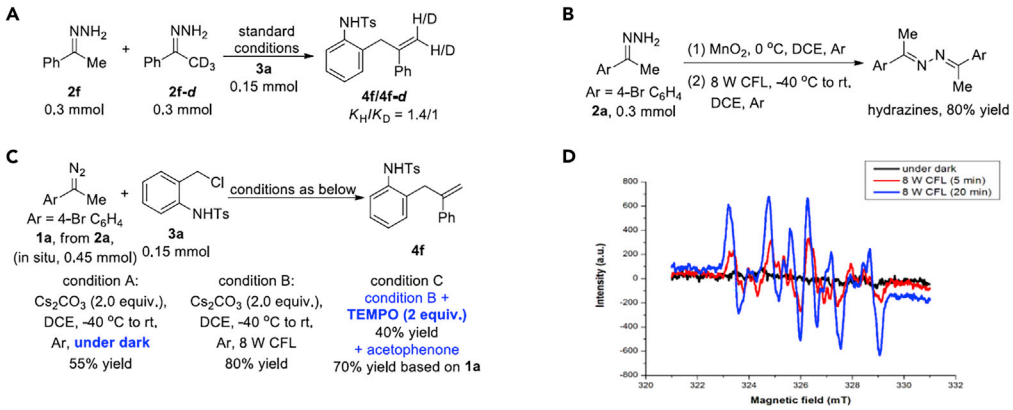

Figure 3. Control Experiments and EPR Analysis

(A) Kinetic isotope effect (KIE) experiment.

(B) Control experiment in the absence of *aza-o*-QMs.

(C) The parallel reactions under dark or in the presence of TEMPO.

(D) Electron paramagnetic resonance (EPR) experiments.

the KIE experiment, see Figure 3A). In the cases of substrates without the adjacent C-H bond, the annulation product **9** could be formed via the [1,3] C-migration pathway. The carbocation intermediate is very unlikely to form as a key intermediate (Suneja and Schneider, 2018; Pandit et al., 2019), which cannot be located as a local minimum computationally, owing to the presence of highly nucleophilic negatively charged C^1 and N atoms. Thus, this alternative mechanistic pathway is discarded. However, other possibility could not be totally ruled out so far.

Recently, elegant cycloannulation reactions of *o*-QMs and diazo ketones/esters were reported by Schneider (Suneja and Schneider, 2018) and Ryu (Pandit et al., 2019), independently. And corresponding cyclopropane derivatives are the key intermediates in these transformations. However, the manner of ring opening is different from ours. Besides, redox-neutral hydrogen transfer processes instead of intramolecular rearrangement (Li et al., 2019; Gandamana et al., 2018; Mavroskoufis et al., 2020; Mori et al., 2018; Kaiser et al., 2019; Tian et al., 2019; Haibach and Seidel, 2014) thereafter took place in our protocol to form the desaturation products (see Note S2 for extended discussion). Moreover, the desaturation product of 2-allyl anilines are prized building blocks for the divergent synthesis of heterocycles through various transformations (Lu et al., 2018; Lin et al., 2017; Wdowik and Chemler, 2017; Jiang et al., 2017; Chemler, 2013; Du et al., 2015; Miyazaki et al., 2014; Pan et al., 2014; Yu et al., 2017). Yet the current methods for the synthesis of these motifs usually took a long synthetic route and with limited substrate scope (Du et al., 2015; Miyazaki et al., 2014; Pan et al., 2014; Yu et al., 2017) (see Note S3 for extended discussion). This method provides a missing link in the synthesis of 2-allyl anilines with high control of the terminal selectivity and broad substrate generality under mild conditions.

To show the synthetic utility of this method, a variety of 5- and 6-membered *N*-heterocycles have be expeditiously synthesized with these obtained 2-allyl aniline products (Figure 6, see also Methods for further transformations in SI). Catalytic 5-*exo*-cyclization, which selectively promoted the formation of new C-N bonds in conjunction with vicinal C-CN (Pan et al., 2014), C-Br (Yu et al., 2017), C-O, C-H, or C-S bonds, delivered the corresponding functionalized indolines **10–14** in high yields. In addition, the 6-*endo*-cyclization products **15** and **16** were smoothly obtained in 70% and 82% yields under catalytic vicinal chlorination and reductive conditions, respectively. Owing to the limitation of diazo compounds, the di-alkyl-substituted alkenes were not directly delivered currently. However, they can be realized by the late-state modifications, i.e., the corresponding 2-allyl aniline **17** could be readily generated from **7a** with lithium aluminum hydride (LAH) in 70% yield, which further demonstrate the utility of our methodology. Comparing with the results of **16** and **17**, we reasoned that the product **16** may come from the annulation under the alkaline condition then reduction. To verify this assumption, the reaction of **7f** was conducted only under the basic condition, and the corresponding annulation product was observed. After screening the bases, we found that DBU is the best one for this annulation. This discovery was applied in the efficient synthesis of **18** (from the generated 2-allyl aniline **7j**), which could be further used for the synthesis of a leukemia inhibitor in three steps with high yields (Figure 7) (Chen et al., 2016).

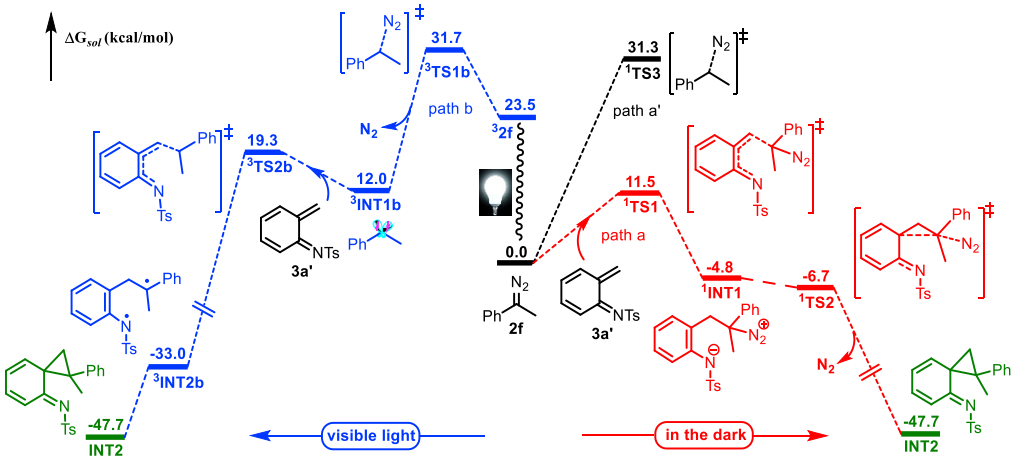

Figure 4. Energy Profile (in kcal/mol) for the Formation of INT2

Conclusion

In summary, we have developed a novel visible-light-enhanced desaturation method for highly site-/regio-controlled synthesis of 2-allylic anilines. Mechanically, two reaction pathways, including a direct electronic addition of diazo compound and light-enhancing induced radical processes, may simultaneously contribute to the formation of closed-shell cyclopropane intermediate, followed by a ring opening and redox-neutral hydrogen transfer process to give the desaturated product. This desaturated approach provides a facile access to a wide range of 2-allyl aniline derivatives under mild conditions with good tolerance of functional groups. Notably, further applications in *N*-heterocycle construction, including 5- and 6-membered-ring with a variety of functional groups, have been explored as well, which show potential in diversity synthesis and drug discovery. Novel desaturation method could be envisioned with this AG-assisted hydrogen transfer strategy.

Limitations of the Study

Owing to the limitation of diazo compounds, the di-alkyl substituted alkenes were not directly delivered currently.

Resource Availability

Lead Contact

Further information and requests for resources and reagents should be directed to and will be fulfilled by the Lead Contact, Xinfang Xu (xinfangxu@suda.edu.cn).

Materials Availability

All unique/stable reagents generated in this study are available from the Lead Contact with a completed Materials Transfer Agreement.

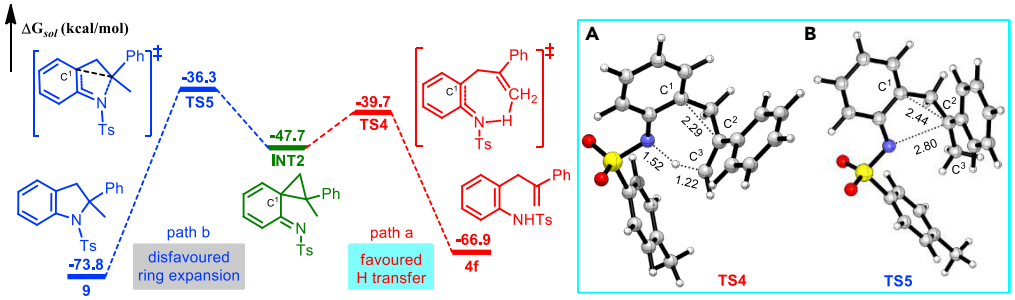

Figure 5. Energy Profiles (in kcal/mol) for the Formation of 4f and 9 from INT2 (A) Optimized transition state of TS4. (B) Optimized transition state of TS5.

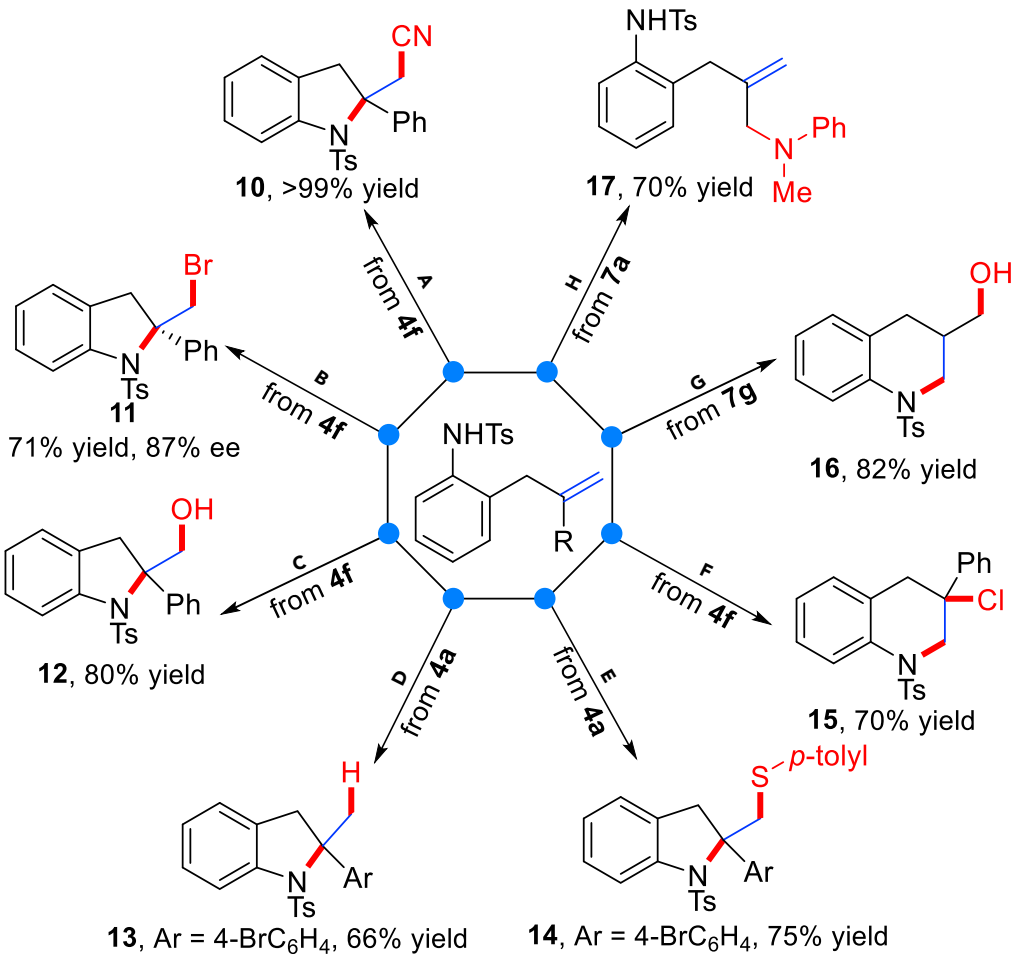

Figure 6. Versatile Transformations with Obtained 2-Allyl Anilines

(A) BrCN, Et_3N, Et_2O, 0°C, 3 h, then $B(C_6F_5)_3$ (20 mol%), PhMe, 100°C, 48 h.

(B) 10 mol% BINAP(*S*), NBS, toluene/CH_2Cl_2, -78°C, 50 h.

(C) m-CPBA, CH_2Cl_2, rt, 36 h.

(D) $NbCl_5$ (2.5 mol %), $AgNTf_2$ (5 mol %), DCE, 80°C, 6 h.

(E) CuCl (20 mol%), B_2Pin_2 (20 mol%), NFSI, CH_3CN, 45°C, 15 h.

(F) $CaCl_2$ (0.50 mmol), $Pd(OAc)_2$ (0.01 mmol) and H_2O_2 (30% aq wt.), HOAc, rt, 30 h.

(G) LiAlH4, THF, 0°C to rt, 3 h.

(H) $LiAlH_4$, THF, 0°C to rt, 3 h.

Data and Code Availability

The crystallography data have been deposited at the Cambridge Crystallographic Data Center (CCDC) under accession number CCDC: 1579217 (**4f**); 1579222 (**9a**); 1579218 (**9d′**) and can be obtained free of charge from www.ccdc.cam.ac.uk/getstructures. Original/source data for Schemes 1 and 2 together with Figures 2, 3, 6, and 7 in the paper is available at https://doi.org/10.17632/k23x374cz3.1.

METHODS

All methods can be found in the accompanying Transparent Methods supplemental file.

SUPPLEMENTAL INFORMATION

Supplemental Information can be found online at https://doi.org/10.1016/j.isci.2020.101168.

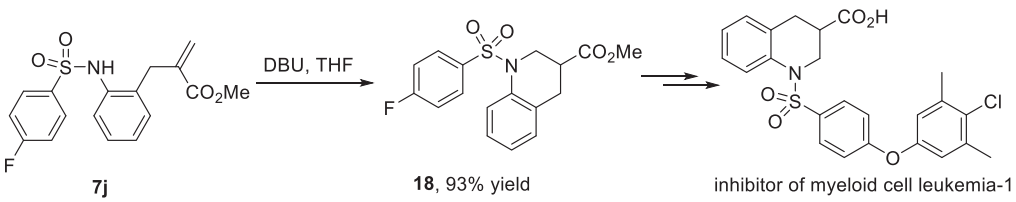

Figure 7. Formal Synthesis of a Leukemia Inhibitor

ACKNOWLEDGMENTS

This project was support by National Natural Science Foundation of China (21971262 to X.X.; 21973068 to X.B.), and the Program for Guangdong Introducing Innovative and Entrepreneurial Teams (No. 2016ZT06Y337 to W.H.) is greatly acknowledged.

AUTHOR CONTRIBUTIONS

X.X. supervised the project. Y.Z., K.H., and S.D. conducted the experimental works. L.Q. performed X-ray analysis. P.D., D.G., L.K., and X.B. performed the computational studies. Y.Z., J.H., W.H., X.B., and X.X. co-wrote the manuscript.

DECLARATION OF INTERESTS

The authors declare no competing interests.

Received: February 25, 2020
Revised: April 16, 2020
Accepted: May 12, 2020
Published: June 26, 2020

REFERENCES

Barluenga, J., and Valdés, C. (2011). Tosylhydrazones: new uses for classic reagents in palladium-catalyzed cross-coupling and metal-free reactions. Angew. Chem. Int. Ed. *50*, 7486–7500.

Barluenga, J., Moriel, P., Valdés, C., and Aznar, F. (2007). *N*-Tosylhydrazones as reagents for cross-coupling reactions: a route to polysubstituted olefins. Angew. Chem. Int. Ed. *46*, 5587–5590.

Bigi, M.A., Reed, S.A., and White, M.C. (2011). Diverting non-haem iron catalyzed aliphatic C–H hydroxylations towards desaturations. Nat. Chem. *3*, 216–222.

Blakemore, P.R. (2002). The modified Julia olefination: alkene synthesis via the condensation of metallated heteroarylalkylsulfones with carbonyl compounds. J. Chem. Soc. Perkin Trans. *1*, 2563–2585.

Boratyński, P.J., Pink, M., Rajca, S., and Rajca, A. (2010). Isolation of the triplet ground state aminyl diradical. Angew. Chem. Int. Ed. *49*, 5459–5462.

Bras, J.L., and Muzart, J. (2011). Intermolecular dehydrogenative Heck reactions. Chem. Rev. *111*, 1170–1214.

Cekovic, Z., Dimitrijevic, L., Djokic, G., and Srnic, T. (1979). Remote functionalization by ferrous ion–cupric ion induced decomposition of alkyl hydroperoxides. Tetrahedron *35*, 2021–2026.

Chemler, S.R. (2013). Copper's contribution to amination catalysis. Science *341*, 624–626.

Chen, K., and Baran, P.S. (2009). Total synthesis of eudesmane terpenes by site-selective C–H oxidations. Nature *459*, 824–828.

Chen, M., and Dong, G. (2019). Copper-catalyzed desaturation of lactones, lactams, and ketones under pH-neutral conditions. J. Am. Chem. Soc. *141*, 14889–14897.

Chen, L., Wilder, P.T., Drennen, B., Tran, J., Roth, B.M., Chesko, K., Shapiroac, P., and Fletcher, S. (2016). Structure-based design of 3-carboxy-substituted 1,2,3,4-tetrahydroquinolines as inhibitors of myeloid cell leukemia-1 (Mcl-1). Org. Biomol. Chem. *14*, 5505–5510.

Chen, M., Rago, A.J., and Dong, G. (2018a). Platinum-catalyzed desaturation of lactams, ketones, and lactones. Angew. Chem. Int. Ed. *57*, 16205–16209.

Cheng, W.-M., Shang, R., and Fu, Y. (2018b). Irradiation-induced palladium-catalyzed decarboxylative desaturation enabled by a dual ligand system. Nat. Commun. *9*, 5215–5223.

Chuentragool, P., Parasram, M., Shi, Y., and Gevorgyan, V. (2018). General, mild, and selective method for desaturation of aliphatic amines. J. Am. Chem. Soc. *140*, 2465–2468.

Dong, K., Yan, B., Chang, S., Chi, Y., Qiu, L., and Xu, X. (2016). Transition-metal-free fluoroarylation of diazoacetamides: a complementary approach to 3-fluorooxindoles. J. Org. Chem. *81*, 6887–6892.

Doyle, M.P., McKervey, M.A., and Ye, T. (1998). Modern Catalytic Methods for Organic Synthesis with Diazo Compounds (John Wiley & Sons).

Du, W., Gu, Q., Li, Z., and Yang, D. (2015). Palladium(II)-catalyzed intramolecular tandem aminoalkylation via divergent C(sp3)–H functionalization. J. Am. Chem. Soc. *137*, 1130–1135.

Gallagher, N., Zhang, H., Junghoefer, T., Giangrisostomi, E., Ovsyannikov, R., Pink, M., Rajca, S., Casu, M.B., and Rajca, A. (2019). Thermally and magnetically robust triplet ground state diradical. J. Am. Chem. Soc. *141*, 4764–4774.

Gandamana, D.A., Wang, B., Tejo, C., Bolte, B., Gagosz, F., and Chiba, S. (2018). Alkyl ethers as traceless hydride donors in Brønsted acid catalyzed intramolecular hydrogen atom transfer. Angew. Chem. Int. Ed. *57*, 6181–6185.

Haibach, M.C., and Seidel, D. (2014). C-H bond functionalization through intramolecular hydride transfer. Angew. Chem. Int. Ed. *53*, 5010–5036.

Hommelsheim, R., Guo, Y., Yang, Z., Empel, C., and Koenigs, R.M. (2019). Blue-light-induced carbene-transfer reactions of diazoalkanes. Angew. Chem. Int. Ed. *58*, 1203–1207.

Jiang, H.-J., Liu, K., Yu, J., Zhang, L., and Gong, L.-Z. (2017). Switchable stereoselectivity in bromoaminocyclizationof olefins: using Brønsted acids of anionic chiral cobalt(III) complexes. Angew. Chem. Int. Ed. *56*, 11931–11935.

Jurberg, I.D., and Davies, H.M.L. (2018). Blue light-promoted photolysis of aryldiazoacetates. Chem. Sci. *9*, 5112–5118.

Kaiser, D., Tona, V., Gonçalves, C.R., Shaaban, S., Oppedisano, A., and Maulide, N. (2019). A general acid-mediated hydroaminomethylation of unactivated alkenes and alkynes. Angew. Chem. Int. Ed. *58*, 14639–14643.

Kang, Z., Wang, Y., Zhang, D., Wu, R., Xu, X., and Hu, W. (2019). Asymmetric counter-anion-directed aminomethylation: synthesis of chiral β-amino acids via trapping of an enol intermediate. J. Am. Chem. Soc. *141*, 1473–1478.

Kolb, H.C., VanNieuwenhze, M.S., and Sharpless, K.B. (1994). Catalytic asymmetric dihydroxylation. Chem. Rev. *94*, 2483–2547.

Lee, A., Younai, A., Price, C.K., Izquierdo, J., Mishra, R.K., and Scheidt, K.A. (2014). Enantioselective annulations for dihydroquinolones by in situ generation of azolium enolates. J. Am. Chem. Soc. *136*, 10589–10592.

Li, J., Preinfalk, A., and Maulide, N. (2019). Enantioselective redox-neutral coupling of aldehydes and alkenes by an iron-catalyzed "catch–release" tethering approach. J. Am. Chem. Soc. *141*, 143–147.

Lin, J.-S., Wang, F.-L., Dong, X.-Y., He, W.-W., Yuan, Y., Chen, S., and Liu, X.-Y. (2017). Catalytic asymmetric radical aminoperfluoroalkylation and aminodifluoromethylation of alkenes to versatile enantioenriched-fluoroalkyl amines. Nat. Commun. *8*, 14841–14852.

Lu, Y., Nakatsuji, H., Okumura, Y., Yao, L., and Ishihara, K. (2018). Enantioselective halo-oxy- and halo-azacyclizations induced by chiral amidophosphate catalysts and halo-Lewis acids. J. Am. Chem. Soc. *140*, 6039–6043.

Ma, C., Xing, D., and Hu, W. (2016). Catalyst-free halogenation of α-diazocarbonyl compounds with *N*-halosuccinimides: synthesis of 3-halooxindoles or vinyl halides. Org. Lett. *18*, 3134–3137.

Mavroskoufis, A., Rajes, K., Golz, P., Agrawal, A., Ruß, V., Göze, J.P., and Hopkinson, M.N. (2020). N-Heterocyclic carbene catalyzed photoenolization/Diels–Alder reaction of acid fluorides. Angew. Chem. Int. Ed. *59*, 3190–3194.

Miyazaki, Y., Ohta, N., Semba, K., and Nakao, Y. (2014). Intramolecular aminocyanation of alkenes by cooperative palladium/boron catalysis. J. Am. Chem. Soc. *136*, 3732–3735.

Mohrig, J.R. (2013). Stereochemistry of 1,2-elimination and proton-transfer reactions: toward a unified understanding. Acc. Chem. Res. *46*, 1407–1416.

Moosophon, P., Kanokmedhakul, S., Kanokmedhakul, K., and Soytong, K. (2009). Prenylxanthones and a bicyclo[3.3.1]nona-2,6-diene derivative from the fungus emericella rugulosa. J. Nat. Prod. *72*, 1442–1446.

Mori, K., Isogai, R., Kamei, Y., Yamanaka, M., and Akiyama, T. (2018). Chiral magnesium bisphosphate-catalyzed asymmetric double C(sp3)–H bond functionalization based on sequential hydride shift/cyclization process. J. Am. Chem. Soc. *140*, 6203–6207.

Negishi, E.-I., Huang, Z., Wang, G., Mohan, S., Wang, C., and Hattori, H. (2008). Recent advances in efficient and selective synthesis of di-, tri-, and tetrasubstituted alkenes via Pd-catalyzed alkenylation-carbonyl olefination synergy. Acc. Chem. Res. *41*, 1474–1485.

Pan, Z., Pound, S.M., Rondla, N.R., and Douglas, C.J. (2014). Intramolecular aminocyanation of alkenes by N-CN bond cleavage. Angew. Chem. Int. Ed. *53*, 5170–5174.

Pandit, R.P., Kim, S.T., and Ryu, D.H. (2019). Asymmetric synthesis of enantioenriched 2-aryl-2,3-dihydrobenzofurans by a Lewis acid catalyzed cyclopropanation/intramolecular rearrangement sequence. Angew. Chem. Int. Ed. *58*, 13427–13432.

Parasram, M., Chuentragool, P., Wang, Y., Shi, Y., and Gevorgyan, V. (2017). General, auxiliary-enabled photoinduced Pd-catalyzed remote desaturation of aliphatic alcohols. J. Am. Chem. Soc. *139*, 14857–14860.

Poplata, S., Tröter, A., Zou, Y.-Q., and Bach, T. (2016). Recent advances in the synthesis of cyclobutanes by olefin [2 + 2] photocycloaddition reactions. Chem. Rev. *116*, 9748–9815.

Rukachaisirikul, V., Rodglin, A., Sukpondma, Y., Phongpaichit, S., Buatong, J., and Sakayaroj, J. (2012). Phthalide and isocoumarin derivatives produced by an *acremonium sp.* isolated from a mangrove rhizophora apiculate. J. Nat. Prod. *75*, 853–858.

Seechurn, C.C.C.J., Kitching, M.O., Colacot, T.J., and Snieckus, V. (2012). Palladium-catalyzed cross-coupling: a historical contextual perspective to the 2010 Nobel Prize. Angew. Chem. Int. Ed. *51*, 5062–5085.

Sha, Q., and Wei, Y. (2013). Base and solvent mediated decomposition of tosylhydrazones: highly selective synthesis of *N*-alkyl substituted hydrazones, dialkylidenehydrazines, and oximes. Tetrahedron *69*, 3829–3835.

Singh, C., Hassam, M., Verma, V.P., Singh, A.S., Naikade, N.K., Puri, S.K., Maulik, P.R., and Kant, R. (2012). Bile acid-based 1,2,4-trioxanes: synthesis and antimalarial assessment. J. Med. Chem. *55*, 10662–10673.

Snyder, G.J., and Dougherty, D.A. (1989). 2,4-Dimethylene-1,3-cyclobutanediyl, the non-kekule isomer of benzene: synthesis, EPR, and electronic spectroscopy. J. Am. Chem. Soc. *111*, 3927–3942.

Suneja, A., and Schneider, C. (2018). Phosphoric acid catalyzed [4 + 1]-cycloannulation reaction of *ortho*-Quinone methides and diazoketones: catalytic, enantioselective access toward cis-2,3-dihydrobenzofurans. Org. Lett. *20*, 7576–7580.

Tian, J.-J., Zeng, N.-N., Liu, N., Tu, X.-S., and Wang, X.-C. (2019). Intramolecular cyclizations of vinyl-substituted *N,N*-dialkyl arylamines enabled by borane-assisted hydride transfer. ACS Catal. *9*, 295–300.

Voica, A.-F., Mendoza, A., Gutekunst, W.R., Fraga, J.O., and Baran, P.S. (2012). Guided desaturation of unactivated aliphatics. Nat. Chem. *4*, 629–635.

Wang, L., Li, S., Blümel, M., Philipps, A.R., Wang, A., Puttreddy, R., Rissanen, K., and Enders, D. (2016). Asymmetric synthesis of spirobenzazepinones with atroposelectivity and spiro-1,2-diazepinones by NHC-catalyzed [3+4] annulation reactions. Angew. Chem. Int. Ed. *55*, 11110–11114.

Wdowik, T., and Chemler, S.R. (2017). Direct synthesis of 2-formylpyrrolidines, 2-pyrrolidinones and 2-dihydrofuranones via aerobic copper-catalyzed aminooxygenation and dioxygenation of 4-pentenylsulfonamides and 4-pentenylalcohols. J. Am. Chem. Soc. *139*, 9515–9518.

Xia, Y., Qiu, D., and Wang, J. (2017). Transition-metal-catalyzed cross-couplings through carbene migratory insertion. Chem. Rev. *117*, 13810–13889.

Yang, B., and Gao, S. (2018). Recent advances in the application of Diels–Alder reactions involving *o*-quinodimethanes, aza-*o*-quinone methides and *o*-quinone methides in natural product total synthesis. Chem. Soc. Rev. *47*, 7926–7953.

Yang, Q., Xiao, C., Lu, L., An, J., Tan, F., Li, B., and Xiao, W. (2012). Synthesis of indoles through highly efficient cascade reactions of sulfur ylides and *N*-(ortho-chloromethyl)aryl amides. Angew. Chem. Int. Ed. *51*, 9137–9140.

Yu, S.-N., Li, Y.-L., and Deng, J. (2017). Enantioselective synthesis of 2-bromomethyl indolines via BINAP(S)-catalyzed bromoaminocyclization of allyl aniline. Adv. Synth. Catal. *359*, 2499–2508.

Zeng, Q., Dong, K., Pei, C., Dong, S., Hu, W., Qiu, L., and Xu, X. (2019). Divergent construction of macrocyclic alkynes via catalytic metal carbene C(sp2)–H insertion and the Buchner reaction. ACS Catal. *9*, 10773–10779.

Zhan, G., Shi, M.-L., He, Q., Du, W., and Chen, Y.-C. (2015). [4 + 3] Cycloadditions with bromo-substituted Morita–Baylis–Hillman adducts of isatins and *N*-(*ortho*-chloromethyl)aryl amides. Org. Lett. *17*, 4750–4753.

Zhang, C., Hong, K., Dong, S., Pei, C., Zhang, X., He, C., Hu, W., and Xu, X. (2019a). Gold(I)-Catalyzed aromatization: expeditious synthesis of polyfunctionalized naphthalenes. iScience *21*, 499–508.

Zhang, Z., Yadagiri, D., and Gevorgyan, V. (2019b). Light-induced metal-free transformations of unactivated pyridotriazoles. Chem. Sci. *10*, 8399–8404.

Zheng, Y., Mao, J., Weng, Y., Zhang, X., and Xu, X. (2015). Cyclopentadiene construction via Rh-catalyzed carbene/alkyne metathesis terminated with intramolecular formal [3 + 2] cycloaddition. Org. Lett. *17*, 5638–5641.

Zheng, Y., Bao, M., Qiu, L., and Xu, X. (2017). Thermally induced reaction of diazoamides with isatins: a complementary approach to the 3,3'-bioxindole derivatives. Tetrahedron Lett. *58*, 3390–3393.

iScience, Volume *23*

Supplemental Information

Desaturation via Redox-Neutral Hydrogen Transfer Process: Synthesis of 2-Allyl Anilines, Mechanism and Applications

Yang Zheng, Ping Dai, Dafang Gao, Kemiao Hong, Luyao Kou, Shanliang Dong, Jundie Hu, Lihua Qiu, Wenhao Hu, Xiaoguang Bao, and Xinfang Xu

Supplemental Figures

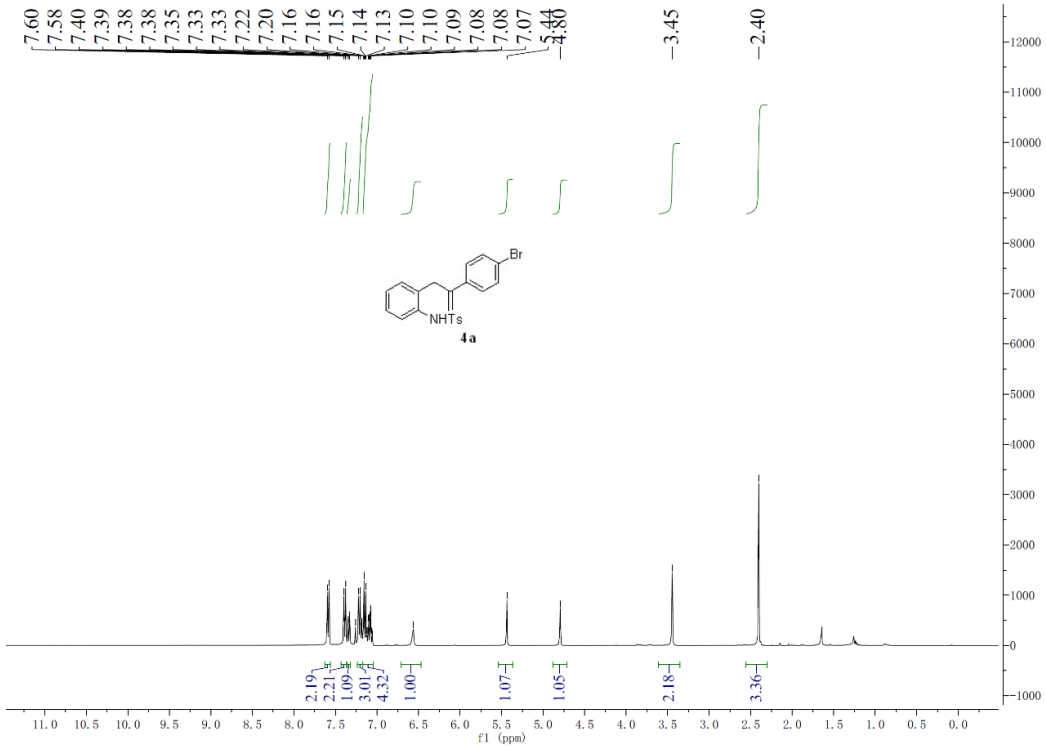

Figure S1. ^{1}H NMR spectra (400 MHz) of **4a** in $CDCl_3$, related to **Table 1** and **Scheme 1**.

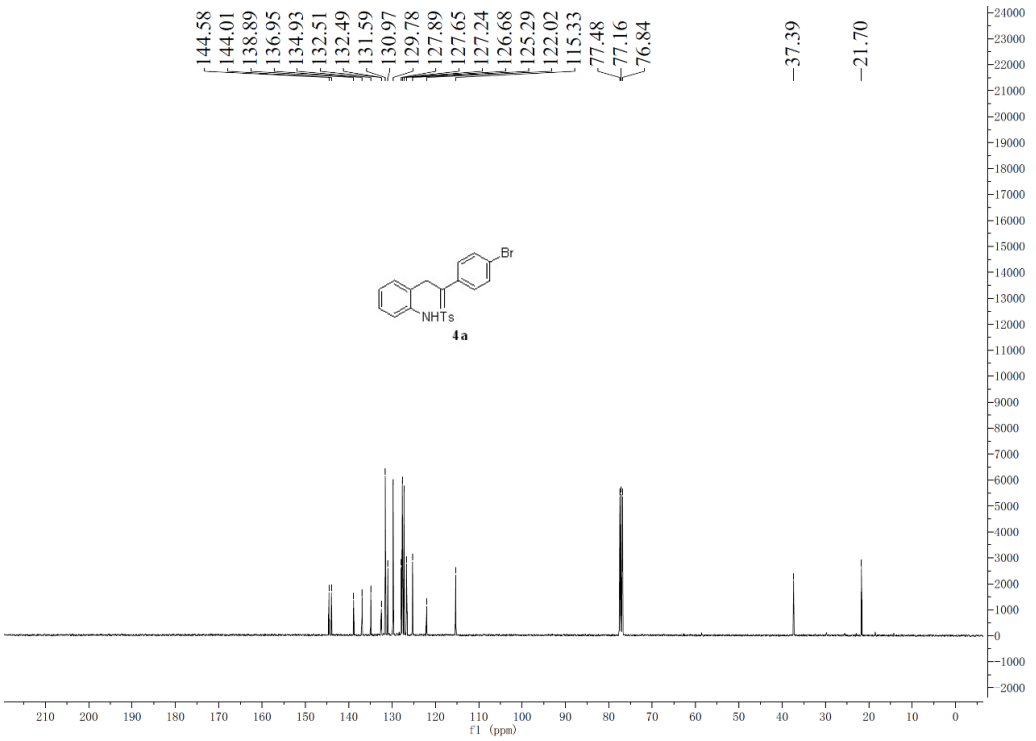

Figure S2. ^{13}C NMR spectra (400 MHz) of **4a** in $CDCl_3$, related to **Table 1** and **Scheme 1**.

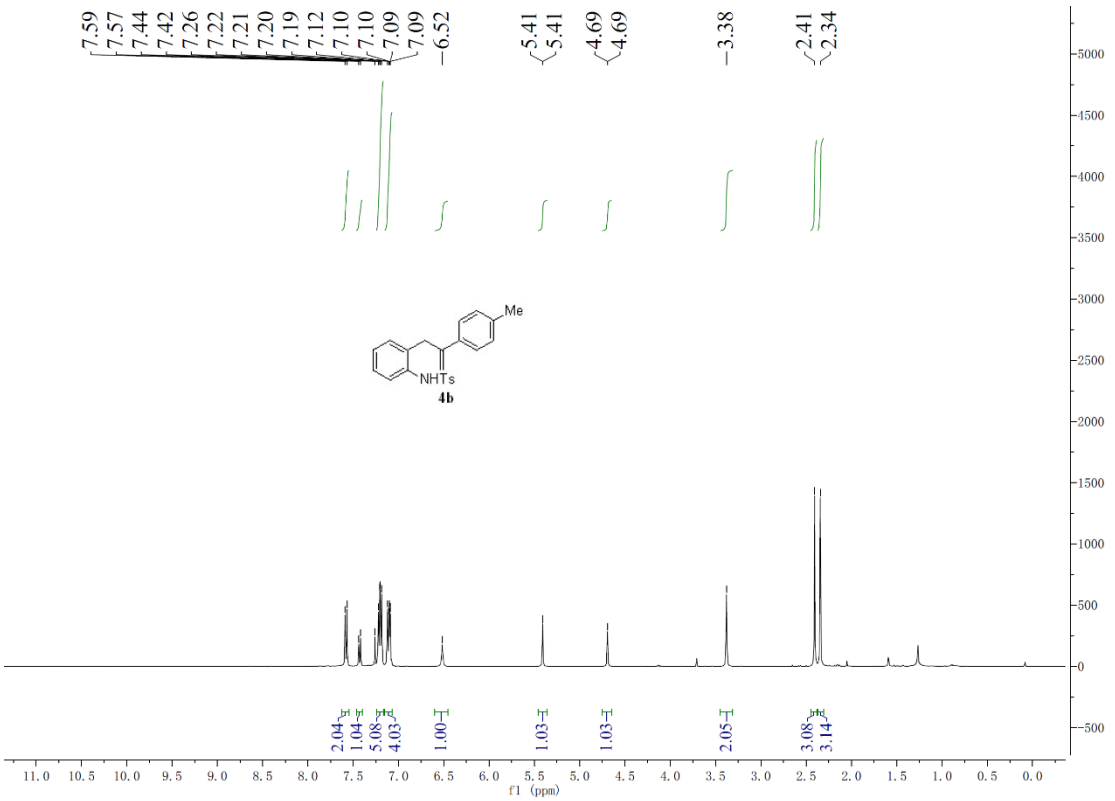

Figure S3. ^{1}H NMR spectra (400 MHz) of **4b** in $CDCl_3$, related to **Scheme 1**.

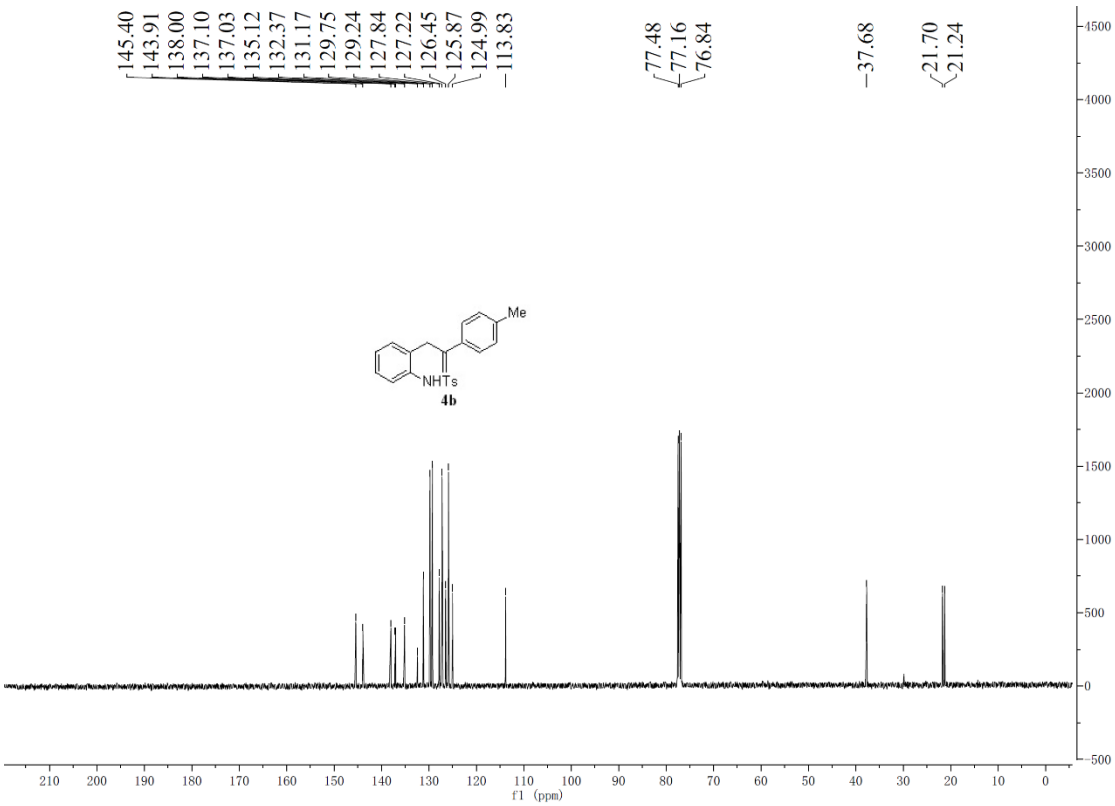

Figure S4. ^{13}C NMR spectra (400 MHz) of **4b** in $CDCl_3$, related to **Scheme 1**.

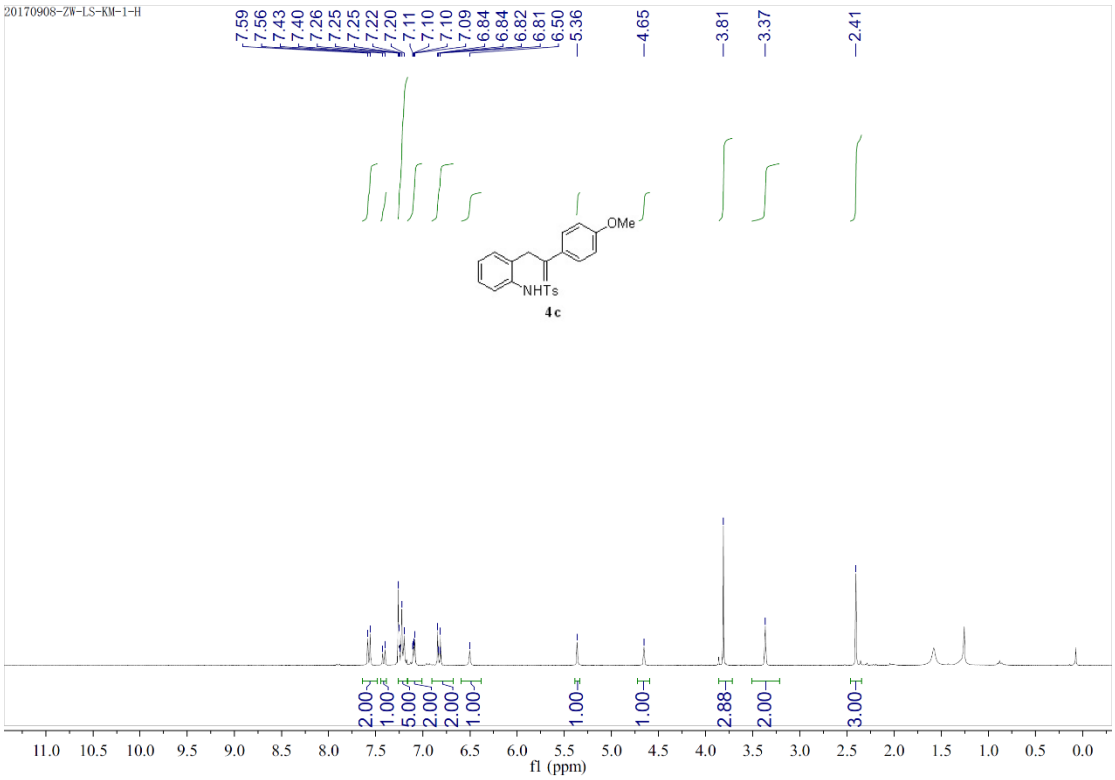

Figure S5. ^{1}H NMR spectra (400 MHz) of **4c** in $CDCl_3$, related to **Scheme 1**.

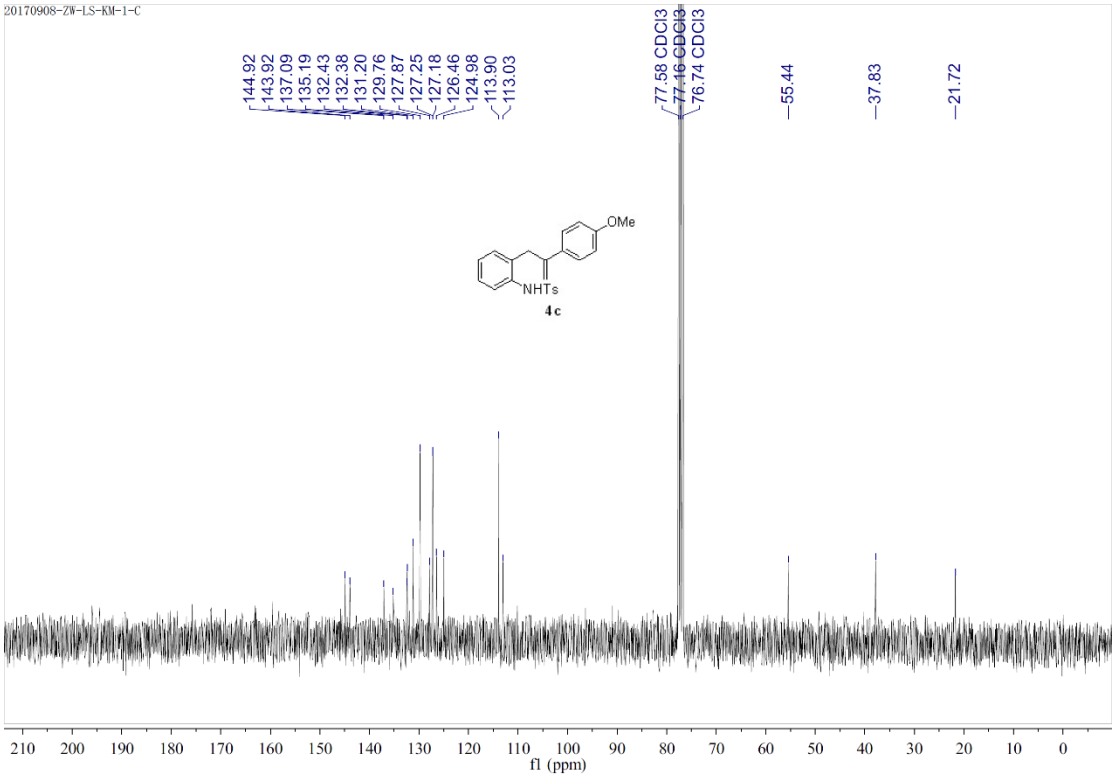

Figure S6. ^{13}C NMR spectra (400 MHz) of **4c** in $CDCl_3$, related to **Scheme 1**.

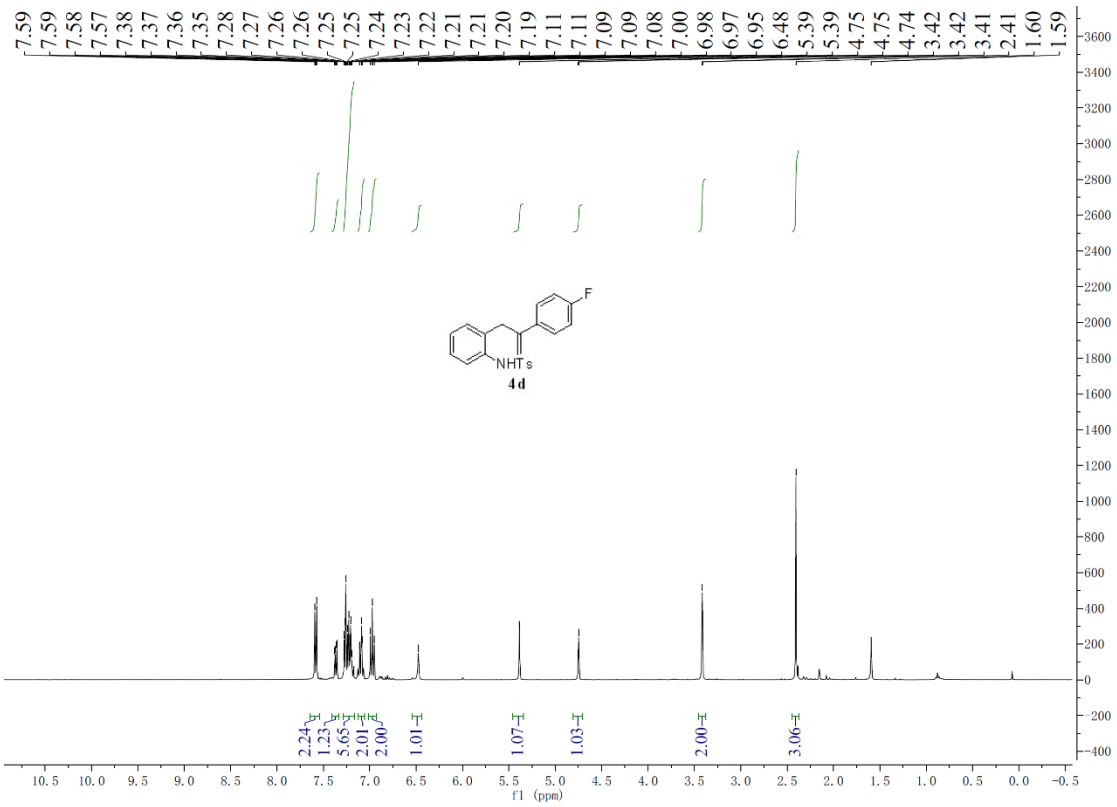

Figure S7. ^{1}H NMR spectra (400 MHz) of **4d** in $CDCl_3$, related to **Scheme 1**.

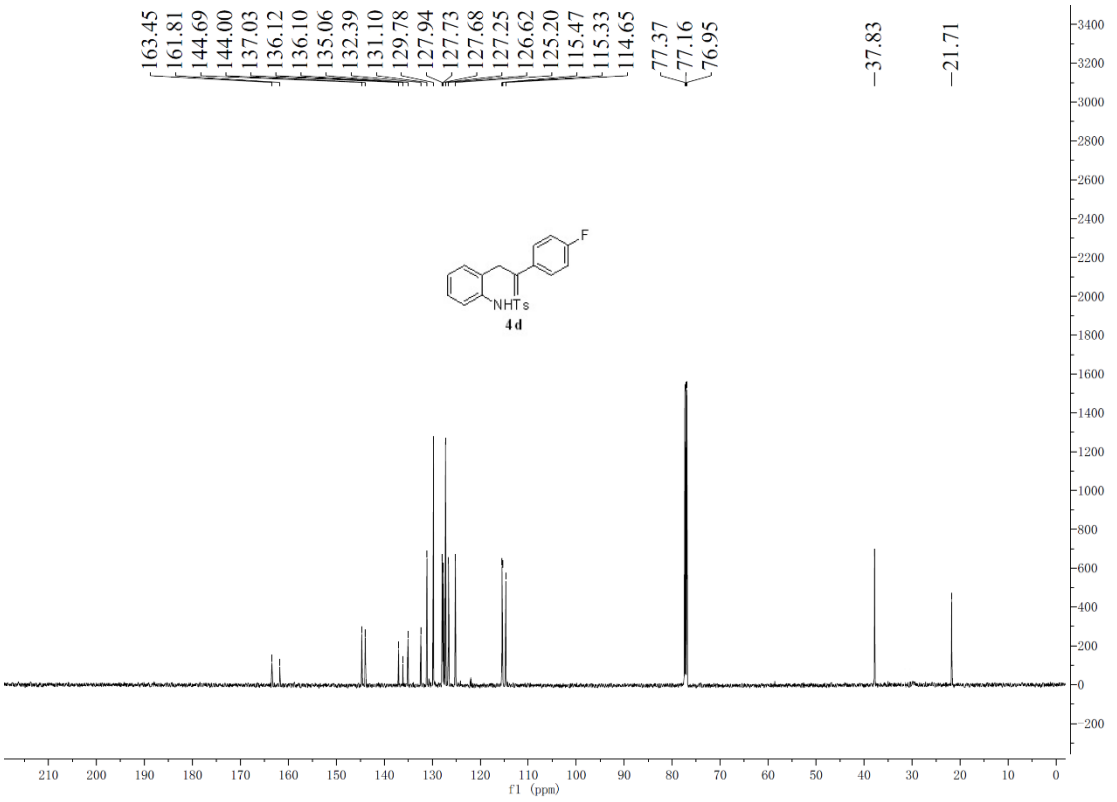

Figure S8. ^{13}C NMR spectra (400 MHz) of **4d** in $CDCl_3$, related to **Scheme 1**.

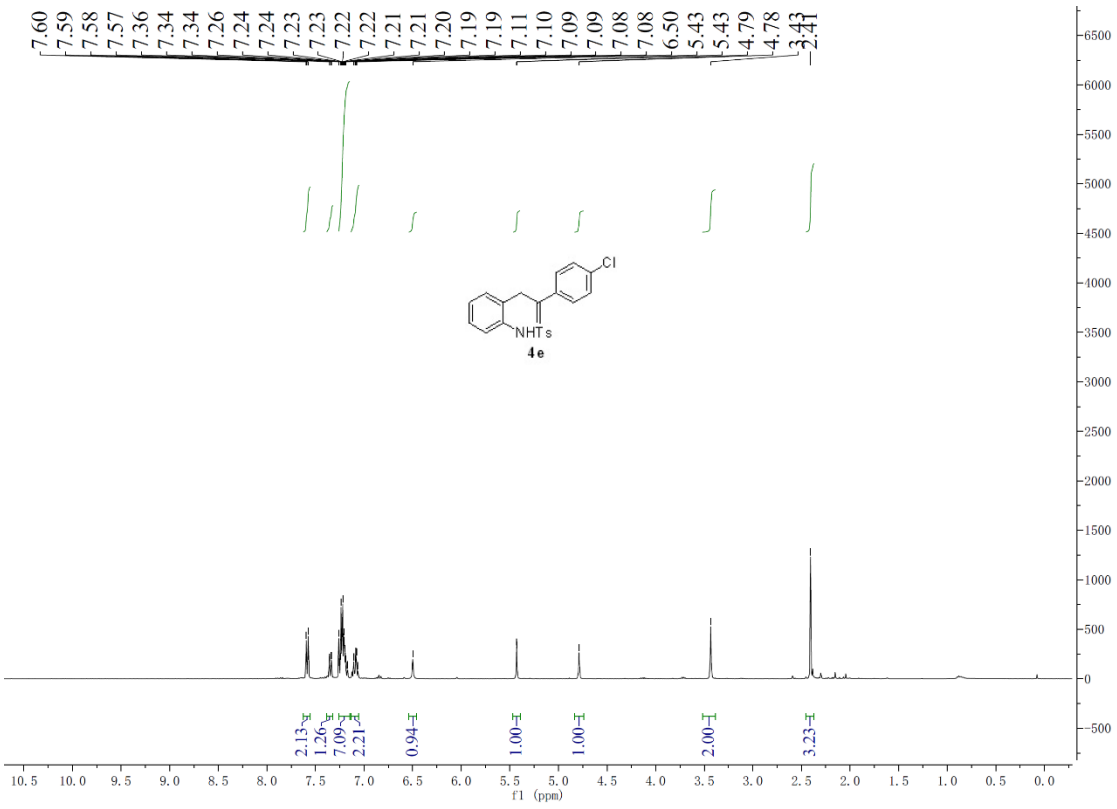

Figure S9. ^{1}H NMR spectra (400 MHz) of **4e** in $CDCl_3$, related to **Scheme 1**.

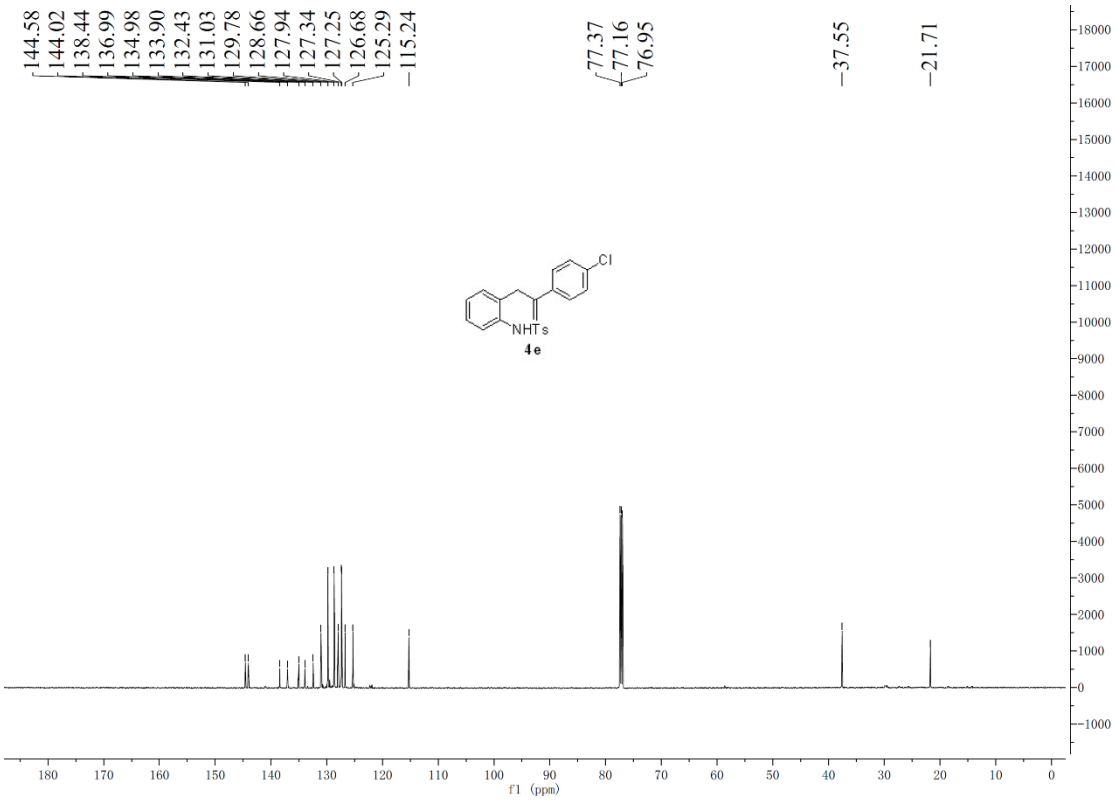

Figure S10. ^{13}C NMR spectra (400 MHz) of **4e** in $CDCl_3$, related to **Scheme 1**.

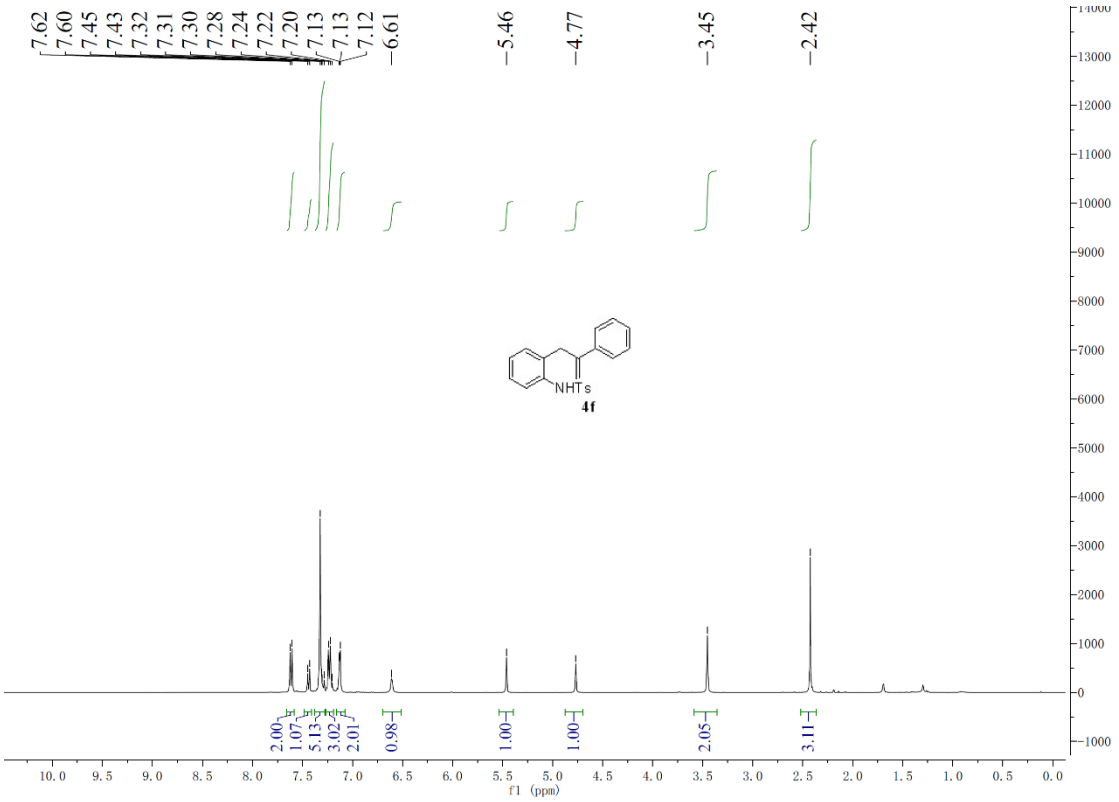

Figure S11. ^{1}H NMR spectra (400 MHz) of **4f** in $CDCl_3$, related to **Scheme 1**.

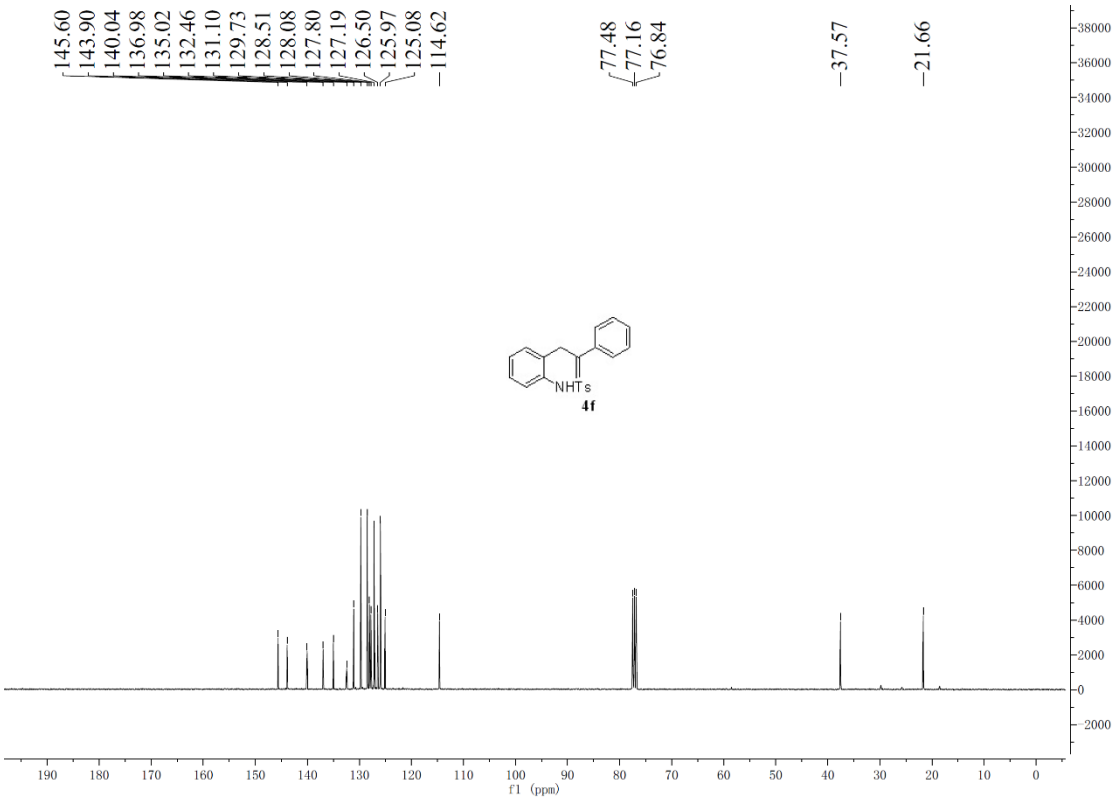

Figure S12. ^{13}C NMR spectra (400 MHz) of **4f** in $CDCl_3$, related to **Scheme 1**.

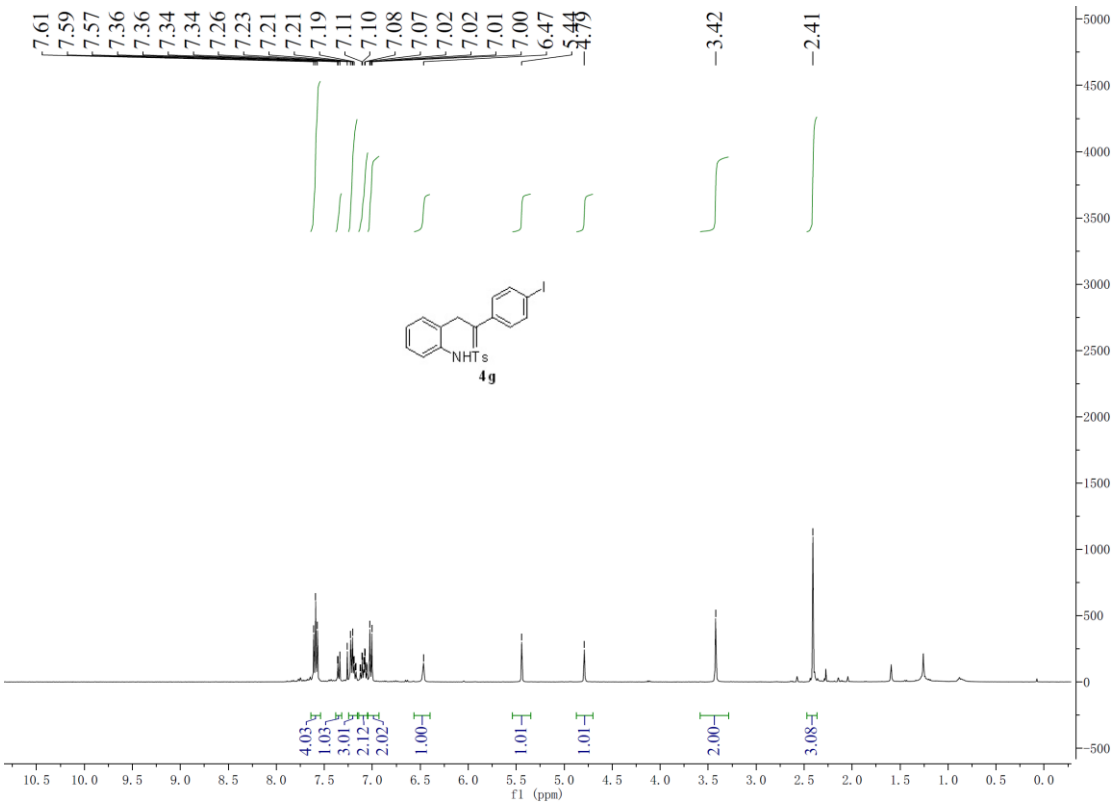

Figure S13. ^{1}H NMR spectra (400 MHz) of **4g** in $CDCl_3$, related to **Scheme 1**.

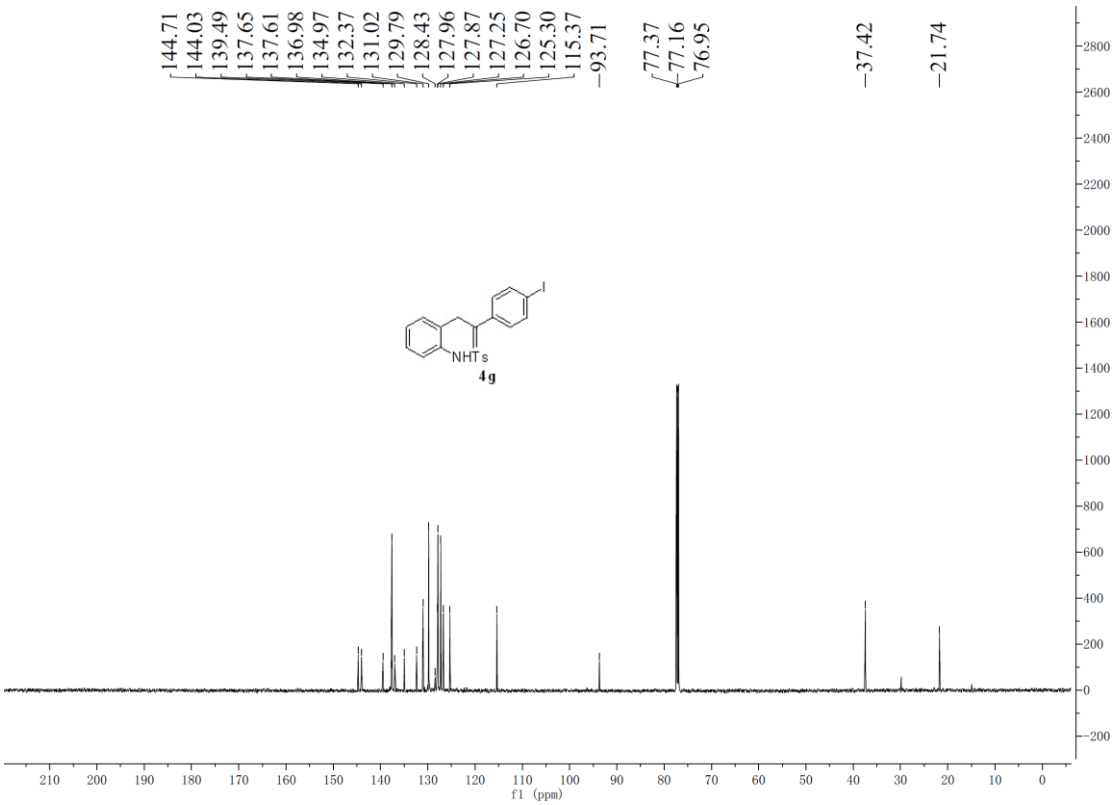

Figure S14. ^{13}C NMR spectra (400 MHz) of **4g** in $CDCl_3$, related to **Scheme 1**.

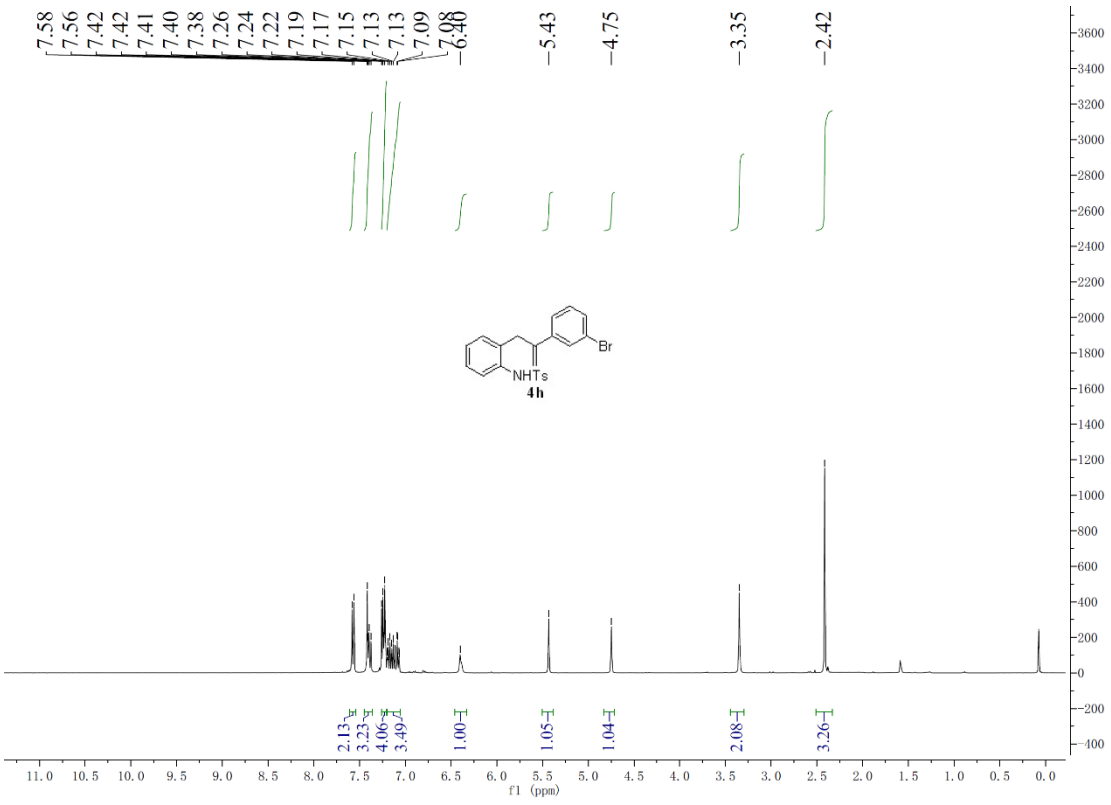

Figure S15. ^{1}H NMR spectra (400 MHz) of **4h** in $CDCl_3$, related to **Scheme 1**.

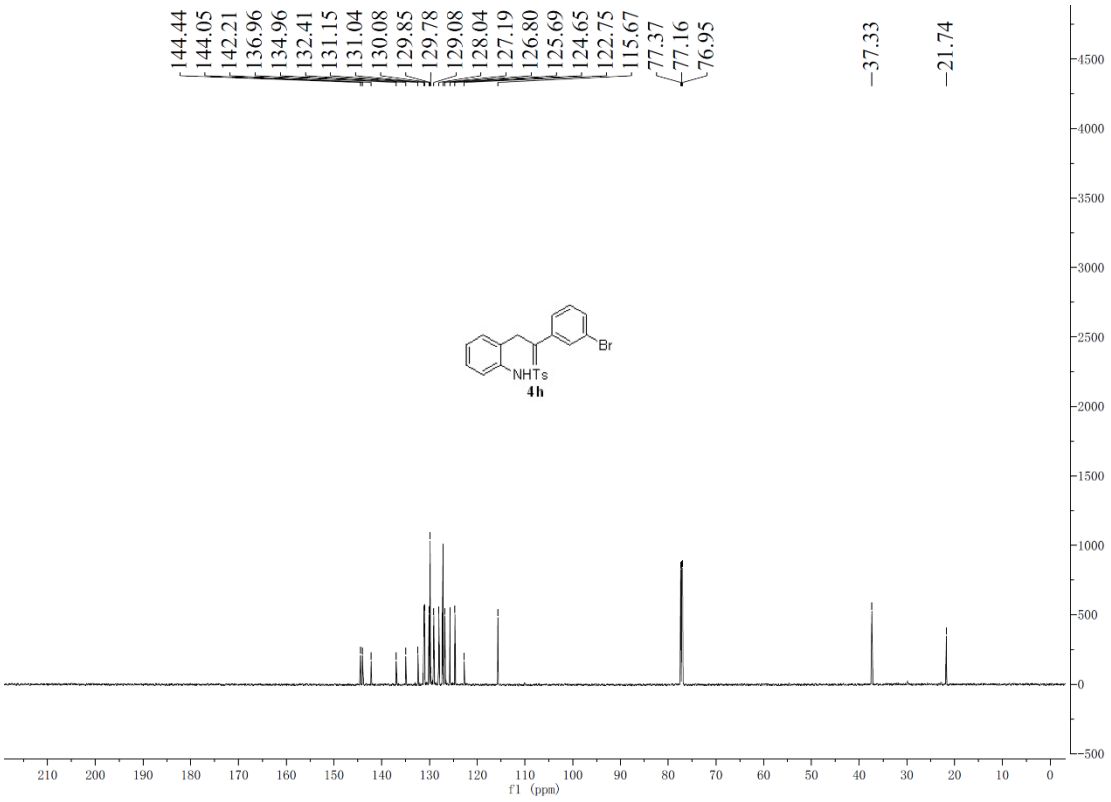

Figure S16. ^{13}C NMR spectra (400 MHz) of **4h** in $CDCl_3$, related to **Scheme 1**.

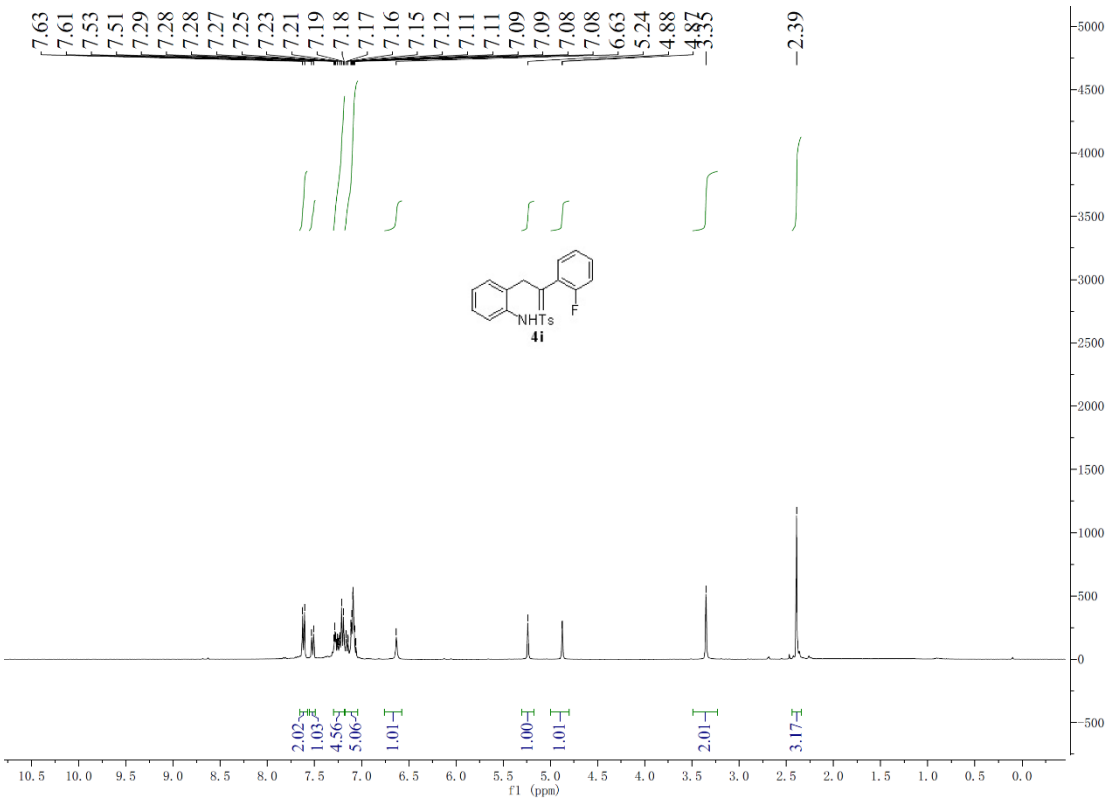

Figure S17. ^{1}H NMR spectra (400 MHz) of **4i** in $CDCl_3$, related to **Scheme 1**.

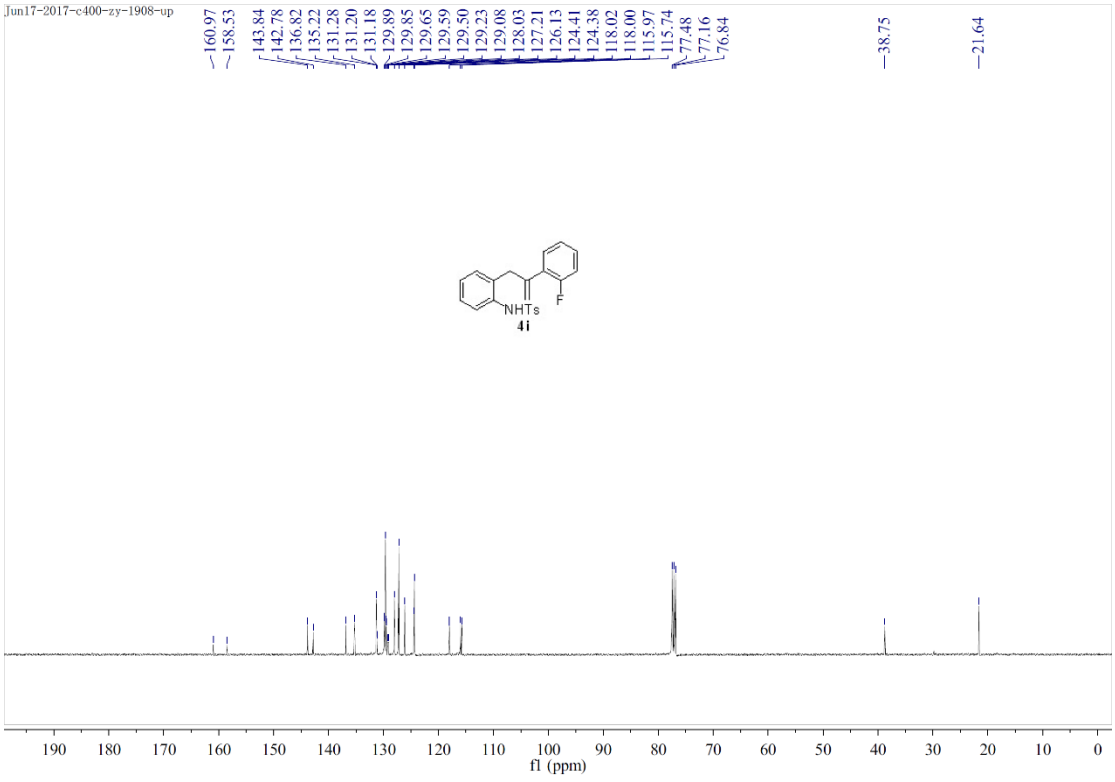

Figure S18. ^{13}C NMR spectra (400 MHz) of **4i** in $CDCl_3$, related to **Scheme 1**.

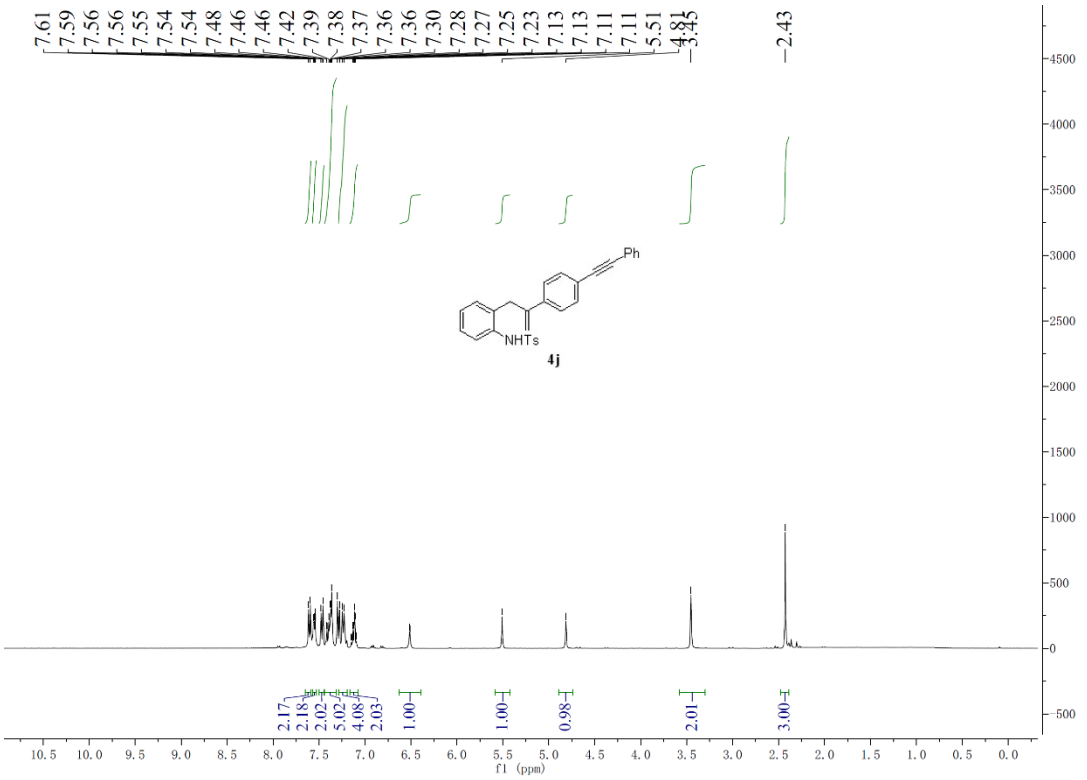

Figure S19. ^{1}H NMR spectra (400 MHz) of **4j** in $CDCl_3$, related to **Scheme 1**.

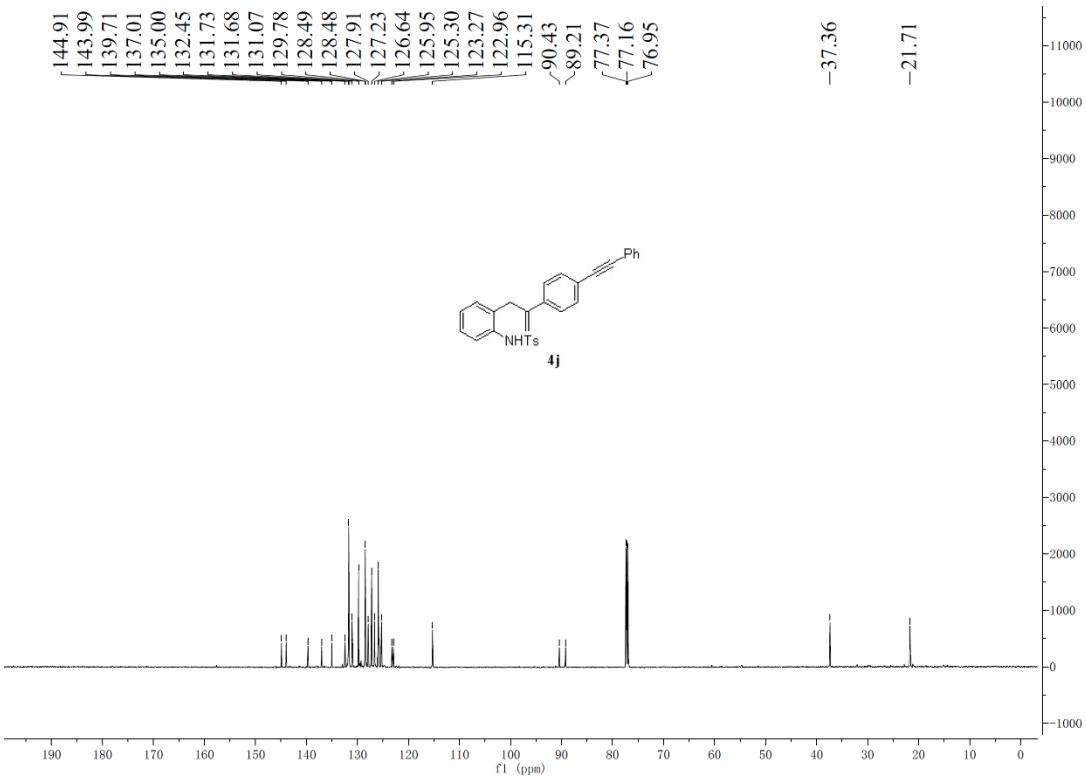

Figure S20. ^{13}C NMR spectra (400 MHz) of **4j** in $CDCl_3$, related to **Scheme 1**.

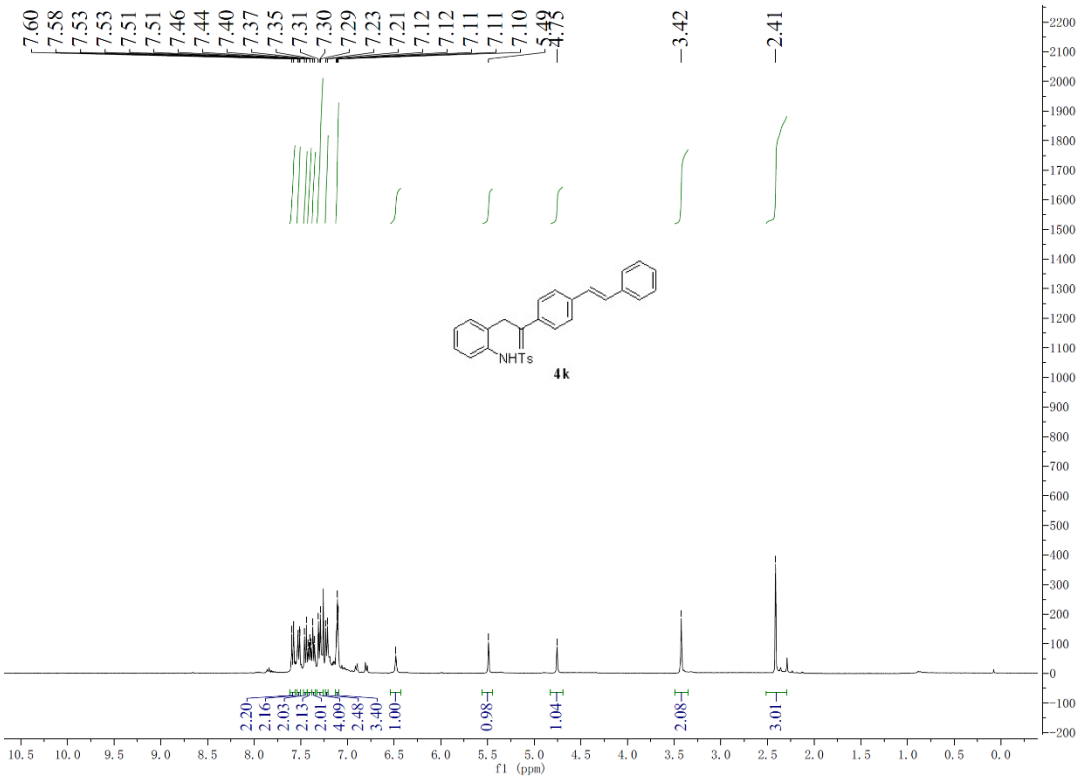

Figure S21. ^{1}H NMR spectra (400 MHz) of **4k** in $CDCl_3$, related to **Scheme 1**.

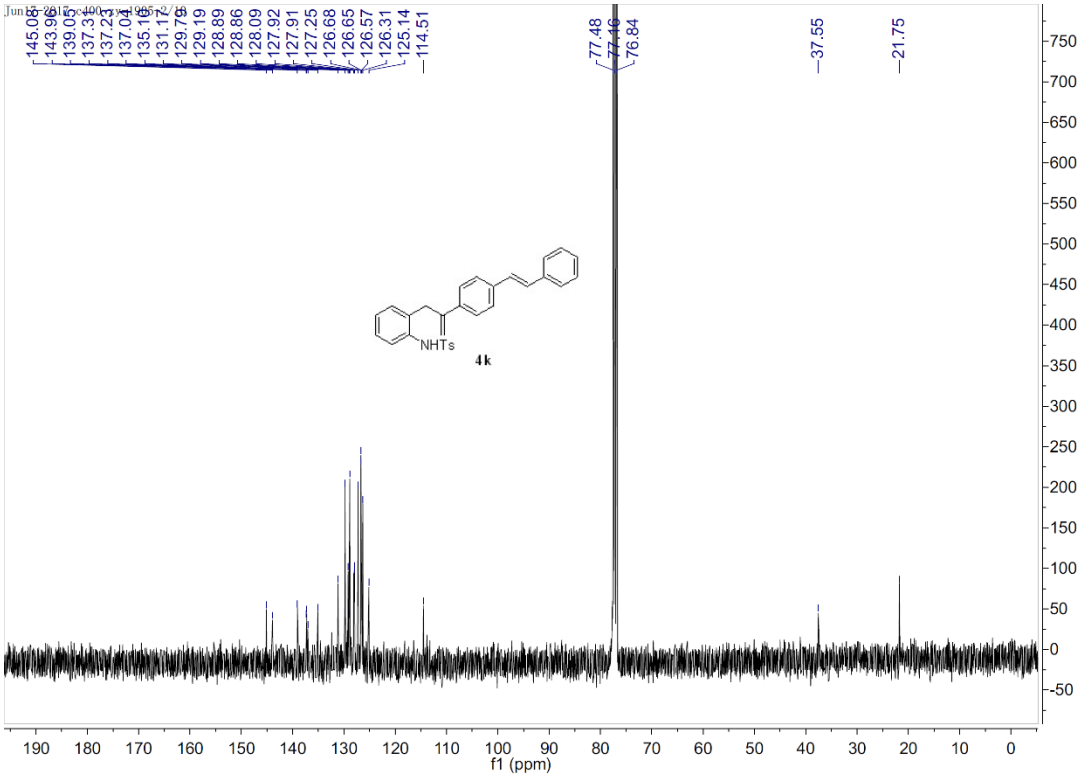

Figure S22. ^{13}C NMR spectra (400 MHz) of **4k** in $CDCl_3$, related to **Scheme 1**.

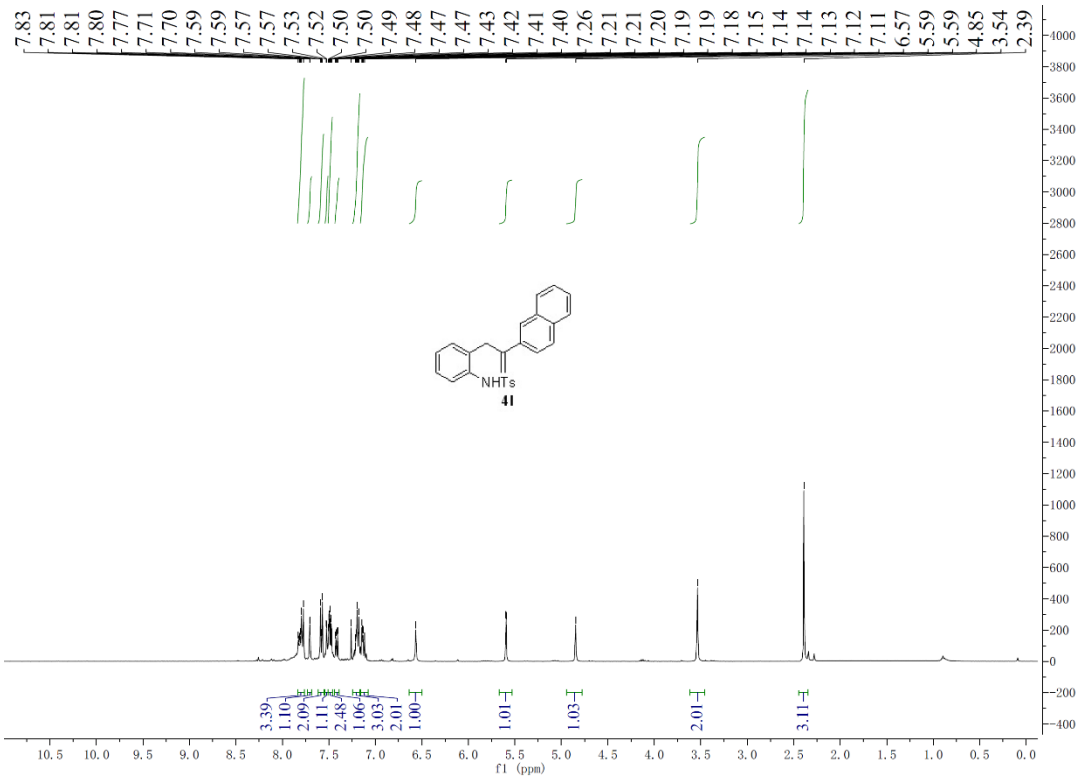

Figure S23. ^{1}H NMR spectra (400 MHz) of **4l** in $CDCl_3$, related to **Scheme 1**.

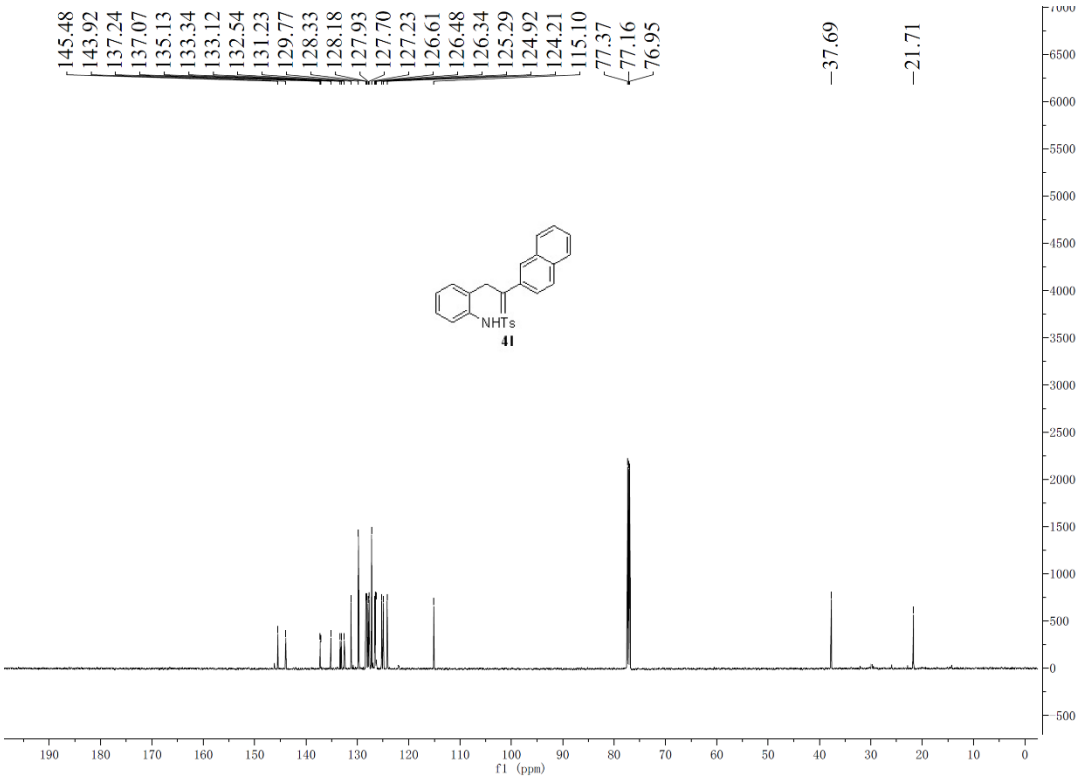

Figure S24. ^{13}C NMR spectra (400 MHz) of **4l** in $CDCl_3$, related to **Scheme 1**.

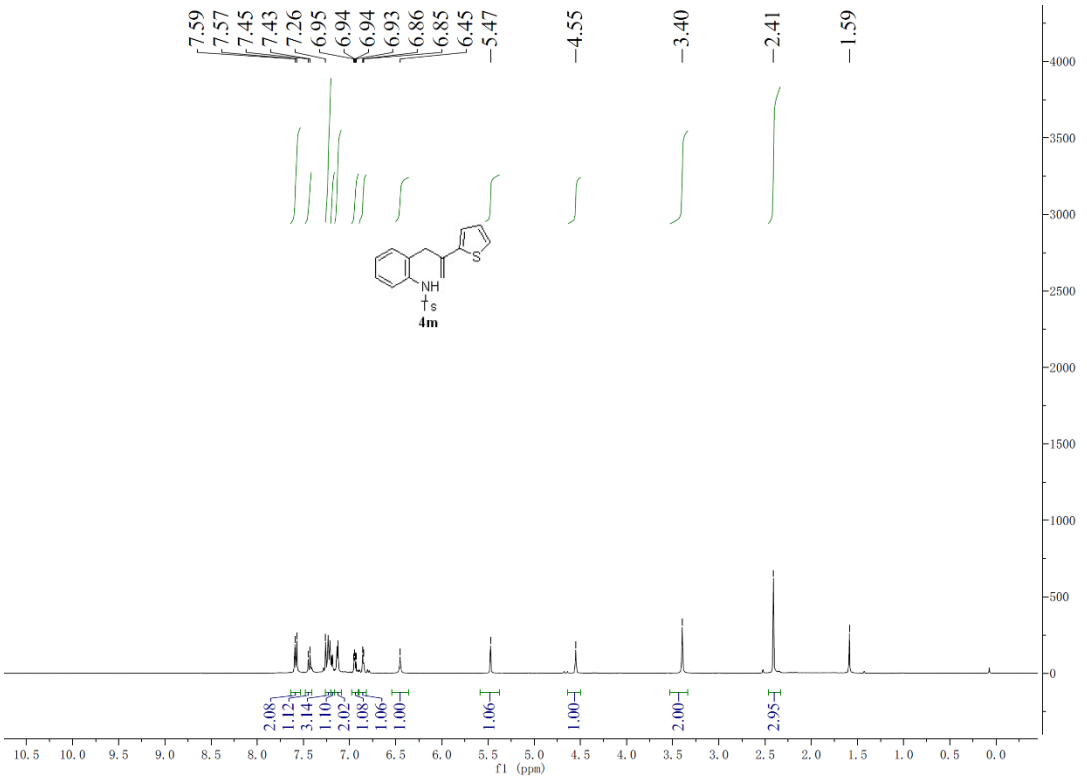

Figure S25. ^{1}H NMR spectra (400 MHz) of **4m** in $CDCl_3$, related to **Scheme 1**.

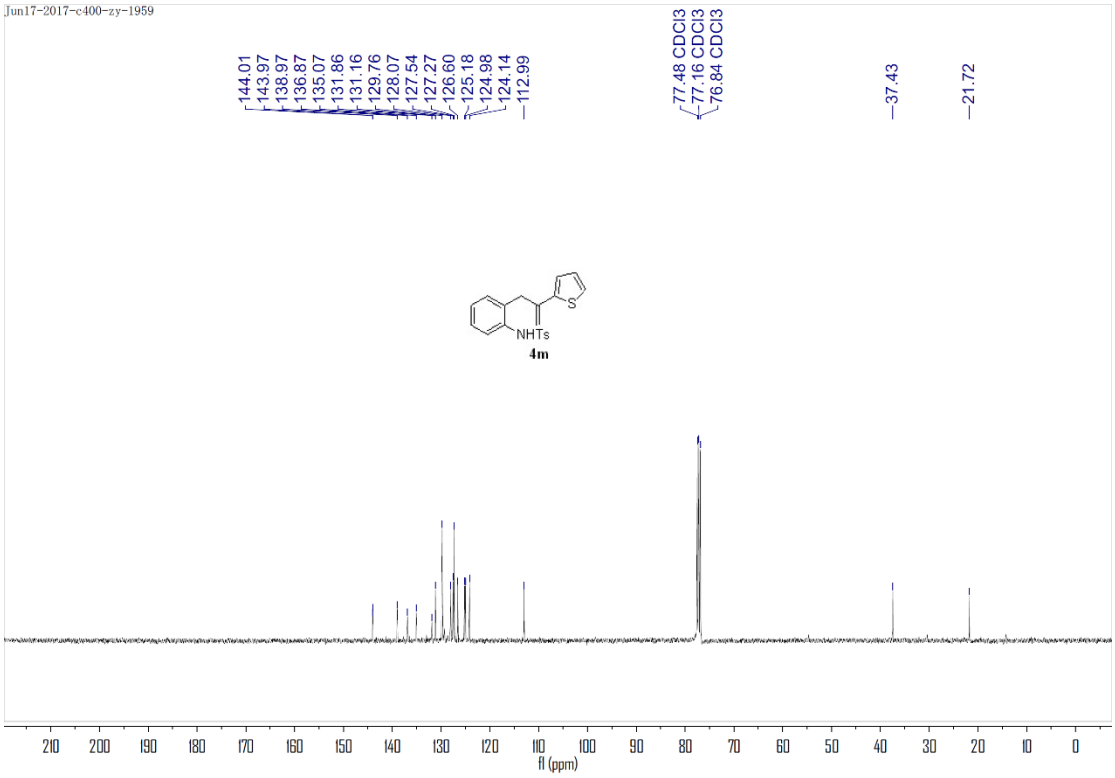

Figure S26. ^{13}C NMR spectra (400 MHz) of **4m** in $CDCl_3$, related to **Scheme 1**.

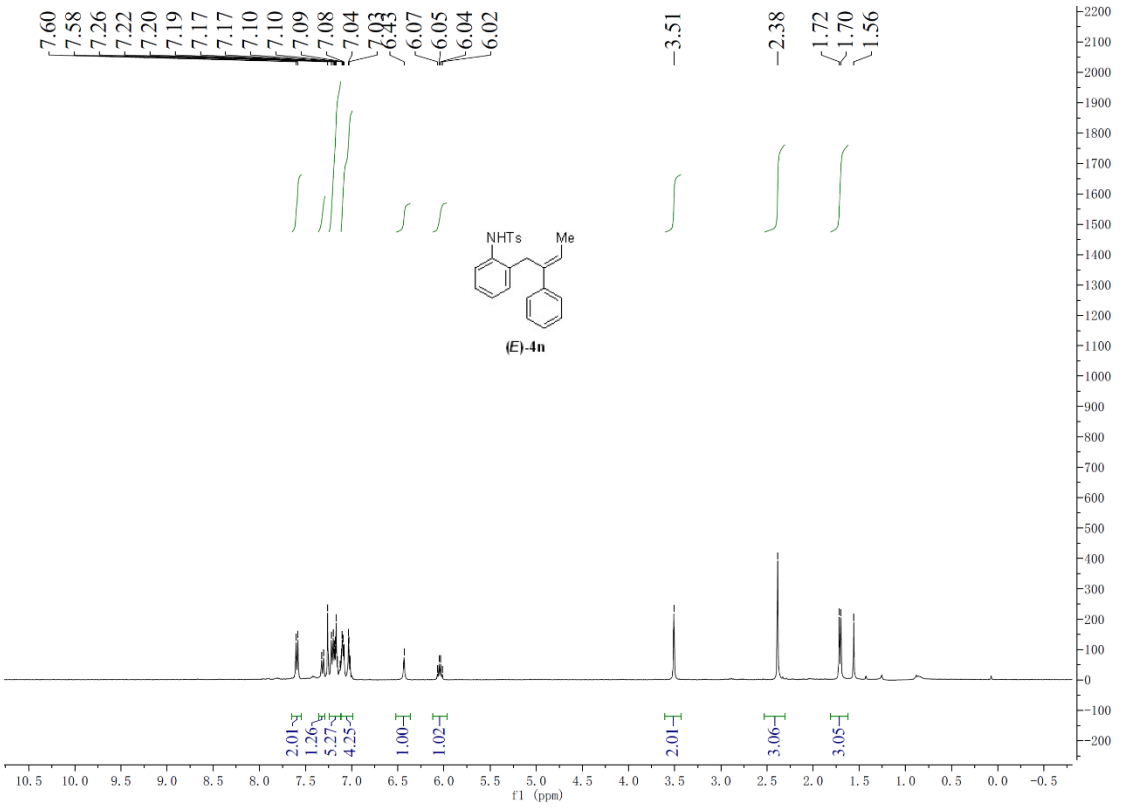

Figure S27. ^{1}H NMR spectra (400 MHz) of (*E*)-**4n** in $CDCl_3$, related to **Scheme 1**.

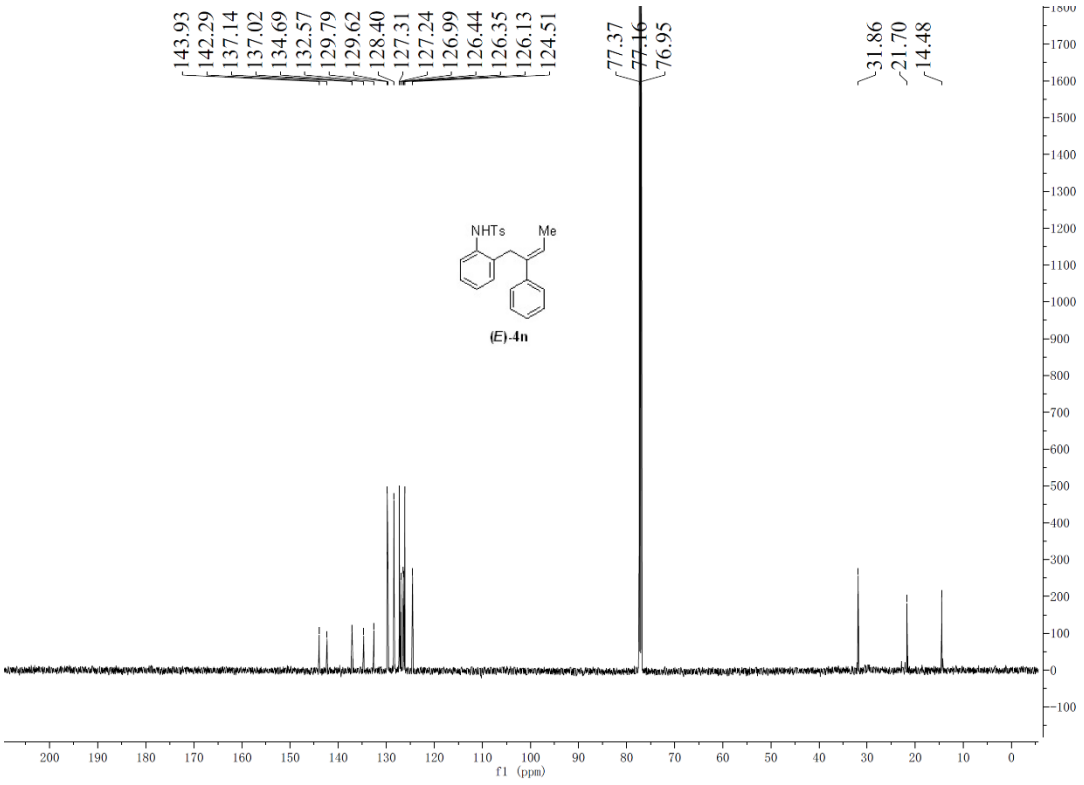

Figure S28. ^{13}C NMR spectra (400 MHz) of (*E*)-**4n** in $CDCl_3$, related to **Scheme 1**.

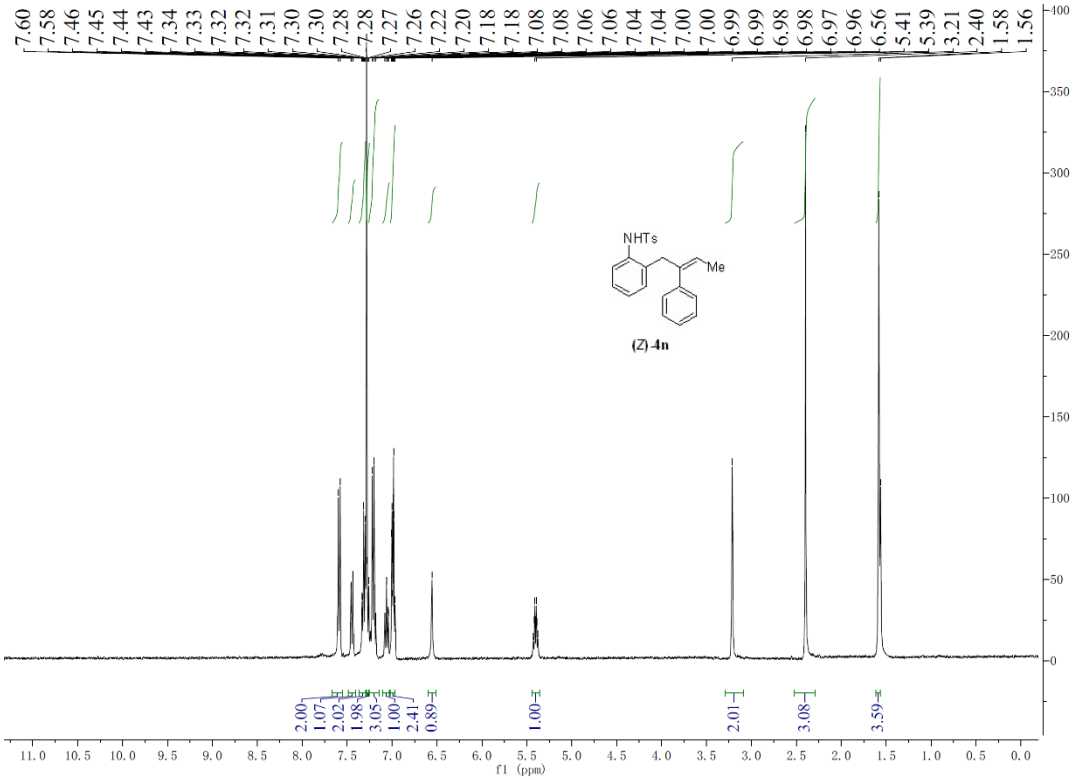

Figure S29. ^{1}H NMR spectra (400 MHz) of (*Z*)-**4n** in $CDCl_3$, related to **Scheme 1**.

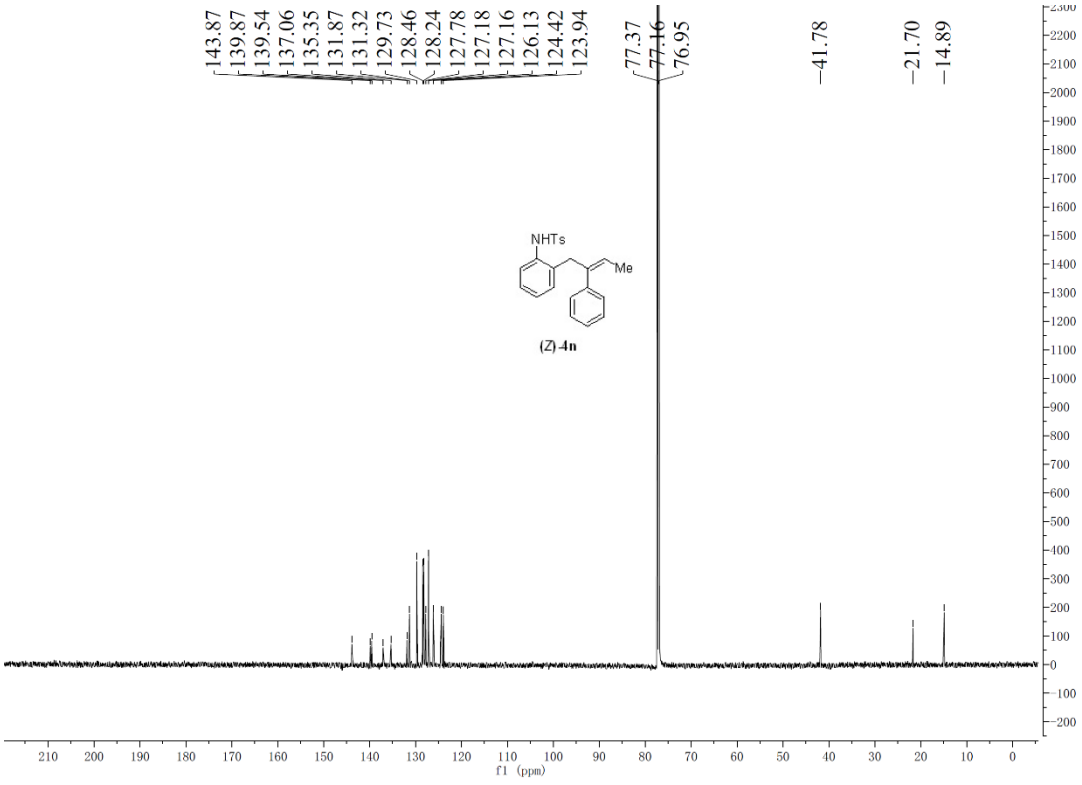

Figure S30. ^{13}C NMR spectra (400 MHz) of (*Z*)-**4n** in $CDCl_3$, related to **Scheme 1**.

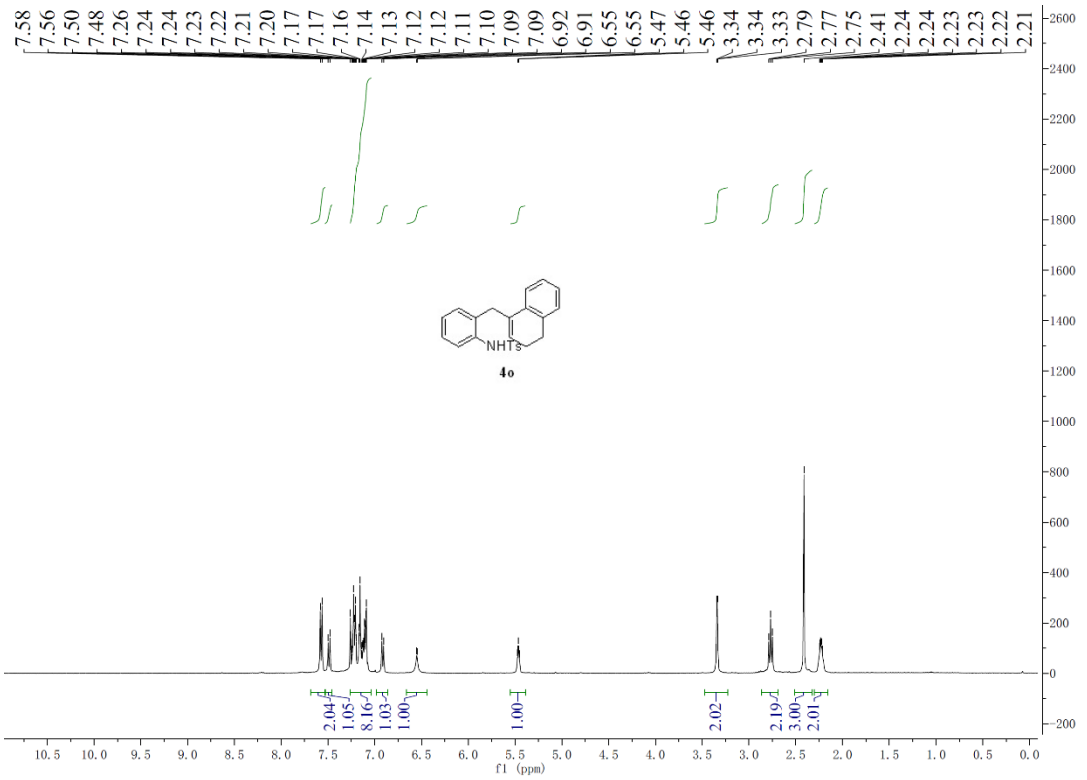

Figure S31. ^{1}H NMR spectra (400 MHz) of **4o** in $CDCl_3$, related to **Scheme 1**.

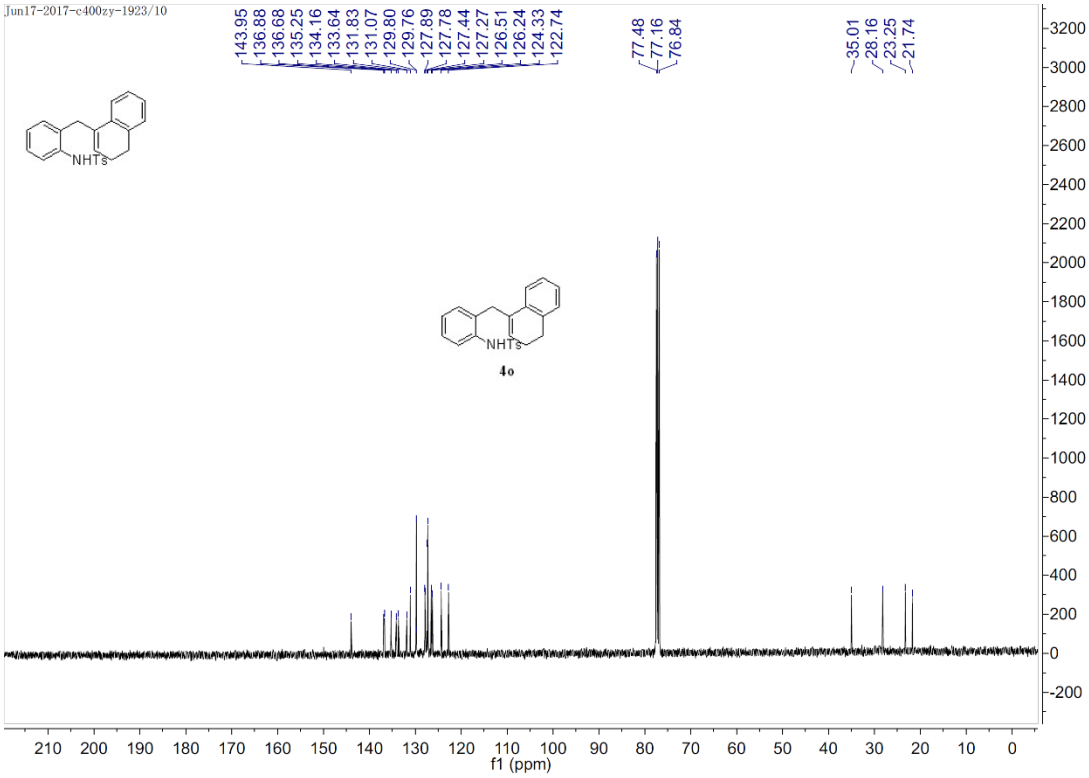

Figure S32. ^{13}C NMR spectra (400 MHz) of **4o** in $CDCl_3$, related to **Scheme 1**.

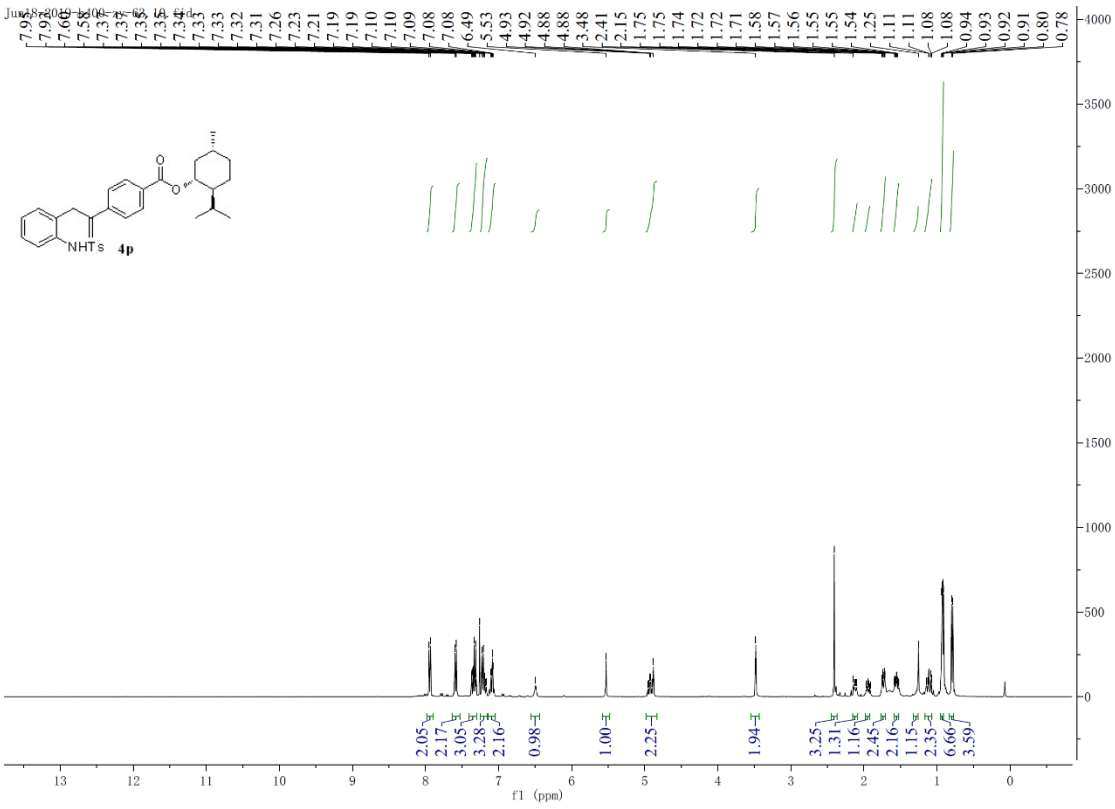

Figure S33. ^{1}H NMR spectra (400 MHz) of **4p** in $CDCl_3$, related to **Scheme 1**.

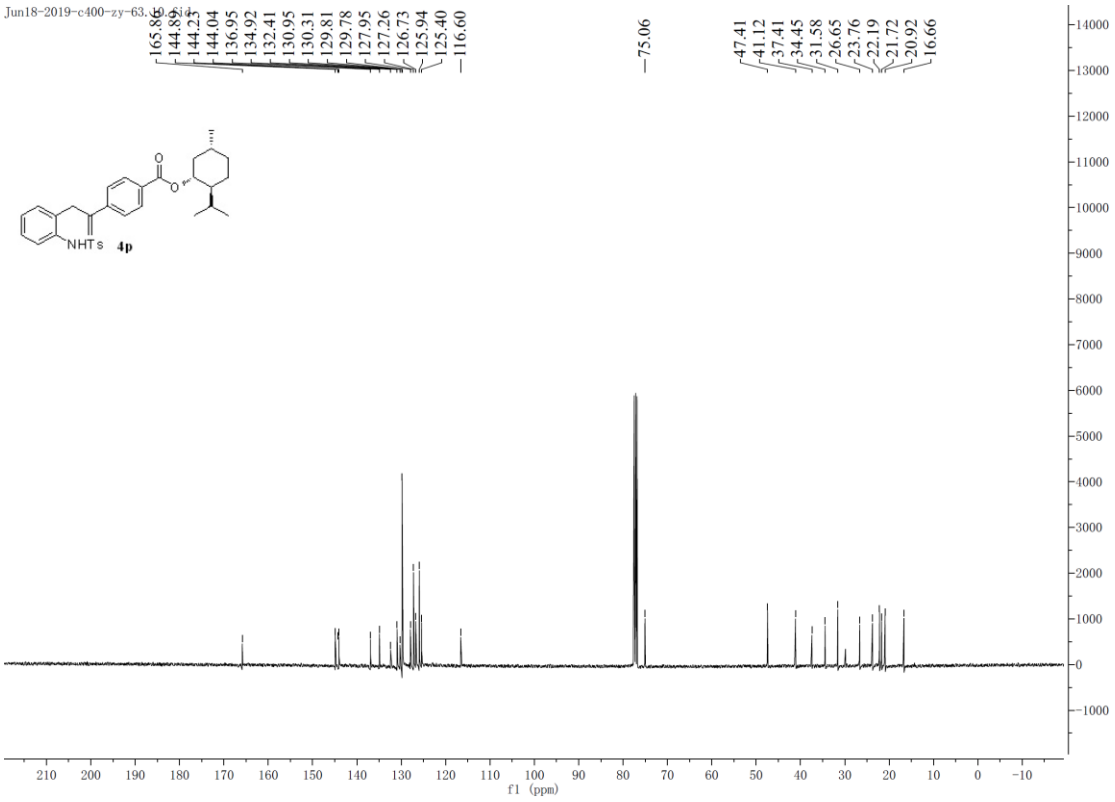

Figure S34. ^{13}C NMR spectra (400 MHz) of **4p** in $CDCl_3$, related to **Scheme 1**.

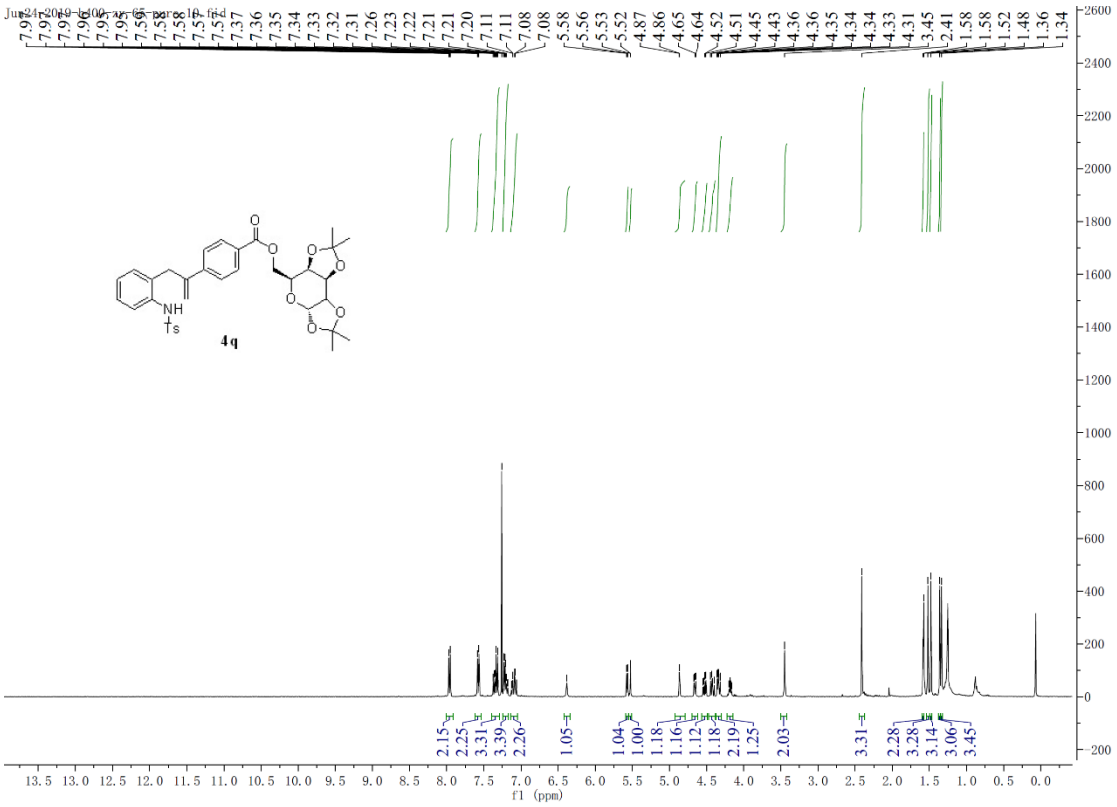

Figure S35. ^{1}H NMR spectra (400 MHz) of **4q** in $CDCl_3$, related to **Scheme 1**.

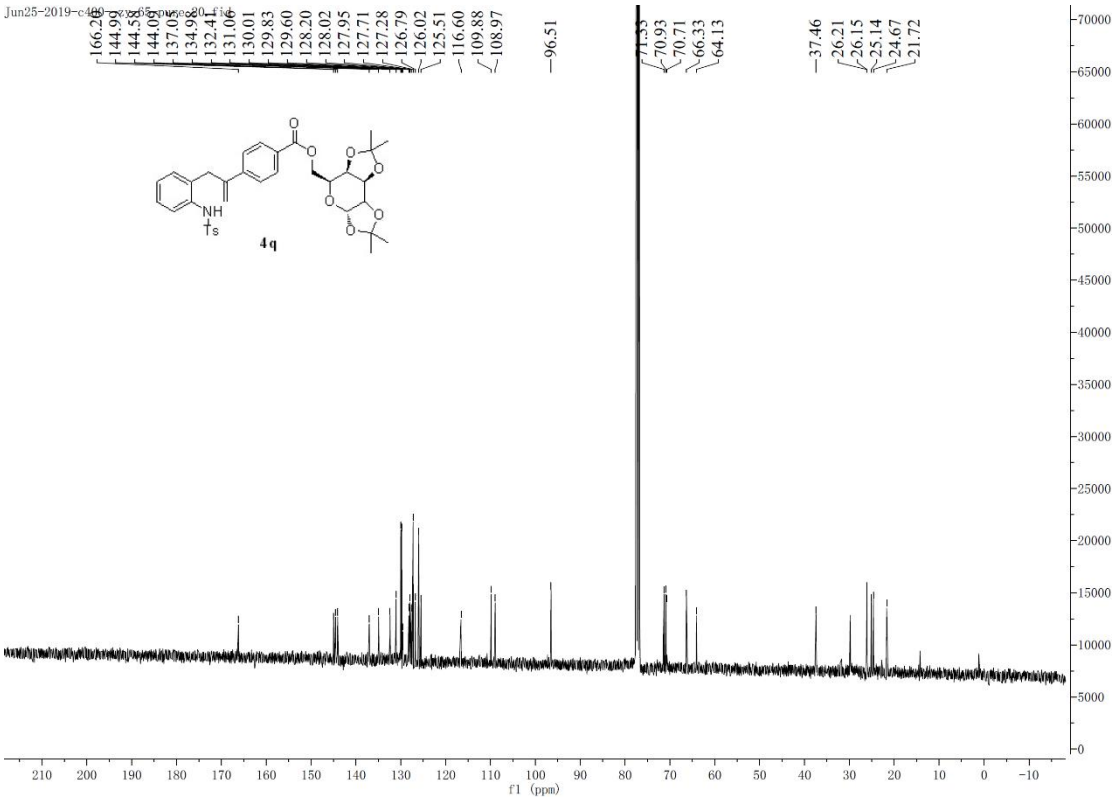

Figure S36. ^{13}C NMR spectra (400 MHz) of **4q** in $CDCl_3$, related to **Scheme 1**.

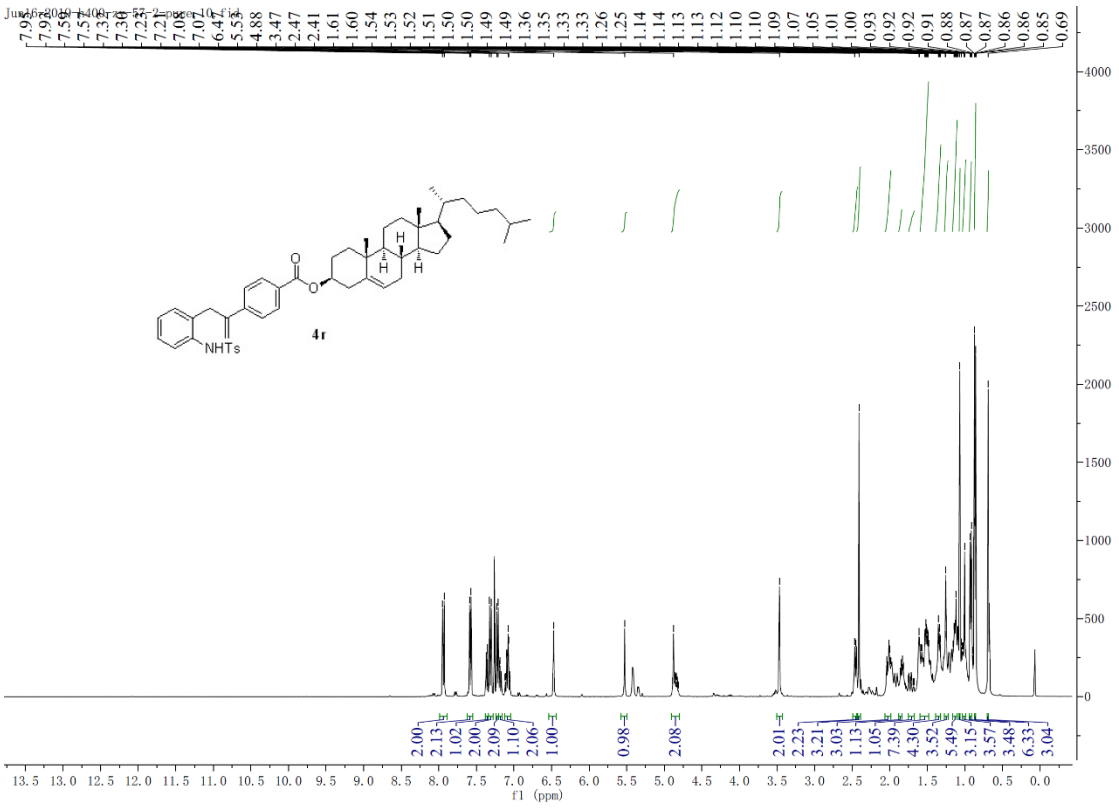

Figure S37. ^{1}H NMR spectra (400 MHz) of **4r** in $CDCl_3$, related to **Scheme 1**.

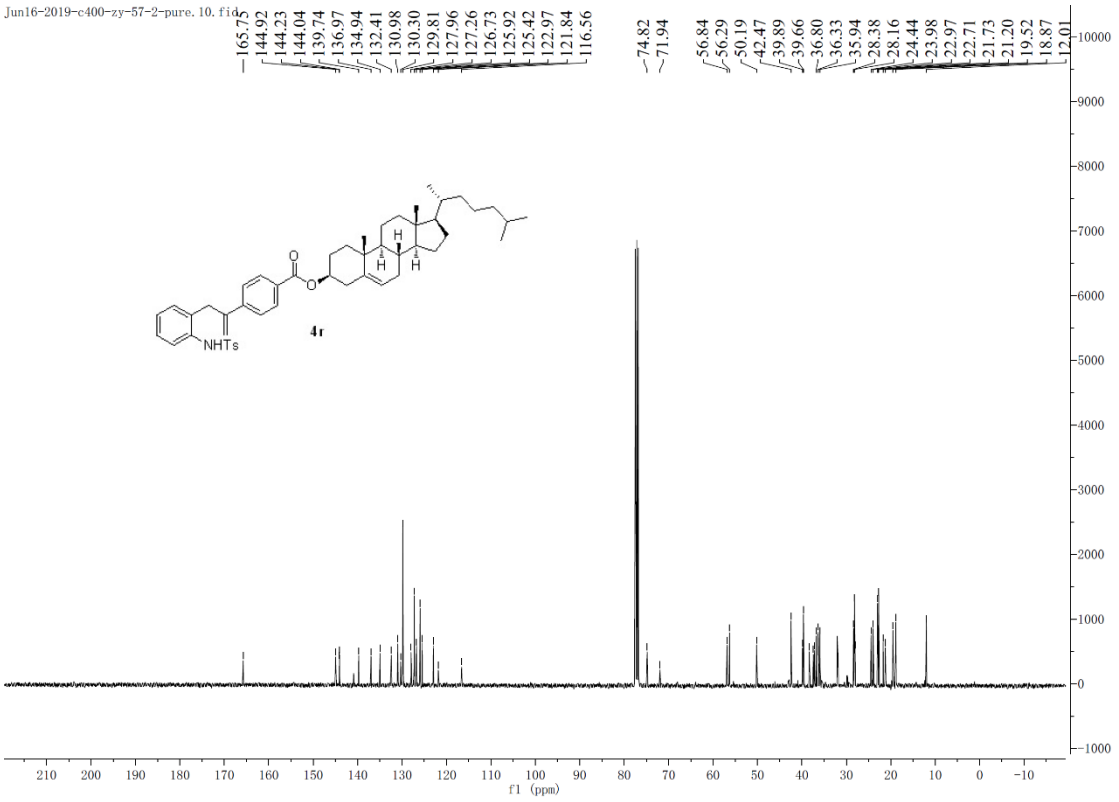

Figure S38. ^{13}C NMR spectra (400 MHz) of **4r** in $CDCl_3$, related to **Scheme 1**.

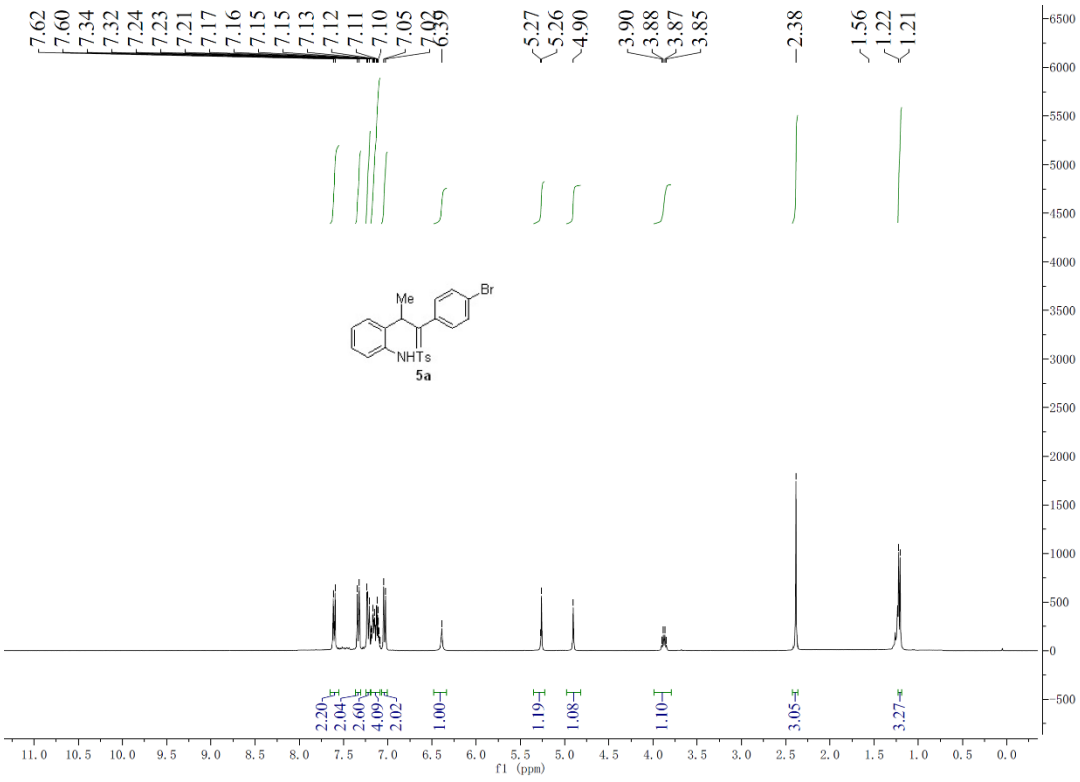

Figure S39. ^{1}H NMR spectra (400 MHz) of **5a** in $CDCl_3$, related to **Scheme 1**.

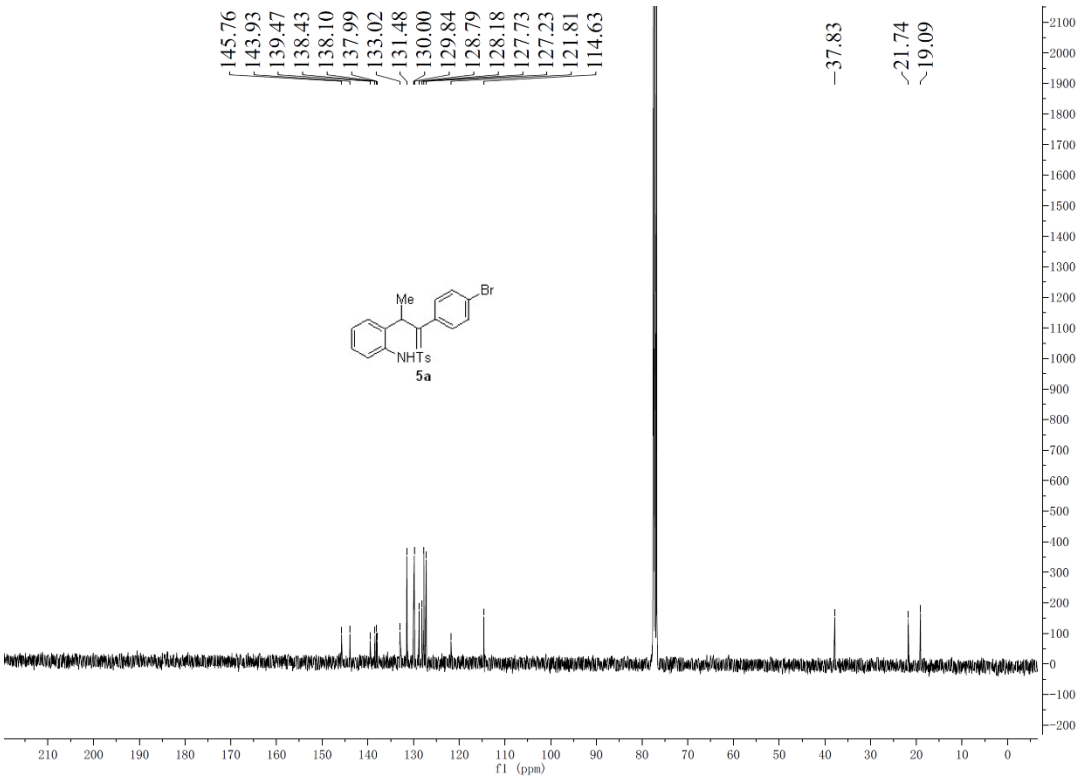

Figure S40. ^{13}C NMR spectra (400 MHz) of **5a** in $CDCl_3$, related to **Scheme 1**.

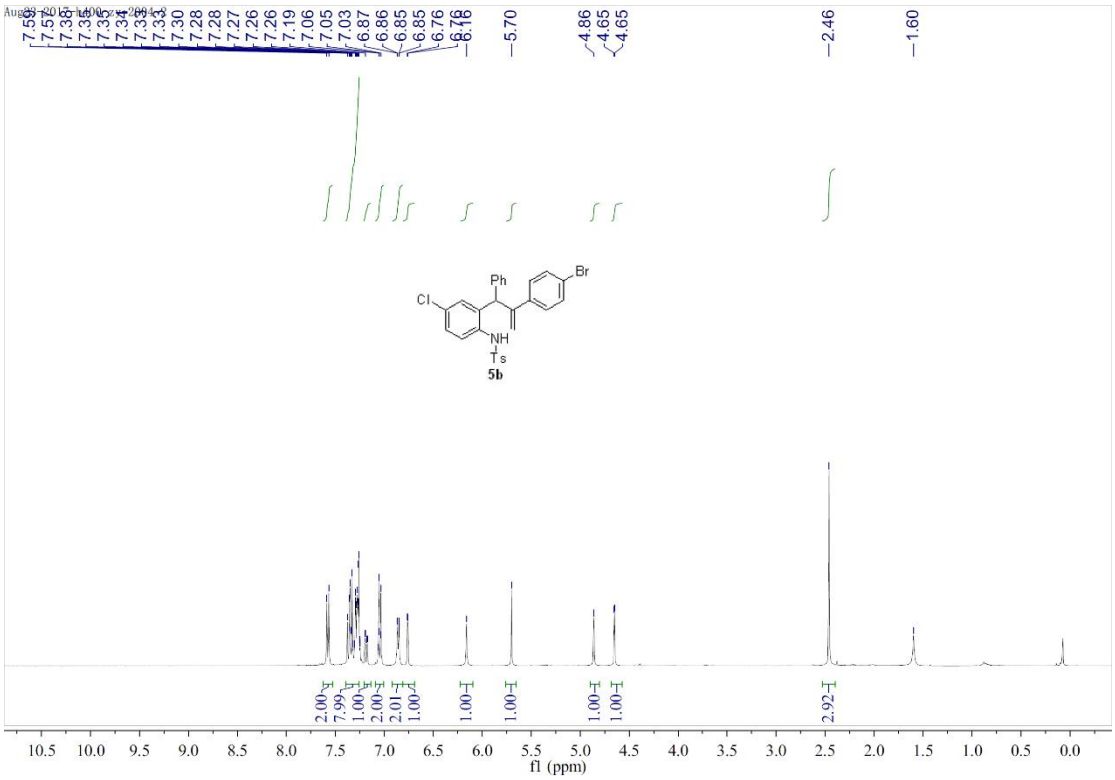

Figure S41. ^{1}H NMR spectra (400 MHz) of **5b** in $CDCl_3$, related to **Scheme 1**.

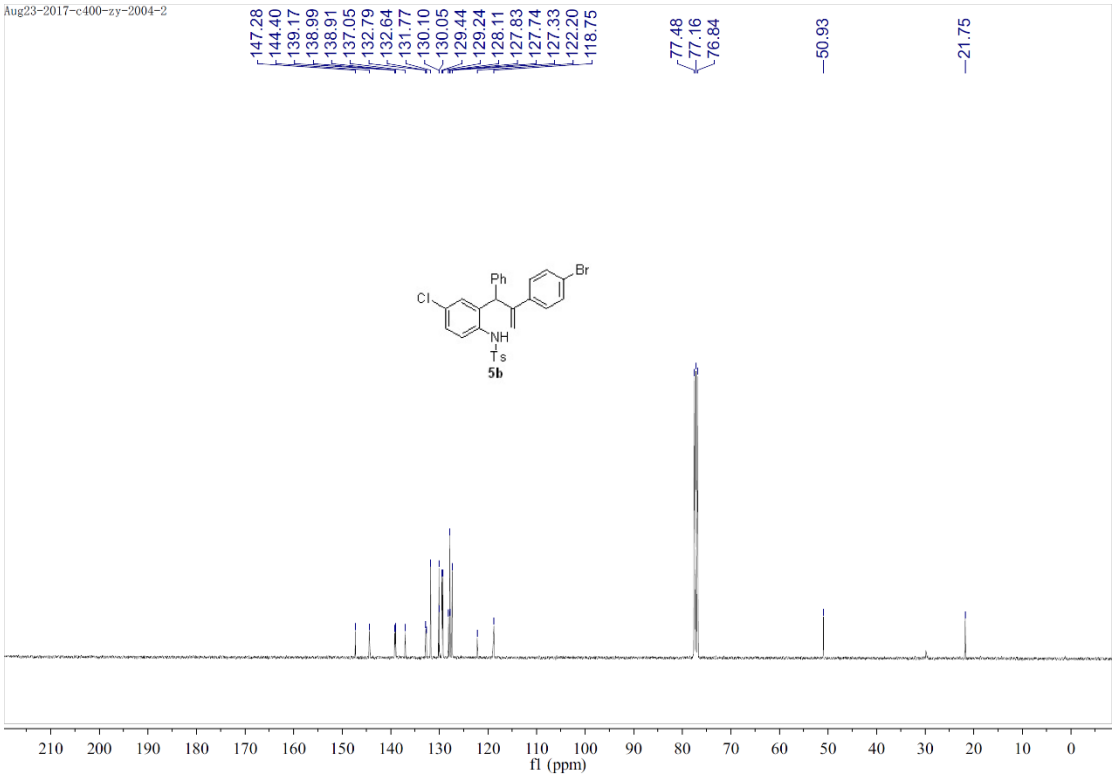

Figure S42. ^{13}C NMR spectra (400 MHz) of **5b** in $CDCl_3$, related to **Scheme 1**.

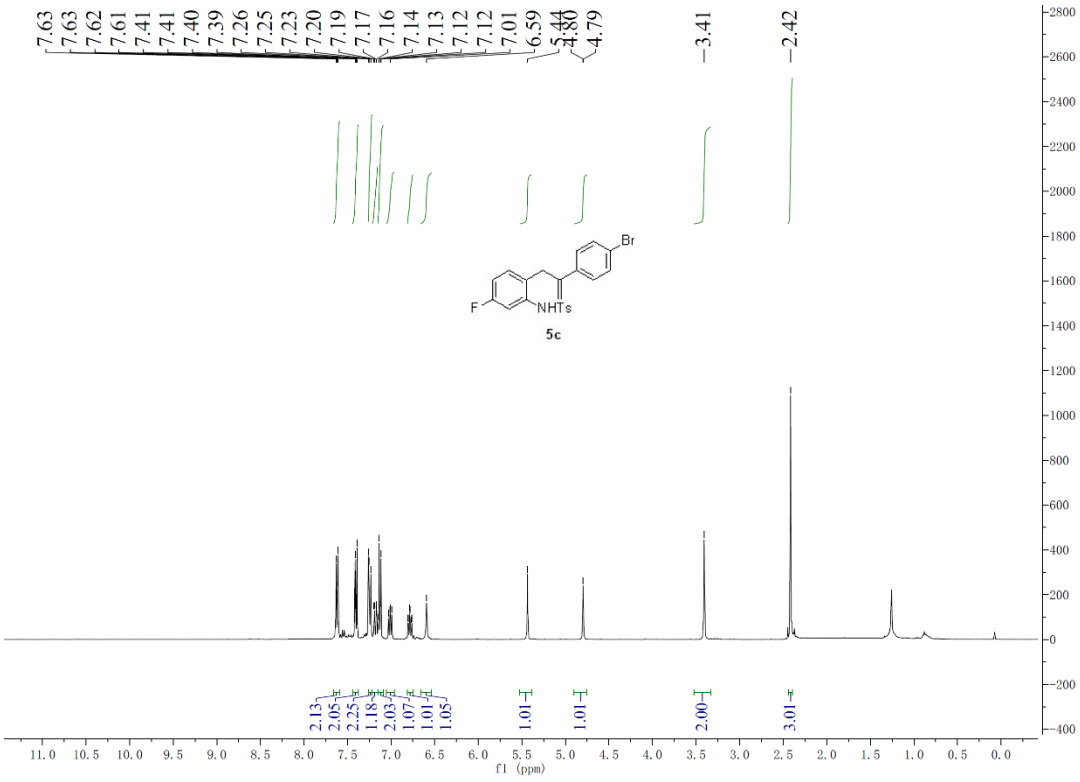

Figure S43. ^{1}H NMR spectra (400 MHz) of **5c** in $CDCl_3$, related to **Scheme 1**.

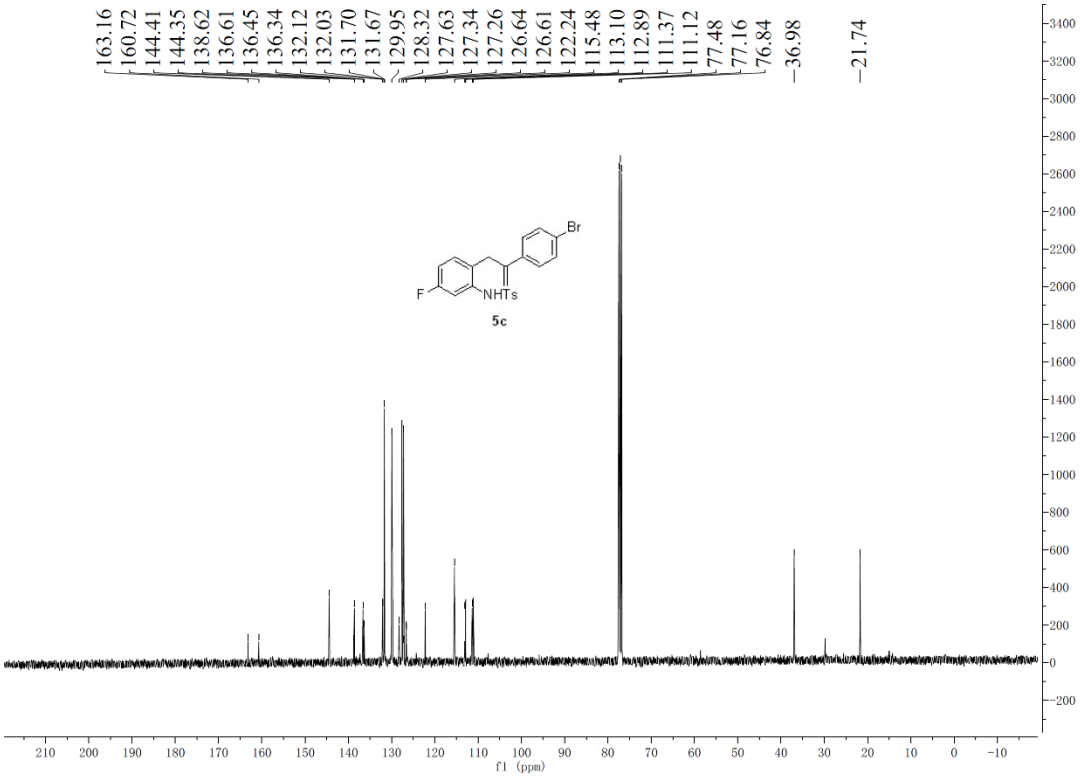

Figure S44. ^{13}C NMR spectra (400 MHz) of **5c** in $CDCl_3$, related to **Scheme 1**.

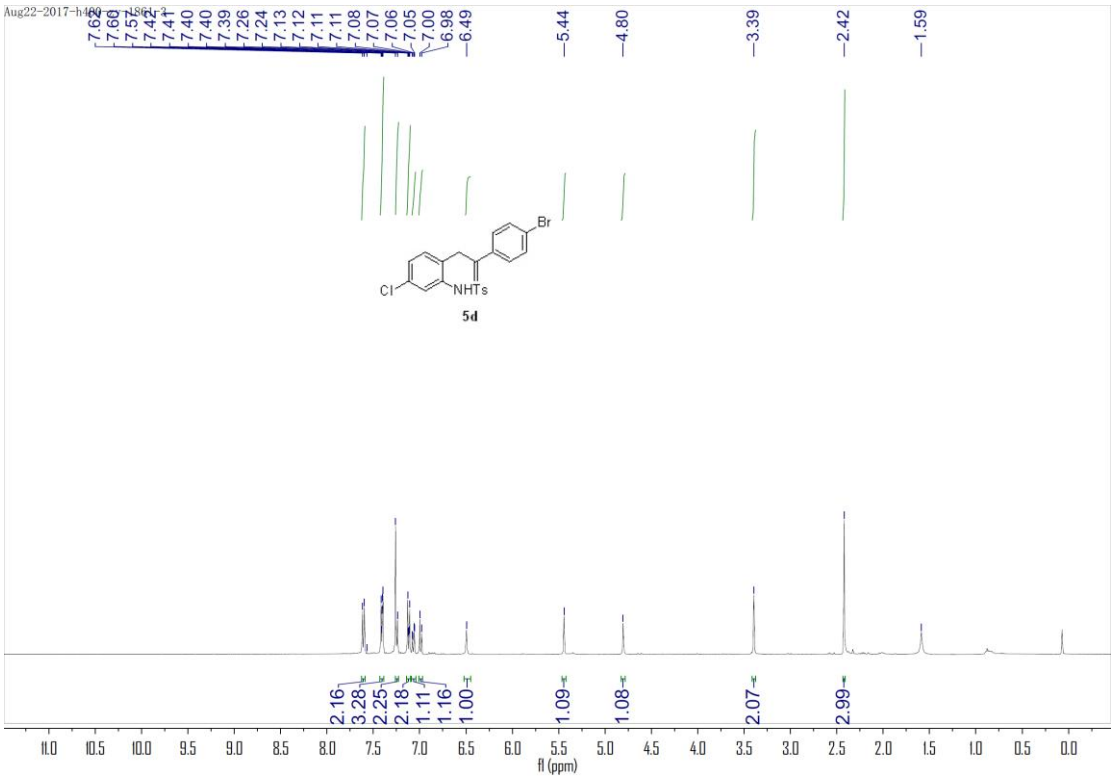

Figure S45. ^{1}H NMR spectra (400 MHz) of **5d** in $CDCl_3$, related to **Scheme 1**.

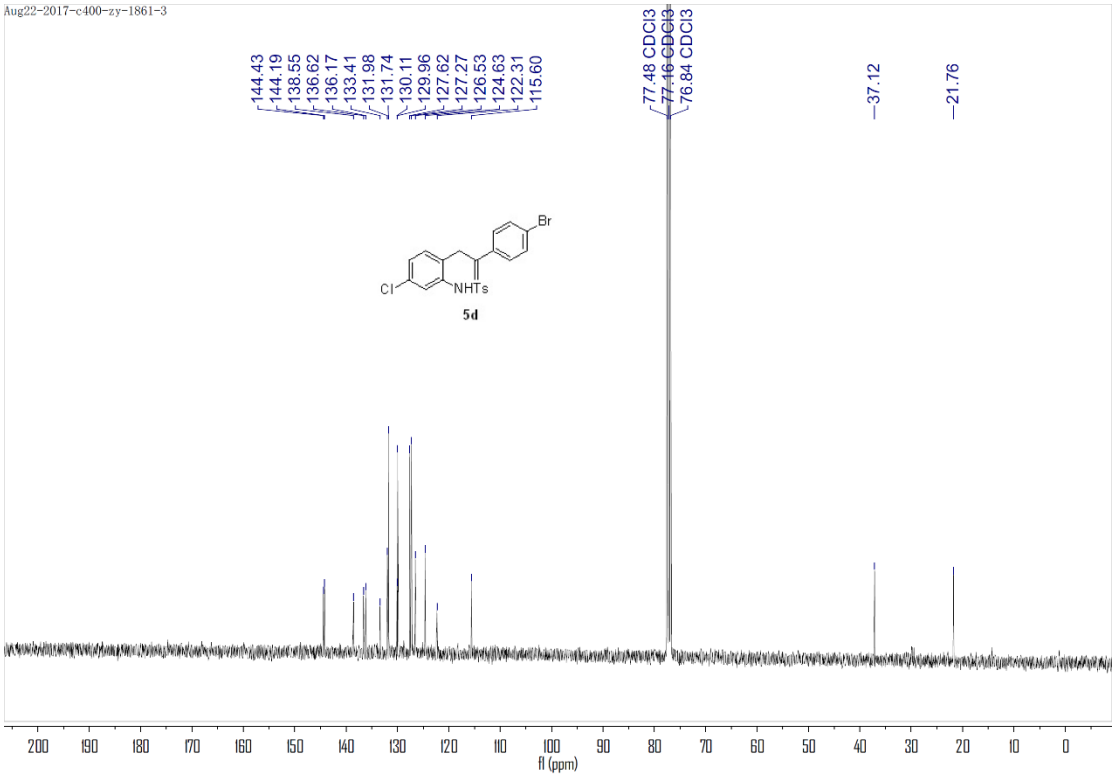

Figure S46. ^{13}C NMR spectra (400 MHz) of **5d** in $CDCl_3$, related to **Scheme 1**.

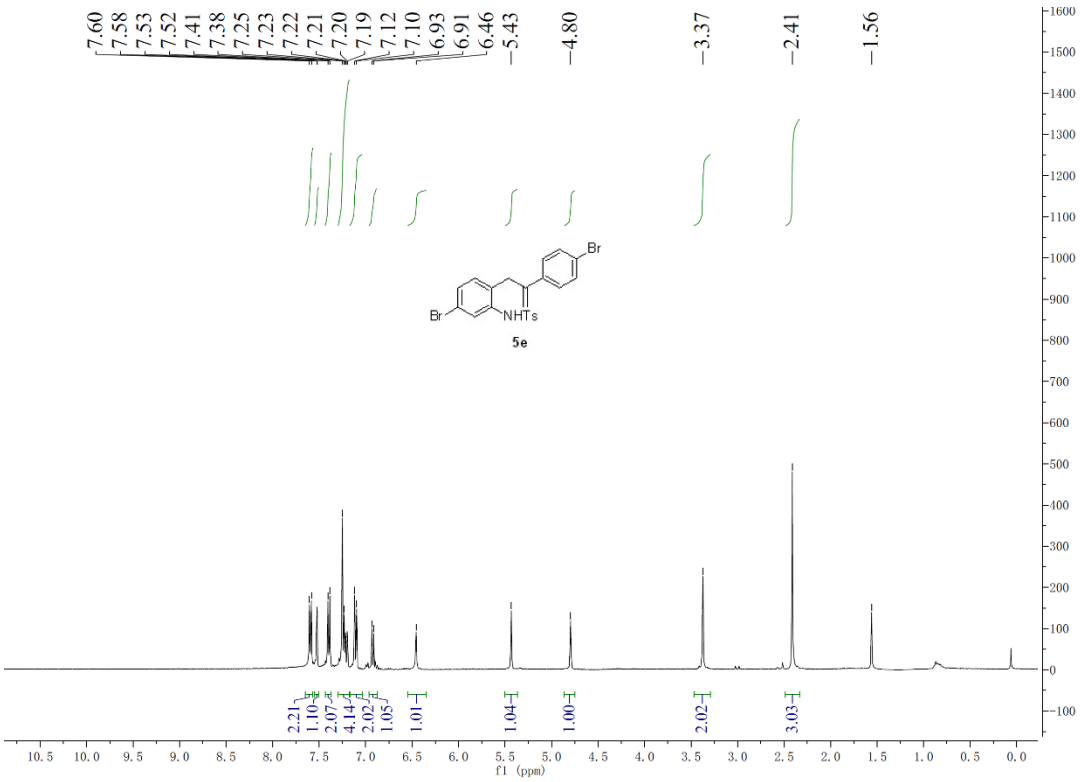

Figure S47. ^{1}H NMR spectra (400 MHz) of **5e** in $CDCl_3$, related to **Scheme 1**.

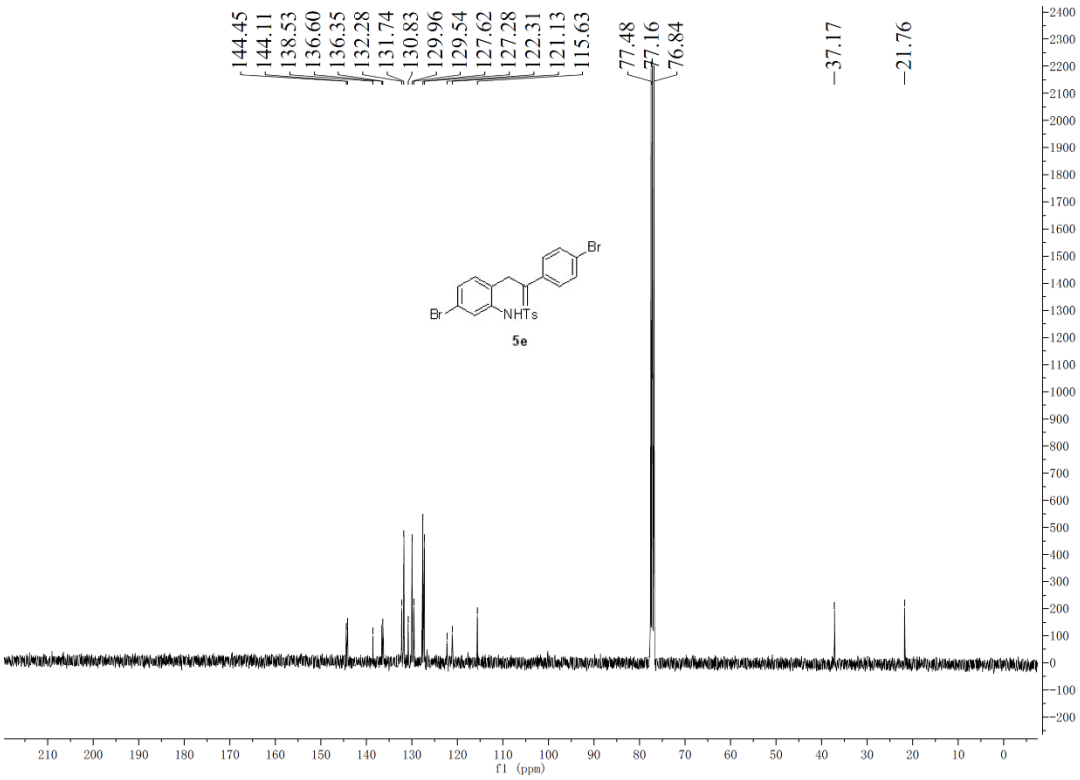

Figure S48. ^{13}C NMR spectra (400 MHz) of **5e** in $CDCl_3$, related to **Scheme 1**.

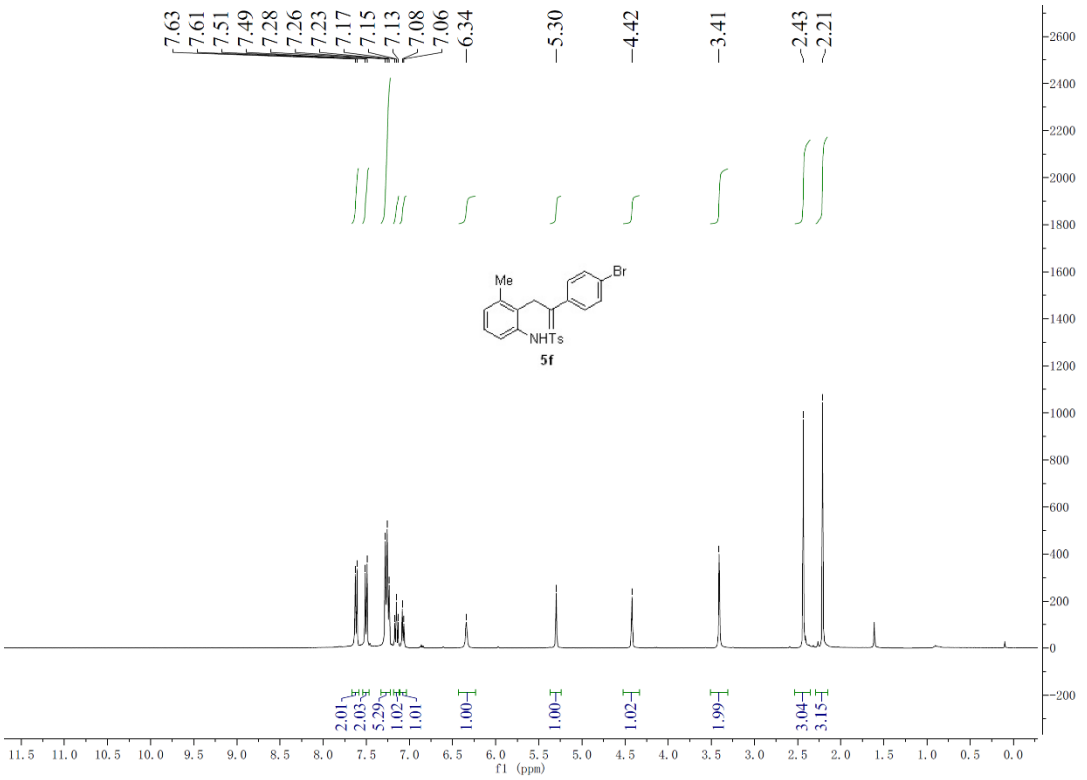

Figure S49. ^{1}H NMR spectra (400 MHz) of **5f** in $CDCl_3$, related to **Scheme 1**.

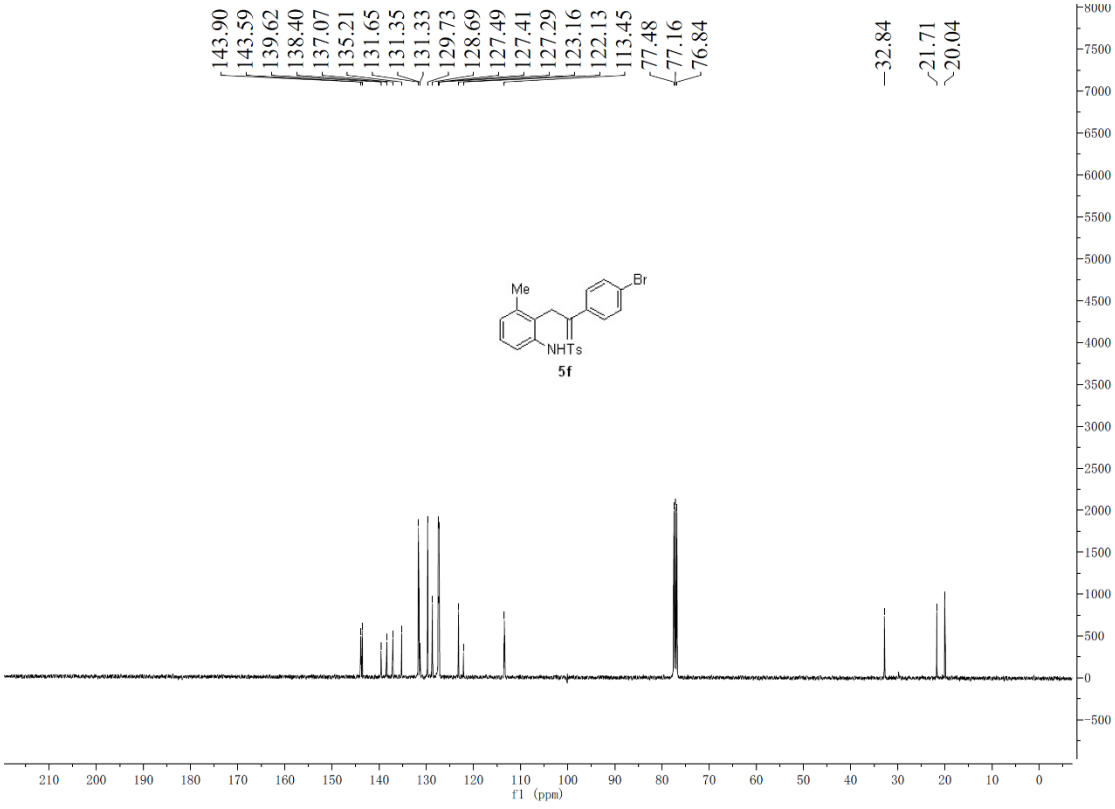

Figure S50. ^{13}C NMR spectra (400 MHz) of **5f** in $CDCl_3$, related to **Scheme 1**.

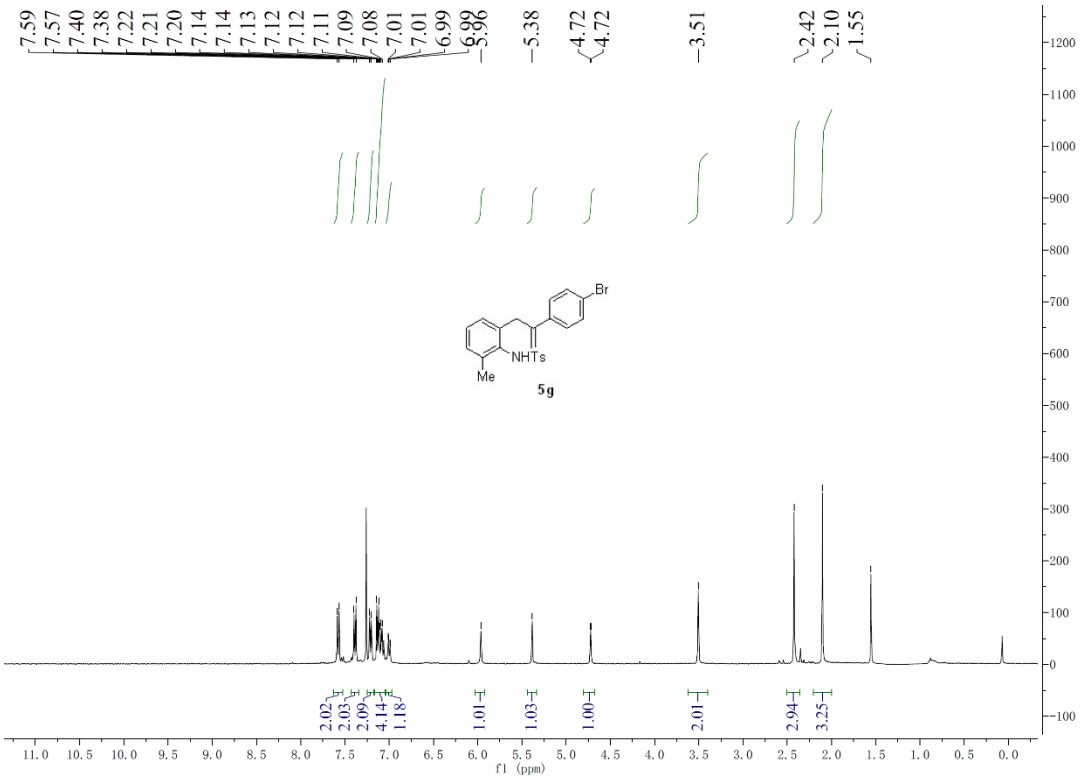

Figure S51. ^{1}H NMR spectra (400 MHz) of **5g** in $CDCl_3$, related to **Scheme 1**.

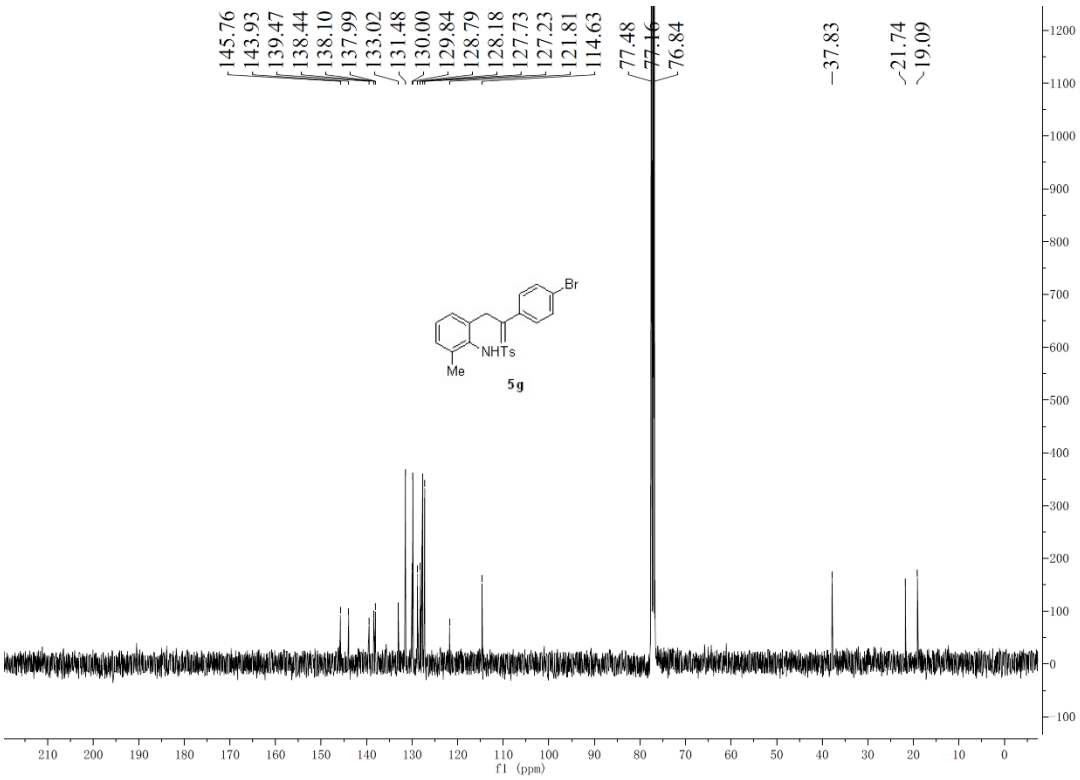

Figure S52. ^{13}C NMR spectra (400 MHz) of **5g** in $CDCl_3$, related to **Scheme 1**.

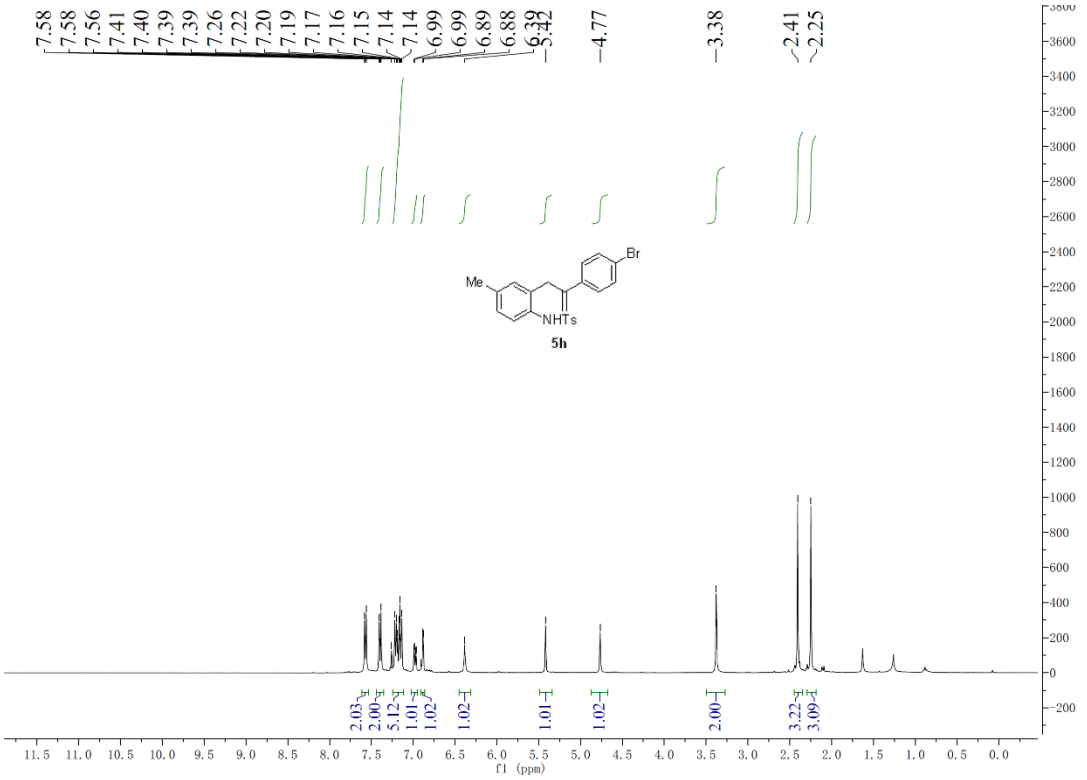

Figure S53. ^{1}H NMR spectra (400 MHz) of **5h** in $CDCl_3$, related to **Scheme 1**.

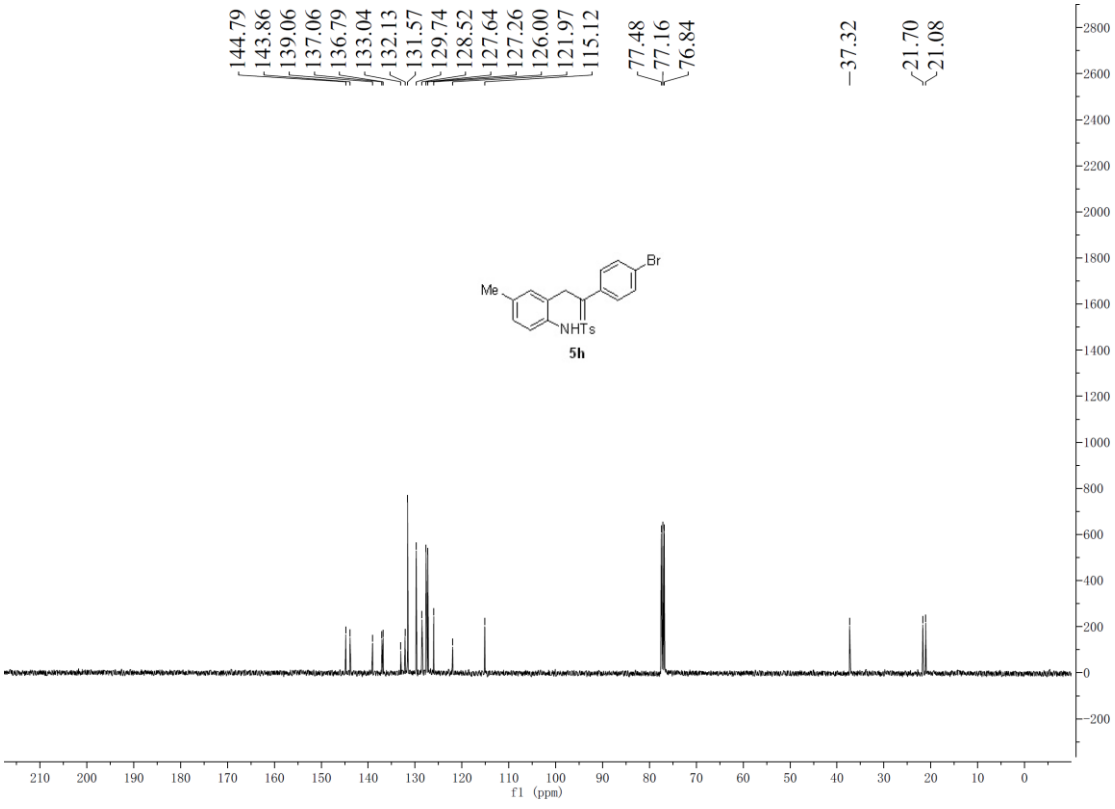

Figure S54. ^{13}C NMR spectra (400 MHz) of **5h** in $CDCl_3$, related to **Scheme 1**.

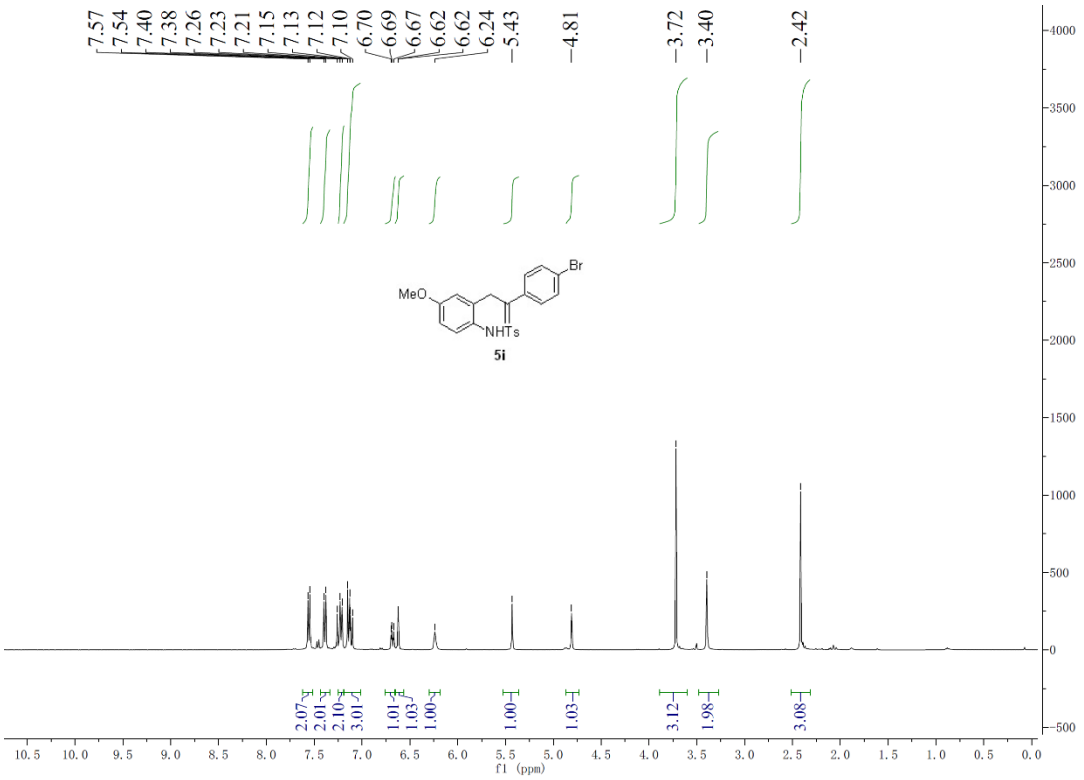

Figure S55. ^{1}H NMR spectra (400 MHz) of **5i** in $CDCl_3$, related to **Scheme 1**.

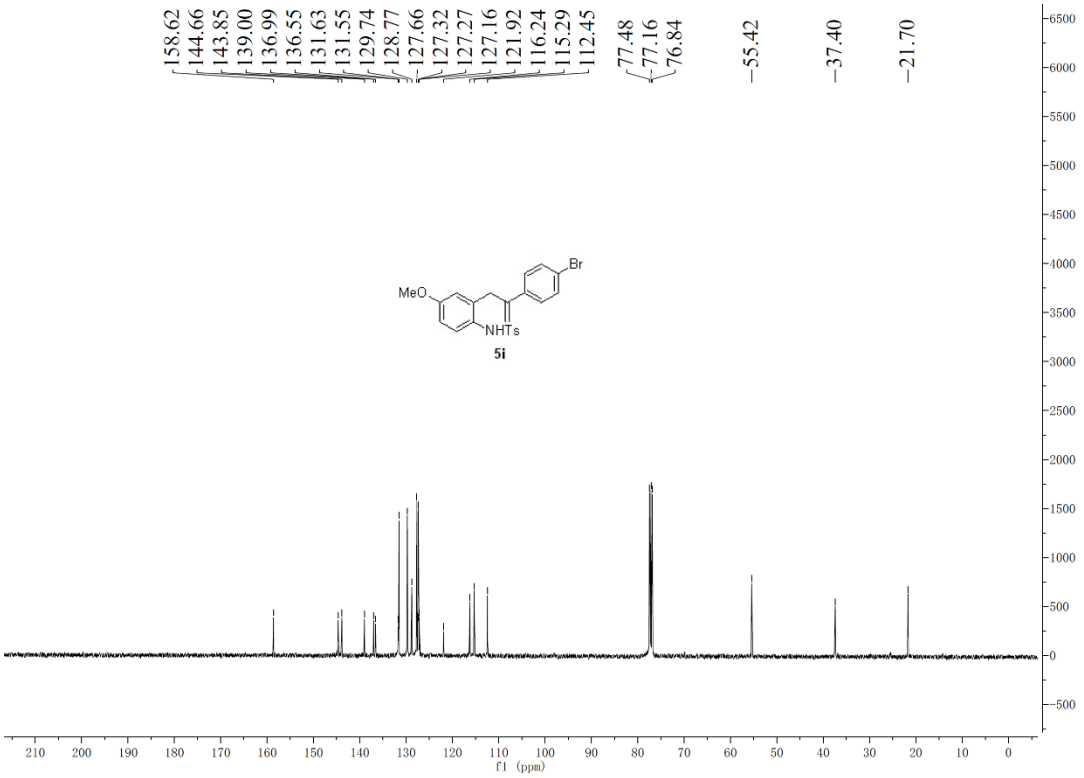

Figure S56. ^{13}C NMR spectra (400 MHz) of **5i** in $CDCl_3$, related to **Scheme 1**.

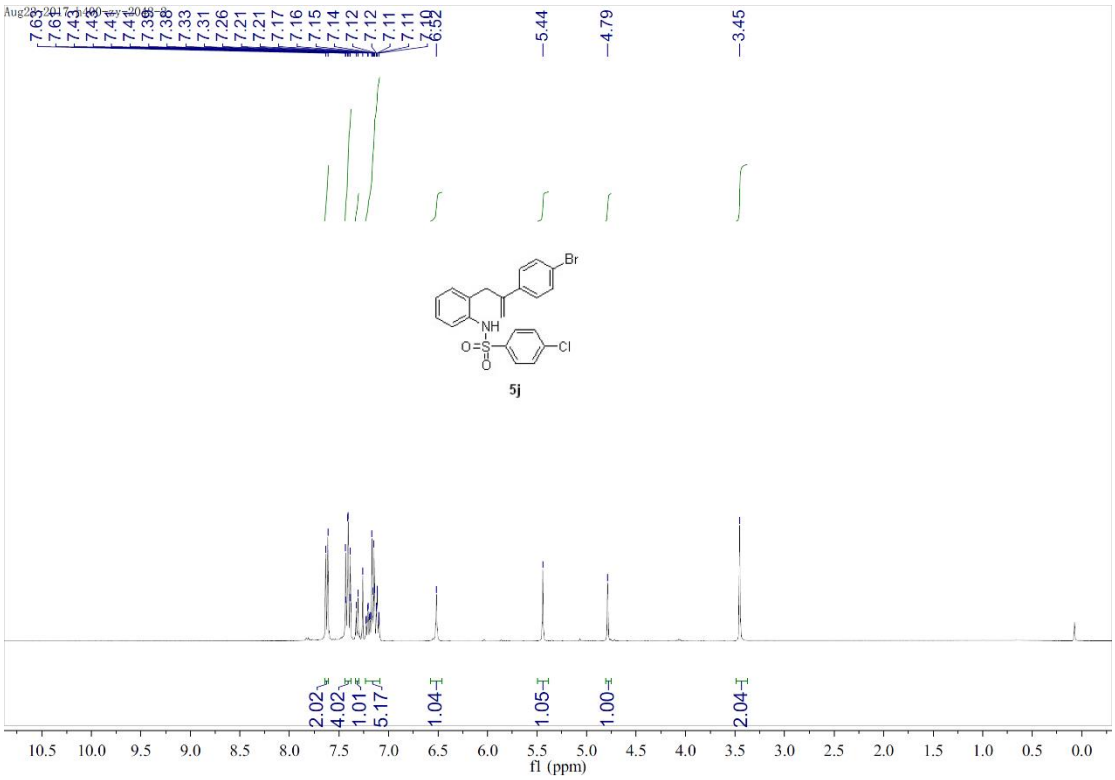

Figure S57. ^{1}H NMR spectra (400 MHz) of **5j** in $CDCl_3$, related to **Scheme 1**.

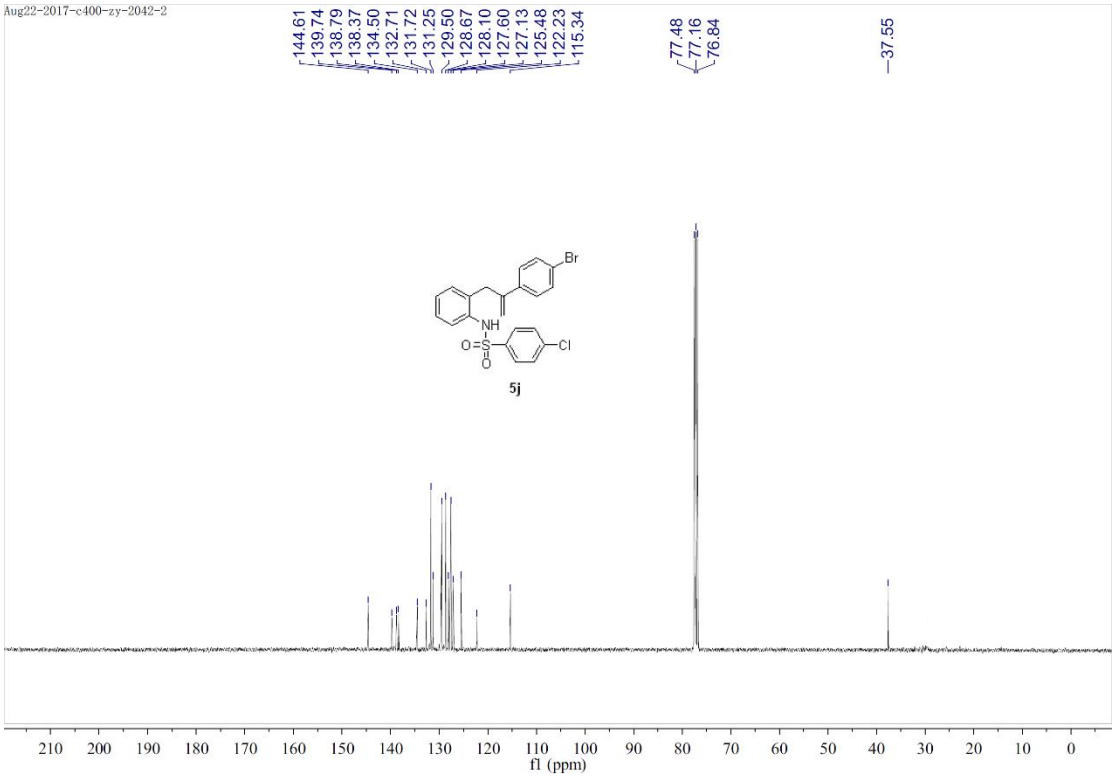

Figure S58. ^{13}C NMR spectra (400 MHz) of **5j** in $CDCl_3$, related to **Scheme 1**.

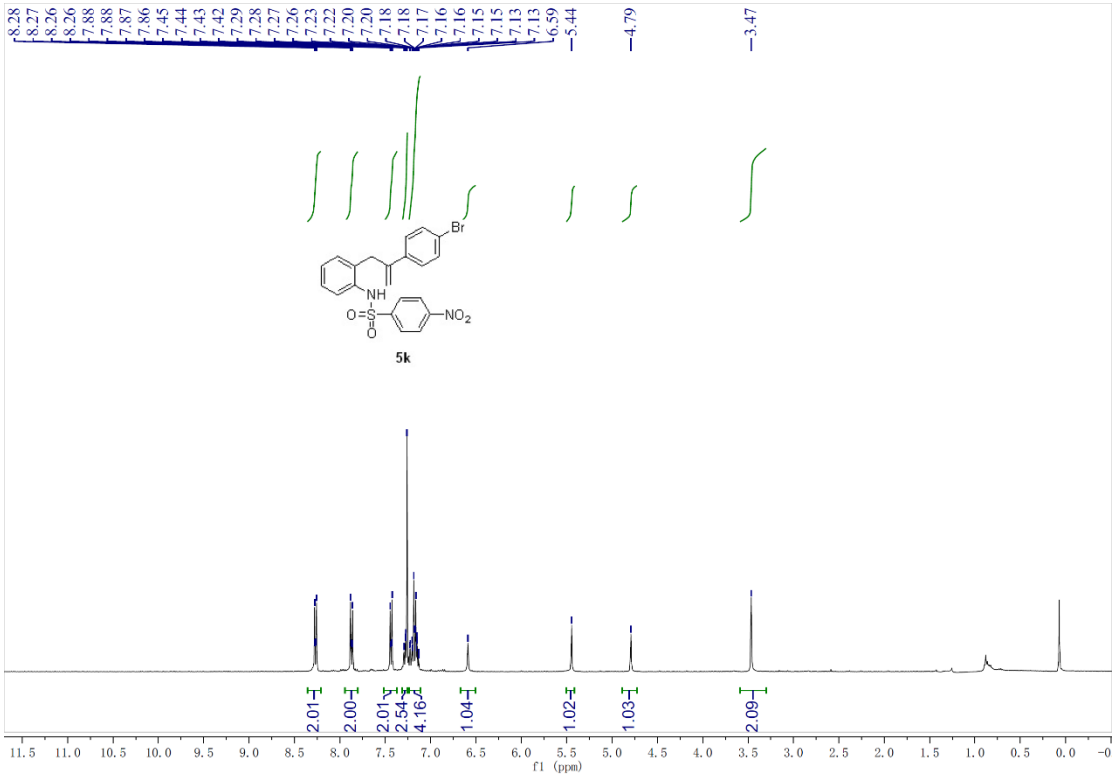

Figure S59. ^{1}H NMR spectra (400 MHz) of **5k** in $CDCl_3$, related to **Scheme 1**.

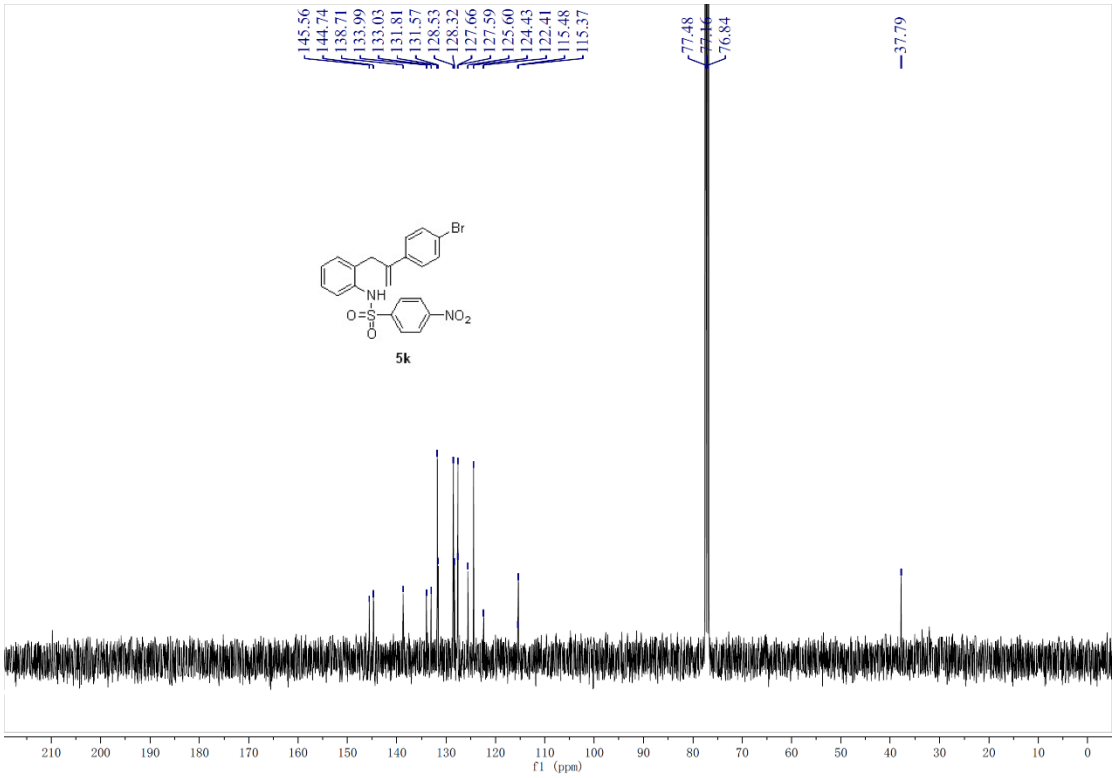

Figure S60. ^{13}C NMR spectra (400 MHz) of **5k** in $CDCl_3$, related to **Scheme 1**.

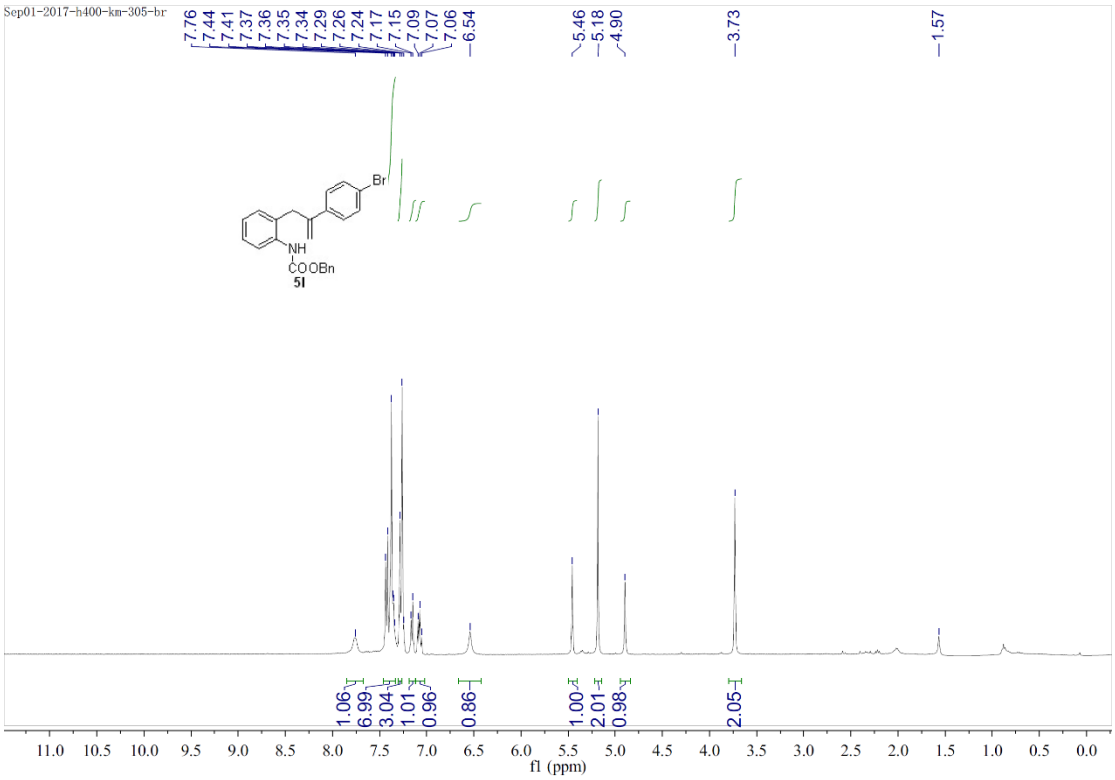

Figure S61. ^{1}H NMR spectra (400 MHz) of **5l** in $CDCl_3$, related to **Scheme 1**.

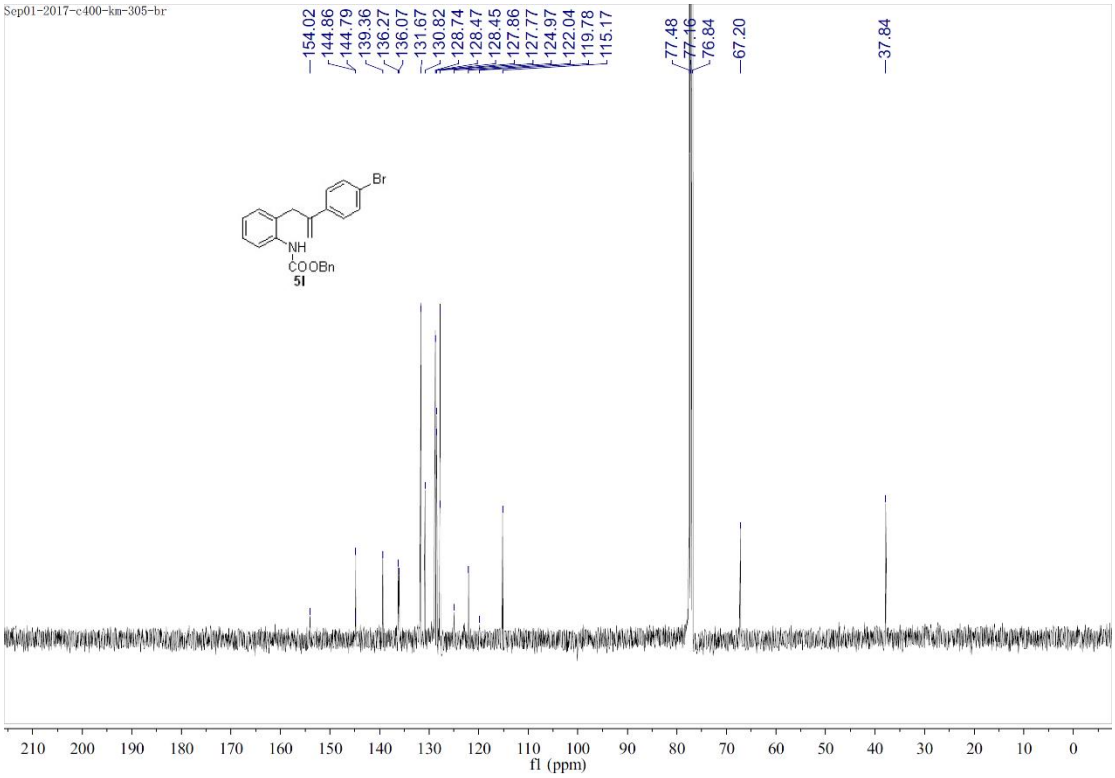

Figure S62. ^{13}C NMR spectra (400 MHz) of **5l** in $CDCl_3$, related to **Scheme 1**.

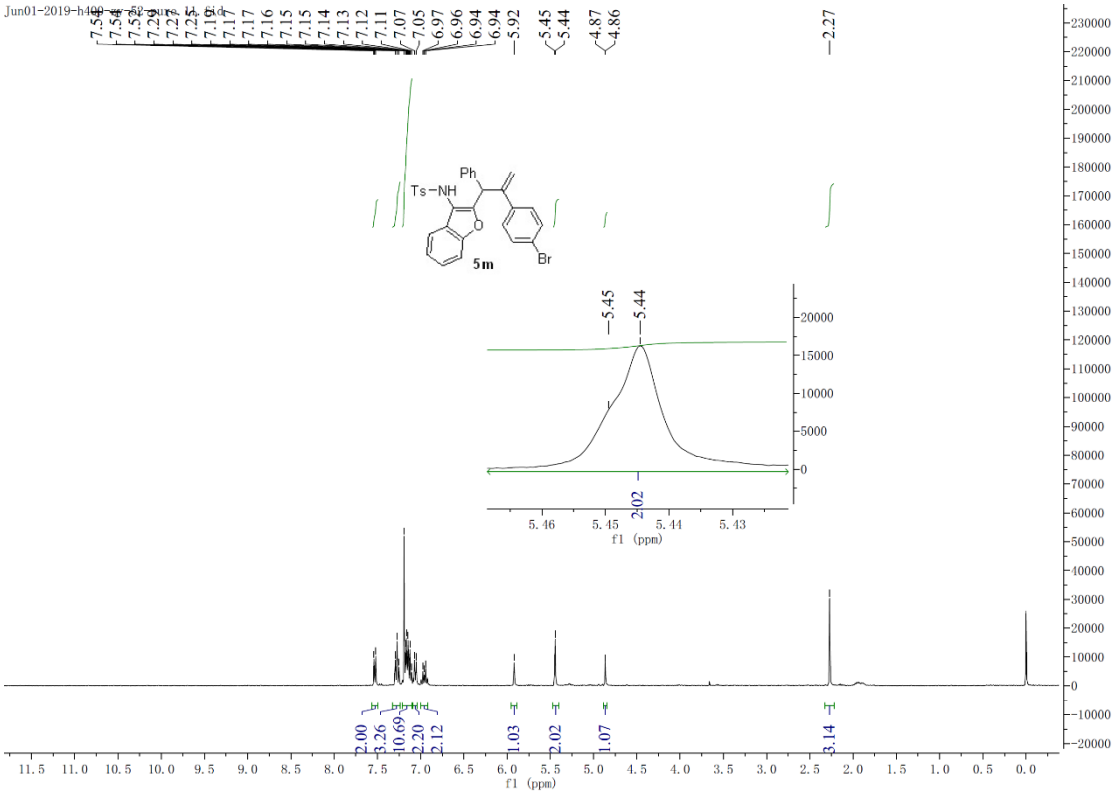

Figure S63. ^{1}H NMR spectra (400 MHz) of **5m** in $CDCl_3$, related to **Scheme 1**.

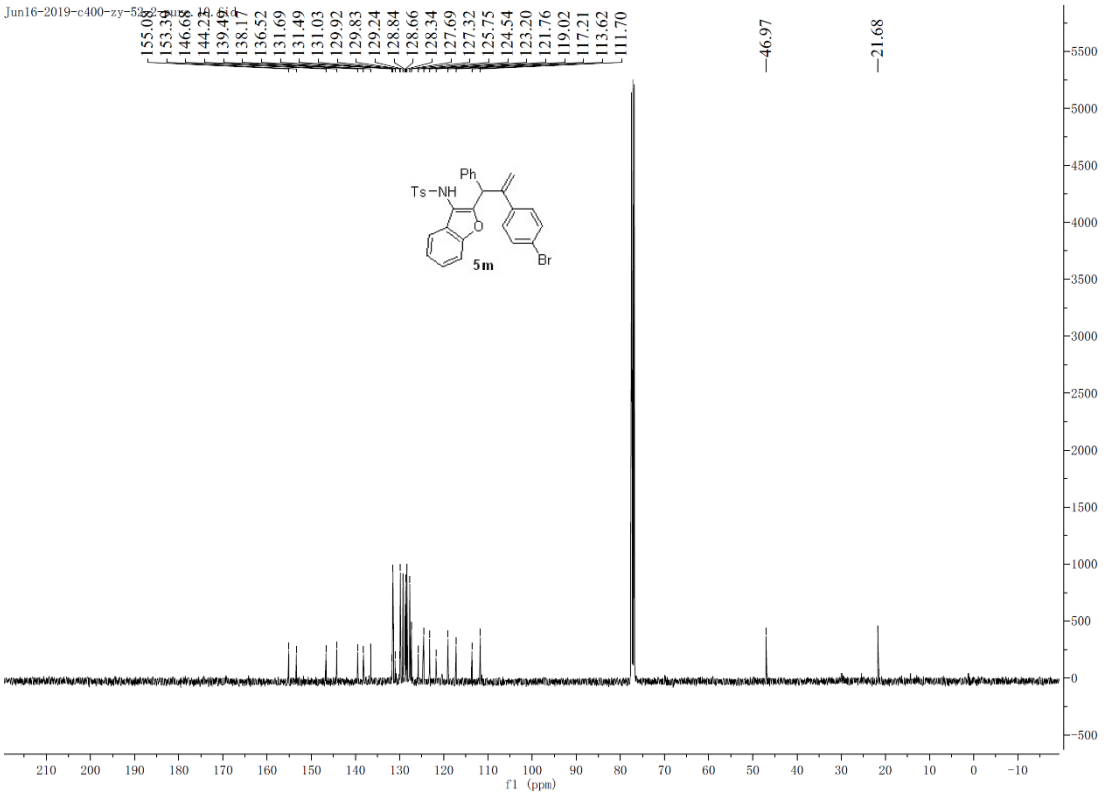

Figure S64. ^{13}C NMR spectra (400 MHz) of **5m** in $CDCl_3$, related to **Scheme 1**.

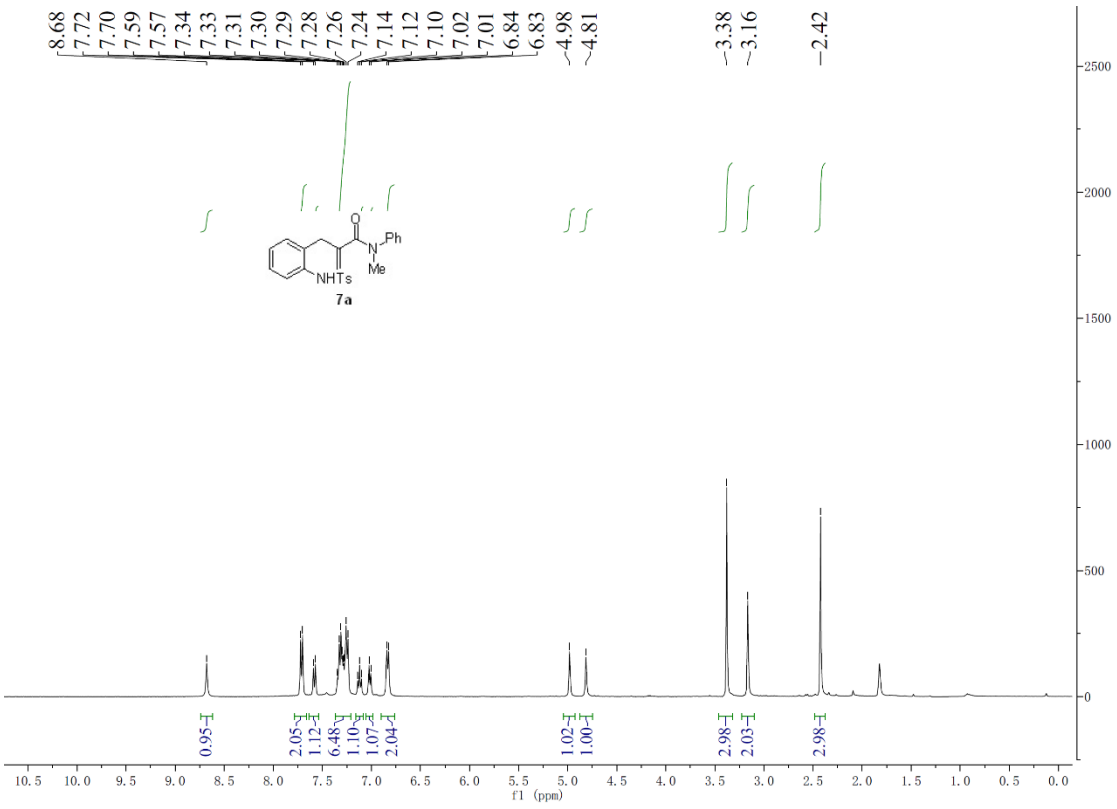

Figure S65. ^{1}H NMR spectra (400 MHz) of **7a** in $CDCl_3$, related to **Scheme 2**.

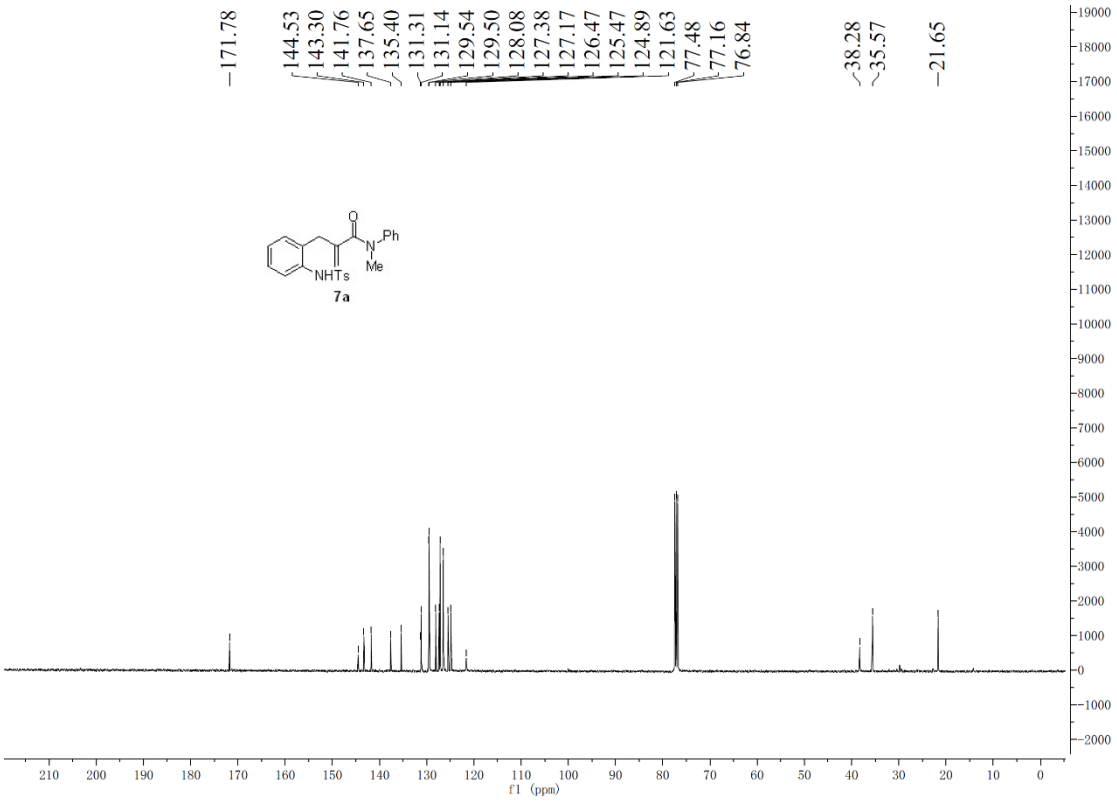

Figure S66. ^{13}C NMR spectra (400 MHz) of **7a** in $CDCl_3$, related to **Scheme 2**.

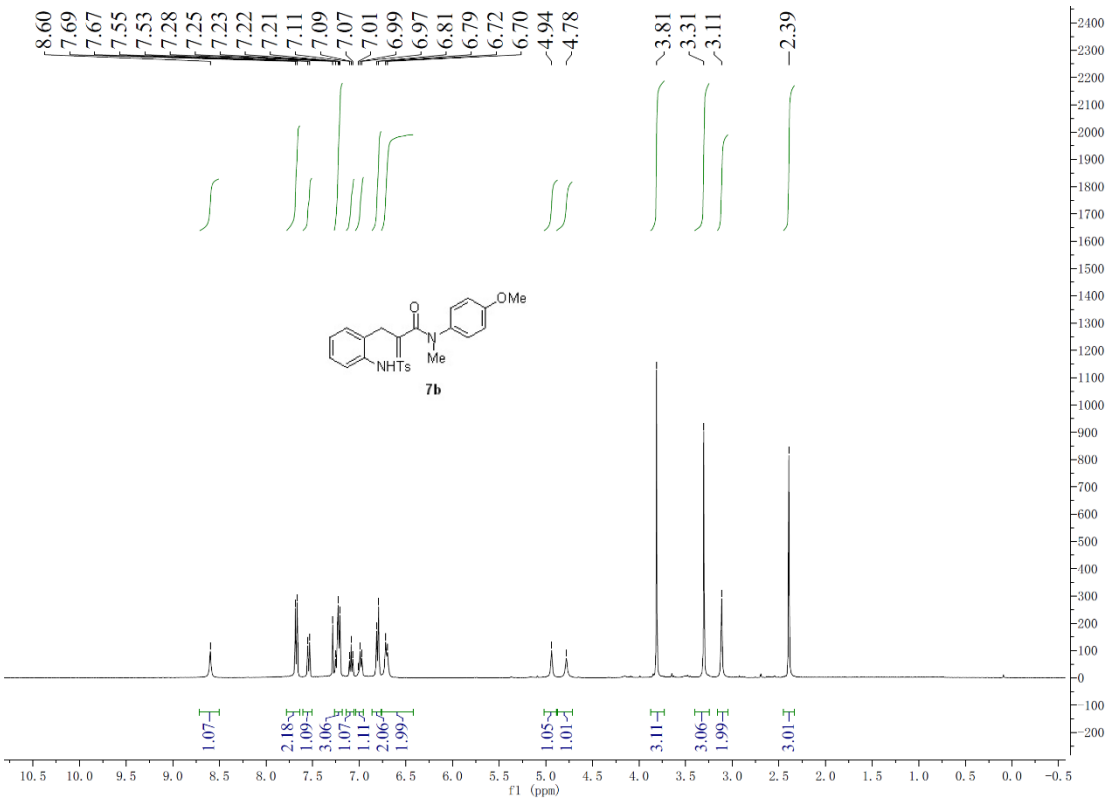

Figure S67. ^{1}H NMR spectra (400 MHz) of **7b** in $CDCl_3$, related to **Scheme 2**.

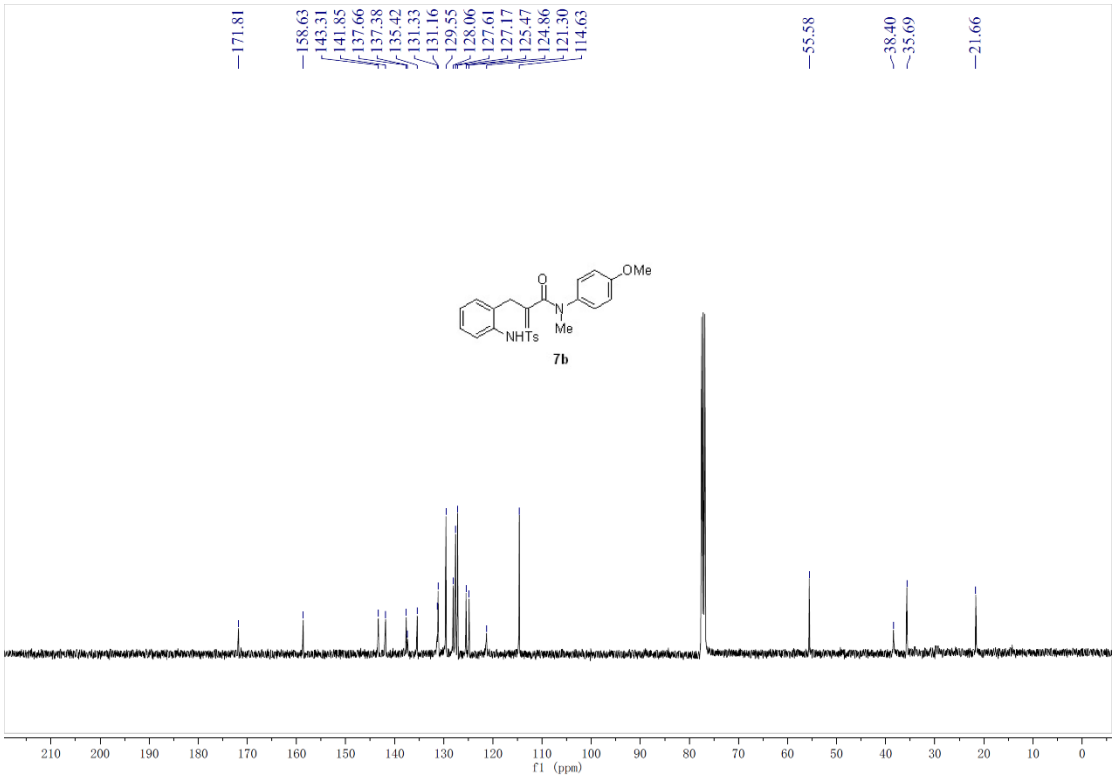

Figure S68. ^{13}C NMR spectra (400 MHz) of **7b** in $CDCl_3$, related to **Scheme 2**.

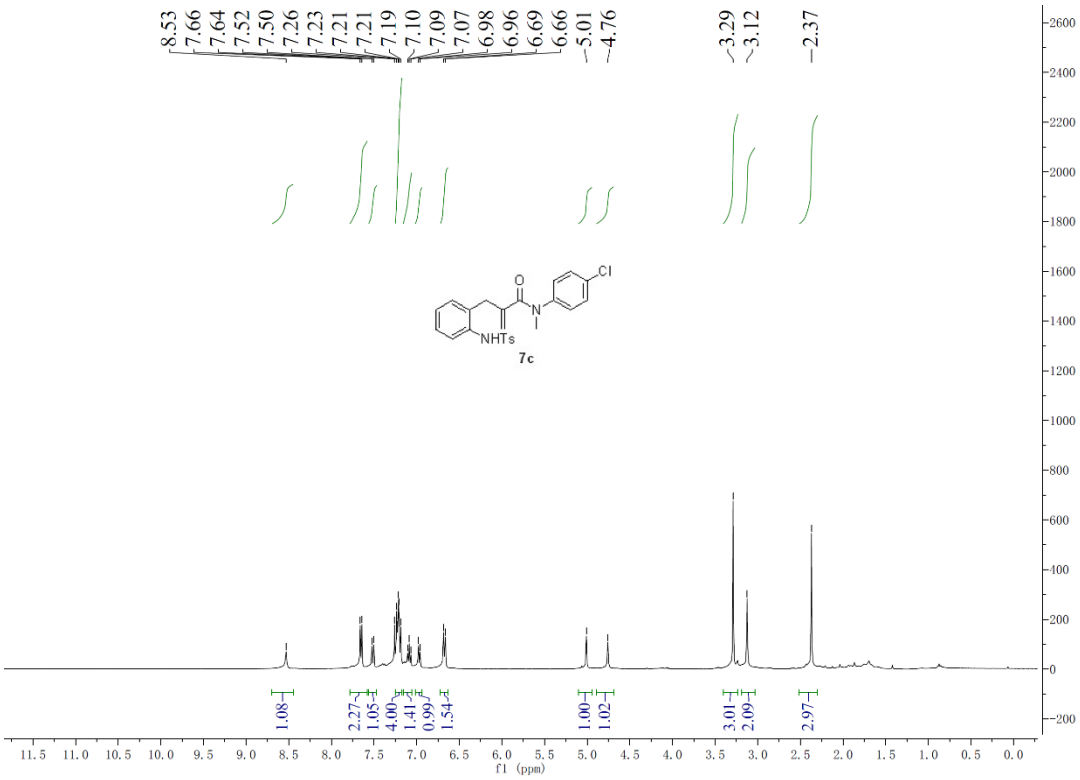

Figure S69. ^{1}H NMR spectra (400 MHz) of **7c** in $CDCl_3$, related to **Scheme 2**.

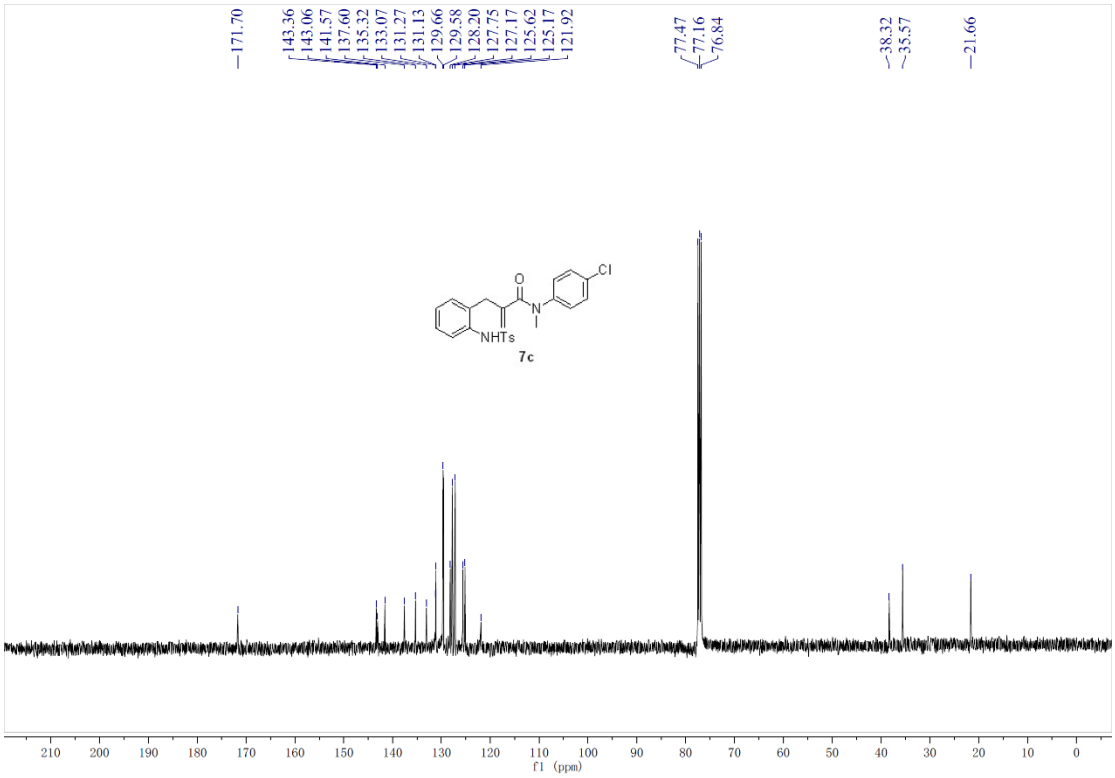

Figure S70. ^{13}C NMR spectra (400 MHz) of **7c** in $CDCl_3$, related to **Scheme 2**.

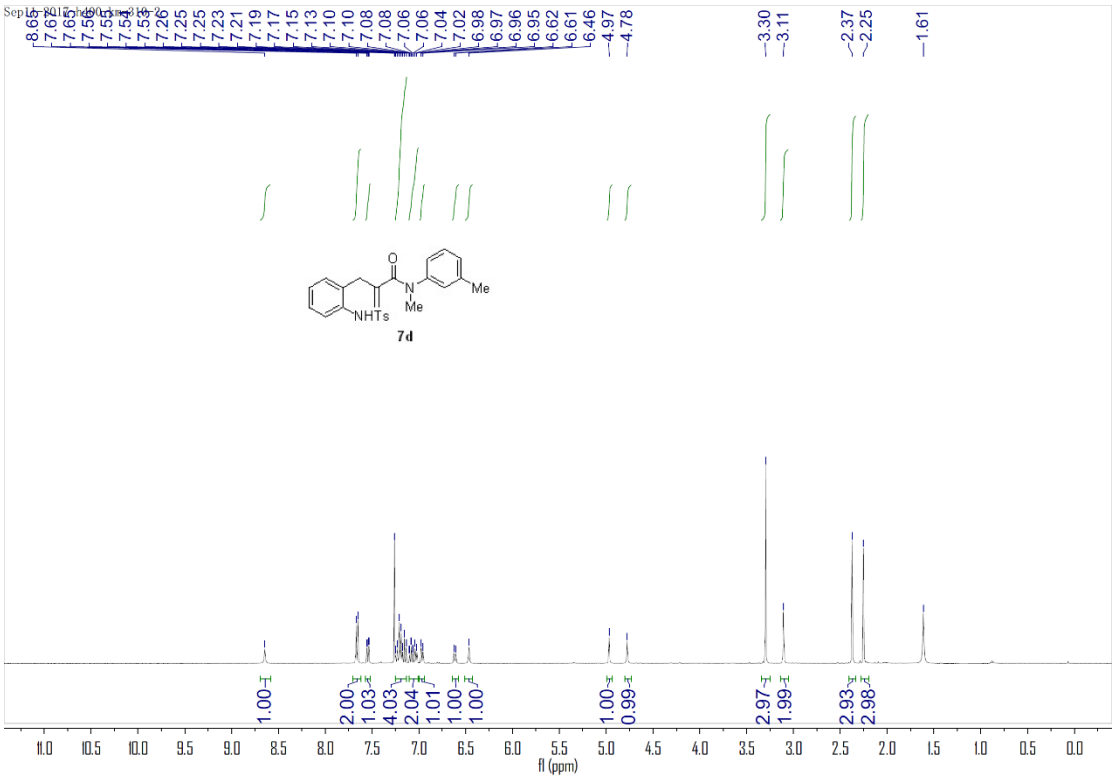

Figure S71. ^{1}H NMR spectra (400 MHz) of **7d** in $CDCl_3$, related to **Scheme 2**.

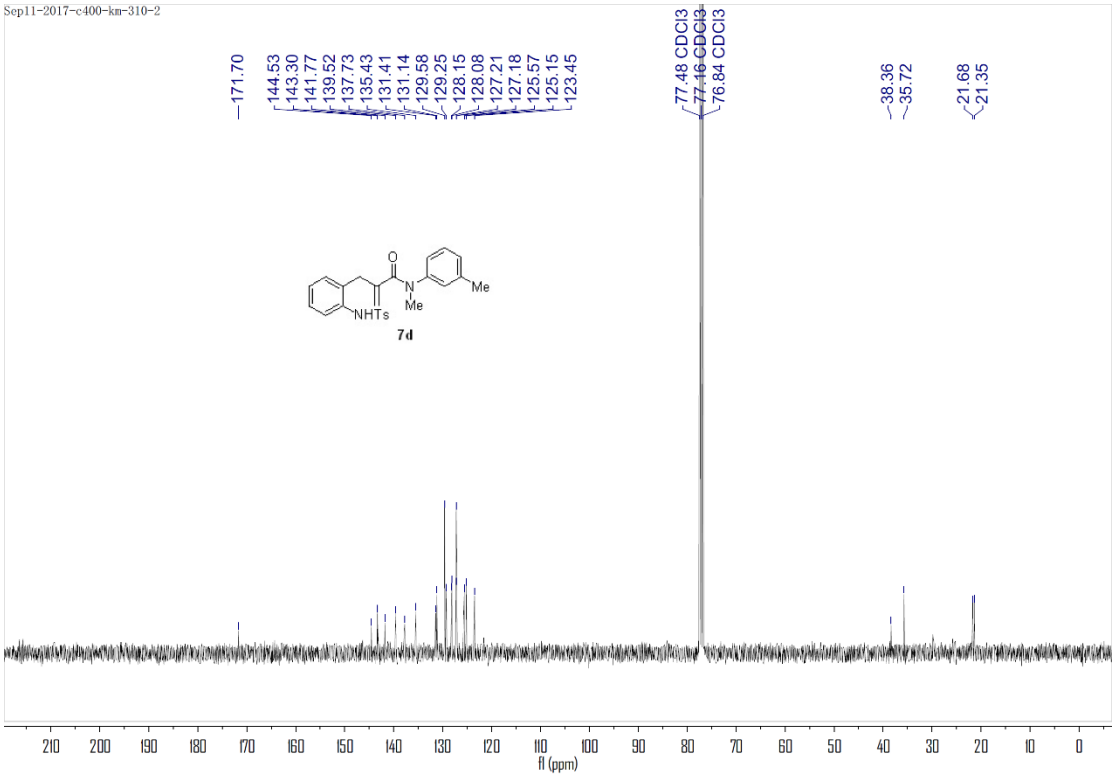

Figure S72. ^{13}C NMR spectra (400 MHz) of **7d** in $CDCl_3$, related to **Scheme 2**.

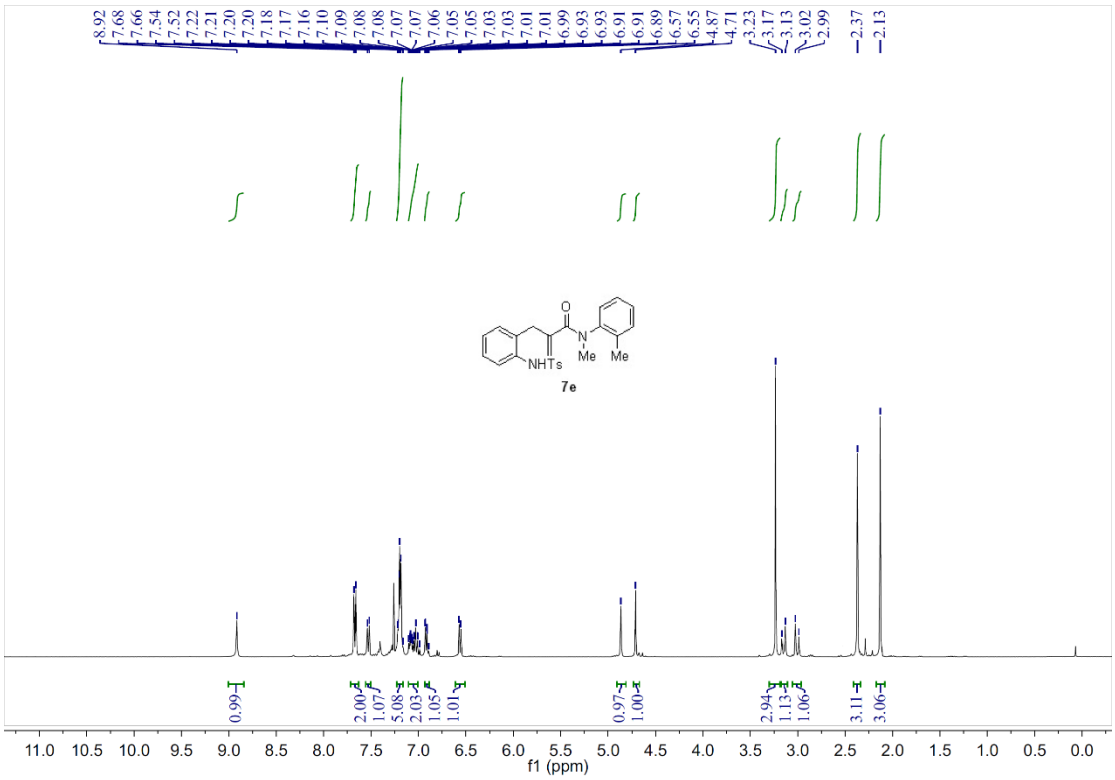

Figure S73. ^{1}H NMR spectra (400 MHz) of **7e** in $CDCl_3$, related to **Scheme 2**.

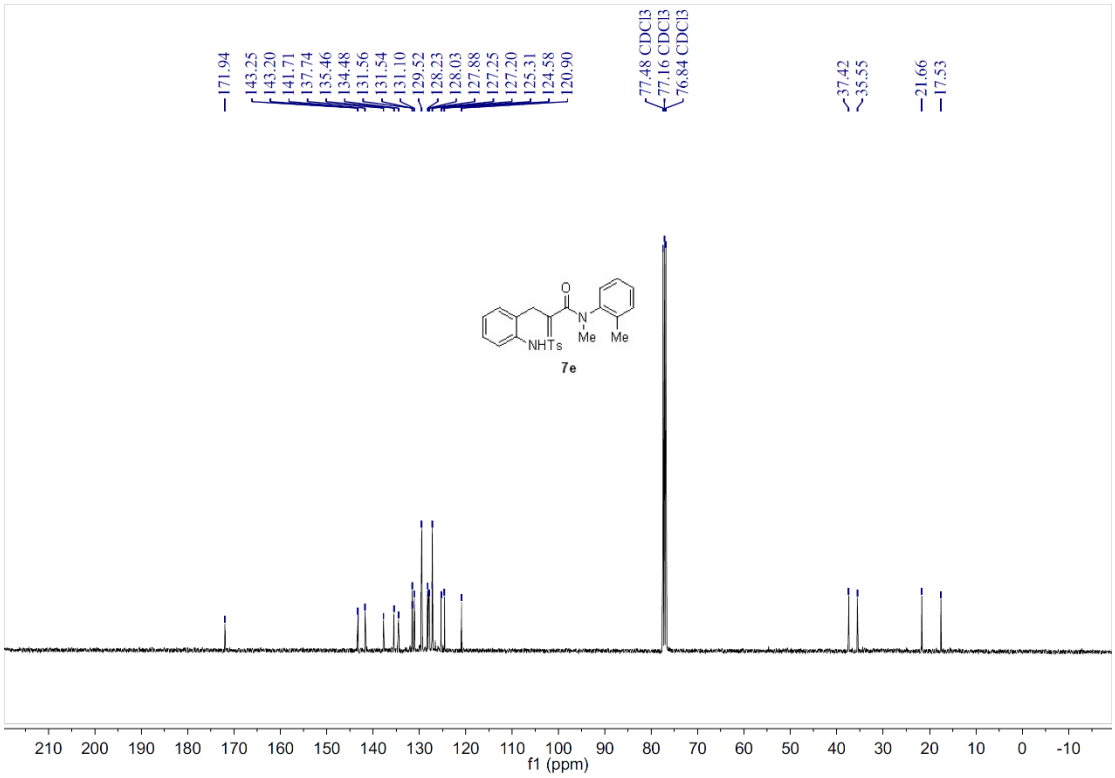

Figure S74. ^{13}C NMR spectra (400 MHz) of **7e** in $CDCl_3$, related to **Scheme 2**.

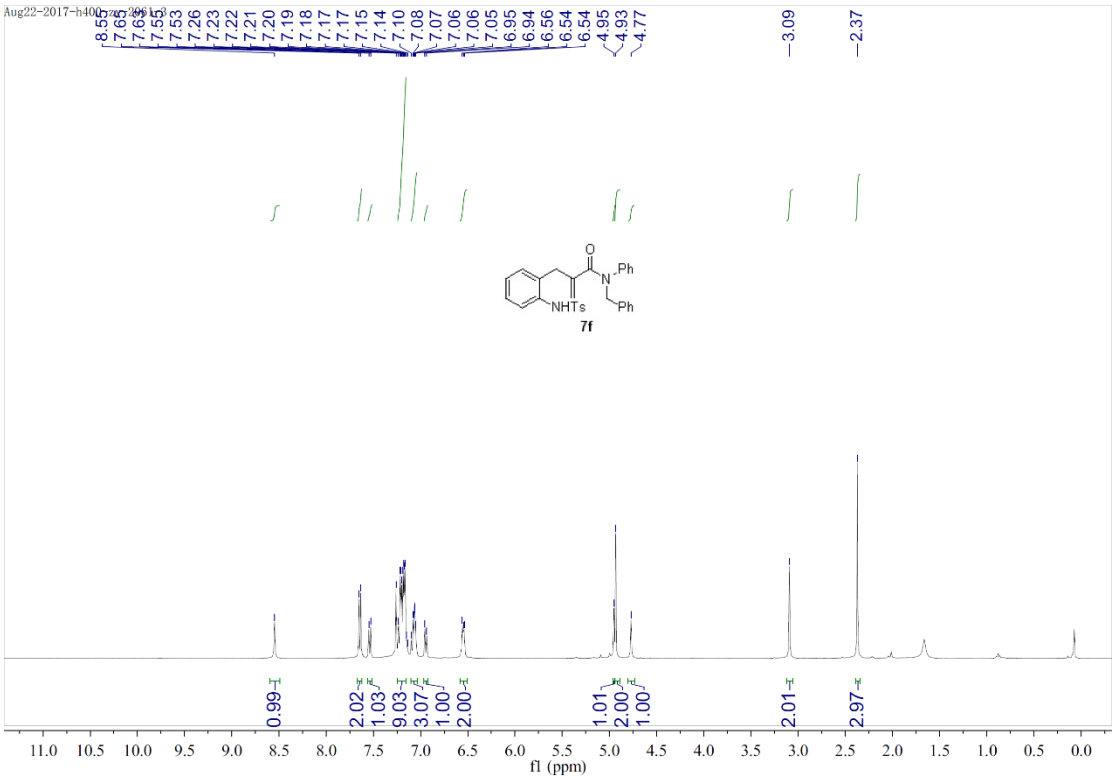

Figure S75. ^{1}H NMR spectra (400 MHz) of **7f** in $CDCl_3$, related to **Scheme 2**.

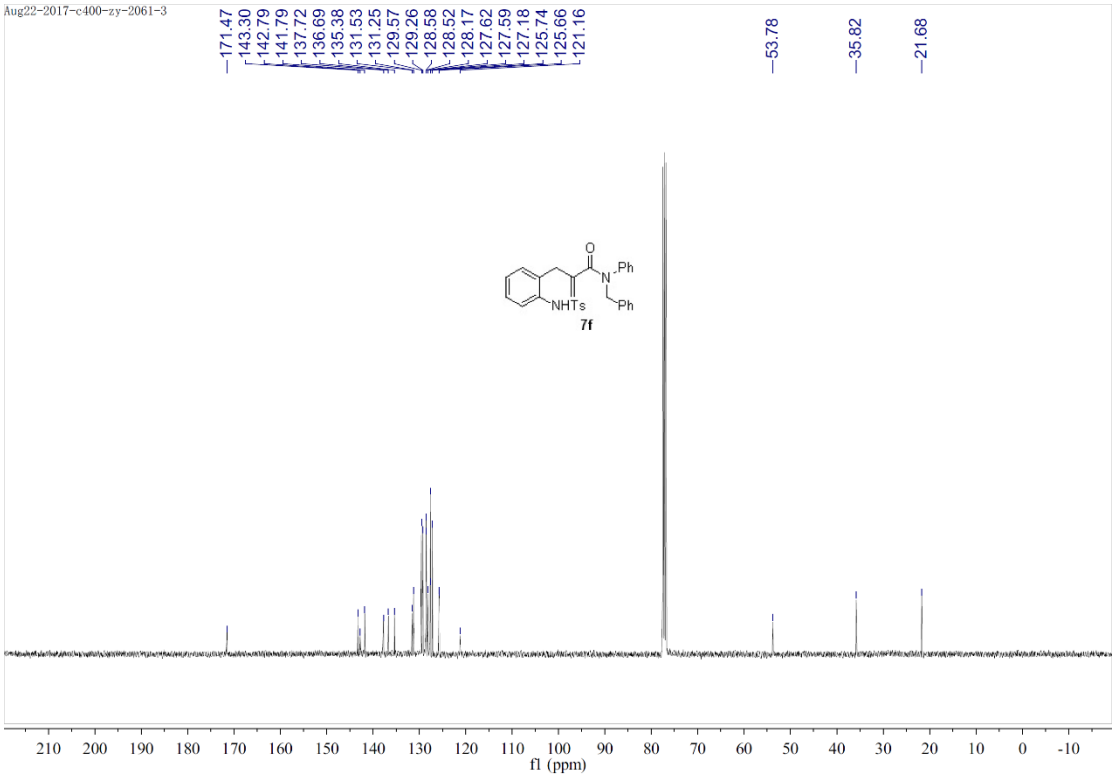

Figure S76. ^{13}C NMR spectra (400 MHz) of **7f** in $CDCl_3$, related to **Scheme 2**.

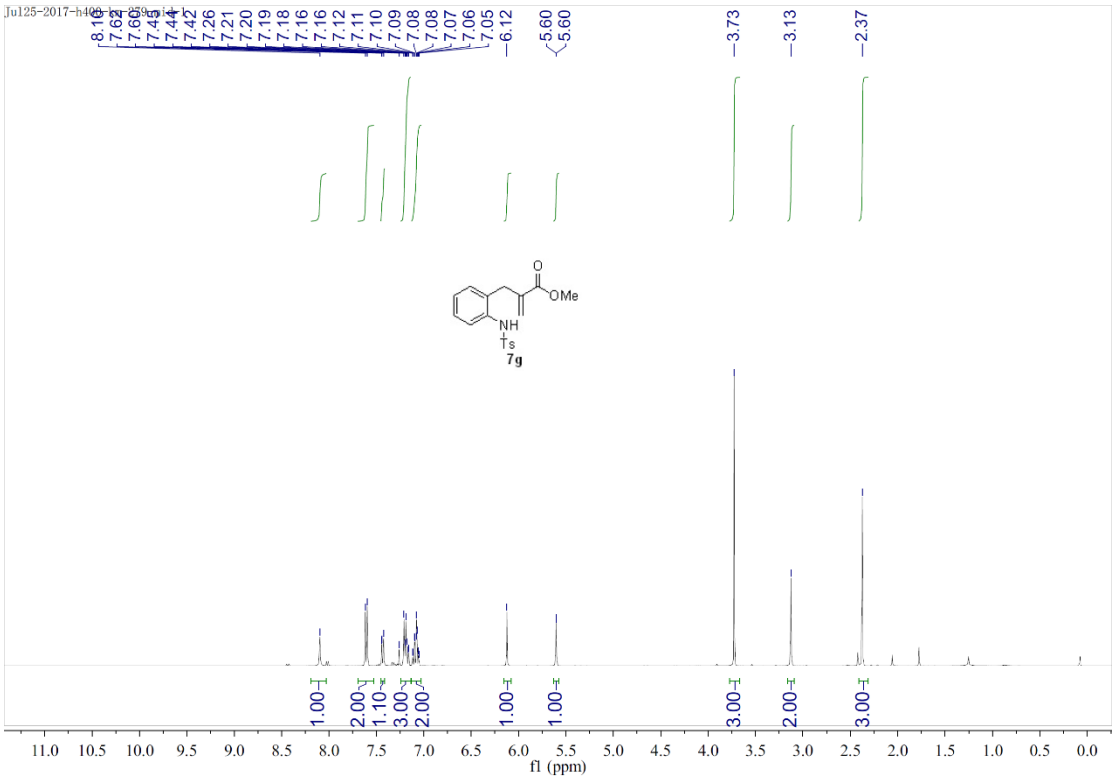

Figure S77. ^{1}H NMR spectra (400 MHz) of **7g** in $CDCl_3$, related to **Scheme 2**.

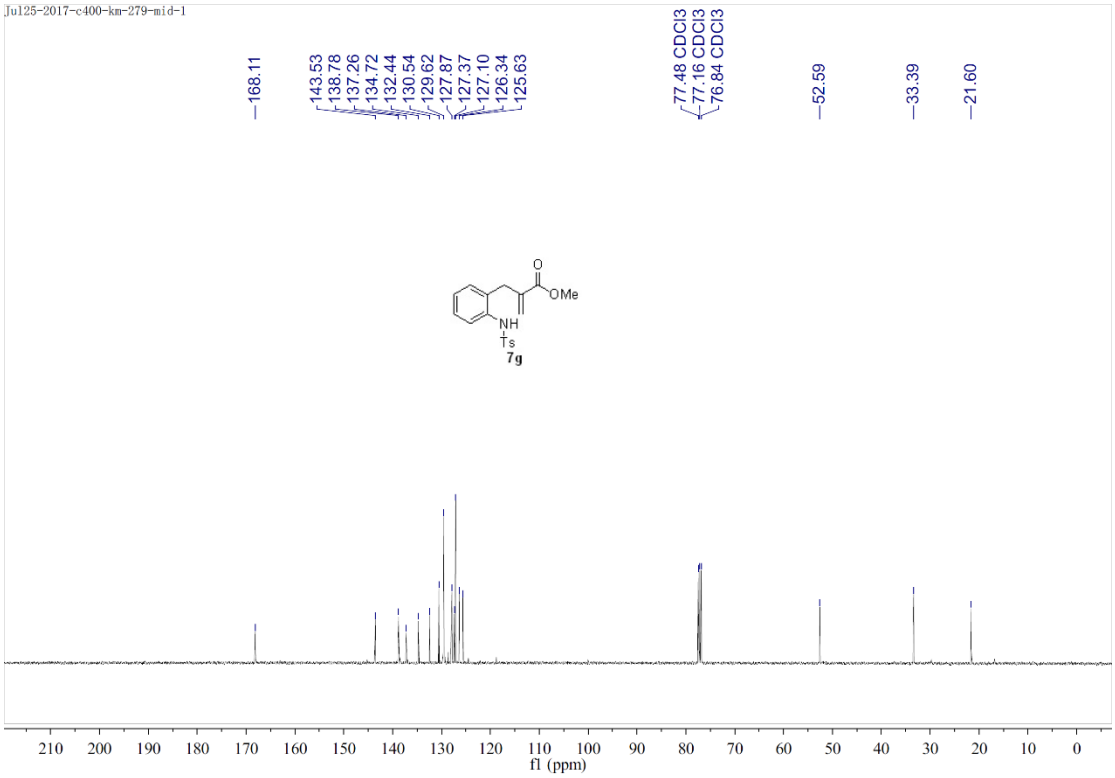

Figure S78. ^{13}C NMR spectra (400 MHz) of **7g** in $CDCl_3$, related to **Scheme 2**.

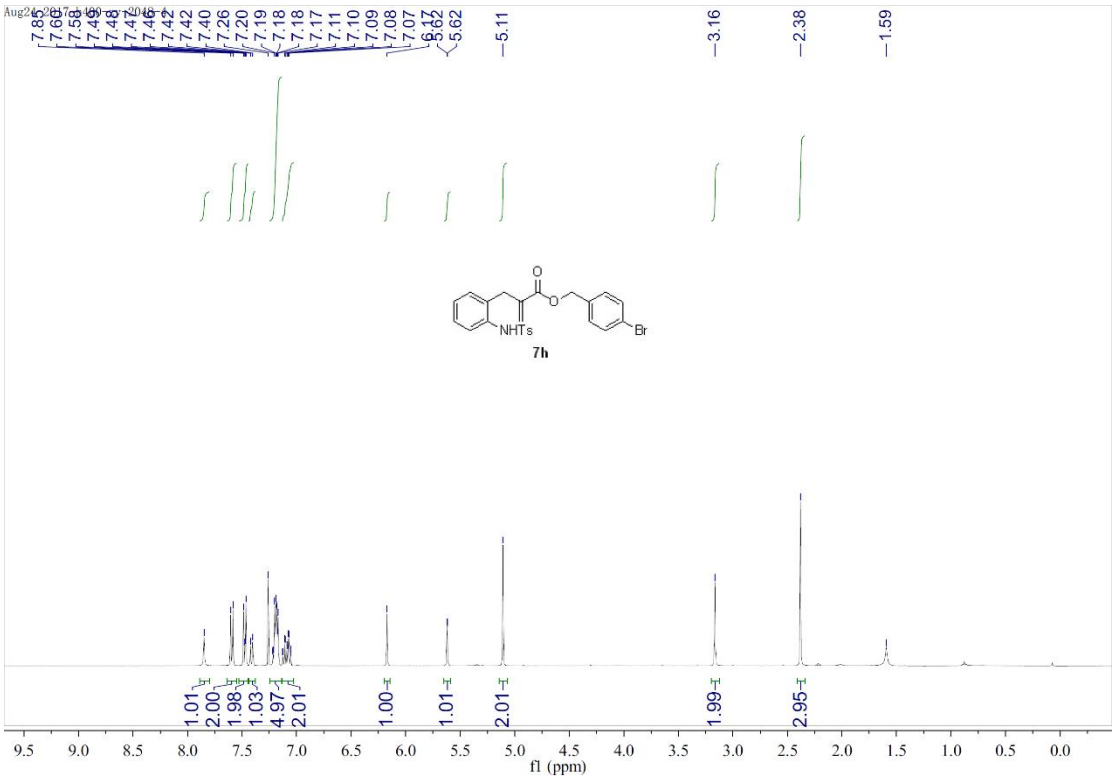

Figure S79. ^{1}H NMR spectra (400 MHz) of **7h** in $CDCl_3$, related to **Scheme 2**.

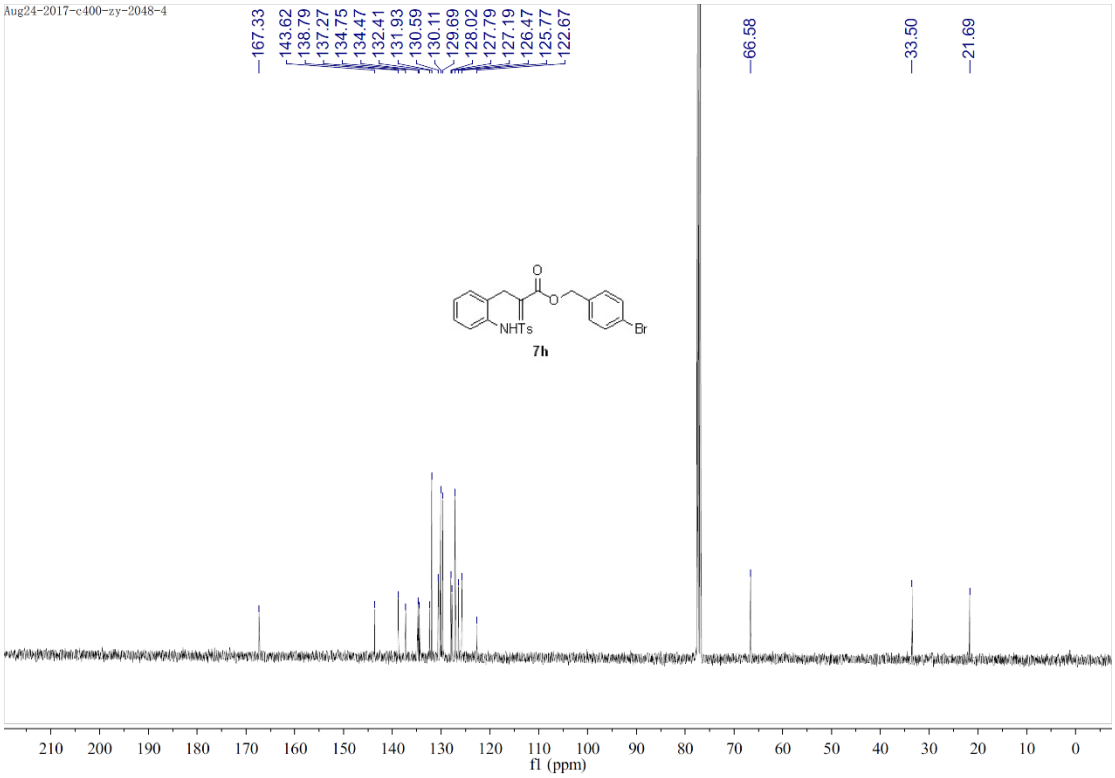

Figure S80. ^{13}C NMR spectra (400 MHz) of **7h** in $CDCl_3$, related to **Scheme 2**.

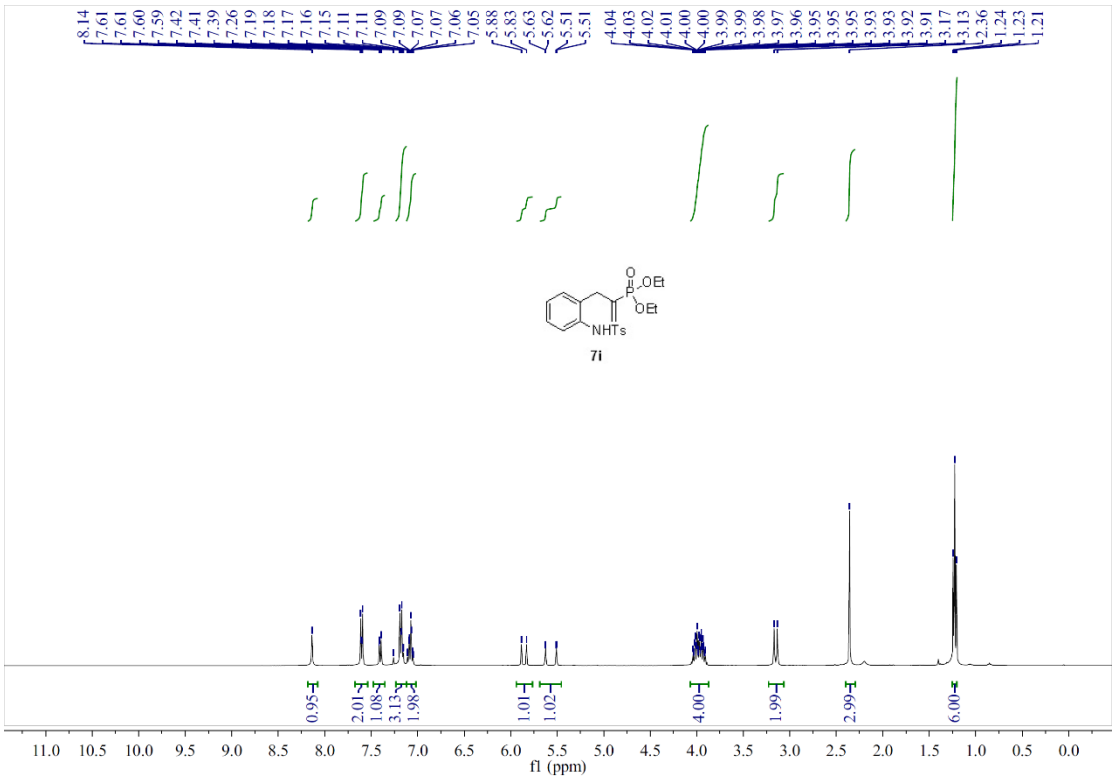

Figure S81. ^{1}H NMR spectra (400 MHz) of **7i** in $CDCl_3$, related to **Scheme 2**.

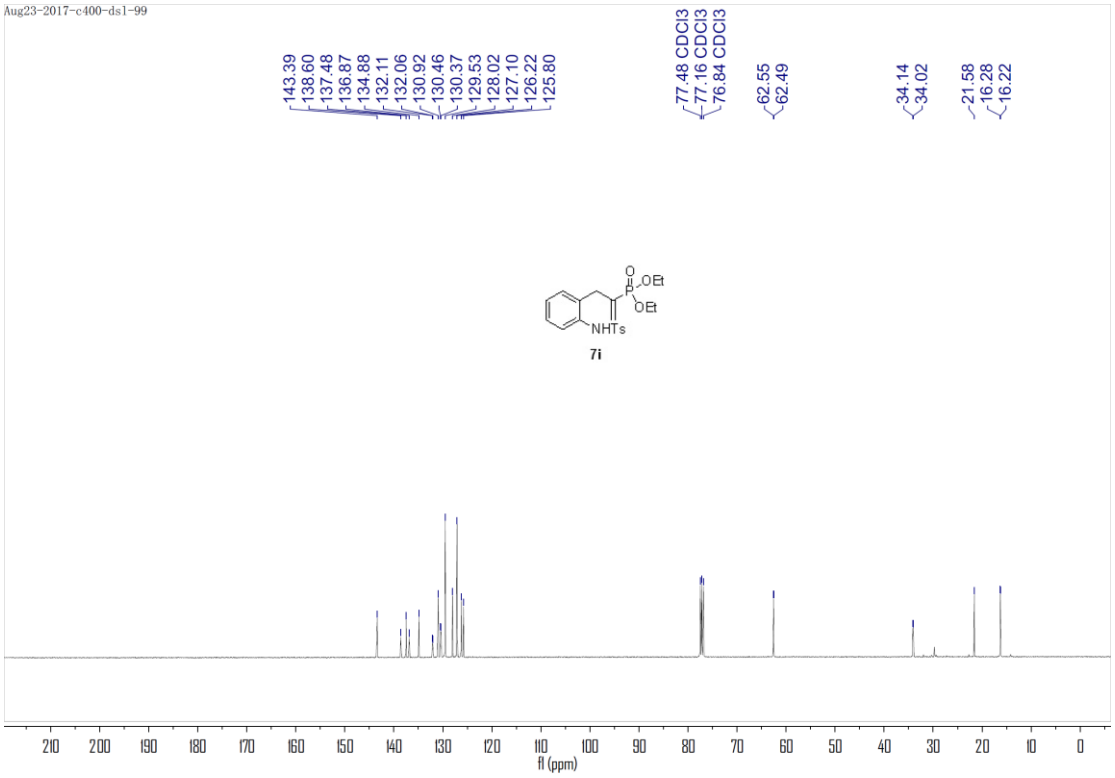

Figure S82. ^{13}C NMR spectra (400 MHz) of **7i** in $CDCl_3$, related to **Scheme 2**.

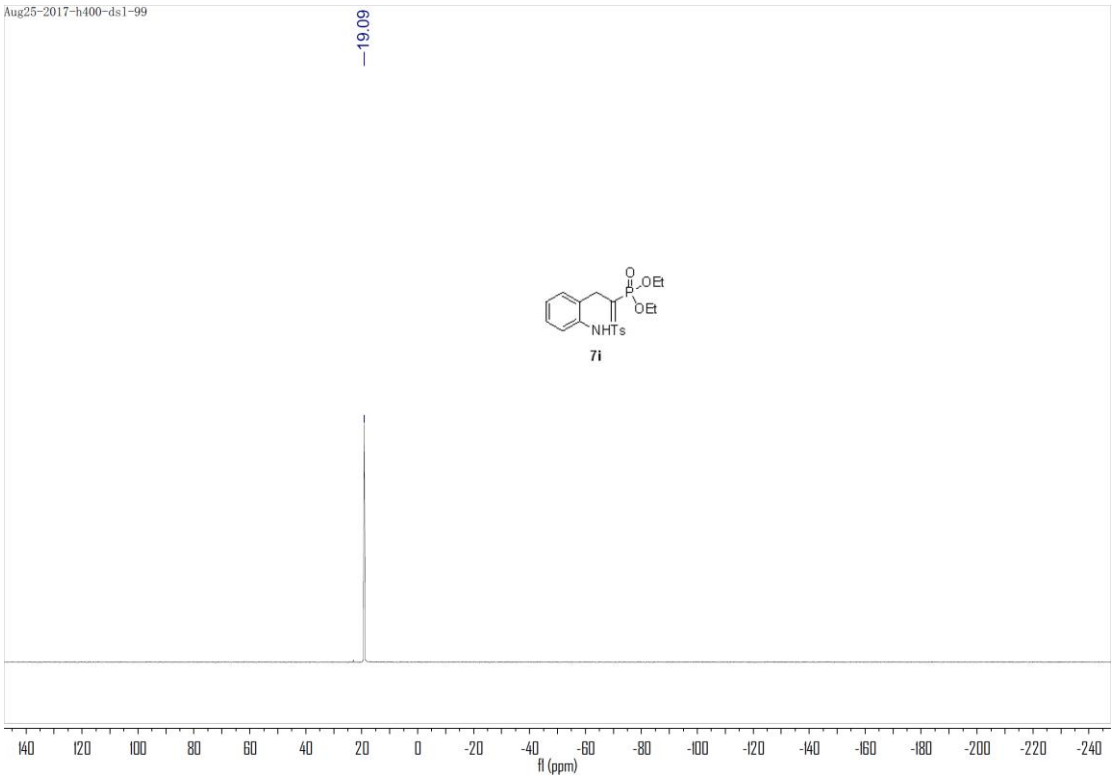

Figure S83. ^{31}P NMR spectra (400 MHz) of **7i** in $CDCl_3$, related to **Scheme 2**.

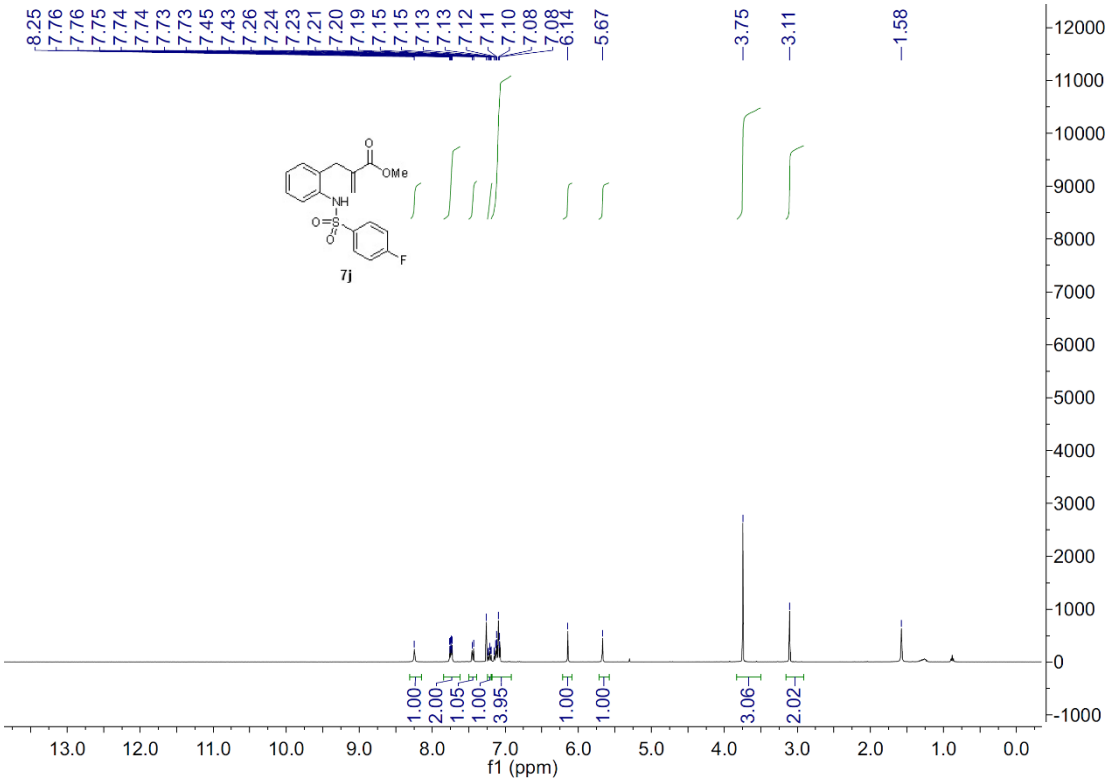

Figure S84. ^{1}H NMR spectra (400 MHz) of **7j** in $CDCl_3$, related to **Scheme 2**.

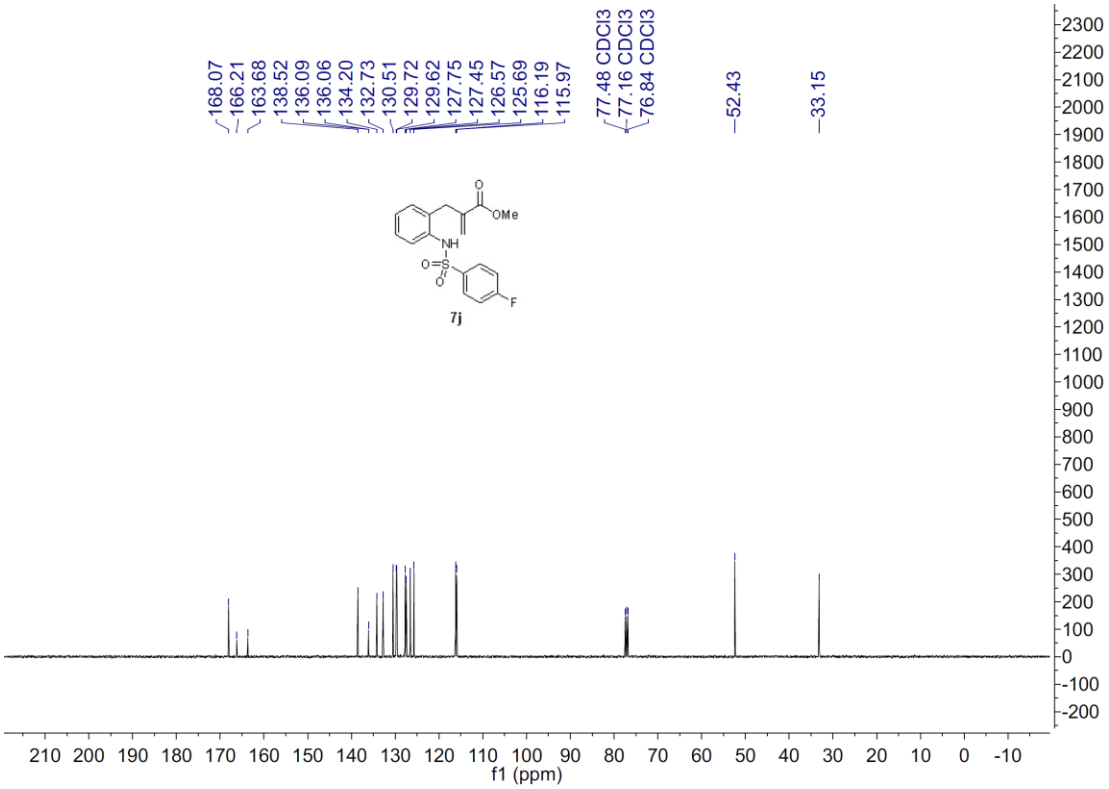

Figure S85. ^{13}C NMR spectra (400 MHz) of **7j** in $CDCl_3$, related to **Scheme 2**.

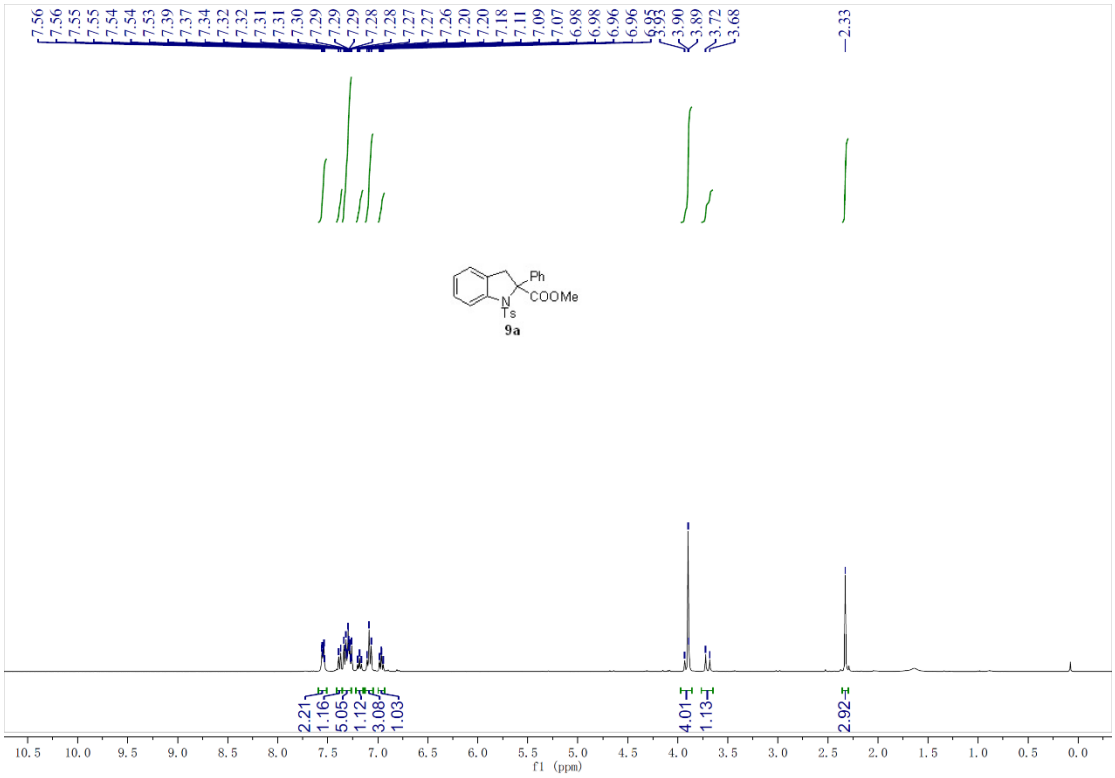

Figure S86. ^{1}H NMR spectra (400 MHz) of **9a** in $CDCl_3$, related to **Figure 2A**.

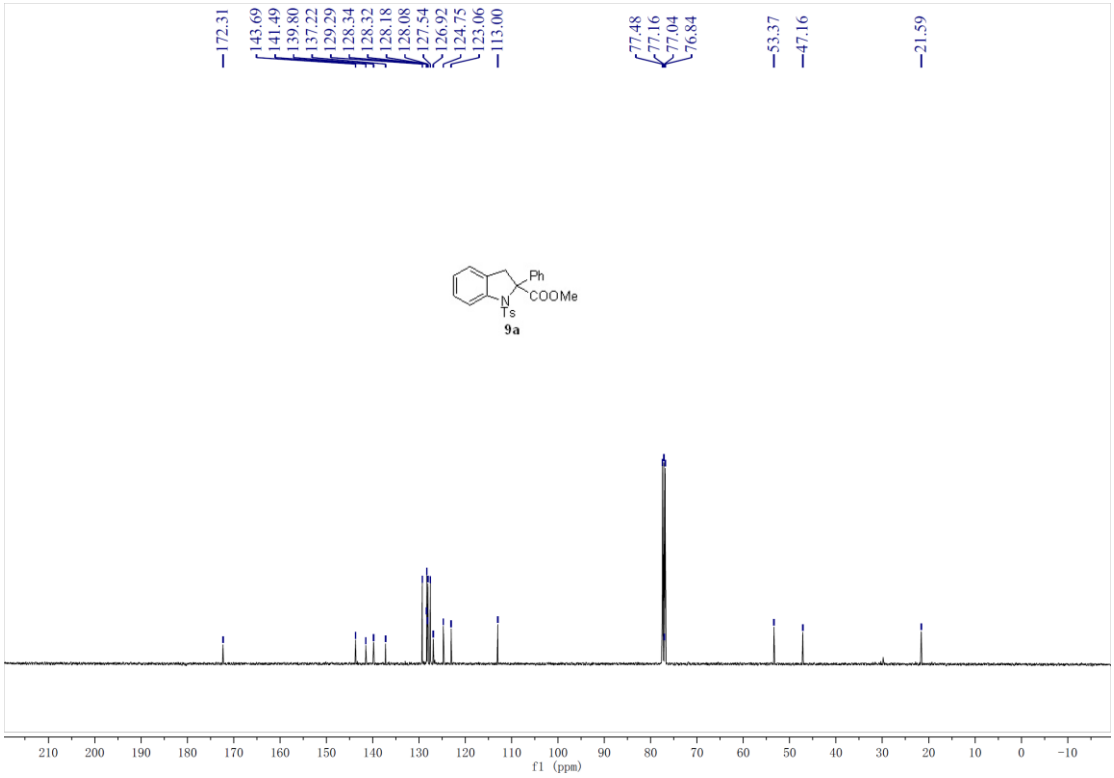

Figure S87. ^{13}C NMR spectra (400 MHz) of **9a** in $CDCl_3$, related to **Figure 2A**.

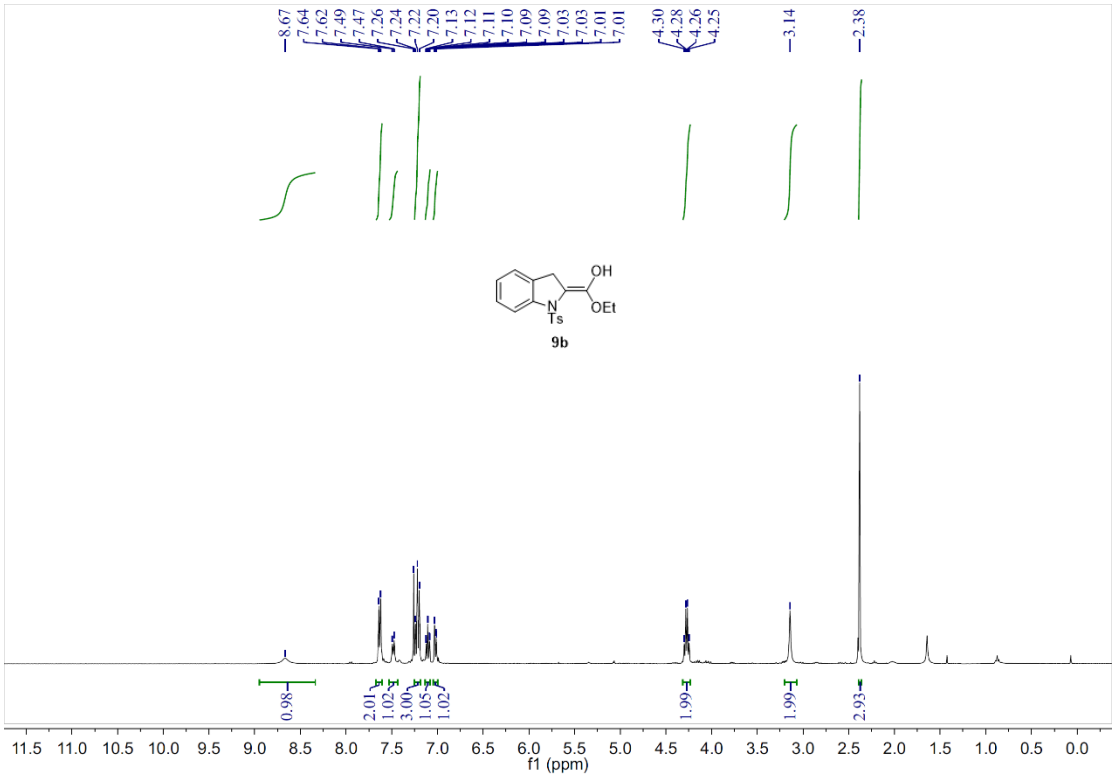

Figure S88. ^{1}H NMR spectra (400 MHz) of **9b** in $CDCl_3$, related to **Figure 2B**.

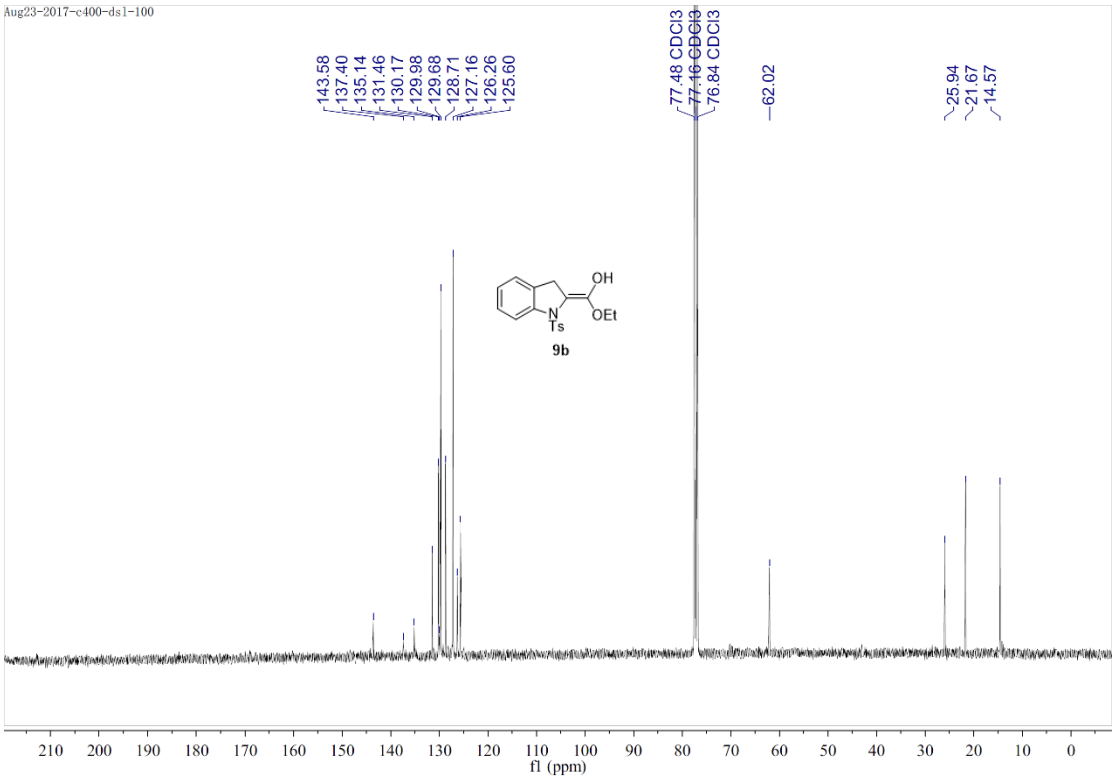

Figure S89. ^{13}C NMR spectra (400 MHz) of **9b** in $CDCl_3$, related to **Figure 2B**.

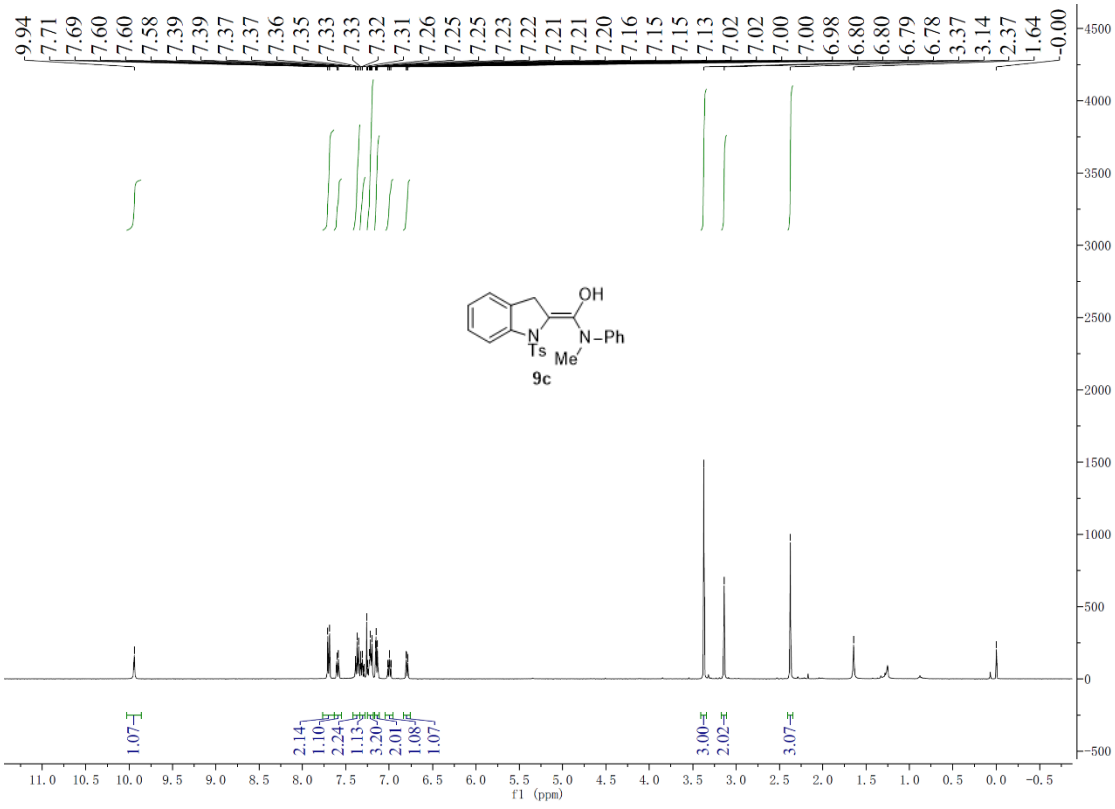

Figure S90. ^{1}H NMR spectra (400 MHz) of **9c** in $CDCl_3$, related to **Figure 2B**.

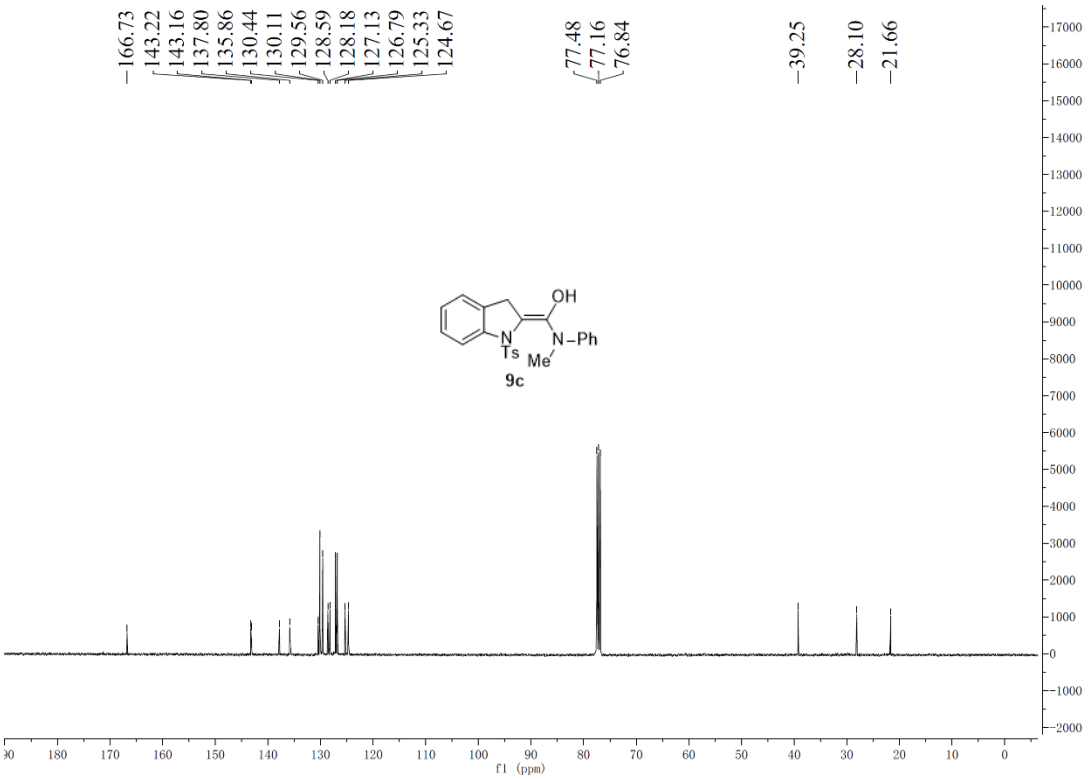

Figure S91. ^{13}C NMR spectra (400 MHz) of **9c** in $CDCl_3$, related to **Figure 2B**.

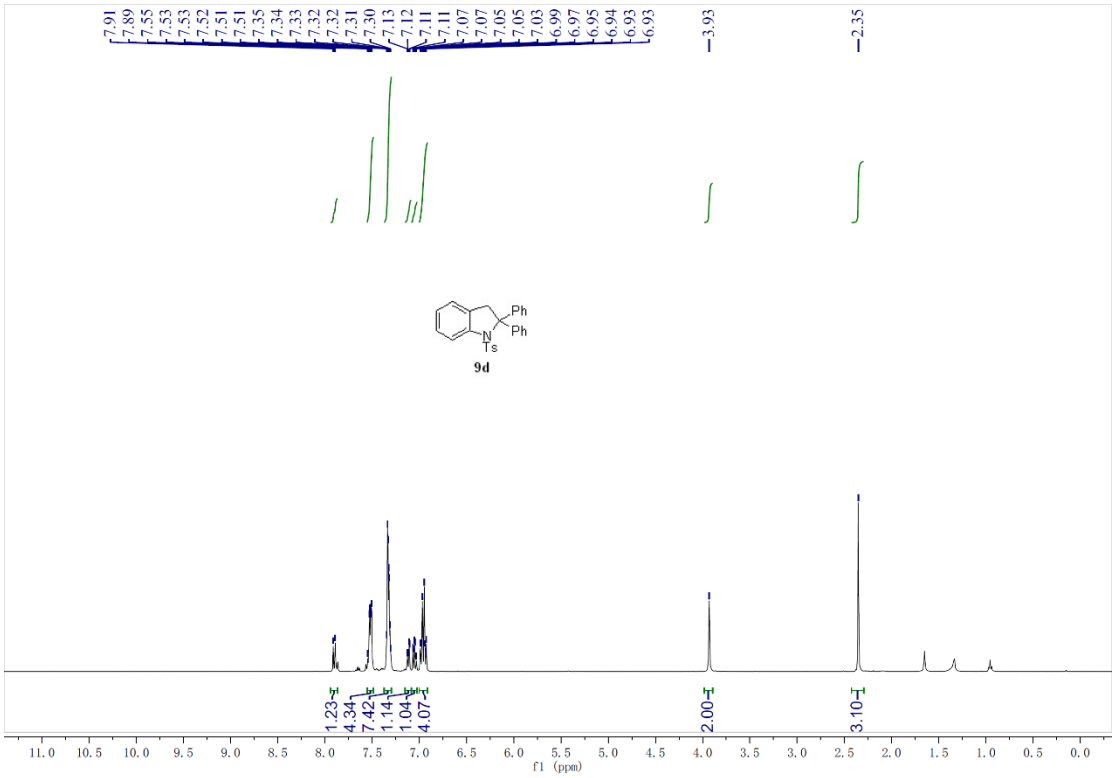

Figure S92. ^{1}H NMR spectra (400 MHz) of **9d** in $CDCl_3$, related to **Figure 2C**.

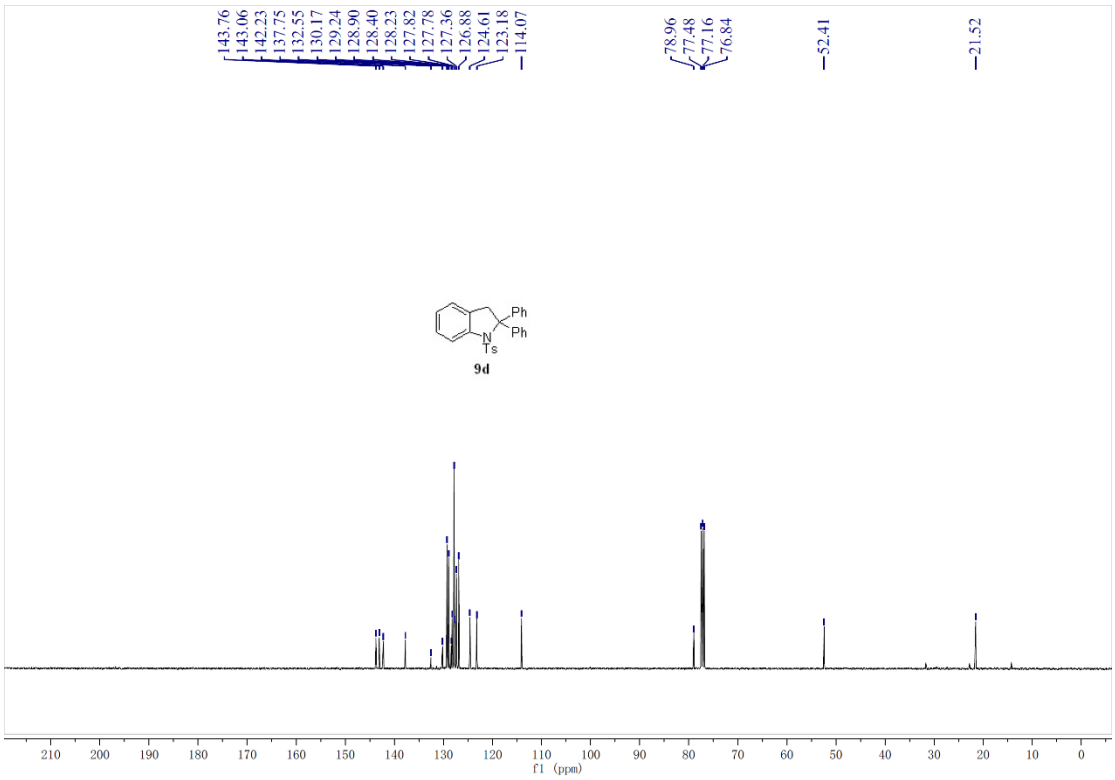

Figure S93. ^{13}C NMR spectra (400 MHz) of **9d** in $CDCl_3$, related to **Figure 2C**.

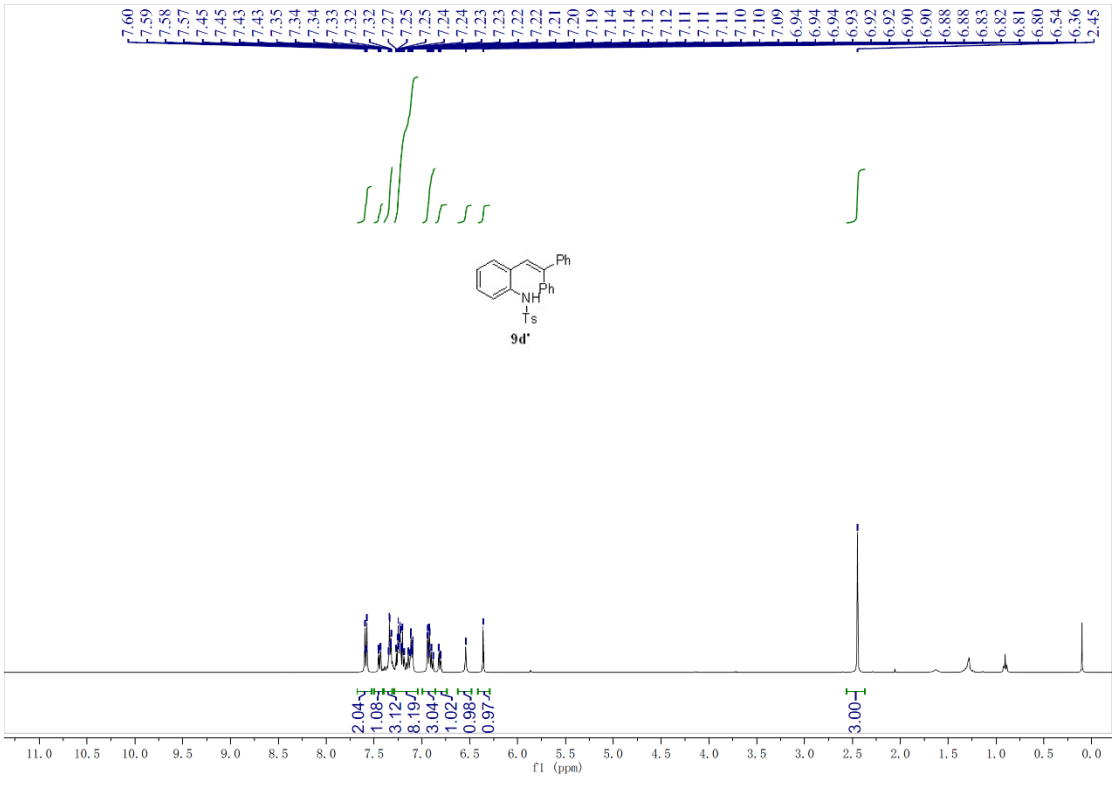

Figure S94. ^{1}H NMR spectra (400 MHz) of **9d'** in $CDCl_3$, related to **Figure 2C**.

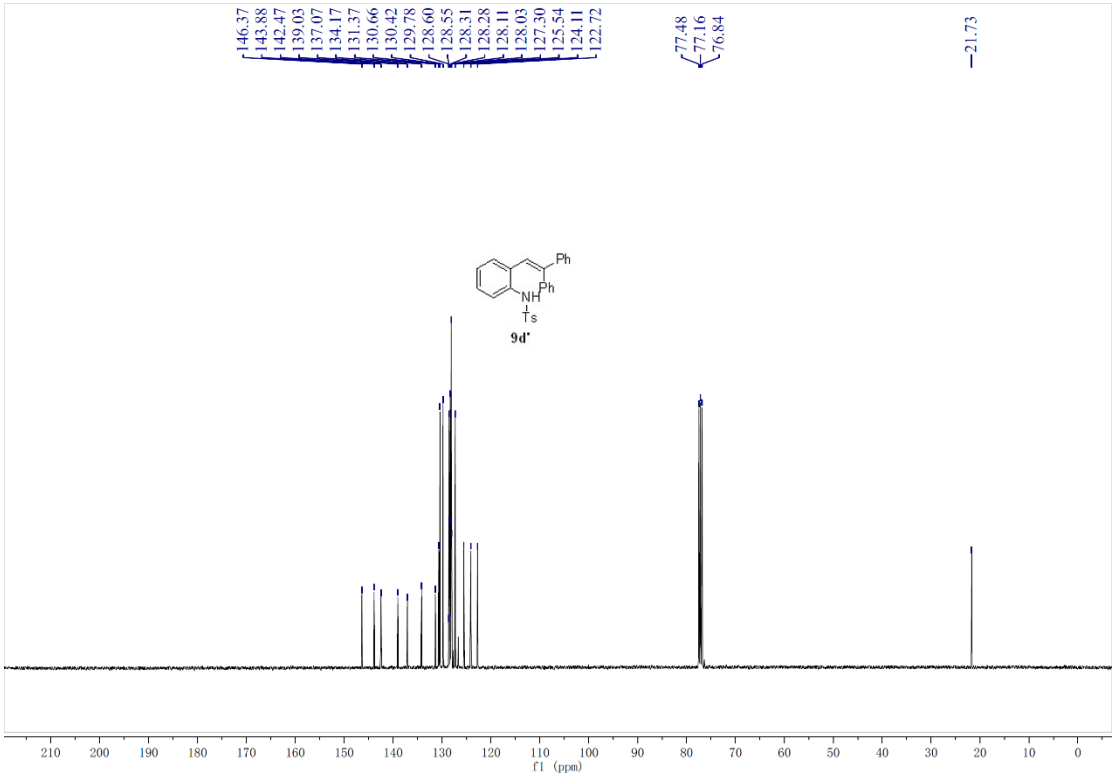

Figure S95. ^{13}C NMR spectra (400 MHz) of **9d'** in $CDCl_3$, related to **Figure 2C**.

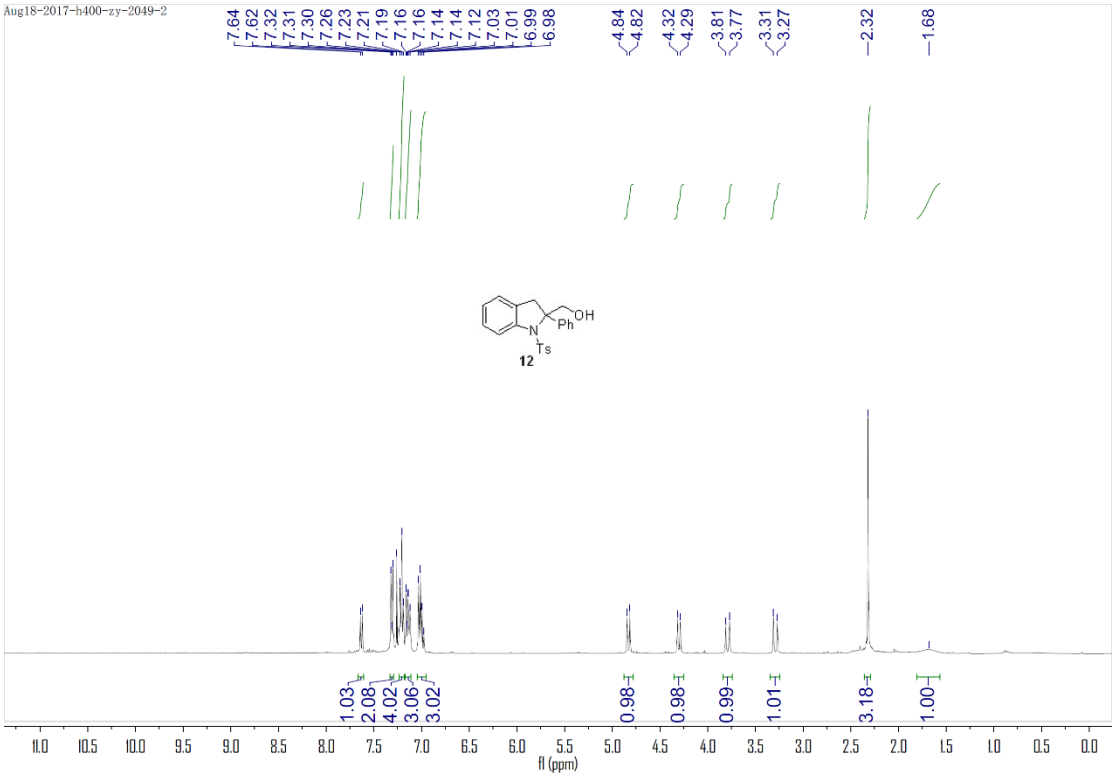

Figure S96. ^{1}H NMR spectra (400 MHz) of **12** in $CDCl_3$, related to **Figure 6C**.

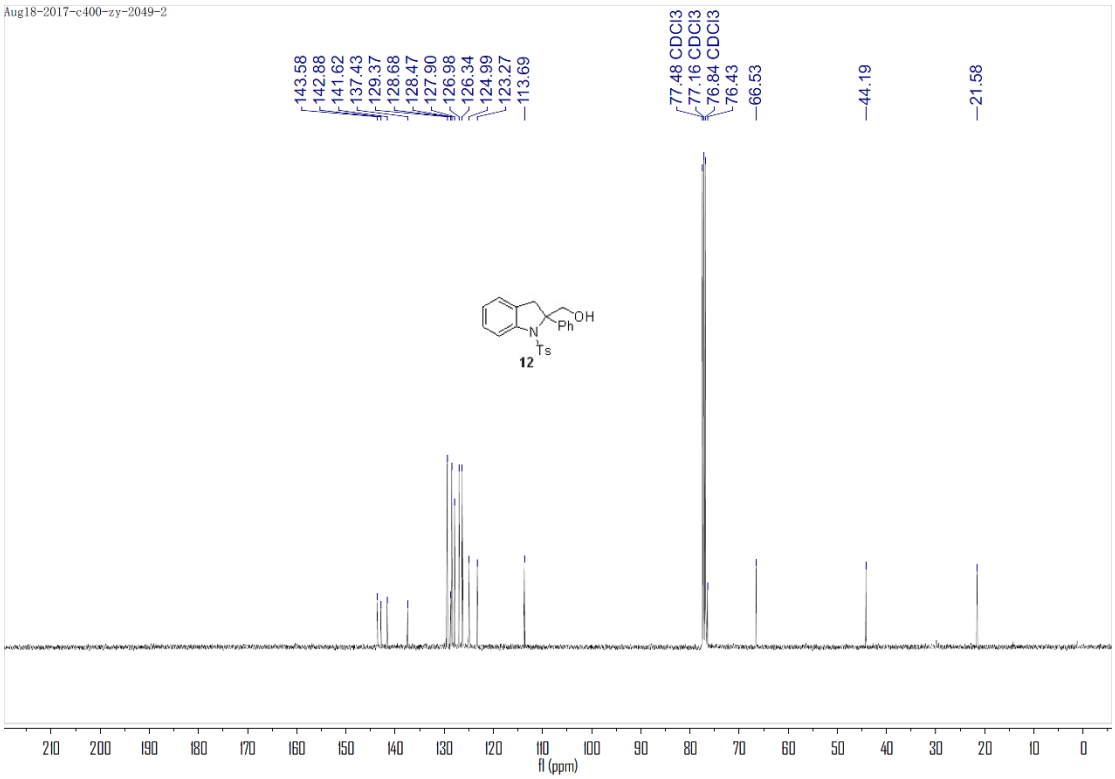

Figure S97. ^{13}C NMR spectra (400 MHz) of **12** in $CDCl_3$, related to **Figure 6C**.

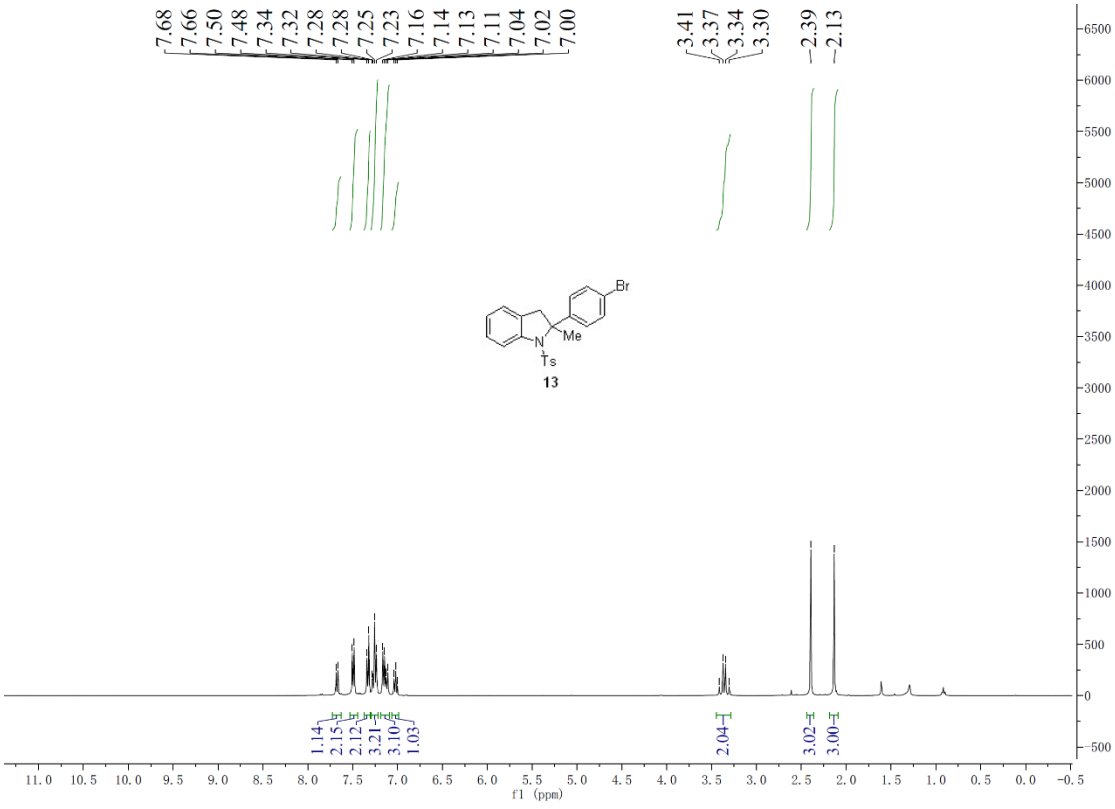

Figure S98. ^{1}H NMR spectra (400 MHz) of **13** in $CDCl_3$, related to **Figure 6D**.

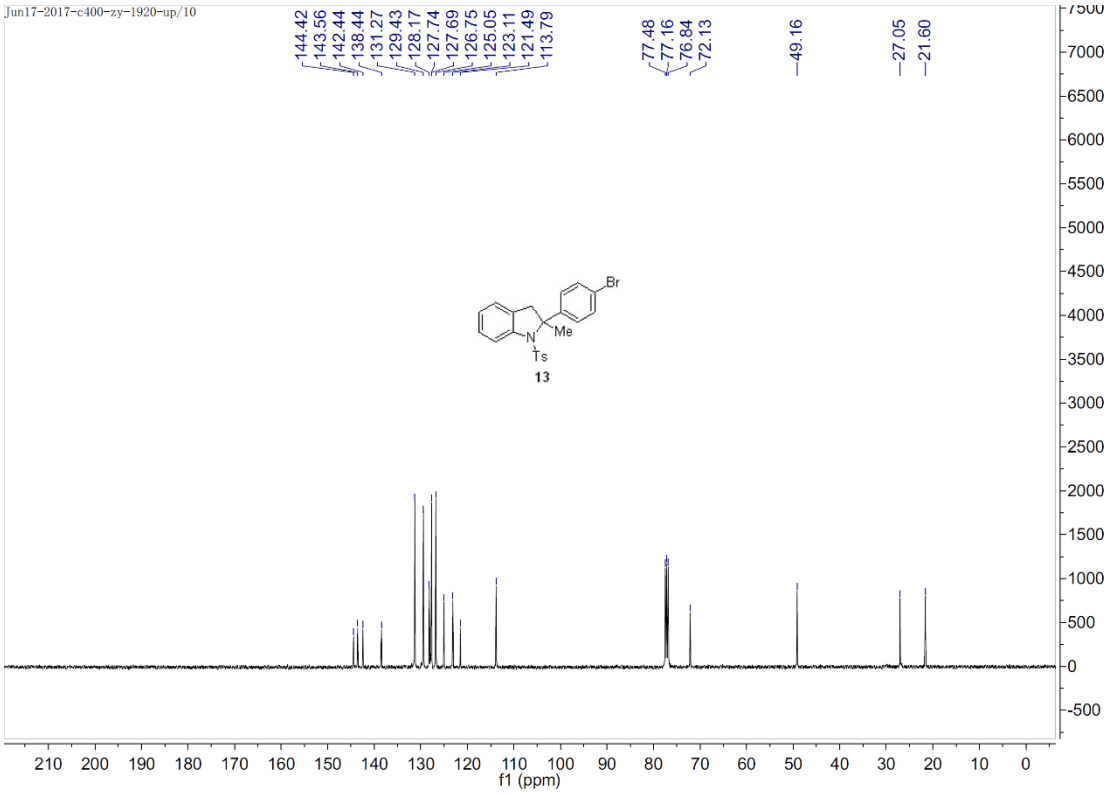

Figure S99. ^{13}C NMR spectra (400 MHz) of **13** in $CDCl_3$, related to **Figure 6D**.

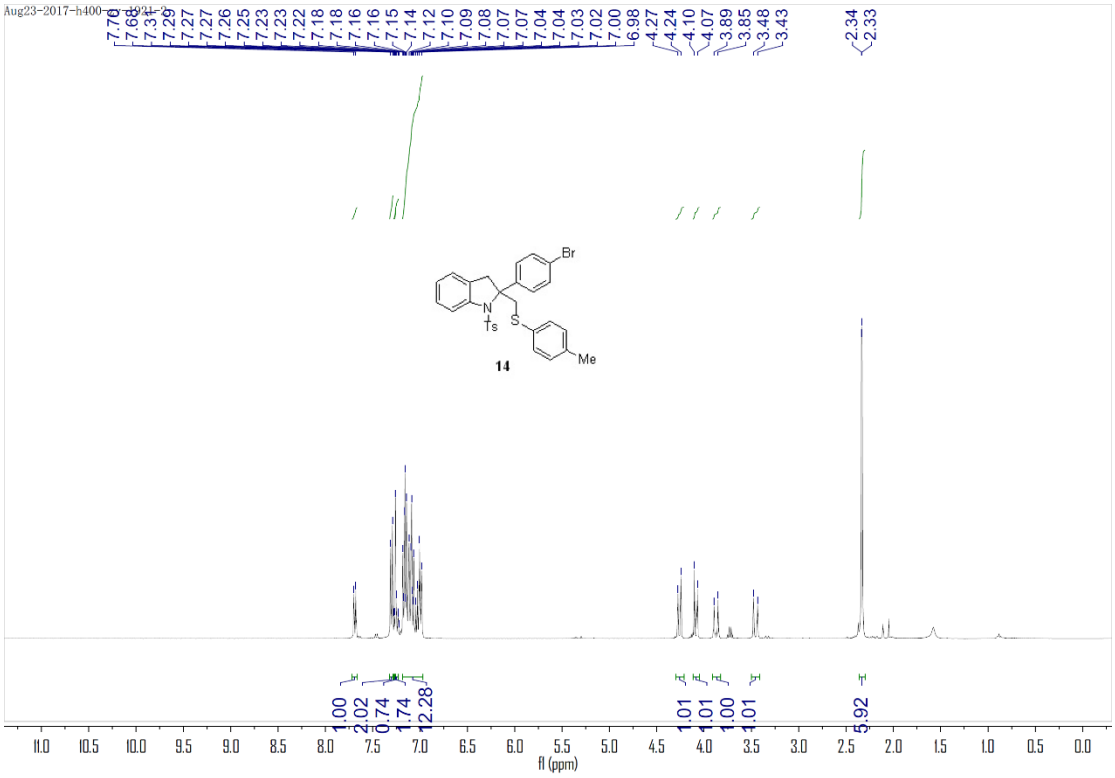

Figure S100. ^{1}H NMR spectra (400 MHz) of **14** in $CDCl_3$, related to **Figure 6E**.

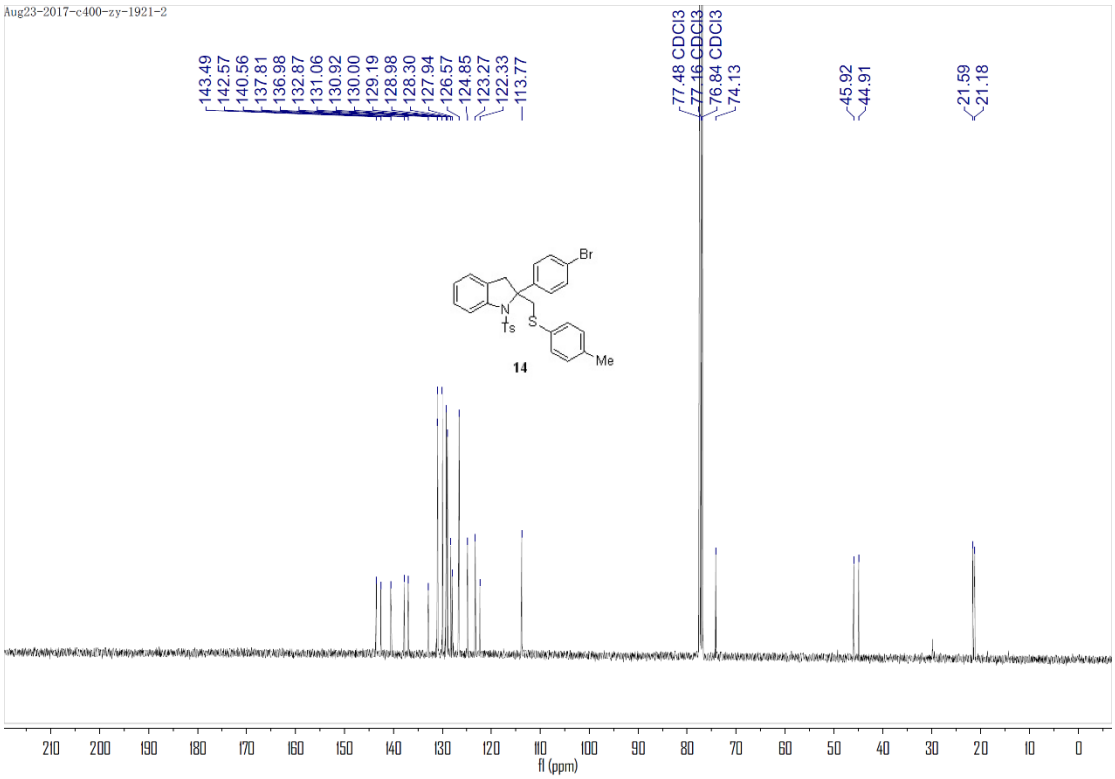

Figure S101. ^{13}C NMR spectra (400 MHz) of **14** in $CDCl_3$, related to **Figure 6E**.

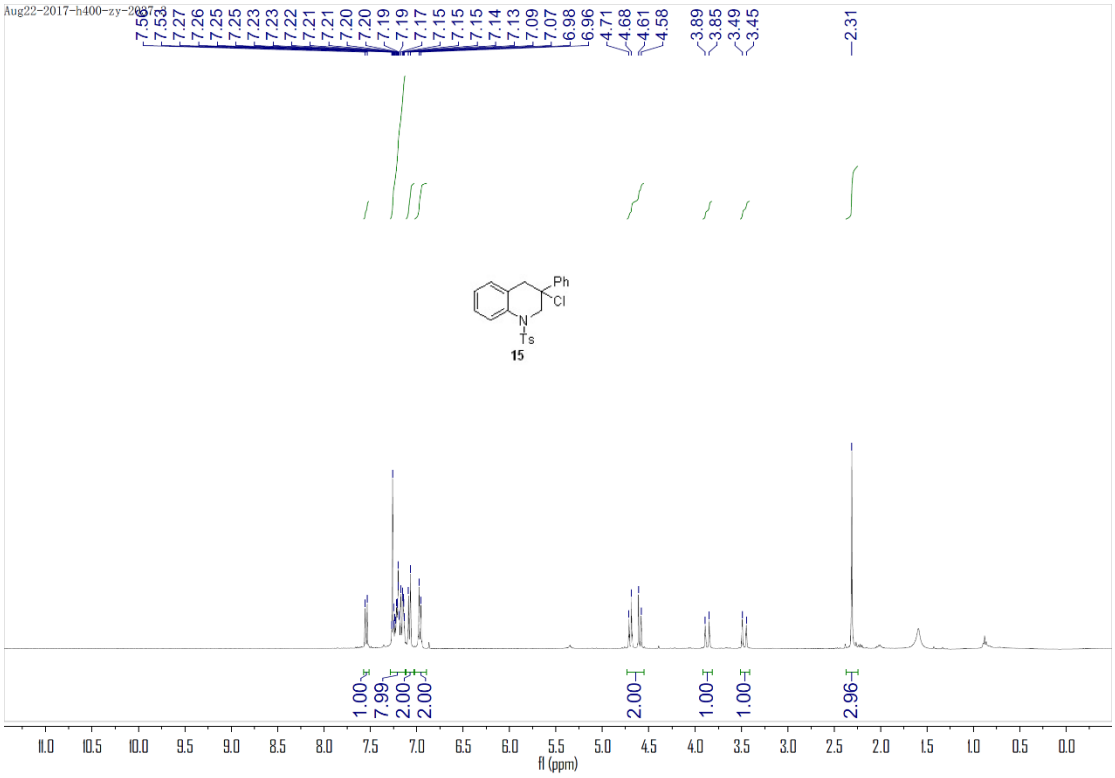

Figure S102. ^{1}H NMR spectra (400 MHz) of **15** in $CDCl_3$, related to **Figure 6F**.

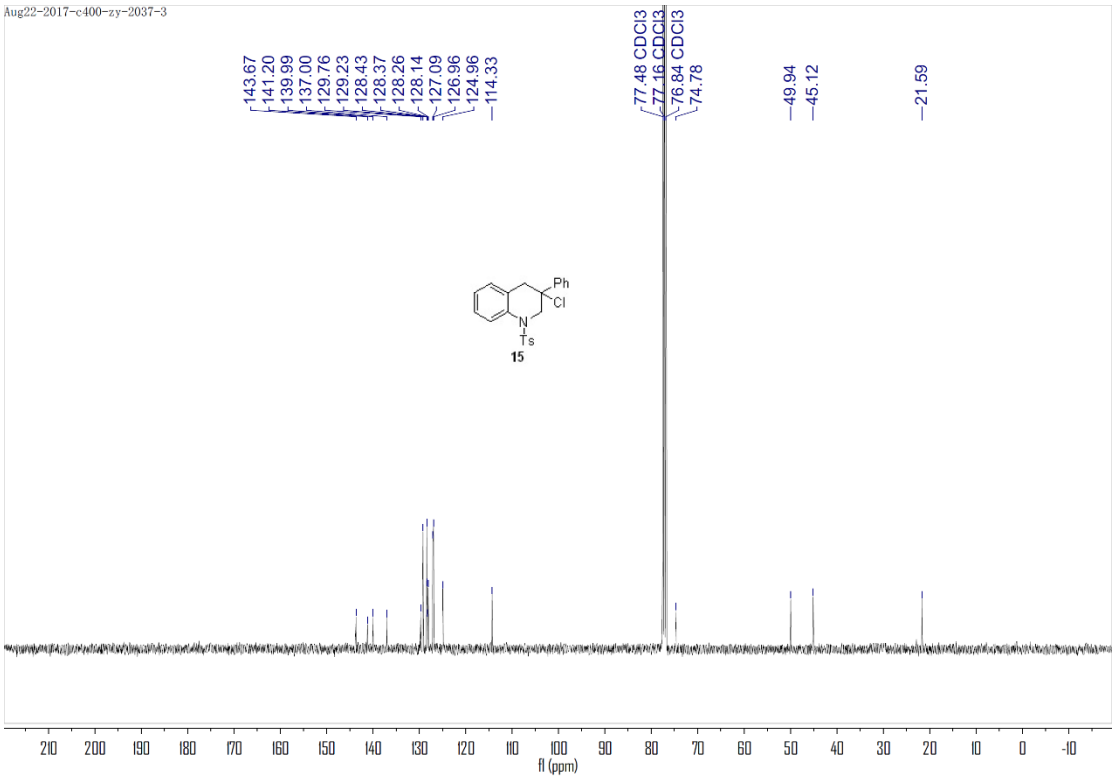

Figure S103. ^{13}C NMR spectra (400 MHz) of **15** in $CDCl_3$, related to **Figure 6F**.

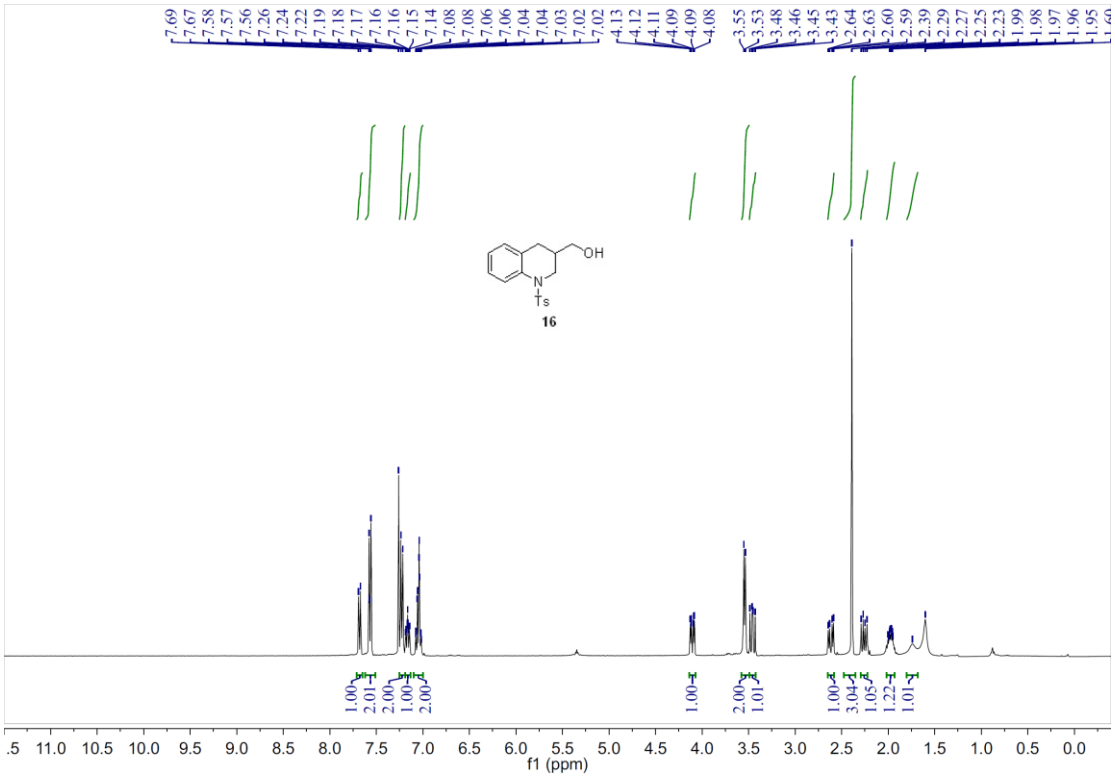

Figure S104. ^{1}H NMR spectra (400 MHz) of **16** in $CDCl_3$, related to **Figure 6G**.

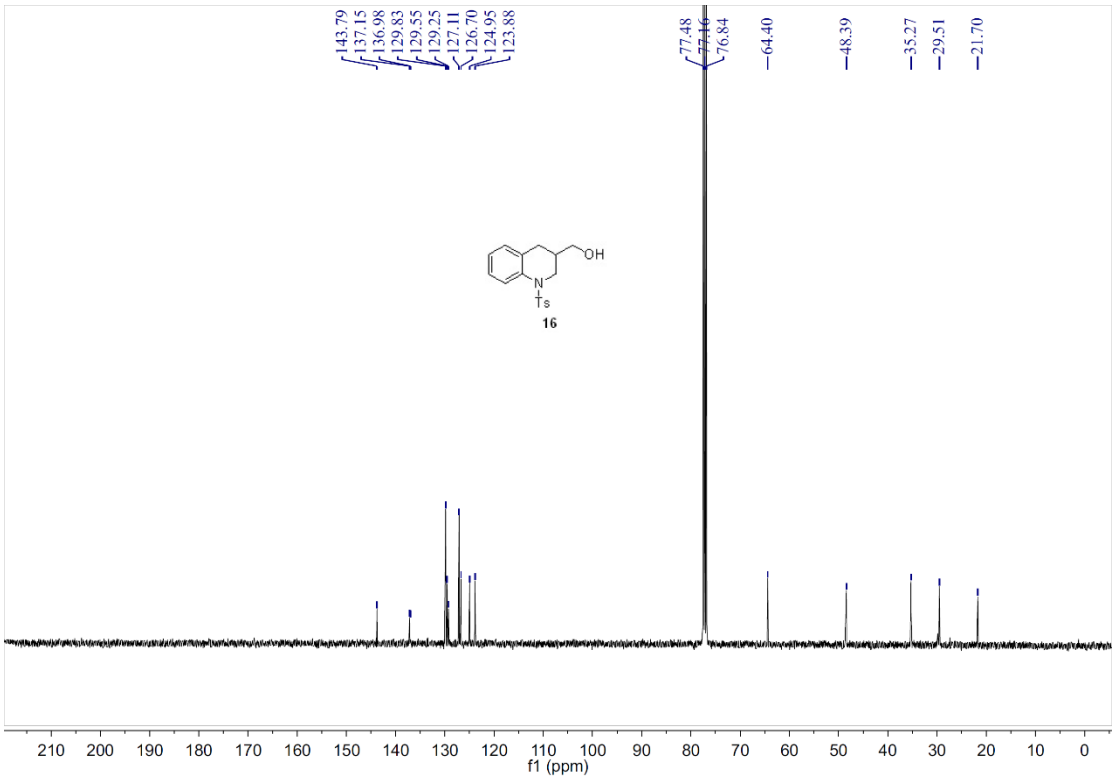

Figure S105. ^{13}C NMR spectra (400 MHz) of **16** in $CDCl_3$, related to **Figure 6G**.

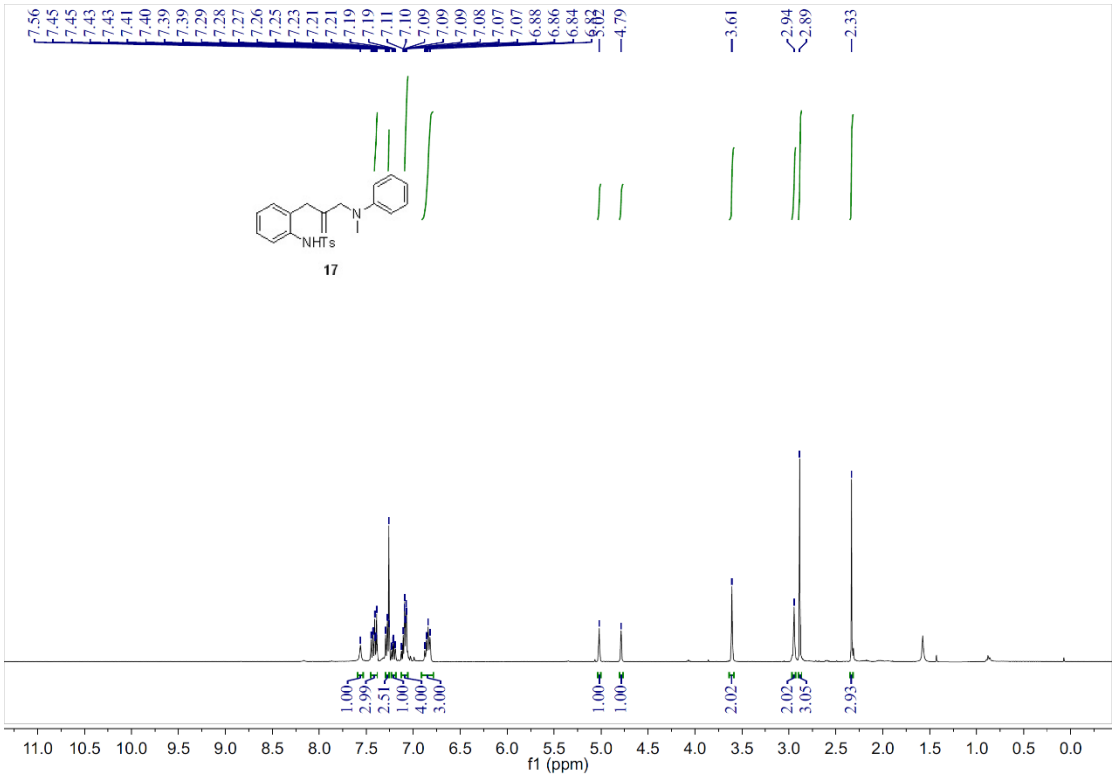

Figure S106. ^{1}H NMR spectra (400 MHz) of **17** in $CDCl_3$, related to **Figure 6H**.

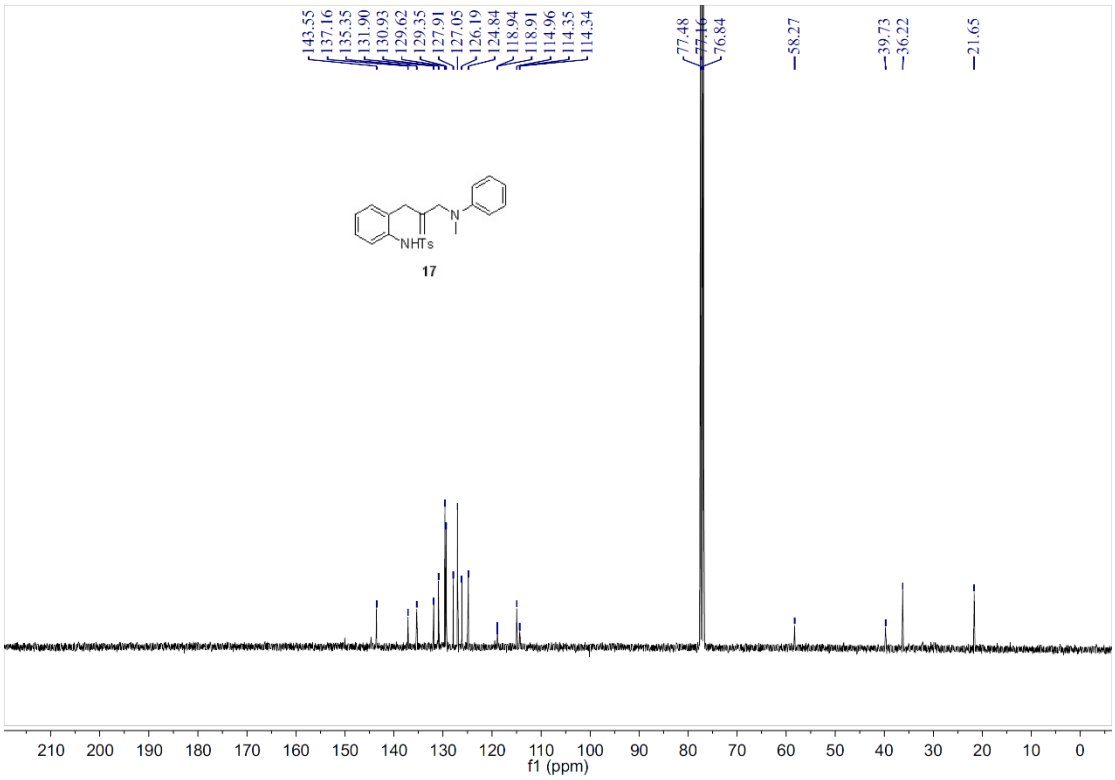

Figure S107. ^{13}C NMR spectra (400 MHz) of **17** in $CDCl_3$, related to **Figure 6H**.

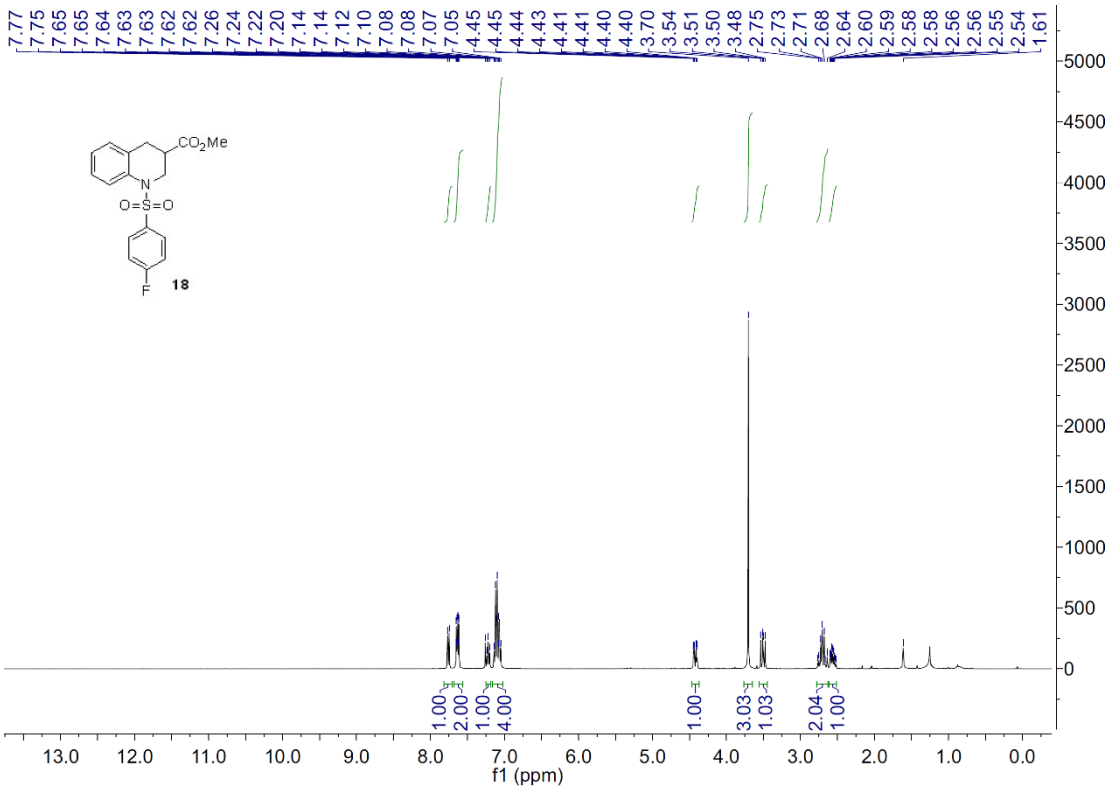

Figure S108. ^{1}H NMR spectra (400 MHz) of **18** in $CDCl_3$, related to **Figure 7**.

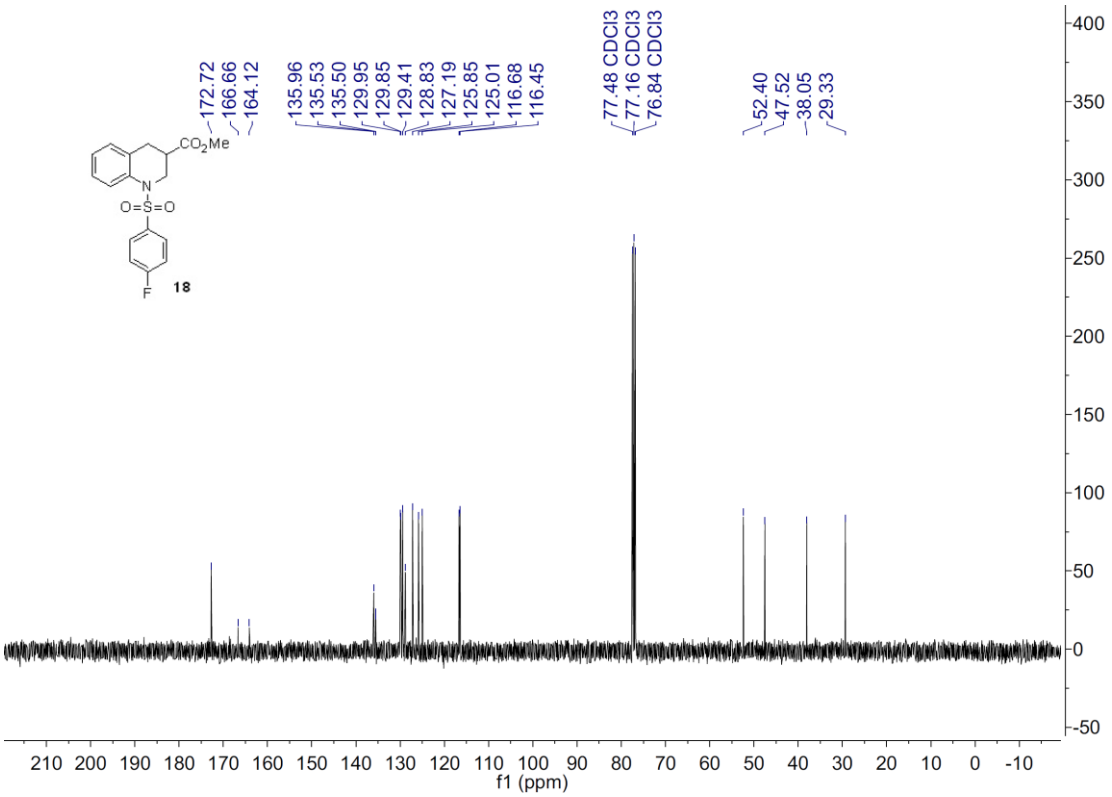

Figure S109. ^{13}C NMR spectra (400 MHz) of **18** in $CDCl_3$, related to **Figure 7**.

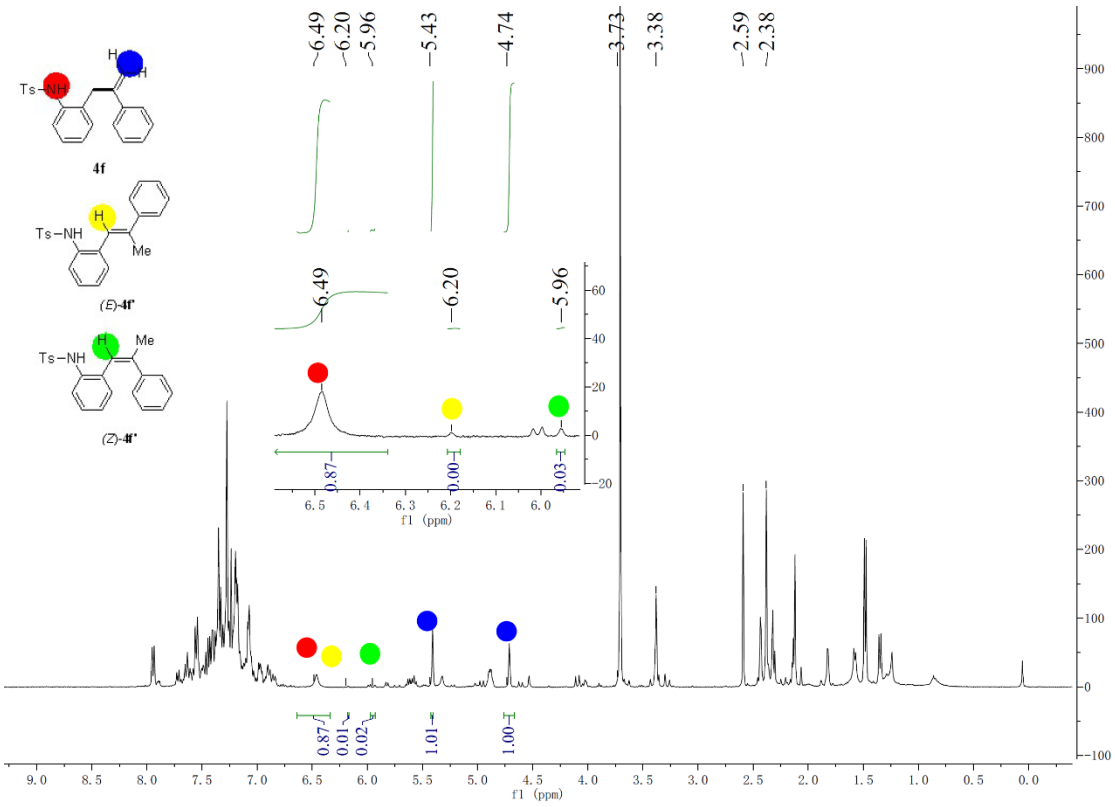

Figure S110. Crude NMR Spectra for the reaction of **2f** and **3a** under the conditions of **Table 1**, **entry 1**, related to **Table 1**. (Note: *E*/*Z*-**4f'** is kown product, see ref.: (2014). Org. Lett. *16*, 3720-3723)

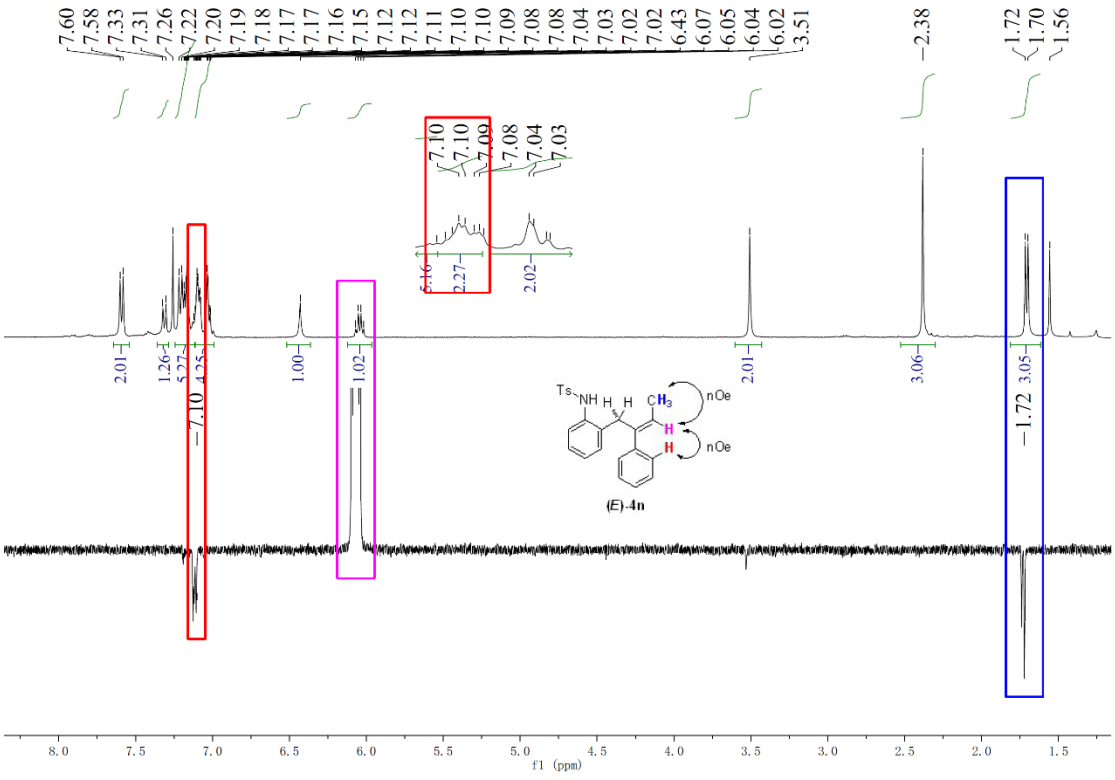

Figure S111. 1D-NOE NMR Spectra for ***E*-4n**, related to **Scheme 1**.

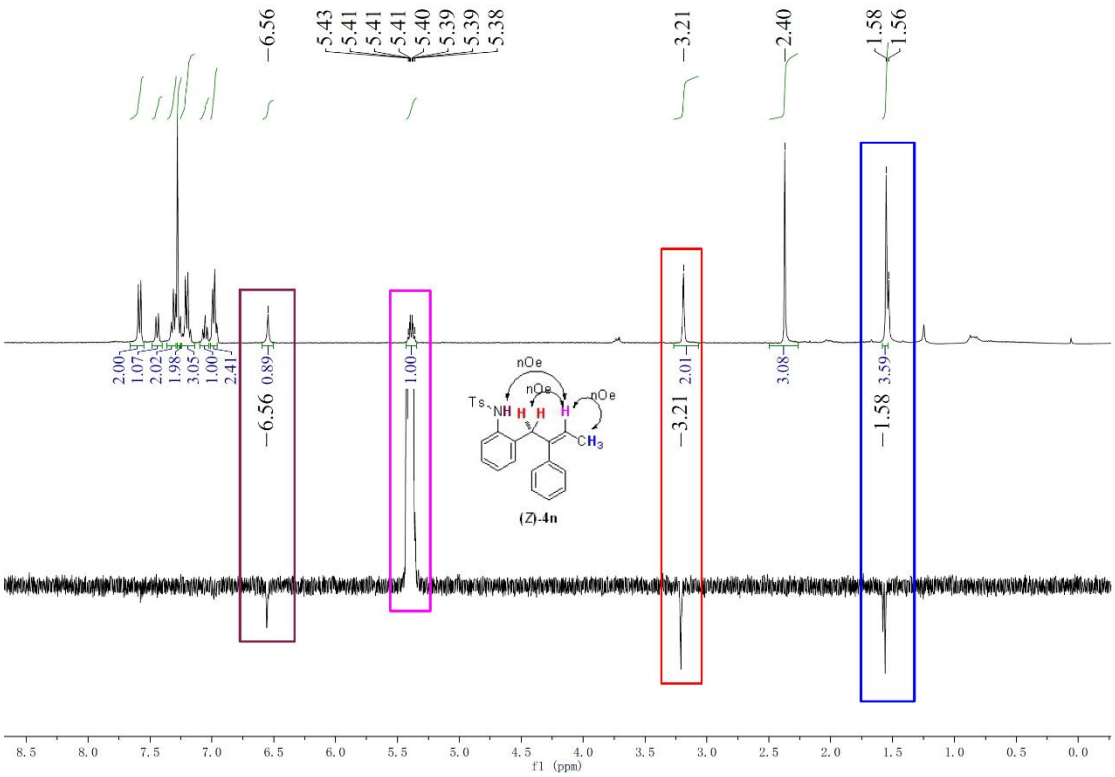

Figure S112. 1D-NOE NMR Spectra for ***Z*-4n**, related to **Scheme 1**.

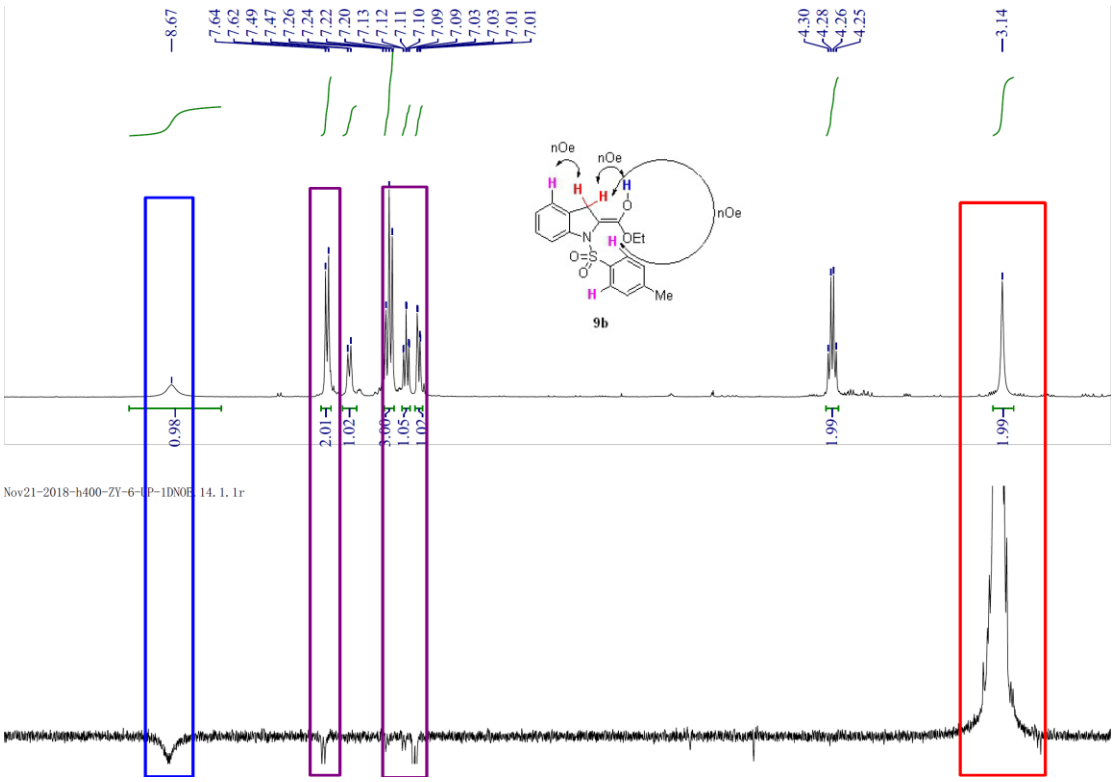

Figure S113. 1D-NOE NMR Spectra for **9b**, related to **Figure 2B.**

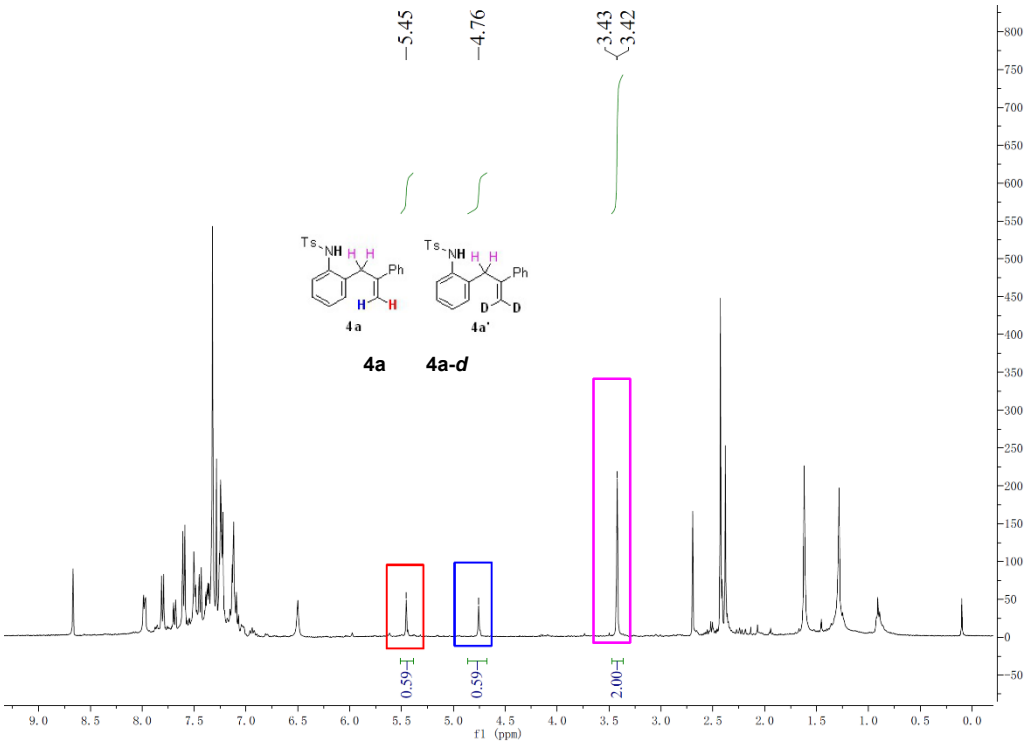

Figure S114. Intermolecular Kinetic Isotope Effect (KIE) Experiment, related to **Figure 3A**.

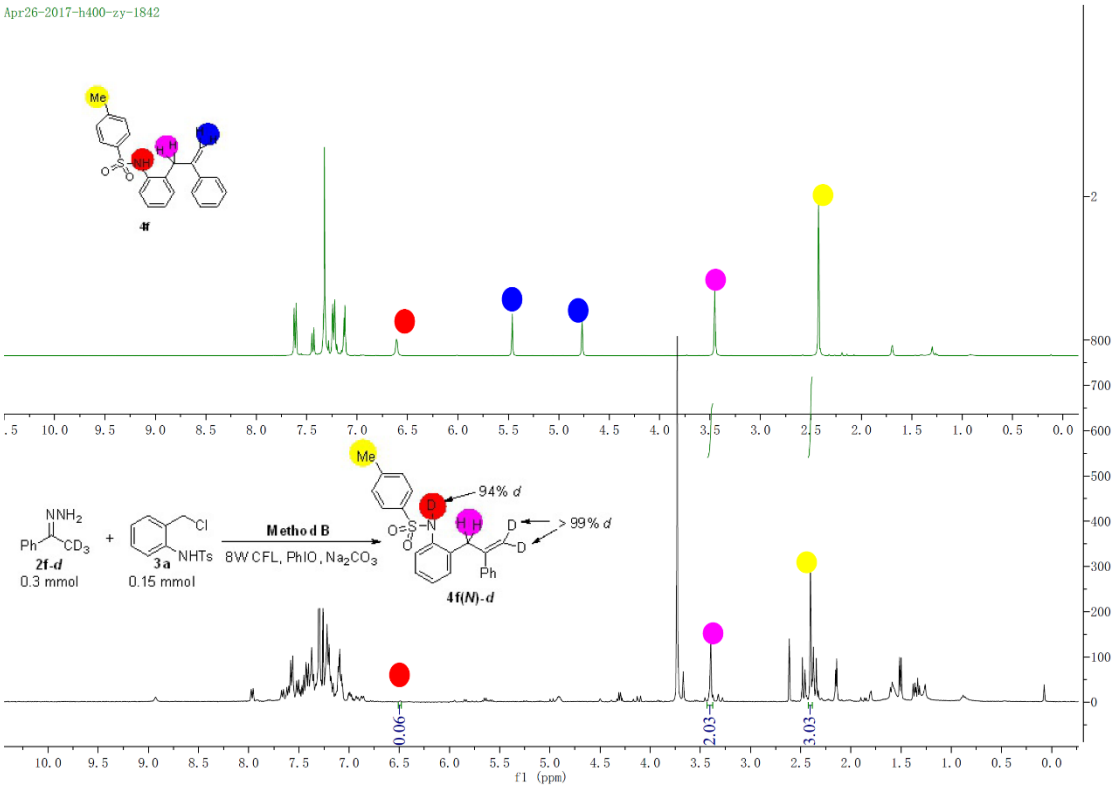

Figure S115. Intramolecular Isotope Labeling Experiment, related to **Figure 3A**.

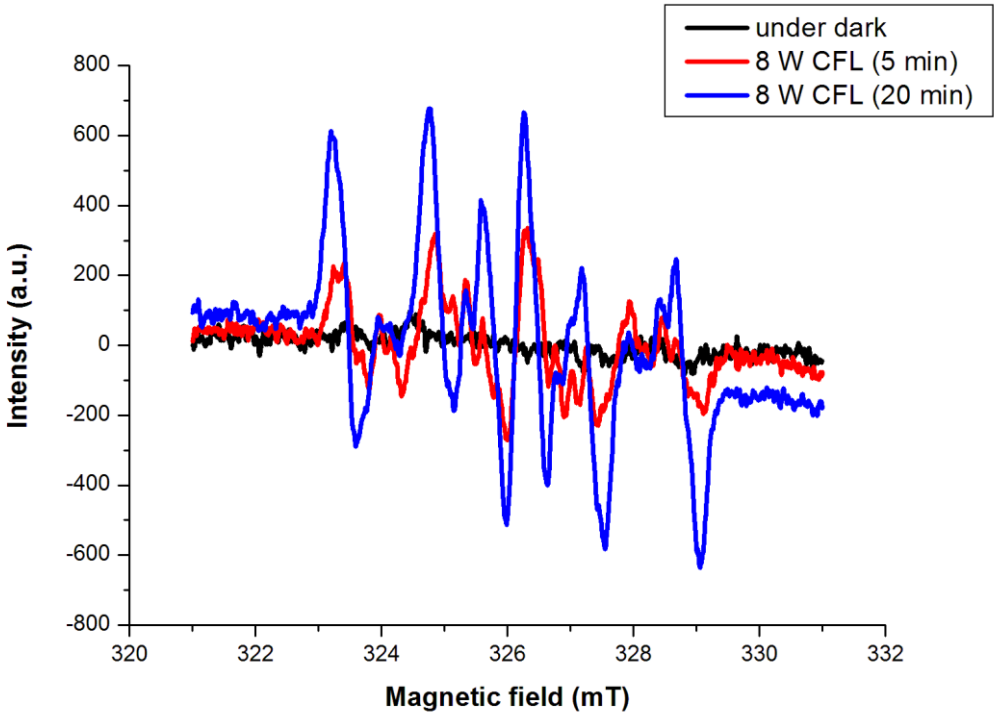

Figure S116. EPR Analysis, related to **Figure 3D**.

Supplemental Tables

Table S1. X-ray crystal structures of 4f, related to Scheme 1.

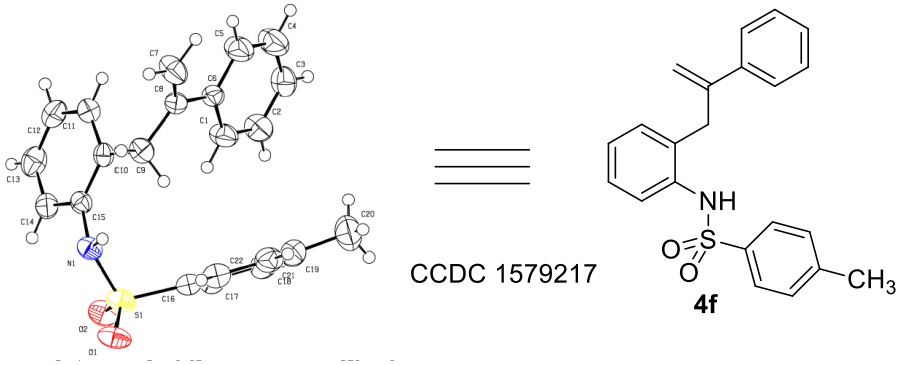

The missing CIF items (i.e., _computing_data_collection; _computing_publication_material) were added as fellow:

ata_xcalibur

_audit_creation_date;

'Mon Dec 12 10:27:52 2016';

_audit_creation_method;

CrysAlisPro, Agilent Technologies,

Version 1.171.36.32

(release 02-08-2013 CrysAlis171 .NET)

(compiled Aug 2 2013,16:46:58);

_computing_data_collection;

CrysAlisPro, Agilent Technologies,

Version 1.171.36.32

(release 02-08-2013 CrysAlis171 .NET)

(compiled Aug 2 2013,16:46:58);

_computing_cell_refinement;

CrysAlisPro, Agilent Technologies,

Version 1.171.36.32

(release 02-08-2013 CrysAlis171 .NET)

(compiled Aug 2 2013,16:46:58);

_computing_data_reduction;

CrysAlisPro, Agilent Technologies,

Version 1.171.36.32

(release 02-08-2013 CrysAlis171 .NET)

(compiled Aug 2 2013,16:46:58)

Table S2. X-ray crystal structures of 9a and 9d, related to Figure 2D.

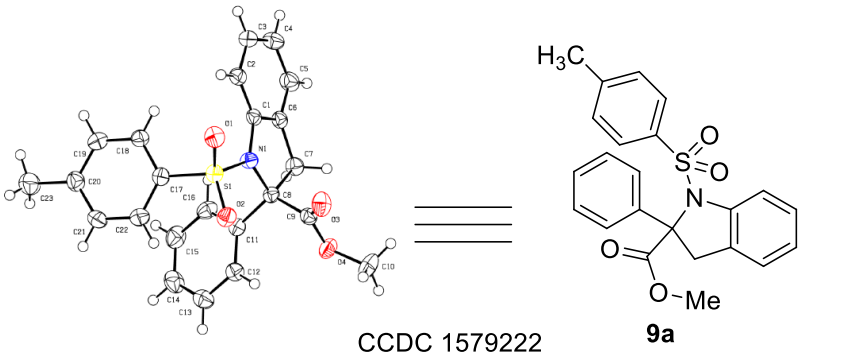

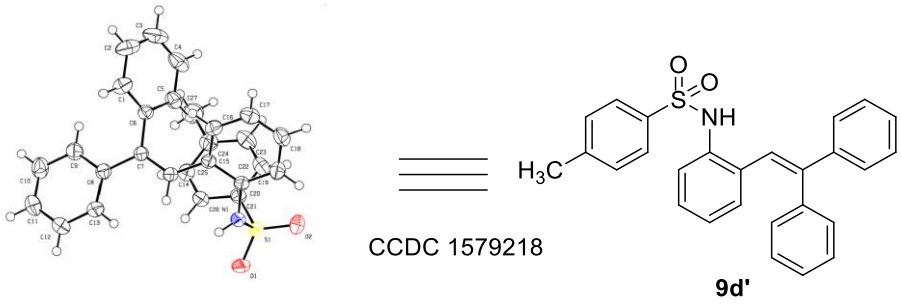

Transparent Methods

General Information

All reactions were carried out in oven-dried (110 °C) glassware under an atmosphere of dry argon. Solvents were dried and degassed by the standard methods. Flash column chromatography was performed using silica gel (300-400 mesh). Analytical thin-layer chromatography was performed using glass plates pre-coated with 200-300 mesh silica gel impregnated with a fluorescent indicator (254 nm). ^{1}H NMR and ^{13}C NMR spectra were recorded in $CDCl_3$ on a 400 MHz spectrometer; chemical shifts are reported in ppm with the solvent signals as reference, and coupling constants (*J*) are given in Hertz. The peak information is described as: br = broad, s = singlet, d = doublet, t = triplet, q = quartet, m = multiplet, comp = composite. High-resolution mass spectra (HRMS) were recorded on a commercial apparatus (ESI or CI Source).

Note S1. Expanded discussion on the formation of linear/branched alkenes via organometal intermediates

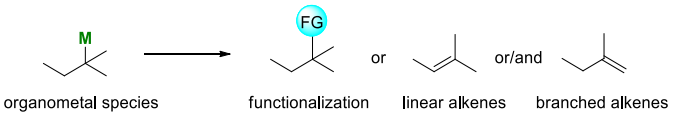

Organometal species, as the very common intermediate, have broadly existed in organic synthesis. Basically, functionalization or β-H elimination are the major reactions based on organometal intermediate. In terms of the β-H elimination, linear alkenes are usually formed as the major products (comparing to branched alkenes) because of the energetically favorable process. For example, the Pd-catalyzed cross coupling reactions of *N*-tosylhydrazones with halides that take place with carbene migratory insertion and β-H elimination to form linear alkenes were well developed by Barluenga ((2007). Angew. Chem. Int. Ed. *46*, 5587–5590.), Valdés ((2011). Angew. Chem. Int. Ed. *50*, 7486−7500.) and Wang ((2017). Chem. Rev. *117*, 13810−13889.). Whilst, the only analogous version for the selective branched alkene formation was disclosed by Barluenga and Valdés through a regioselective β-H elimination via a steric less hindered transition state ((2010). Angew. Chem. Int. Ed. *49*, 6856−6859.), demonstrating that highly regioselective access to branched alkenes are much more challenging ((2017). J. Am. Chem. Soc. *139*, 6086−6089.).

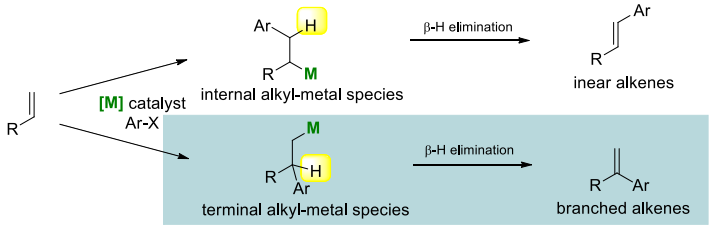

To overcome the problem of selectivity for the branched alkenes, the strategy through the catalytic formation of terminal alkyl-metal species in Heck alkenylation was developed last decade. Representative works were reported by Jamison ((2011). J. Am. Chem. Soc. *133*, 19020−19023; (2013). J. Am. Chem. Soc. *135*, 1585−1592; (2014). Angew. Chem. Int. Ed. *53*, 1858−1861.), Zhou ((2012). Angew. Chem. Int. Ed. *51*, 5915–5919.), Stahl ((2012). J. Am. Chem. Soc. *134*, 16496−16499; (2015). Chem. Commun. *51*, 12771−12774.), Goossen ((2016). Angew. Chem. Int. Ed. *55*, 11296−11299.), and Bower ((2018). Angew. Chem. Int. Ed. *57*, 14198−14202.), independently. Despite of these advances, the development of alternative methods for the effective synthesis of branched alkenes are still highly demand.

Note S2. Expanded discussion on the reactions of *o*-QMs/*aza-o*-QMs with diazo-compounds

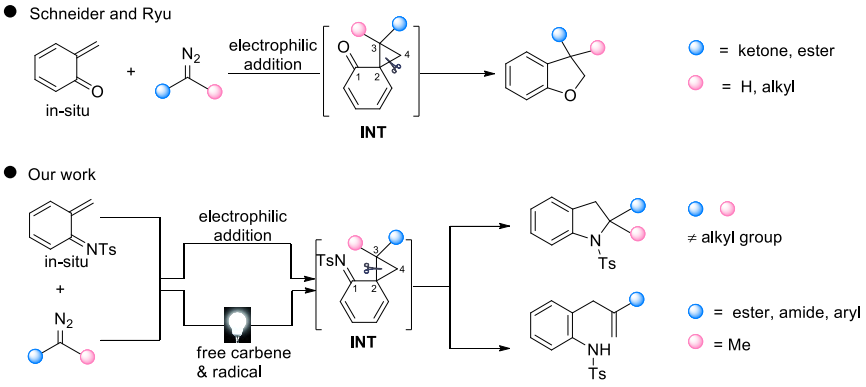

When we prepared this work, elegant cycloannulation reactions of *o*-QMs and diazo ketones/esters were recently reported by Schneider and Ryu, independently. However, the chemistries are quite different: (1) the substrates (*o*-QMs versus *aza-o*-QMs. In addition, the more reactive alkyl diazocomounds were also investigated in our protocol); (2) the pathways to the INT (besides the traditional way of electrophilic addition, we also found a visible light promoted path, which include free carbene and radical species; (3) the manner of ring opening (C_2–C_4 bond cleavage versus C_2–C_3 bond cleavage); (4) the reactions (cycloannulation versus desaturation).

Highlights (1) and (4) can be observed in the manuscript and the reported papers. Hight (2) is supported by control experiments and DFT calculations. Hight (3) can also be verified by our cycloannulation products (**Figure 2**).

Note S3. Expanded discussion on the strategies for the synthesis of 2-allyl anilines

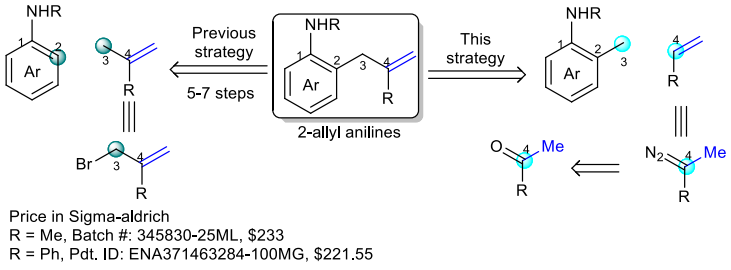

Based on the reported literature ((2015). J. Am. Chem. Soc. *137*, 1130−1135; (2014). J. Am. Chem. Soc. *136*, 3732−3735; (2014). Angew. Chem. Int. Ed. *53*, 5170−5174; (2017). Adv. Synth. Catal. *359*, 2499−2508.), we found that the strategies they used are usually coupling with C_2 and C_3. In this context, allylation of the ortho-halo -anilines or -nitrobenzene following by reduction are usually employed. However, the main problem needs to overcome is the compatibility of aniline. Many steps were taken to protect and de-protect the amine group. Moreover, the substrates (branched alkenes) are not easy to obtained, which largely limited the scopes.

In this new developed strategy, C_3 catch C_4 by the electrophilic addition without transition metal catalyst, which perfectly overcome the compatibility of aniline. Besides, the precursors of the two partners are commercially available and not expensive. With this method, a wide spectrum of 2-allyl anilines can be provided.

In terms of C_3-C_4 bond formation strategy, the alkenylation of the benzylic halides was also evaluated. However, to the best of knowledge ((2011). J. Am. Chem. Soc. *133*, 19020−19023; (2013). J. Am. Chem. Soc. *135*, 1585−1592), the substrates of ortho-amine benzylic halides were not involved in the scopes.

Experimental procedure

General procedure for the preparation of 2-allyl anilines 4 and 5 (Method A, related to Table 1 and Scheme 1).

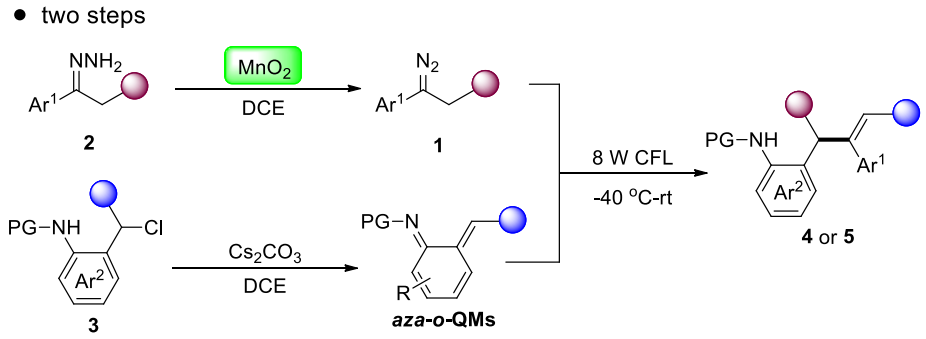

To a 10 mL oven-dried flask containing a magnetic stirring bar, hydrazone **2** (0.45 mmol), anhydrous $MgSO_4$ (60 mg), MnO_2 (312.0 mg, 8.0 equiv), and 1,2-dichloroethane (3.0 mL) were added in sequence under argon atmosphere. Then the flask was wrapped in foil and the reaction mixture was allowed to stir for 45 min at 0 °C. After that, removing the solid by filtering through a pad of Celite with Teflon filter (0.22 μm) at the bottom, we could obtain the pink solution as the diazo compound **1**.

To a 10 mL oven-dried vial, which contains a magnetic stirring bar, *N*-(2-chloromethylaryl) amide **3** (0.15 mmol), Cs_2CO_3 (97.7 mg, 2.0 equiv) under argon atmosphere at -40 °C, the above-mentioned pink solution was added via syringe. The reaction was carried out by irradiation of visible light (8 W CFL) and warm to room temperature slowly. When the reaction was completed (monitored by TLC), the reaction mixture was quenched by saturated NH_4Cl (aq), extracted with ethyl acetate (15 X 3 mL), and wahsed with brine (50 mL). The organic phase was dried with Na_2SO_4 and evaporated *in vacuo*. The resulting residue was purified by

column chromatography on silica gel with hexanes/ethyl acetate (20:1 to 10:1) as the eluent to give the desired pure products **4** or **5** in moderate to good or high yields.

General procedure for the preparation of 2-allyl anilines 4 and 5 (Method B, related to Table 1 and Scheme 1).

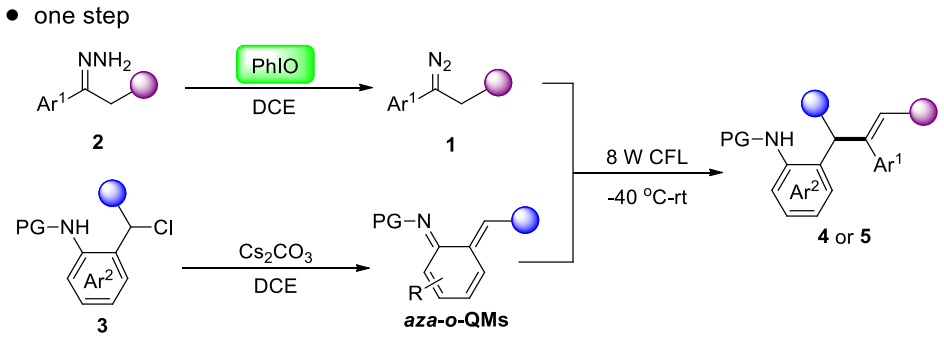

To a 10 mL oven-dried vial, which contains a magnetic stirring bar, hydrazone **2** (0.30 mmol), *N*-(2-chloromethylaryl) amide **3** (0.15 mmol), Cs_2CO_3 (97.7 mg, 2.0 equiv) and PhIO (66.0 mg, 0.30 mmol) in DCE (2 mL) under argon atmosphere at -40 °C. The reaction was carried out by irradiation of visible light (8 W CFL) and warm to room temperature slowly. When the reaction was completed (monitored by TLC), the reaction mixture was quenched by saturated NH_4Cl (aq), extracted with ethyl acetate (15 X 3 mL), and wahsed with brine (50 mL). The organic phase was dried with Na_2SO_4 and evaporated in vacuo. The organic layer was dried over Na_2SO_4, filtered, and concentrated. The resulting residue was purified by column chromatography on silica gel with hexanes/ethyl acetate (20:1 to 10:1) as the eluent to give the desired pure products **4** or **5** in moderate to good or high yields.

***N*-{2-[2-(4-Bromophenyl)allyl]phenyl}-4-methylbenzenesulfonamide (4a).**

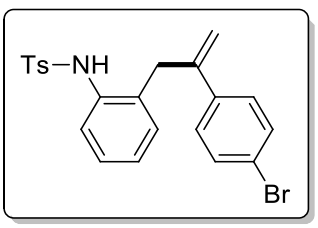

Following the general procedure A, 53.7 mg, 81% yield. Yellow solid, mp: 150-151 °C. ^1H NMR (400 MHz, $CDCl_3$) (δ, ppm) 7.58 (d, *J* = 8.2 Hz, 2H), 7.40 (d, *J* = 8.4 Hz, 2H), 7.35 (d, *J* =

7.9 Hz, 1H), 7.23-7.19 (m, 3H), 7.17-7.06 (comp, 4H), 6.48 (s, 1H), 5.44 (s, 1H), 4.80 (s, 1H), 3.43 (s, 2H), 2.41 (s, 3H); ^{13}C NMR (100 MHz, $CDCl_3$) (δ, ppm) 144.6, 144.0, 138.9, 136.9, 134.9, 132.5, 131.6, 130.9, 129.8, 127.9, 127.7, 127.2, 126.7, 125.3, 122.0, 115.3, 37.4, 21.7. HRMS (TOF MS ESI$^+$) calculated for $C_{22}H_{21}BrNO_2S$ [M+H]$^+$: 442.0471, found 442.0468.

4-Methyl-*N*-{2-[2-(*p*-tolyl)allyl]phenyl}benzenesulfonamide (4b).

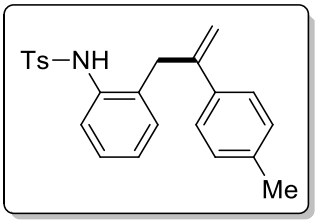

Following the general procedure A, 46.4 mg, 82% yield. Yellow solid, mp: 141-142 °C. ^{1}H NMR (400 MHz, $CDCl_3$) (δ, ppm) 7.58 (d, *J* = 8.3 Hz, 2H), 7.43 (d, *J* = 8.0 Hz, 1H), 7.22-7.19 (comp, 5H), 7.12-7.09 (comp, 4H), 6.52(s, 1H), 5.41 (s, 1H), 4.69 (s, 1H), 3.38 (s, 2H), 2.41 (s, 3H), 2.34 (s, 3H); ^{13}C NMR (100 MHz, $CDCl_3$) (δ, ppm) 145.4, 143.9, 138.0, 137.1, 137.0, 135.1, 132.4, 131.2, 129.8, 129.2, 127.8, 127.2, 126.5, 125.9, 124.9, 113.8, 37.7, 21.7, 21.2. HRMS (TOF MS ESI$^+$) calculated for $C_{23}H_{24}NO_2S$ [M+H]$^+$: 378.1522, found 378.1527.

***N*-{2-[2-(4-Methoxyphenyl)allyl]phenyl}-4-methylbenzenesulfonamide (4c).**

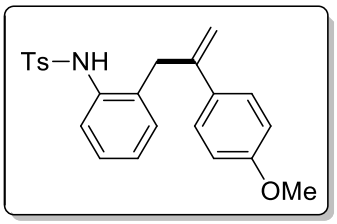

Following the general procedure A, 49.6 mg, 84% yield. Yellow solid, mp: 143-145 °C. ^{1}H NMR (400 MHz, $CDCl_3$) (δ, ppm) 7.58 (d, *J* = 11.2 Hz, 2H), 7.41 (d, *J* = 10.4 Hz, 1H), 7.25-7.20 (comp, 5H), 7.11-7.09 (m, 2H), 6.84-6.81 (m, 2H), 6.50 (br, 1H), 5.36 (s, 1H), 4.65 (s, 1H), 3.81 (s, 3H), 3.37 (s, 2H), 2.41 (s, 3H); ^{13}C NMR (100 MHz, $CDCl_3$) (δ, ppm) 144.9, 143.9, 137.1, 135.2, 132.4, 132.3, 131.2, 129.8, 127.9, 127.3, 127.2, 126.5, 124.9, 113.9, 113.0, 55.4, 37.8,

21.7. HRMS (TOF MS ESI$^+$) calculated for $C_{23}H_{24}NO_3S$ [M+H]$^+$ 394.1471, found 394.1467.

***N*-{2-[2-(4-Fluorophenyl)allyl]phenyl}-4-methylbenzenesulfonamide (4d).**

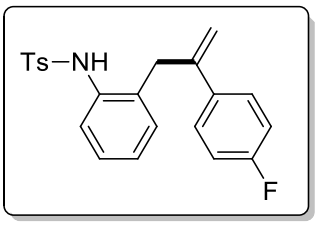

Following the general procedure A, 45.7 mg, 80% yield. Yellow solid, mp: 95-96 °C. ^{1}H NMR (400 MHz, $CDCl_3$) (δ, ppm) 7.58 (d, *J* = 8.3 Hz, 2H), 7.36 (d, *J* = 7.7 Hz, 1H), 7.28-7.27 (m, 1H), 7.25-7.17 (comp, 4H), 7.13-7.06 (comp, 2H), 7.00-6.94 (comp, 2H), 6.48 (s, 1H), 5.39 (s, 1H), 4.75 (s, 1H), 3.42 (s, 2H), 2.41 (s, 3H) ; ^{13}C NMR (150 MHz, $CDCl_3$) (δ, ppm) 162.6 (d, *J* = 246.2 Hz), 144.7, 144.0, 137.0, 136.1 (d, *J* = 3.1 Hz), 135.1, 132.4, 131.1, 129.8, 127.9, 127.7 (d, *J* = 8.0 Hz), 127.3, 126.6, 125.2, 115.4 (d, *J* = 21.3 Hz), 114.7, 37.8, 21.7. HRMS (TOF MS ESI$^+$) calculated for $C_{22}H_{21}FNO_2S$ [M+H]$^+$: 382.1272, found 382.1282.

***N*-{2-[2-(4-Chlorophenyl)allyl]phenyl}-4-methylbenzenesulfonamide (4e).**

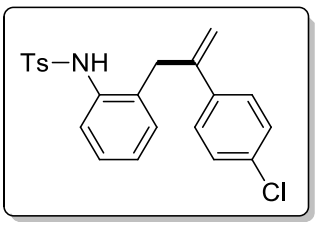

Following the general procedure A, 45.9 mg, 77% yield. Yellow solid, mp: 155-156 °C. ^{1}H NMR (400 MHz, $CDCl_3$) (δ, ppm) 7.58 (d, *J* = 8.3 Hz, 2H), 7.35 (d, *J* = 7.6 Hz, 1H), 7.25-7.17 (comp, 7H), 7.13-7.06 (comp, 2H), 6.50 (s, 1H), 5.43 (s, 1H), 4.79 (s, 1H), 3.43 (s, 2H), 2.41 (s, 3H); ^{13}C NMR (100 MHz, $CDCl_3$) (δ, ppm) 144.6, 144.0, 138.4, 136.9, 134.9, 133.9, 132.4, 131.0, 129.8, 128.7, 127.9, 127.3, 127.2, 126.7,125.3, 115.2, 37.6, 21.7. HRMS (TOF MS ESI$^+$) calculated for $C_{22}H_{21}ClNO_2S$ [M+H]$^+$: 398.0976, found 398.0979.

4-Methyl-*N*-[2-(2-phenylallyl)phenyl]benzenesulfonamide （4f）.

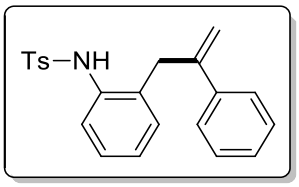

Following the general procedure A, 46.9 mg, 86% yield; Following the general procedure B, 39.8 mg, 73% yield. Yellow solid, mp: 140-141 °C. ^{1}H NMR (400 MHz, $CDCl_3$) (δ, ppm) 7.59 (d, *J* = 8.2 Hz, 2H), 7.41 (d, *J* = 7.9 Hz, 1H), 7.30-7.28 (comp, 5H), 7.22-7.18 (comp, 3H), 7.11-7.10 (comp, 2H), 6.59 (s, 1H), 5.44 (s, 1H), 4.75 (s, 1H), 3.43 (s, 2H), 2.40 (s, 3H); ^{13}C NMR (100 MHz, $CDCl_3$) (δ, ppm) 145.6, 143.9, 140.0, 136.9, 135.0, 132.5, 131.1, 129.7, 128.5, 128.1, 127.8, 127.2, 126.5, 125.9, 125.1, 114.6, 37.6, 21.7. HRMS (TOF MS ESI$^+$) calculated for $C_{22}H_{22}NO_2S$ $[M+H]^+$: 364.1366, found 364.1378.

***N*-{2-[2-(4-Iodophenyl)allyl]phenyl}-4-methylbenzenesulfonamide (4g).**

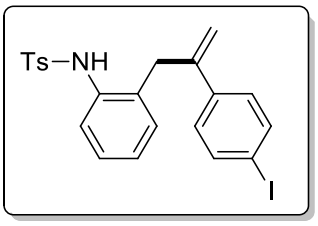

Following the general procedure A, 55.8 mg, 76% yield. Yellow solid, mp: 150-151 °C. ^{1}H NMR (400 MHz, $CDCl_3$) (δ, ppm) 7.61-7.57 (comp, 4H), 7.35 (d, *J* = 7.9 Hz, 1H), 7.23-7.17 (m, 3H), 7.12-7.06 (comp, 2H), 7.02- 7.00 (comp, 2H), 6.47 (s, 1H), 5.44 (s, 1H), 4.79 (s, 1H), 3.42 (s, 2H), 2.41 (s, 3H); ^{13}C NMR (100 MHz, $CDCl_3$) (δ, ppm) 144.7, 144.0, 139.5, 137.6, 136.9, 134.9, 132.4, 131.0, 129.8, 127.9, 127.8, 127.3, 126.7, 125.3, 115.4, 93.7, 37.4, 21.7. HRMS (TOF MS ESI$^+$) calculated for $C_{22}H_{21}INO_2S$ $[M+H]^+$: 490.0332, found 490.0319.

***N*-{2-[2-(3-Bromophenyl)allyl]phenyl}-4-methylbenzenesulfonamide (4h).**

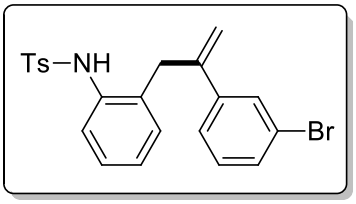

Following the general procedure A, 53.0 mg, 80% yield; Following the general procedure B, 43.1 mg, 65% yield. Yellow solid, mp: 135-136 °C. ^{1}H NMR (400 MHz, $CDCl_3$) (δ, ppm) 7.57 (d, *J* = 8.3 Hz, 2H), 7.42-7.38 (comp, 3H), 7.24-7.22 (m, 4H), 7.20-7.07 (comp, 3H), 6.40 (s, 1H), 5.43 (s, 1H), 4.75 (s, 1H), 3.35 (s, 2H), 2.42 (s, 3H); ^{13}C NMR (150 MHz, $CDCl_3$) (δ, ppm) 144.4, 144.1, 142.2, 136.9, 134.9, 132.4, 131.2, 131.0, 130.1, 129.9, 129.1, 128.0, 127.2, 126.8, 125.7, 124.7, 122.8, 115.7, 37.3, 21.7. HRMS (TOF MS ESI$^+$) calculated for $C_{22}H_{21}BrNO_2S$ $[M+H]^+$: 442.0471, found 442.0472.

***N*-{2-[2-(2-Fluorophenyl)allyl]phenyl}-4-methylbenzenesulfonamide (4i).**

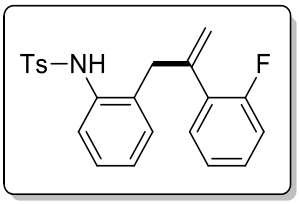

Following the general procedure A, 48.1 mg, 84% yield. Yellow solid, mp: 70-71 °C. ^{1}H NMR (400 MHz, $CDCl_3$) (δ, ppm) 7.59 (d, *J* = 8.2 Hz, 2H), 7.50 (d, *J* = 8.1 Hz, 2H), 7.25-7.16 (comp, 4H), 7.14-7.04 (comp, 5H), 6.61 (s, 1H), 5.22 (s, 1H), 4.85 (s, 1H), 3.33 (s, 2H), 2.37 (s, 3H); ^{13}C NMR (100 MHz, $CDCl_3$) (δ, ppm) 160.9, 158.5, 143.8, 142.8, 136.8, 135.2, 131.2, 131.19 (d, *J* = 3.2 Hz), 129.9 (d, *J* = 4.2 Hz), 129.6, 129.5 (d, *J* = 8.5 Hz), 129.2 (d, *J* = 14.3 Hz), 128.0, 127.2, 126.1, 124.4, 124.3, 118.0 (d, *J* = 3.2 Hz), 115.9 (d, *J* = 22.7 Hz), 38.7, 21.7. HRMS (TOF MS ESI$^+$) calculated for $C_{22}H_{21}FNO_2S$ $[M+H]^+$: 382.1272, found 382.1273.

4-Methyl-*N*-{2-[2-(4-(phenylethynyl)phenyl)allyl]phenyl}benzenesulfonamide (4j).

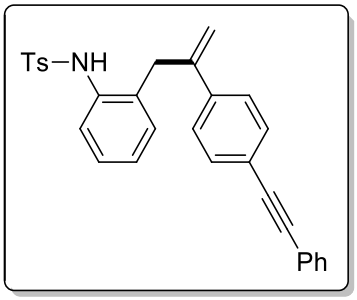

Following the general procedure A, 55.6 mg, 80% yield. Yellow solid, mp: 180-181 °C. ^{1}H NMR (400 MHz, $CDCl_3$) (δ, ppm) 7.56 (d, *J* = 8.2 Hz, 2H), 7.52-7.50 (m, 2H), 7.43 (d, *J* = 8.3 Hz, 2H), 7.39-7.32 (comp, 5H), 7.24-7.19 (comp, 4H), 7.11-7.05 (m, 2H), 6.47 (s, 1H), 5.47 (s, 1H), 4.77 (s, 1H), 3.41 (s, 2H), 2.39 (s, 3H); ^{13}C NMR (100 MHz, $CDCl_3$) (δ, ppm) 144.9, 143.9, 139.7, 137.0, 135.0, 132.5, 131.73, 131.68, 131.1, 129.8, 128.49, 128.48, 127.9, 127.2, 126.6, 125.9, 125.3, 123.3, 122.9, 115.3, 90.4, 89.2, 37.4, 21.7. HRMS (TOF MS ESI$^+$) calculated for $C_{30}H_{26}NO_2S$ [M+H]$^+$: 464.1679, found 464.1674.

4-Methyl-*N*-{2-[2-(4-styrylphenyl)allyl]phenyl}benzenesulfonamide (4k).

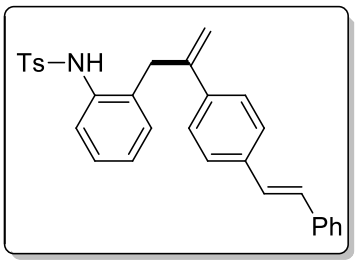

Following the general procedure A, 57.9 mg, 83% yield. Yellow solid, mp: 127-128 °C. ^{1}H NMR (400 MHz, $CDCl_3$) (δ, ppm) 7.60-7.58 (m, 2H), 7.53-7.51 (m, 2H), 7.46-7.44 (m, 2H), 7.42-7.39 (m, 2H), 7.37-7.35 (m, 2H), 7.31-7.28 (comp, 4H), 7.32-7.21 (m, 2H), 7.12-7.10 (comp, 3H), 6.48 (br, 1H), 5.49 (s, 1H), 4.75 (s, 1H), 3.42 (s, 2H), 2.41 (s, 3H); ^{13}C NMR (100 MHz, $CDCl_3$) (δ, ppm) 145.1, 144.0, 139.1, 137.3, 137.2, 137.0, 135.1, 131.1, 129.8, 129.2, 128.89, 128.86, 128.1, 127.92, 129.91, 127.3, 126.68, 126.65, 126.57, 126.3, 125.1, 114.5, 37.6, 21.8. HRMS (TOF MS ESI$^+$) calculated for $C_{30}H_{28}NO_2S$ [M+H]$^+$: 466.1835, found 466.1831.

4-Methyl-*N*-{2-[2-(naphthalen-2-yl)allyl]phenyl}benzenesulfonamide (4l).

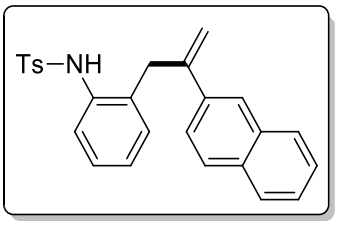

Following the general procedure A, 47.1 mg, 76% yield; Following the general procedure B, 36.6 mg, 59% yield. Yellow solid, mp: 122-123 °C. ^{1}H NMR (400 MHz, $CDCl_3$) (δ, ppm) 7.85-7.77 (comp, 3H), 7.70 (d, *J* = 1.2 Hz, 1H), 7.58 (d, *J* = 8.3 Hz, 2H), 7.53-7.52 (m, 1H), 7.50-7.47 (comp, 2H), 7.42 (d, *J* = 7.4 Hz, 1H), 7.23-7.10 (comp, 5H), 6.57 (s, 1H), 5.59 (s, 1H), 4.85 (s, 1H), 3.54 (s, 2H), 2.39 (s, 3H); ^{13}C NMR (100 MHz, $CDCl_3$) (δ, ppm) 145.5, 143.9, 137.2, 137.1, 135.1, 133.3, 133.1, 132.5, 131.2, 129.8, 128.3, 128.2, 127.9, 127.7, 127.2, 126.6, 126.5, 126.3, 125.3, 124.9, 124.2, 115.1, 37.7, 21.7. HRMS (TOF MS ESI$^+$) calculated for $C_{26}H_{24}NO_2S$ $[M+H]^+$: 414.1522, found 414.1526.

4-Methyl-*N*-{2-[2-(thiophen-2-yl)allyl]phenyl}benzenesulfonamide (4m).

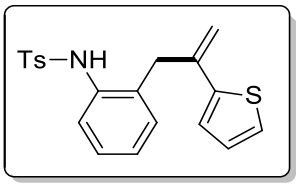

Following the general procedure A, 43.2 mg, 78% yield. Yellow solid, mp: 112-113 °C. ^{1}H NMR (400 MHz, $CDCl_3$) (δ, ppm) 7.58 (d, *J* = 8.2 Hz, 2H), 7.44 (d, *J* = 8.1 Hz, 1H), 7.23-7.21 (m, 3H), 7.19 (d, *J* = 5.1 Hz, 1H), 7.13 (d, *J* = 4.2 Hz, 2H), 6.95-6.93 (m, 1H), 6.86-6.85 (m, 1H), 6.45 (s, 1H), 5.47 (s, 1H), 4.55 (s, 1H), 3.40 (s, 2H), 2.41(s, 3H); ^{13}C NMR (100 MHz, $CDCl_3$) (δ, ppm) 144.0, 143.9, 138.9, 136.9, 135.1, 131.9, 131.2, 129.8, 128.1, 127.5, 127.3, 126.6, 125.2, 124.9, 124.1, 112.9, 37.4, 21.7. HRMS (TOF MS ESI$^+$) calculated for $C_{20}H_{20}NO_2S_2$ $[M+H]^+$: 370.0930, found 370.0939.

4-Methyl-*N*-[2-(2-phenylbut-2-en-1-yl)phenyl]benzenesulfonamide (4n).

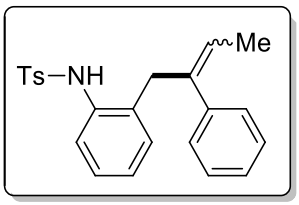

Following the general procedure A, 46.9 mg, 83% overall yield. (*E* : *Z* = 1.2 : 1). ***E*:** ^{1}H NMR (400 MHz, $CDCl_3$) (δ, ppm) 7.59 (d, *J* = 8.2 Hz, 2H), 7.32 (d, *J* = 7.9 Hz, 1H), 7.22-7.15 (comp, 5H), 7.13-7.00 (comp, 5H), 6.43 (s, 1H), 6.05 (q, *J* = 6.9 Hz, 1H), 3.51 (s, 2H), 2.38 (s, 3H), 1.71 (d, *J* = 6.9 Hz, 3H); ^{13}C NMR (100 MHz, $CDCl_3$) (δ, ppm) 143.9, 142.3, 137.1, 137.0, 134.7, 132.6, 129.8, 129.6, 128.4, 127.3, 127.2, 126.9, 126.4, 126.3, 126.1, 124.5, 31.9, 21.7, 14.5. HRMS (TOF MS ESI$^+$) calculated for $C_{23}H_{24}NO_2S$ [M+H]$^+$: 378.1522, found 378.1528. ***Z*:** ^{1}H NMR (400 MHz, $CDCl_3$) (δ, ppm) 7.56 (d, *J* = 8.3 Hz, 2H), 7.42 (d, *J* = 8.0 Hz, 1H), 7.31-7.27 (m, 2H), 7.25-7.23 (m, 2H), 7.20-7.16 (comp, 3H), 7.06-7.02 (m, 1H), 6.98-6.96 (m, 2H), 6.53 (s, 1H), 5.38 (q, *J* = 7.0 Hz, 1H), 3.19 (s, 2H), 2.37 (s, 3H), 1.54 (s, 3H); ^{13}C NMR (150 MHz, $CDCl_3$) (δ, ppm) 143.9, 139.9, 139.5, 137.1, 135.3, 131,9, 131.3, 129.7, 128.5, 128.2, 127.8, 127.2, 127.1, 126.1, 124.4, 123.9, 41.8, 21.7, 14.9. HRMS (TOF MS ESI$^+$) calculated for $C_{23}H_{24}NO_2S$ [M+H]$^+$: 378.1522, found 378.1526.

_N_-{2-[(3,4-Dihydronaphthalen-1-yl)methyl]phenyl}-4-methylbenzenesulfonamide (4o).

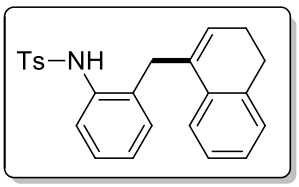

Following the general procedure A, 45.6 mg, 78% yield; Following the general procedure B, 37.4 mg, 64% yield. Yellow solid, mp: 120-121 °C. ^{1}H NMR (400 MHz, $CDCl_3$) (δ, ppm) 7.57 (d, *J* = 8.2 Hz, 2H), 7.49 (d, *J* = 8.0 Hz, 1H), 7.23-7.09 (comp, 8H), 6.91 (d, *J* = 7.4 Hz, 1H), 6.55 (s, 1H), 5.46 (t, *J* = 4.4 Hz, 1H), 3.34 (s, 2H), 2.77 (t, *J* = 8.0 Hz, 2H), 2.41(s, 3H), 2.23-2.20 (m, 2H); ^{13}C NMR (100 MHz, $CDCl_3$) (δ, ppm) 144.0, 136.9, 136.7, 135.3, 134.2, 133.6, 131.8, 131.1, 129.80, 129.76, 127.9, 127.7, 127.4, 127.3, 126.5, 126.2, 124.3, 122.7, 35.0, 28.2, 23.3, 21.7. HRMS (TOF MS ESI$^+$) calculated for $C_{24}H_{24}NO_2S$ [M+H]$^+$: 390.1522, found 390.1517.

(1*S*,2*R*,5*S*)-2-Isopropyl-5-methylcyclohexyl 4-{3-[2-(4-methylphenylsulfonamido)phenyl]prop-1-en-2-yl}benzoate (4p).

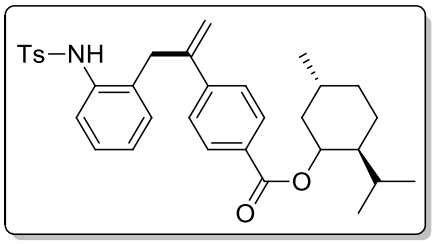

Following the general procedure A, 58.5 mg, 71% yield; Following the general procedure B, 47.8 mg, 58% yield. Yellow oil. ^{1}H NMR (400 MHz, $CDCl_3$) (δ, ppm) 7.94 (d, *J* = 8.0 Hz, 2H), 7.59 (d, *J* = 8.0 Hz, 2H), 7.37-7.31 (comp, 3H), 7.23-7.17 (comp, 3H), 7.10-7.18 (m, 2H), 6.49 (br, 1H), 5.53 (s, 1H), 4.96-4.89 (m, 1H), 4.88 (s, 1H), 3.48 (s, 2H), 2.40 (s, 3H), 2.15-2.10 (m, 1H), 1.97-1.91 (m, 1H), 1.75-1.71 (m, 2H), 1.60-1.51 (m, 2H), 1.32-1.27 (m, 1H), 1.16-1.06 (m, 1H), 0.94-0.91 (comp, 6H), 0.79 (d, *J* = 8.0 Hz, 3H); ^{13}C NMR (100 MHz, $CDCl_3$) (δ, ppm) 165.9, 144.9, 144.2, 144.0, 136.9, 134.9, 132.4, 130.9, 130.3, 129.8, 127.9, 127.3, 126.7, 125.9, 125.4, 116.6, 75.1, 47.4, 41.1, 37.4, 34.5, 31.6, 26.7, 23.8, 22.2, 21.7, 20.9, 16.7. HRMS (TOF MS ESI$^+$) calculated for $C_{33}H_{40}NO_4S$ $[M+H]^+$: 546.2678, found 546.2687.

{(3a*R*,5*R*,5a*S*,8a*S*,8b*R*)-2,2,7,7-tetramethyltetrahydro-3a*H*-bis([1,3]dioxolo)[4,5-*b*:4',5'-d]pyran-5-yl}methyl 4-{3-[2-(4-methylphenylsulfonamido)phenyl]prop-1-en-2-yl}benzoate (4q).

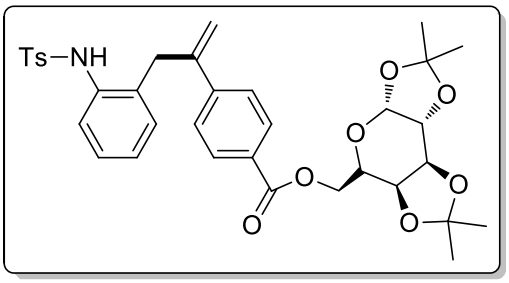

Following the general procedure A, 60.4 mg, 62% yield; Following the general procedure B, 52.6 mg, 54% yield. Yellow oil. ^{1}H NMR (400 MHz, $CDCl_3$) (δ, ppm) 7.97 (d, *J* = 8.0 Hz, 2H),

7.58 (d, *J* = 8.0 Hz, 2H), 7.38-7.31 (comp, 3H), 7.24-7.18 (comp, 3H), 7.13-7.06 (m, 2H), 6.38 (br, 1H), 5.57 (d, *J* = 5.6 Hz, 1H), 5.53 (s, 1H), 4.86 (s, 1H), 4.67-4.64 (m, 1H), 4.55-4.51 (m, 1H), 4.45-4.40 (m, 1H), 4.36-4.31 (m, 2H), 4.20-4.16 (m, 1H), 3.45 (s, 2H), 2.41 (s, 3H), 1.58 (m, 2H), 1.52 (s, 3H), 1.48 (s, 3H), 1.36 (s, 3H), 1.34 (s, 3H); ^{13}C NMR (100 MHz, $CDCl_3$) (δ, ppm) 166.2, 145.0, 144.6, 144.1, 137.1, 135.0, 132.4, 131.1, 130.0, 129.8, 129.6, 128.2, 128.0, 127.9, 127.7, 127.3, 126.8, 126.0, 125.5, 116.6, 109.9, 109.0, 96.5, 71.3, 70.9, 70.7, 66.3, 64.1, 37.5, 26.2, 26.2, 25.1, 24.7, 21.7. HRMS (TOF MS ESI$^+$) calculated for $C_{35}H_{40}NO_9S$ [M+H]$^+$: 650.2424, found 650.2430.

(3*S*,8*R*,9*S*,10*S*,13*R*,14*S*,17*R*)-10,13-dimethyl-17-[(*R*)-6-methylheptan-2-yl]hexadecahydro-1*H*-cyclopenta[*a*]phenanthren-3-yl 4-{3-[2-(4-methylphenylsulfonamido)phenyl]prop-1-en-2-yl}benzoate (4r).

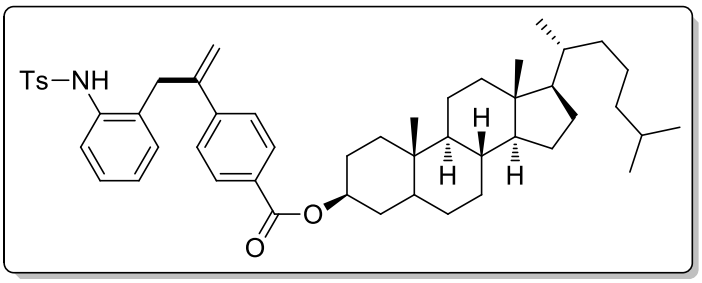

Following the general procedure A, 70.0 mg, 60% yield; Following the general procedure B, 57.2 mg, 49% yield. Yellow oil. ^{1}H NMR (400 MHz, $CDCl_3$) (δ, ppm) 7.94 (d, *J* = 8.0 Hz, 2H), 7.58 (d, *J* = 8.0 Hz, 2H), 7.36 (d, *J* = 7.4 Hz, 1H), 7.31 (d, *J* = 7.3 Hz, 2H), 7.22 (d, *J* = 7.3 Hz, 2H), 7.19-7.17 (m, 1H), 7.12-7.05 (m, 2H), 6.47 (br, 1H), 5.53 (s, 1H), 4.89-4.81 (comp, 2H), 3.47 (s, 2H), 2.46 (d, *J* = 2.5 Hz, 2H), 2.41 (s, 3H), 2.04-1.99 (comp, 3H), 1.86-1.82 (m, 1H), 1.75-1.68 (m, 1H), 1.61-1.48 (comp, 7H), 1.36-1.33 (comp, 4H), 1.27-1.22 (comp, 3H), 1.16-1.09 (comp, 5H), 1.07 (s, 3H), 1.05-1.00 (comp, 3H), 0.92-0.90 (comp, 3H), 0.88-0.85 (comp, 6H), 0.69 (s, 3H); ^{13}C NMR (100 MHz, $CDCl_3$) (δ, ppm) 165.8, 144.9, 144.2, 144.0, 139.7, 137.0, 134.9, 132.4, 131.0, 130.3, 129.8, 128.0, 127.3, 126.7, 125.9, 125.4, 123.0, 121.8, 116.6, 74.8, 71.9, 56.8, 56.3, 50.2, 42.5, 39.9, 39.7, 38.4, 37.4, 37.2, 36.8, 36.3, 35.9, 32.1, 28.4, 28.2, 28.0, 24.4, 24.0, 23.0, 22.7, 21.7, 21.2, 19.5, 18.8, 12.0. HRMS (TOF MS ESI$^+$) calculated for $C_{50}H_{68}NO_4S$ [M+H]$^+$: 778.4869, found 778.4888.

***N*-{2-[3-(4-Bromophenyl)but-3-en-2-yl]phenyl}-4-methylbenzenesulfonamide (5a).**

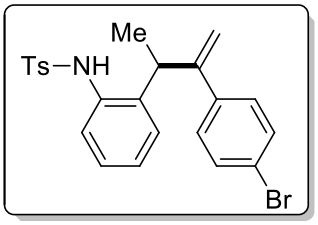

Following the general procedure A, 54.7 mg, 80% yield. Yellow solid, mp: 104-105 °C. ^{1}H NMR (400 MHz, $CDCl_3$) (δ, ppm) 7.63 (d, *J* = 8.3 Hz, 2H), 7.36 (d, *J* = 8.5 Hz, 2H), 7.25-7.23 (m, 2H), 7.21-7.11 (comp, 4H), 7.06 (d, *J* = 8.5 Hz, 2H), 6.41 (s, 1H), 5.28 (s, 1H), 4.92 (s, 1H), 3.90 (t, *J* = 6.9 Hz, 1H), 2.41 (s, 3H), 1.24 (d, *J* = 7.0 Hz, 3H); ^{13}C NMR (100 MHz, $CDCl_3$) (δ, ppm) 145.8, 143.9, 139.5, 138.4, 138.1, 137.9, 133.0, 131.5, 130.0, 129.8, 128.8, 128.2, 127.7, 127.2, 121.8, 114.6, 37.8, 21.7, 19.1. HRMS (TOF MS ESI$^+$) calculated for $C_{23}H_{23}BrNO_2S$ $[M+H]^+$: 456.0627, found 456.0638.

***N*-{2-[2-(4-Bromophenyl)-1-phenylallyl]-4-chlorophenyl}-4-methylbenzenesulfonamide (5b).**

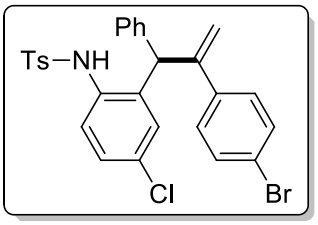

Following the general procedure A, 68.0 mg, 82% yield. Yellow solid, mp: 154-155 °C. ^{1}H NMR (400 MHz, $CDCl_3$) (δ, ppm) 7.58 (d, *J* = 8.2 Hz, 2H), 7.38-7.26 (comp, 8H), 7.20-7.17 (m, 1H), 7.05 (d, *J* = 8.5 Hz, 2H), 6.86 (d, *J* = 6.2 Hz, 2H), 6.76 (d, *J* =2.3 Hz, 1H), 6.17 (s, 1H), 5.70 (s, 1H), 4.87 (s, 1H), 4.65 (s, 1H), 2.46 (s, 3H); ^{13}C NMR (100 MHz, $CDCl_3$) (δ, ppm) 147.3, 144.4, 139.2, 138.99, 138.91, 137.1, 132.8, 132.6, 131.8, 130.1, 130.0, 129.4, 129.2, 128.1, 127.8, 127.7, 127.3, 122.2, 118.8, 50.9, 21.8. HRMS (TOF MS ESI$^+$) calculated for $C_{28}H_{23}BrClNO_2SNa$ $[M+Na]^+$: 574.0214, found 574.0199.

***N*-{2-[2-(4-Bromophenyl)allyl]-5-fluorophenyl}-4-methylbenzenesulfonamide (5c).**

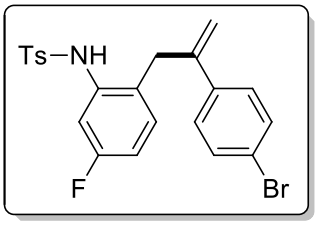

Following the general procedure A, 57.9 mg, 84% yield. Yellow solid, mp: 135-136 °C. ^{1}H NMR (400 MHz, $CDCl_3$) (δ, ppm) 7.62 (d, *J* = 8.3 Hz, 2H), 7.42-7.39 (m, 2H), 7.24 (d, *J* = 8.1 Hz, 2H), 7.20-7.16 (m, 1H), 7.14-7.11 (m, 2H), 7.03-6.99 (m, 1H), 6.81-6.76 (m, 1H), 6.59 (s, 1H), 5.43 (s, 1H), 4.80 (s, 1H), 3.41 (s, 2H), 2.42 (s, 3H); ^{13}C NMR (100 MHz, $CDCl_3$) (δ, ppm) 161.9 (d, *J* = 244.5 Hz), 144.4, 144.3, 138.6, 136.6, 136.4 (d, *J* = 10.6 Hz), 132.1 (d, *J* = 9.0 Hz), 131.7, 129.9, 128.3, 127.6, 127.3, 126.6 (d, *J* = 3.4 Hz), 122.2, 115.5, 113.0 (d, *J* = 21.1 Hz), 111.3 (d, *J* = 25.2 Hz), 36.9, 21.7. HRMS (TOF MS ESI$^+$) calculated for $C_{22}H_{20}BrFNO_2S$ [M+H]$^+$: 460.0377, found 460.0368.

_N_-{2-[2-(4-Bromophenyl)allyl]-5-chlorophenyl}-4-methylbenzenesulfonamide (5d).

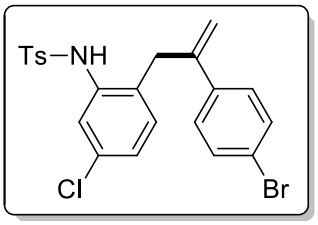

Following the general procedure A, 57.8 mg, 81% yield. Yellow solid, mp: 132-134 °C. ^{1}H NMR (400 MHz, $CDCl_3$) (δ, ppm) 7.61 (d, *J* = 8.2 Hz, 2H), 7.42-7.39 (comp, 3H), 7.26-7.24 (m, 2H), 7.13-7.05 (comp, 3H), 7.00-6.98 (m, 1H), 6.49 (s, 1H), 5.44 (s, 1H), 4.81 (s, 1H), 3.40 (s, 2H), 2.42 (s, 3H); ^{13}C NMR (100 MHz, $CDCl_3$) (δ, ppm) 144.4, 144.2, 138.6, 136.6, 136.2, 133.4, 131.9, 131.7, 130.1, 129.9, 127.6, 127.3, 126.5, 124.6, 122.3, 115.6, 37.1, 21.8. HRMS (TOF MS ESI$^+$) calculated for $C_{22}H_{20}BrClNO_2S$ [M+H]$^+$: 476.0081, found 476.0080.

_N_-{5-Bromo-2-[2-(4-bromophenyl)allyl]phenyl}-4-methylbenzenesulfonamide (5e).

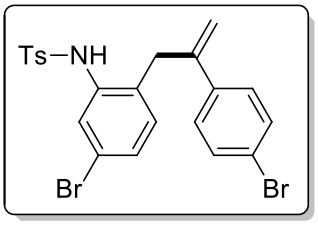

Following the general procedure A, 61.7 mg, 79% yield. Yellow solid, mp: 137-138 °C. ^{1}H NMR (400 MHz, $CDCl_3$) (δ, ppm) 7.57 (d, *J* = 8.4 Hz, 2H), 7.53-7.50 (m, 1H), 7.37 (d, *J* = 8.4 Hz, 2H), 7.22-7.17 (comp, 4H), 7.08 (d, *J* = 8.5 Hz, 2H), 6.90 (d, *J* = 8.2 Hz, 1H), 6.43 (s, 1H), 5.41 (s, 1H), 4.77 (s, 1H), 3.35 (s, 2H), 2.39 (s, 3H); ^{13}C NMR (100 MHz, $CDCl_3$) (δ, ppm) 144.4, 144.1, 138.5, 136.6, 136.4, 132.3, 131.7, 130.8, 129.9, 129.5, 127.63, 127.61, 127.3, 122.3, 121.1, 115.6, 37.2, 21.8. HRMS (TOF MS ESI$^+$) calculated for $C_{22}H_{19}Br_2NO_2SNa$ [M+Na]$^+$: 543.9375, found 543.9363.

***N*-{2-[2-(4-Bromophenyl)allyl]-3-methylphenyl}-4-methylbenzenesulfonamide (5f).**

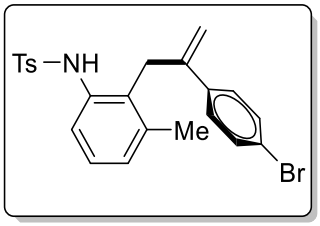

Following the general procedure A, 56.7 mg, 83% yield. Yellow solid, mp: 114-115 °C. ^{1}H NMR (400 MHz, $CDCl_3$) (δ, ppm) 7.60 (d, *J* = 8.2 Hz, 2H), 7.48 (d, *J* = 8.2 Hz, 2H), 7.26-7.21 (comp, 5H), 7.13 (t, *J* = 7.8 Hz, 1H), 7.05 (d, *J* = 7.4 Hz, 1H), 6.32 (s, 1H), 5.28 (s, 1H), 4.40 (s, 1H), 3.39 (s, 1H), 2.41 (s, 3H), 2.19 (s, 3H); ^{13}C NMR (100 MHz, $CDCl_3$) (δ, ppm) 143.9, 143.6, 139.6, 138.4, 137.1, 135.2, 131.6, 131.3, 129.7, 128.7, 127.5, 127.4, 127.3, 123.2, 122.1, 113.5, 32.8, 21.7, 20.0. HRMS (TOF MS ESI$^+$) calculated for $C_{23}H_{23}BrNO_2S$ [M+H]$^+$: 456.0627, found 456.0615.

***N*-{2-[2-(4-Bromophenyl)allyl]-6-methylphenyl}-4-methylbenzenesulfonamide (5g).**

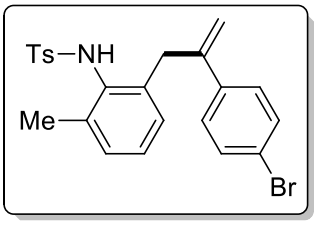

Following the general procedure A, 56.0 mg, 82% yield. Yellow solid, mp: 157-158 °C. ^{1}H NMR (400 MHz, $CDCl_3$) (δ, ppm) 7.58 (d, *J* = 8.2 Hz, 2H), 7.39 (d, *J* = 8.5 Hz, 2H), 7.21 (d, *J* = 8.2 Hz, 2H), 7.13 (d, *J* = 8.5 Hz, 2H), 7.11-7.06 (m, 2H), 7.01-6.99 (m, 1H), 5.96 (s, 1H), 5.38 (s, 1H), 4.72 (s, 1H), 3.51 (s, 2H), 2.42 (s, 3H), 2.10 (s, 3H); ^{13}C NMR (100 MHz, $CDCl_3$) (δ, ppm) 145.8, 143.9, 139.5, 138.4, 138.1, 137.9, 133.0, 131.5, 130.0, 129.8, 128.8, 128.2, 127.7, 127.2, 121.8, 114.6, 37.8, 21.7, 19.1. HRMS (TOF MS ESI$^+$) calculated for $C_{23}H_{23}BrNO_2S$ $[M+H]^+$: 456.0627, found 456.0612.

***N*-{2-[2-(4-Bromophenyl)allyl]-4-methylphenyl}-4-methylbenzenesulfonamide (5h).**

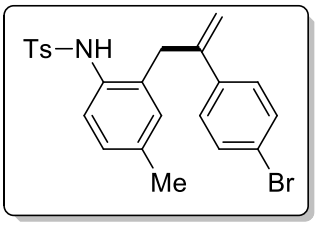

Following the general procedure A, 53.4 mg, 78% yield. Yellow solid, mp: 149-150

°C. ^{1}H NMR (400 MHz, $CDCl_3$) (δ, ppm) 7.57 (d, *J* = 8.2 Hz, 2H), 7.40 (d, *J* = 8.5 Hz, 2H), 7.22-7.14 (comp, 5H), 6.98 (d, *J* = 8.1 Hz, 1H), 6.88 (s, 1H), 6.39 (s, 1H), 5.42 (s, 1H), 4.77 (s, 1H), 3.88 (s, 2H), 2.41 (s, 3H), 2.25 (s, 3H); ^{13}C NMR (100 MHz, $CDCl_3$) (δ, ppm) 144.8, 143.9, 139.1, 137.1, 136.8, 133.06, 133.04, 132.1, 131.6, 129.7, 128.5, 127.6, 127.3, 126.0, 121.9, 115.1, 37.3, 21.7, 21.1. HRMS (TOF MS ESI$^+$) calculated for $C_{23}H_{23}BrNO_2S$ $[M+H]^+$: 456.0627, found

456.0615.

***N*-{2-[2-(4-Bromophenyl)allyl]-4-methoxyphenyl}-4-methylbenzenesulfonamide (5i).**

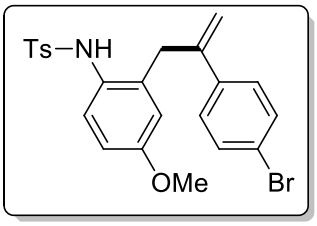

Following the general procedure A, 53.8 mg, 76% yield. Yellow solid, mp: 129-130 °C. ^{1}H NMR (400 MHz, $CDCl_3$) (δ, ppm) 7.55 (d, *J* = 8.2 Hz, 2H), 7.39 (d, *J* = 8.5 Hz, 2H), 7.22 (d, *J* = 8.2 Hz, 2H), 7.15-7.10 (comp, 3H), 6.70-6.67 (m, 1H), 6.62 (d, *J* = 2.8 Hz, 1H), 6.24 (s, 1H), 5.43 (s, 1H), 4.81 (s, 1H), 3.72 (s, 3H), 3.40 (s, 2H), 2.42 (s, 3H); ^{13}C NMR (100 MHz, $CDCl_3$) (δ, ppm) 158.6, 144.7, 143.8, 139.0, 136.9, 136.6, 131.6, 129.7, 128.8, 127.7, 127.3, 127.2, 121.9, 116.2, 115.3, 112.5, 55.4, 37.4, 21.7. HRMS (TOF MS ESI$^+$) calculated for $C_{23}H_{23}BrNO_3S$ $[M+H]^+$: 472.0577, found 472.0565.

***N*-{2-[2-(4-Bromophenyl)allyl]phenyl}-4-chlorobenzenesulfonamide (5j).**

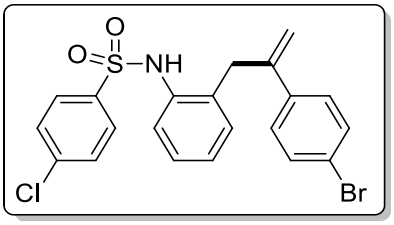

Following the general procedure A, 52.7 mg, 76% yield. Yellow solid, mp: 134-135 °C. ^{1}H NMR (400 MHz, $CDCl_3$) (δ, ppm) 7.62 (d, *J* = 8.6 Hz, 2H), 7.43-7.38 (comp, 4H), 7.32 (d, *J* = 7.8 Hz, 1H), 7.23-7.09 (comp, 5H), 6.52 (s, 1H), 5.44 (s, 1H), 4.79 (s, 1H), 3.45 (s, 2H); ^{13}C NMR (100 MHz, $CDCl_3$) (δ, ppm) 144.6, 139.7, 138.8, 138.4, 134.5, 132.7, 131.7, 131.3, 129.5, 128.7, 128.1, 127.6, 127.1, 125.5, 122.2, 115.3, 37.6. HRMS (TOF MS ESI$^+$) calculated for $C_{21}H_{18}BrClNO_2S$ $[M+H]^+$: 461.9925, found 461.9918.

***N*-{2-[2-(4-Bromophenyl)allyl]phenyl}-4-nitrobenzenesulfonamide (5k).**

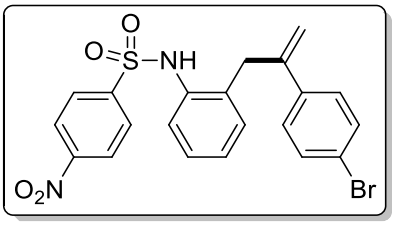

Following the general procedure A, 56.0 mg, 79% yield. Yellow solid, mp: 140-141 °C. ^{1}H NMR (400 MHz, $CDCl_3$) (δ, ppm) 8.27 (d, *J* = 8.8 Hz, 2H), 7.87 (d, *J* = 8.8 Hz, 2H), 7.43 (d, *J* = 8.4 Hz, 2H), 7.29-7.25 (m, 2H), 7.23-7.13 (comp, 4H), 6.59 (s, 1H), 5.44 (s, 1H), 4.79 (s, 1H), 3.47 (s, 2H); ^{13}C NMR (100 MHz, $CDCl_3$) (δ, ppm) 145.56, 144.74, 138.71, 134.0, 133.0, 131.8, 131.6, 128.5, 128.3, 127.7, 127.6, 125.6, 124.4, 122.4, 115.5, 115.4, 37.8. HRMS (TOF MS ESI$^+$) calculated for $C_{21}H_{17}BrN_2O_4SNa$ [M+Na]$^+$: 494.9985, found 494.9975.

Benzyl {2-[2-(4-bromophenyl)allyl]phenyl}carbamate (5l).

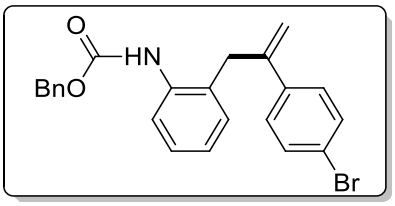

Following the general procedure A, 41.2 mg, 65% yield. Yellow solid, mp: 90-91 °C. ^{1}H NMR (400 MHz, $CDCl_3$) (δ, ppm) 7.76 (br, 1H), 7.44-7.34 (comp, 7H), 7.29-7.24 (comp, 3H), 7.17-7.15 (m, 1H), 7.09-7.06 (m, 1H), 6.54 (s, 1H), 5.48 (s, 1H), 5.18 (s, 2H), 4.90 (s, 1H), 3.73 (s, 2H); ^{13}C NMR (100 MHz, $CDCl_3$) (δ, ppm) 154.0, 144.9, 144.8, 139.4, 136.3, 136.1, 131.7, 130.8, 128.7, 128.47, 128.45, 127.9, 127.8, 124.9, 122.0, 119.8, 115.2, 67.2, 37.8. HRMS (TOF MS ESI$^+$) calculated for $C_{23}H_{20}BrNO_2Na$ [M+Na]$^+$: 444.0570, found 444.0563.

***N*-{2-(2-(4-Bromophenyl)-1-phenylallyl)benzofuran-3-yl)-4-methylbenzenesulfonamide (5m).**

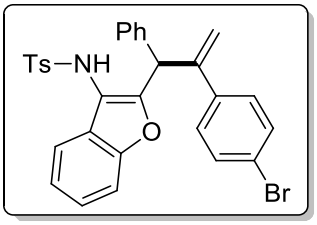

Following the general procedure B in the absence of Cs_2CO_3, 56.1 mg, 67% yield. Yellow oil. ^{1}H NMR (400 MHz, $CDCl_3$) (δ, ppm) 7.60 (d, *J* = 7.60 Hz, 2H), 7.36-7.31 (comp, 3H), 7.26-7.14 (comp, 10H), 7.04-7.69 (m, 2H), 5.99 (s, 1H), 5.51 (comp, 2H), 4.93 (s, 1H), 2.34 (s, 3H); ^{13}C NMR (100 MHz, $CDCl_3$) (δ, ppm) 155.1, 153.4, 146.7, 144.2, 139.5, 138.2, 136.5, 131.5, 129.8, 129.2, 128.7, 128.3, 127.7, 127.3, 125.8, 124.5, 123.2, 121.8, 119.0, 117.2, 113.6, 111.7, 47.0, 21.7. HRMS (TOF MS ESI$^+$) calculated for $C_{30}H_{25}BrNO_3S$ [M+H]$^+$: 558.0739, found: 558.0730.

General Procedure for the Preparation of Terminal Alkenes 7 (Method C, , related to Scheme 2).

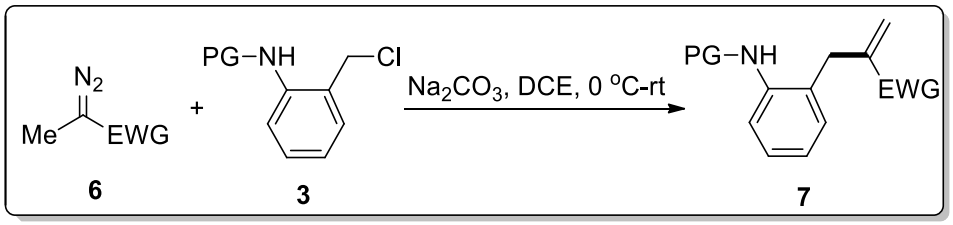

To a 10 mL oven-dried flask containing a magnetic stirring bar, sulfonaminobenzyl chloride **3a** (59.2 mg, 0.2 mmol), α-methyl diazo compounds **6** (0.15 mmol), Na_2CO_3 (25.4 mg, 0.24 mmol) and DCE (2.0 mL) were added in sequence at 0 °C under argon atmosphere. The reaction mixture was stirred under these conditions for 8 h and the temperature was warmed to room temperature slowly. Then the reaction mixture was quenched with H_2O and extracted with DCM (15 X 3 mL). The organic phase was dried with anhydrous Na_2SO_4 and the solvent was evaporated under vacuum after filtration. The resulting residues was purified by column chromatography on silica gel with hexanes/ethyl acetate (10:1 to 5:1) as the eluent to give the desired pure products **7** in moderate to good or high yields.

***N*-Methyl-2-{2-[(4-methylphenyl)sulfonamide]benzyl}-*N*-phenylacrylamide (7a).**

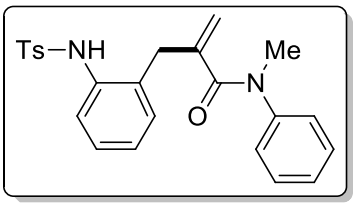

50.4 mg, 80% yield. Yellow solid, mp: 131-132 °C. ^{1}H NMR (400 MHz, $CDCl_3$) (δ, ppm) 8.68 (s, 1H), 7.71 (d, *J* = 8.0 Hz, 2H), 7.58 (d, *J* = 8.0 Hz, 1H), 7.34-7.24 (comp, 6H), 7.12 (t, *J* = 7.4 Hz, 1H), 7.02 (d, *J* = 7.3 Hz, 1H), 6.83 (d, *J* = 7.2 Hz, 2H), 4.98 (s, 1H), 4.81 (s, 1H), 3.38 (s, 3H), 3.16 (s, 2H), 2.42 (s, 3H); ^{13}C NMR (100 MHz, $CDCl_3$) (δ, ppm) 171.8, 144.5, 143.3, 141.8, 137.7, 135.4, 131.3, 131.1, 129.54, 129.50, 128.1, 127.4, 127.2, 126.5, 125.5, 124.9, 121.6, 38.3, 35.6, 21.7. HRMS (TOF MS ESI$^+$) calculated for $C_{24}H_{25}N_2O_3S$ $[M+H]^+$: 421.1580, found 421.1596.

***N*-(4-Methoxyphenyl)-*N*-methyl-2-{2-[(4-methylphenyl)sulfonamido]benzyl}acrylamide (7b).**

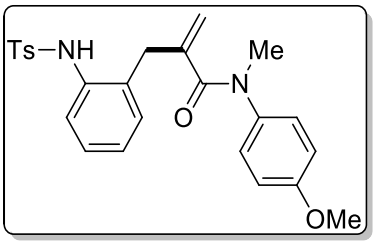

56.7 mg, 84% yield. Yellow solid, mp: 123-124 °C. ^{1}H NMR (400 MHz, $CDCl_3$) (δ, ppm) 8.57 (s, 1H), 7.65 (d, *J* = 8.2 Hz, 2H), 7.52 (d, *J* = 8.0 Hz, 1H), 7.23-7.18 (comp, 3H), 7.06 (t, *J* = 7.4 Hz, 1H), 6.96 (d, *J* = 7.4 Hz, 1H), 6.78 (d, *J* = 8.8 Hz, 2H), 6.68 (d, *J* = 8.2 Hz, 2H), 4.91 (s, 1H), 4.76 (s, 1H), 3.79 (s, 3H), 3.28 (s, 3H), 3.09 (s, 2H), 2.37 (s, 3H); ^{13}C NMR (100 MHz, $CDCl_3$) (δ, ppm) 171.8, 158.6, 143.3, 141.9, 137.7, 137.4, 135.4, 131.3, 131.2, 129.6, 128.1, 127.6, 127.2, 125.5, 124.9, 121.3, 114.6, 55.6, 38.4, 35.7, 21.7. HRMS (TOF MS ESI$^+$) calculated for $C_{25}H_{26}N_2O_4S$ $[M+H]^+$: 451.1686, found 451.1691.

***N*-(4-Chlorophenyl)-*N*-methyl-2-{2-[(4-methylphenyl)sulfonamido]benzyl}acrylamide**

(7c).

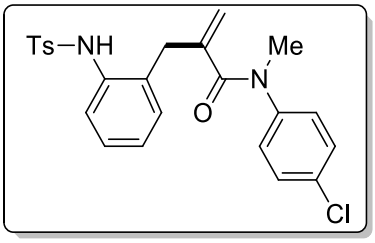

51.9 mg, 76% yield. Yellow solid, mp: 131-132 °C. ^{1}H NMR (400 MHz, $CDCl_3$) (δ, ppm) 8.53 (s, 1H), 7.65 (d, *J* = 8.0 Hz, 2H), 7.51 (d, *J* = 8.1 Hz, 1H), 7.26-7.19 (comp, 5H), 7.09 (t, *J* = 7.4 Hz, 1H), 6.97 (d, *J* = 7.1 Hz, 1H), 6.67 (d, *J* = 8.5 Hz, 1H), 5.01 (s, 1H), 4.76 (s, 1H), 3.29 (s, 3H), 3.12 (s, 2H), 2.37 (s, 3H); ^{13}C NMR (100 MHz, $CDCl_3$) (δ, ppm) 171.7, 143.4, 143.1, 141.6, 137.6, 135.3, 133.1, 131.3, 131.1, 129.7, 129.6, 128.2, 127.8, 127.2, 125.6, 125.2, 121.9, 38.3, 35.6, 21.7. HRMS (TOF MS ESI$^+$) calculated for $C_{24}H_{24}ClN_2O_3S$ [M+H]$^+$: 455.1191, found 455.1195.

***N*-Methyl-2-[2-(4-methylphenylsulfonamido)benzyl]-*N*-(*m*-tolyl)acrylamide (7d).**

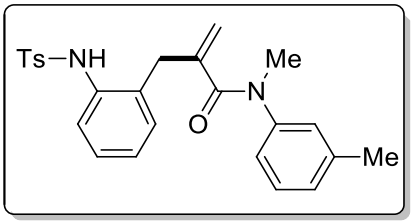

50.2 mg, 77% yield. Yellow solid, mp: 108-109 °C. ^{1}H NMR (400 MHz, $CDCl_3$) (δ, ppm) 8.65 (s, 1H), 7.66 (d, *J* = 8.0 Hz, 2H), 7.56-7.53 (m, 1H), 7.25-7.13 (comp, 4H), 7.10-7.02 (comp, 2H), 6.98-6.95 (m, 1H), 6.62-6.61 (m, 1H), 6.46 (s, 1H), 4.97 (s, 1H), 4.78 (s, 1H), 3.30 (s, 3H), 3.11 (s, 2H), 2.37 (s, 3H), 2.25 (s, 3H); ^{13}C NMR (100 MHz, $CDCl_3$) (δ, ppm) 171.1, 144.5, 143.3, 141.8, 139.5, 137.7, 135.4, 131.4, 131.1, 129.6, 129.3, 128.2, 128.0, 127.2, 127.18, 125.6, 125.2, 123.5, 38.4, 35.7, 21.7, 21.4. HRMS (TOF MS CI$^+$) calculated for $C_{25}H_{27}N_2O_3S$ [M+H]$^+$: 435.1737, found 435.1740.

***N*-Methyl-2-[2-(4-methylphenylsulfonamido)benzyl]-*N*-(*o*-tolyl)acrylamide (7e).**

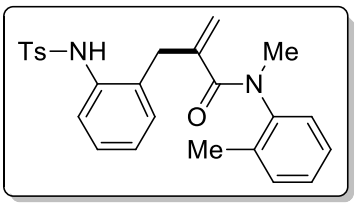

32.6 mg, 50% yield. Yellow oil. ^{1}H NMR (400 MHz, $CDCl_3$) (δ, ppm) 8.92 (s, 1H), 7.67 (d, *J* = 8.0 Hz, 2H), 7.54-7.52 (m, 1H), 7.22-7.16 (comp, 5H), 7.10-7.01 (comp, 2H), 6.93-6.89 (m, 1H), 6.57-6.55 (m, 1H), 4.87 (s, 1H), 4.71 (s, 1H), 3.23 (s, 3H), 3.15 (d, *J* = 15.2 Hz, 1H), 3.01 (d, *J* = 15.2 Hz, 1H), 2.37 (s, 3H), 2.13 (s, 3H); ^{13}C NMR (100 MHz, $CDCl_3$) (δ, ppm) 171.9, 143.3, 143.2, 141.7, 137.7, 135.5, 134.5, 131.6, 131.5, 131.0, 129.5, 128.2, 128.0, 127.9, 127.3, 127.2, 125.3, 124.6, 120.9, 37.4, 35.6, 21.7, 17.5. HRMS (TOF MS CI$^+$) calculated for $C_{25}H_{27}N_2O_3S$ $[M+H]^+$: 435.1737, found 435.1740.

_N_-Benzyl-2-{2-[(4-methylphenyl)sulfonamido]benzyl}-_N_-phenylacrylamide (7f).

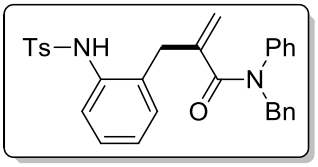

51.4 mg, 69% yield. Yellow solid, mp: 101-102 °C. ^{1}H NMR (400 MHz, $CDCl_3$) (δ, ppm) 8.55 (s, 1H), 7.64 (d, *J* = 8.4 Hz, 2H), 7.54 (d, *J* = 8.0 Hz, 1H), 7.23-7.14 (comp, 9H), 7.10-7.05 (comp, 3H), 6.94 (d, *J* = 7.4 Hz, 1H), 6.56-6.54 (m, 2H), 4.95 (s, 1H), 4.93 (s, 2H), 4.77 (s, 1H), 3.09 (s, 2H), 2.37 (s, 3H); ^{13}C NMR (100 MHz, $CDCl_3$) (δ, ppm) 171.5, 143.3, 142.8, 141.8, 137.7, 136.7, 135.4, 131.5, 131.3, 129.6, 129.3, 128.6, 128.5, 128.2, 127.6, 127.5, 127.2, 125.7, 125.6, 121.2, 53.8, 35.8, 21.7. HRMS (TOF MS ESI$^+$) calculated for $C_{30}H_{29}N_2O_3S$ $[M+H]^+$: 497.1893, found 497.1897.

Methyl 2-{2-[(4-methylphenyl)sulfonamido]benzyl}acrylate (7g).

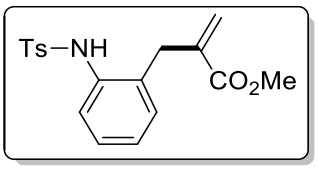

30.0 mg, 58% yield. White solid, mp: 161-162 °C. ^{1}H NMR (400 MHz, $CDCl_3$) (δ, ppm) 8.10 (s, 1H), 7.61 (d, *J* = 8.3 Hz, 2H), 7.45-7.42 (m, 1H), 7.21-7.16 (comp, 3H), 7.12-7.05 (m, 2H), 6.12 (s, 1H), 5.60 (s, 1H), 3.73 (s, 3H), 3.13 (s, 2H), 2.37 (s, 3H); ^{13}C NMR (100 MHz, $CDCl_3$) (δ, ppm) 168.1, 143.5, 138.8, 137.3, 134.7, 132.4, 130.5, 129.6, 127.9, 127.4, 127.1, 126.3, 125.6, 52.6, 33.4, 21.6. HRMS (TOF MS ESI$^+$) calculated for $C_{18}H_{20}NO_4S$ $[M+H]^+$: 346.1108, found 346.1112.

4-Bromobenzyl-2-{2-[(4-methylphenyl)sulfonamido]benzyl}acrylate (7h).

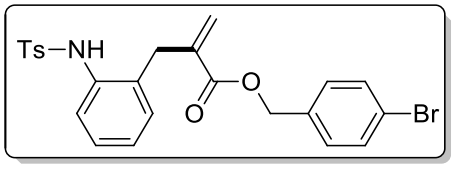

41.2 mg, 55% yield. Yellow solid, mp: 135-138 °C. ^{1}H NMR (400 MHz, $CDCl_3$) (δ, ppm) 7.85 (s, 1H), 7.59 (d, *J* = 8.3 Hz, 2H), 7.49-7.46 (m, 2H), 7.42-7.40 (m, 1H), 7.22-7.17 (comp, 5H), 7.13-7.05 (m, 2H), 6.17 (s, 1H), 5.62 (s, 1H), 5.11 (s, 2H), 3.16 (s, 2H), 2.38 (s, 3H); ^{13}C NMR (100 MHz, $CDCl_3$) (δ, ppm) 167.3, 143.6, 138.8, 137.3, 134.8, 134.5, 132.4, 131.9, 130.6, 130.1, 129.7, 128.0, 127.8, 127.2, 126.5, 125.8, 122.7, 66.6, 33.5, 21.7. HRMS (TOF MS ESI$^+$) calculated for $C_{24}H_{23}BrNO_4S$ $[M+H]^+$: 500.0526, found 500.0531.

Diethyl {3-[2-(4-methylphenylsulfonamido)phenyl]prop-1-en-2-yl}phosphonate (7i).

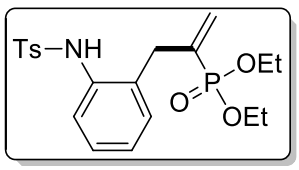

30.5 mg, 48% yield. Yellow solid, mp: 104-105 °C. ^{1}H NMR (400 MHz, $CDCl_3$) (δ, ppm) 8.14 (s,

1H), 7.60 (d, *J* = 8.0 Hz, 2H), 7.42-7.39 (m, 1H), 7.18-7.15 (comp, 3H), 7.11-7.05 (m, 2H), 5.88-5.83 (m, 1H), 5.63-5.51 (m, 1H), 4.09-3.91 (m, 4H), 3.17-3.13 (m, 2H), 2.36 (s, 3H), 1.23 (t, *J* = 7.2 Hz, 6H); ^{13}C NMR (100 MHz, $CDCl_3$) (δ, ppm) 143.4, 138.6, 137.5, 136.9, 134.9, 132.1 (d, *J* = 5.4 Hz), 130.9, 130.4 (d, *J* = 46.1 Hz), 129.5, 128.0, 127.1, 126.2, 125.8, 62.5 (d, *J* = 5.9 Hz), 34.1 (d, *J* = 12.7 Hz), 21.6, 16.2 (d, *J* = 6.2 Hz); ^{31}P{^{1} H} NMR (162 MHz): δ 19.1. HRMS (TOF MS ESI$^+$) calculated for $C_{20}H_{27}NO_5PS$ [M+H]$^+$: 424.1342, found 424.1350.

Methyl 2-(2-(4-fluorophenylsulfonamido)benzyl)acrylate (7j).

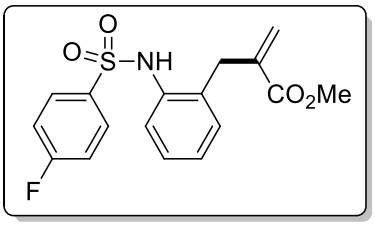

32.0 mg, 61% yield. Yellow oil. ^{1}H NMR (400 MHz, $CDCl_3$) (δ, ppm) 8.25 (br, 1H), 7.76-7.73 (m, 2H), 7.44 (d, *J* = 7.4 Hz, 1H), 7.24-7.19 (m, 1H), 7.15-7.08 (comp, 4H), 6.14 (s, 1H), 5.76 (s, 1H), 3.75 (s, 3H), 3.11 (s, 2H); ^{13}C NMR (100 MHz, $CDCl_3$) (δ, ppm) 168.1, 166.2, 163.7, 138.5, 136.1, 136.1, 134.2, 132.7, 130.5, 129.7, 129.6, 127.8, 127.5, 126.6, 125.7, 116.2, 116.0, 52.4, 33.2. HRMS (TOF MS ESI$^+$) calculated for $C_{17}H_{17}FNO_4S$ [M+H]$^+$: 350.0862, found 350.0880.

General procedure for the preparation of cyclization products 9 (Method D, related to Figure 2).

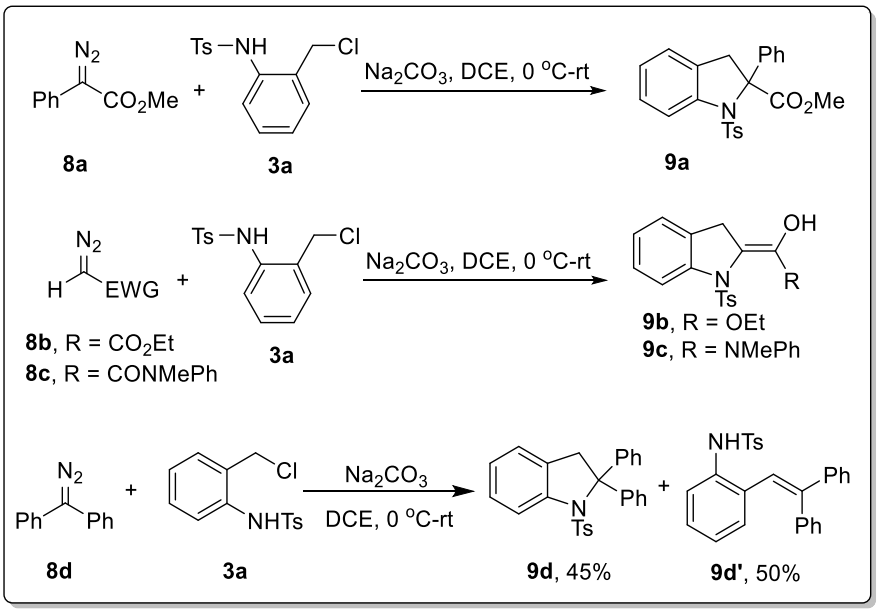

To a 10 mL oven-dried flask containing a magnetic stirring bar, sulfonaminobenzyl chloride **3a** (59.2 mg, 0.20 mmol), diazo compound **8** (0.15 mmol), Na_2CO_3 (25.4 mg, 0.24 mmol) and DCE (2.0 mL) were added in sequence at 0 °C under argon atmosphere. The reaction mixture was stirred under these conditions for 8 h and the temperature was warmed to room temperature slowly. Then the reaction mixture was quenched with H_2O and extracted with DCM (15 X 3 mL). The organic phase was dried with anhydrous Na_2SO_4 and the solvent was evaporated under vacuum after filtration. The resulting residues was purified by column chromatography on silica gel with hexanes/ethyl acetate (10:1 to 5:1) as the eluent to give the desired pure products **9a**-**9c**.

Methyl 2-phenyl-1-tosylindoline-2-carboxylate (9a).

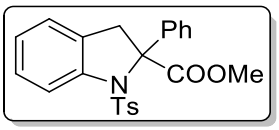

33.6 mg, 55% yield. White solid, mp: 225-226 °C. ^{1}H NMR (400 MHz, $CDCl_3$) (δ, ppm) 7.56-7.53 (m, 2H), 7.39-7.37 (m, 1H), 7.34-7.37 (comp, 5H), 7.20-7.16 (m, 1H), 7.11-7.07 (comp, 3H), 6.98-6.94 (m, 1H), 3.91 (d, *J* = 16.4 Hz, 1H), 3.90 (s, 3H), 3.70 (d, *J* = 16.4 Hz, 1H), 2.33 (s, 3H); ^{13}C NMR (100 MHz, $CDCl_3$) (δ, ppm) 172.3, 143.7, 141.5, 139.8, 137.2, 129.3, 128.34,

128.32, 128.2, 128.1, 127.5, 126.9, 124.8, 123.1, 113.0, 77.0, 53.4, 47.2, 21.6. HRMS (TOF MS CI$^+$) calculated for $C_{23}H_{22}NO_4S$ [M+H]$^+$: 408.1264, found 408.1275.

Ethoxy (1-tosylindolin-2-ylidene)methanol (9b).

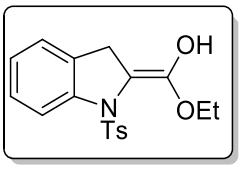

32.0 mg, 62% yield. Yellow oil. ^{1}H NMR (400 MHz, $CDCl_3$) (δ, ppm) 8.67 (br, 1H), 7.63 (d, *J* = 8.0 Hz, 2H), 7.49-7.47 (m, 1H), 7.24-7.20 (comp, 3H), 7.13-7.09 (m, 1H), 7.03-7.01 (m, 1H), 4.27 (q, *J* = 7.0 Hz, 2H), 3.14 (s, 2H), 2.38 (s, 3H); ^{13}C NMR (100 MHz, $CDCl_3$) (δ, ppm) 143.6, 137.4, 135.1, 131.5, 130.2, 130.0, 129.7, 128.7, 127.2, 126.3, 125.6, 62.0, 25.9, 21.7, 14.6. HRMS (TOF MS CI$^+$) calculated for $C_{18}H_{20}NO_4S$ [M+H]$^+$: 346.1108, found 346.1119.

Methyl (phenyl)amino(1-tosylindolin-2-ylidene)methanol (9c).

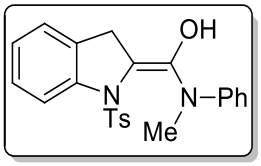

42.7 mg, 70% yield. Yellow oil. ^{1}H NMR (400 MHz, $CDCl_3$) (δ, ppm) 9.94 (s, 1H), 7.70 (d, *J* = 8.4 Hz, 2H), 7.60-7.58 (m, 1H), 7.39-7.35 (m, 2H), 7.33-7.29 (m, 1H), 7.25-7.20 (comp, 3H), 7.16-7.13 (m, 2H), 7.02-6.98 (m, 1H), 6.80-6.78 (m, 1H), 3.37 (s, 3H), 3.14 (s, 2H), 2.37 (s, 3H); ^{13}C NMR (100 MHz, $CDCl_3$) (δ, ppm) 166.7, 143.2, 143.1, 137.8, 135.9, 130.4, 130.1, 129.6, 128.6, 128.2, 127.1, 126.8, 125.3, 124.7, 39.3, 28.1, 21.7. HRMS (TOF MS CI$^+$) calculated for $C_{23}H_{23}N_2O_3S$ [M+H]$^+$: 407.1424, found 407.1435.

2,2-Diphenyl-1-tosylindoline (9d).

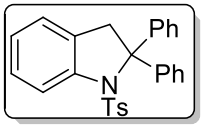

28.7 mg, 45% yield. White solid, mp: 227-228 °C. ^{1}H NMR (400 MHz, $CDCl_3$) (δ, ppm) 7.90 (d, *J* = 8.0 Hz, 1H), 7.55-7.51 (comp, 4H), 7.35-7.30 (comp, 7H) 7.13-7.11 (m, 1H), 7.07-7.03 (m, 1H), 6.99-6.93 (comp, 4H), 3.93 (s, 2H), 2.35 (s, 3H); ^{13}C NMR (100 MHz, $CDCl_3$) (δ, ppm) 143.8, 143.1, 142.2, 137.8, 132.5, 130.2, 129.2, 128.9, 128.4, 128.2, 127.8, 127.8, 127.4, 126.9, 124.6, 123.2, 114.1, 78.9, 52.4, 21.5. HRMS (TOF MS CI$^+$) calculated for $C_{27}H_{24}NO_2S$ $[M+H]^+$: 426.1522, found 426.1536.

***N*-[2-(2,2-diphenylvinyl)phenyl]-4-methylbenzenesulfonamide (9d').**

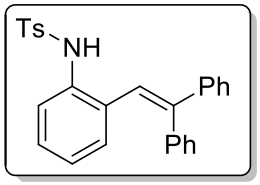

31.8 mg, 50% yield. Yellow solid, mp: 127-128 °C. ^{1}H NMR (400 MHz, $CDCl_3$) (δ, ppm) 7.58 (d, *J* = 8.4 Hz, 2H), 7.45-7.43 (m, 1H), 7.35-7.32 (comp, 3H), 7.25-7.09 (comp, 8H), 6.94-6.88 (comp, 3H), 6.83-6.80 (m, 1H), 6.54 (s, 1H), 6.36 (s, 1H), 2.45 (s, 3H); ^{13}C NMR (100 MHz, $CDCl_3$) (δ, ppm) 146.4, 143.9, 142.5, 139.0, 137.1, 134.2, 131.4, 130.7, 130.4, 129.8, 128.6, 128.5, 128.31, 128.28, 128.1, 128.0, 127.3, 125.5, 124.1, 122.7, 21.7. HRMS (TOF MS CI$^+$) calculated for $C_{27}H_{24}NO_2S$ $[M+H]^+$: 426.1522, found 426.1534.

Methods for further transformations (related to Figure 6 and Figure 7)

Procedure for the preparation of 12 (Liu et al., 2015).

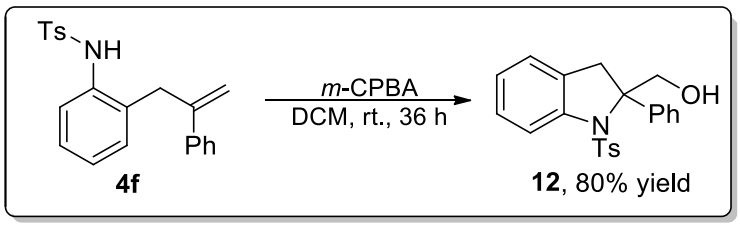

To a 10 mL oven-dried vial containing a magnetic stirring bar, alkenylamine **4f** (36.4 mg,

0.1 mmol), *m*-CPBA (20.7 mg, 0.12 mmol) and DCM (3.0 mL) were added in sequence, and the reaction mixture was stirred at room temperature for 36 h. After the reaction completed, DCM (10 mL) was then added and the mixture was washed with aqueous $Na_2S_2O_3$ (20 mL) and aqueous $NaHCO_3$ (20 mL) in sequence, and the organic phase was dried over $MgSO_4$, and the solvent was evaporated under vacuum after filtration. The resulting residues was purified by column chromatography on silica gel with hexanes/ethyl acetate (10:1 to 5:1) as the eluent to give the desired product **12** in 80% yield, 30.4 mg. Yellow oil. ^{1}H NMR (400 MHz, $CDCl_3$) (δ, ppm) 7.63 (d, *J* = 8.2 Hz, 1H), 7.32-7.30 (m, 2H), 7.23-7.19 (comp, 4H), 7.16-7.12 (comp, 3H), 7.03-6.98 (m, 3H), 4.83 (d, *J* = 11.8 Hz, 2H), 4.30 (d, *J* = 11.8 Hz, 1H), 3.79 (d, *J* = 16.4 Hz, 1H), 3.29 (d, *J* = 16.4 Hz, 1H), 2.32 (s, 3H), 1.68 (s, 1H); ^{13}C NMR (100 MHz, $CDCl_3$) (δ, ppm) 143.6, 142.9, 141.6, 137.4, 129.4, 128.7, 128.5, 127.9, 126.9, 126.3, 124.9, 123.3, 113.7, 76.4, 66.5, 44.2, 21.6. HRMS (TOF MS CI$^+$) calculated for $C_{22}H_{22}NO_3S$ $[M+H]^+$: 380.1315, found 380.1326.

Procedure for the preparation of 13 (Ferrand et al., 2017).

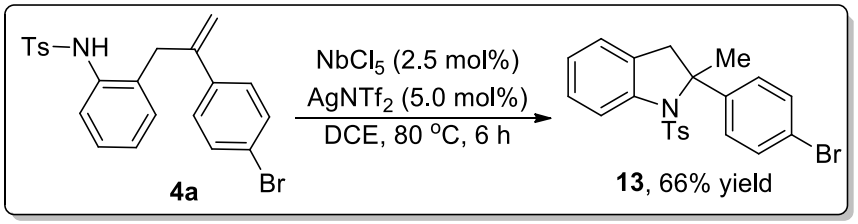

To an oven-dried schlenk flask containing a magnetic stirring bar, $NbCl_5$ (2.5 mol %, 0.0025 mmol, 0.7 mg) and $AgNTf_2$ (5 mol %, 0.005 mmol, 2.0 mg), and fresh distilled DCE (1.5 mL) were added under argon atmosphere. The reaction mixture was allowed to stir at 80 °C for 10 min. Then a solution of alkenylamine **4a** (1.0 equiv., 44.2 mg, 0.1 mmol) in DCE (1.5 mL) was added via syringe. The reaction mixture was allowed to stir at 80 °C for 6 h, then filtered through a pad of silica, washed with Et_2O, and the solvent was evaporated under vacuum. The resulting residues was purified by flash chromatography on silica gel with hexanes/ethyl acetate (20:1 to 10:1) as the eluent to afforded desired product **13** in 66% yield, 29.2 mg. Yellow solid, 131-132 °C. ^{1}H NMR (400 MHz, $CDCl_3$) (δ, ppm) 7.67 **(**d, *J* = 8.4

Hz, 1H), 7.49 (d, *J* = 8.0 Hz, 2H), 7.33 (d, *J* = 8.8 Hz, 2H), 7.28-7.23 (comp, 3H), 7.16-7.11 (comp, 3H), 7.04-7.00 (m, 1H), 3.35 (q, *J* = 16.4 Hz, 2H), 2.39 (s, 3H), 2.13 (s, 3H); ^{13}C NMR (100 MHz, $CDCl_3$) (δ, ppm) 144.4, 143.5, 142.4, 138.4, 131.3, 129.4, 128.2, 127.71, 127.69, 126.8, 125.1, 123.1, 121.5, 113.8, 72.1, 49.2, 27.1, 21.6. HRMS (TOF MS CI$^+$) calculated for $C_{22}H_{21}BrNO_2S$ [M+H]$^+$: 442.0471, found 442.0477.

Procedure for the preparation of 14 (Li et al., 2017).

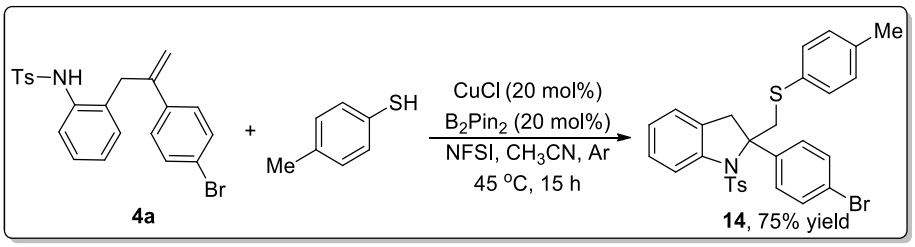

To an oven-dried schlenk flask containing a magnetic stirring bar, alkenylamine **4a** (1 equiv., 44.2 mg, 0.1 mmol) and thiols (18.6 mg, 0.15 mmol), NFSI (47.3 mg, 0.15 mmol), CuCl (2.0 mg, 20 mol%), B_2Pin_2 (5.1 mg, 20 mol%), and CH_3CN (1.5 mL) were added under argon atmosphere. Then the mixture was heated to 45 °C for 15 h. After the reaction was completed (monitored by TLC), it was cooled to room temperature and concentrated under reduced pressure. The residues was purified by flash chromatography on silica gel with hexanes/ethyl acetate (20:1 to 10:1) as the eluent to give the desired product **14** in 75% yield, 42.3 mg. ^{1}H NMR (400 MHz, $CDCl_3$) (δ, ppm); 7.73 (d, *J* = 8.4 Hz, 1H), 7.34-7.32 (m, 2H), 7.30-7.27 (m, 1H), 7.21-7.18 (comp, 4H), 7.15-7.07 (comp, 5H), 7.06-7.01 (comp, 3H), 4.29 (d, *J* = 12.4 Hz, 1H), 4.13 (d, *J* = 12.4 Hz, 1H), 3.90 (d, *J* = 16.8 Hz, 1H), 3.49 (d, *J* = 16.8 Hz, 1H), 2.37 (s, 3H), 2.36 (s, 3H). ^{13}C NMR (100 MHz, $CDCl_3$) (δ, ppm) 143.5, 142.6, 140.6, 137.8, 136.9, 132.9, 131.1, 130.9, 130.0, 129.2, 128.9, 128.3, 127.9, 126.6, 124.9, 123.3, 122.3, 113.8, 74.1, 45.9, 44.9, 21.6, 21.2. HRMS (TOF MS CI$^+$) calculated for $C_{29}H_{27}BrNO_2S_2$ [M+H]$^+$: 564.0661, found 564.0665.

Procedure for the Preparation of 15 (Yin et al., 2014).

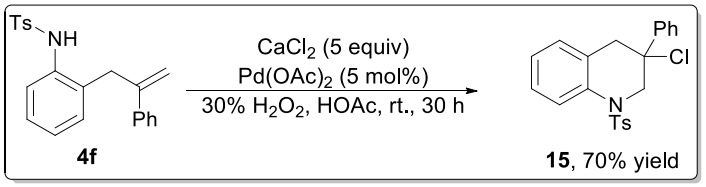

To a 5 mL oven-dried vial containing a magnetic stirring bar, alkenylamine **4f** (1.0 equiv., 44.2 mg, 0.10 mmol), $CaCl_2$ (55.6 mg, 0.50 mmol), and dry acetic acid (0.8 mL) were added at room temperture. After stirring for 5 minutes at room temperture, $Pd(OAc)_2$ (1.2 mg, 0.01 mmol) and H_2O_2 (30% aq wt., 23 μL, 0.20 mmol) were added, and the reaction mixture was stirred at room temperature for about 30 h. Until **4f** was consumed (monitored by thin layer chromatography). Diethyl ether (15 mL) was added and the mixture was filtered through a pad of Celite to remove the solid. Then the mixture was concentrated in vacuum and the resulting residues was purified by silica gel column chromatography with hexanes/ethyl acetate (20:1 to 10:1) as the eluent to give the corresponding product **15** in 70% yield, 41.7 mg. ^{1}H NMR (400 MHz, $CDCl_3$) (δ, ppm) 7.54 (d, *J* = 8.7 Hz, 1H), 7.27-7.13 (comp, 8H), 7.08 (d, *J* = 8.4 Hz, 2H), 6.97 (d, *J* = 8.1 Hz, 2H), 4.65 (dd, *J* = 40,8, 11.4 Hz, 2H), 3.87 (d, *J* = 17.2 Hz, 1H), 3.47 (d, *J* = 17.3 Hz, 1H), 2.31 (s, 3H); ^{13}C NMR (100 MHz, $CDCl_3$) (δ, ppm) 143.7, 141.2, 139.9, 137.0, 129.8, 129.2, 128.4, 128.3, 128.2, 128.1, 127.1, 126.9, 124.9, 114.3, 74.8, 49.9, 45.1, 21.6. HRMS (TOF MS CI$^+$) calculated for $C_{22}H_{21}ClNO_2S$ $[M+H]^+$: 398.0976, found 398.0983.

Procedure for the preparation of 16.

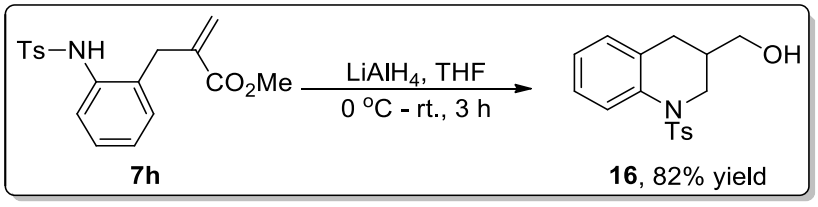

To a 10 mL oven-dried vial containing a magnetic stirring bar, **7h** (51.8 mg, 0.15 mmol) in dry THF (5.0 mL), was added Lithium aluminium hydride (28.5 mg, 0.75 mmol) at 0 °C. The reaction mixture was stirred under this condition for 3 h and the temperature was warmed to room temperature slowly. Then reaction was quenched with $Na_2SO_4 \cdot 10H_2O$, filtered through

a pad of Celite and washed with EtOAc (15 mL). The filtrate was concentrated under reduced pressure to give crude product. The obtained residues was purified by flash column chromatography on silica gel (Hexanes : EtOAc = 20:1 to 10:1) to give the pure product **16** in 82% yield, 39.0 mg, yellow oil. ^{1}H NMR (400 MHz, $CDCl_3$) (δ, ppm) 7.68 (d, *J* = 8.4 Hz, 1H), 7.57 (d, *J* = 8.0 Hz, 2H), 7.23 (d, *J* = 8.4 Hz, 2H), 7.19-7.14 (m, 1H), 7.08-7.02 (m, 2H), 4.13-4.08 (m, 1H), 3.54 (d, *J* = 6.4 Hz, 2H), 3.48-3.43 (m, 1H), 2.64-2.59 (m, 1H), 2.39 (s, 3H), 2.29-2.23 (m, 1H), 2.00-1.95 (m, 1H), 1.74 (br, 1H); ^{13}C NMR (100 MHz, $CDCl_3$) (δ, ppm) 143.8, 137.2, 136.9, 129.8, 129.5, 129.3, 127.1, 126.7, 124.9, 123.9, 64.4, 48.4, 35.3, 29.5, 21.7. HRMS (TOF MS CI$^+$) calculated for $C_{17}H_{20}NO_3S$ $[M+H]^+$: 318.1158, found 318.1156.

Procedure for the preparation of 17.

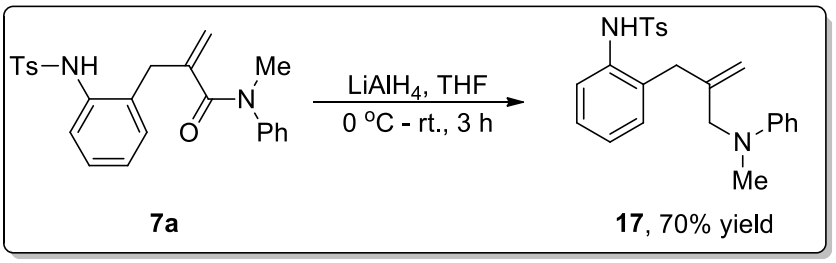

To a 10 mL oven-dried vial containing a magnetic stirring bar, **7a** (63.0 mg, 0.15 mmol) in dry THF (5 mL), was added Lithium aluminium hydride (28.5 mg, 0.75 mmol) at 0 °C. The reaction mixture was stirred under this condition for 3 h and the temperature was warmed to room temperature slowly. Then reaction was quenched with $Na_2SO_4{\cdot}10H_2O$, filtered through a pad of Celite and washed with EtOAc (15 mL). The filtrate was concentrated under reduced pressure to give crude product. The obtained residues was purified by flash column chromatography on silica gel (Hexanes : EtOAc = 20:1 to 10:1) to give the pure product **17** in 70% yield, 42.6 mg, yellow oil. ^{1}H NMR (400 MHz, $CDCl_3$) (δ, ppm) 7.56 (br, 1H), 7.45-7.39 (comp, 3H), 7.29-7.25 (m, 2H), 7.23-7.19 (m, 1H), 7.13-7.07 (comp, 4H), 6.88-6.82 (comp, 3H), 5.02 (s, 1H), 4.79 (s, 1H), 3.61 (s, 2H), 2.94 (s, 2H), 2.89 (s, 3H), 2.33 (s, 3H); ^{13}C NMR (100 MHz, $CDCl_3$) (δ, ppm) 143.6, 137.2, 135.4, 131.9, 130.9, 129.6, 129.4, 127.9, 127.1, 126.2, 124.8, 118.94, 118.91, 114.9, 114.35, 114.34, 58.3, 39.7, 36.2, 21.7. HRMS (TOF MS CI$^+$) calculated for $C_{24}H_{27}N_2O_2S$ $[M+H]^+$: 407.1788, found 407.1790.

Procedure for the preparation of 18.

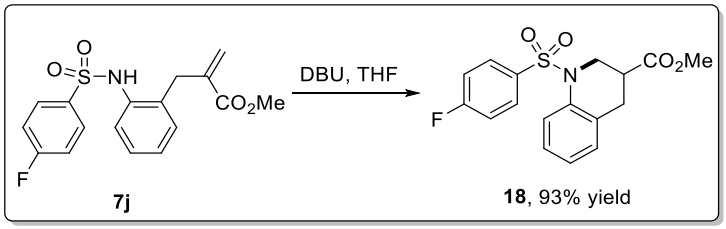

To a 10 mL oven-dried vial containing a magnetic stirring bar, **7j** (52.4 mg, 0.15 mmol) in dry THF (2 mL) was added DBU (27.4 mg, 1.2 equiv.). The reaction mixture was stirred under this condition for 8 h. When the reaction was completed (monitored by TLC), the reaction mixture was quenched by saturated NH_4Cl (aq), extracted with ethyl acetate (15 X 3 mL), and washed with brine (50 mL). The organic phase was dried with Na_2SO_4 and evaporated *in vacuo*. The resulting residue was purified by the flash column to afford the product **18** in 93% yield. After that, according to the literature, inhibitor Mcl-1 can be easily obtained within two steps. ^{1}H NMR (400 MHz, $CDCl_3$) (δ, ppm) 7.76 (d, *J* = 7.8 Hz, 1H), 7.65-7.62 (m, 2H), 7.24-7.20 (m, 1H), 7.14-7.05 (comp, 4H), 4.45-4.40 (m, 1H), 3.70 (s, 3H), 3.54-3.48 (m, 1H), 2.77-2.64 (m, 2H), 2.60-2.52 (m, 1H); ^{13}C NMR (100 MHz, $CDCl_3$) (δ, ppm) 172.7, 166.7, 164.1, 136.0, 135.5, 135.5, 130.0, 129.9, 129.4, 128.8, 127.2, 125.9, 125.0, 116.7, 116.5, 52.4, 47.5, 38.1, 29.3.

Methods for mechanistic studies

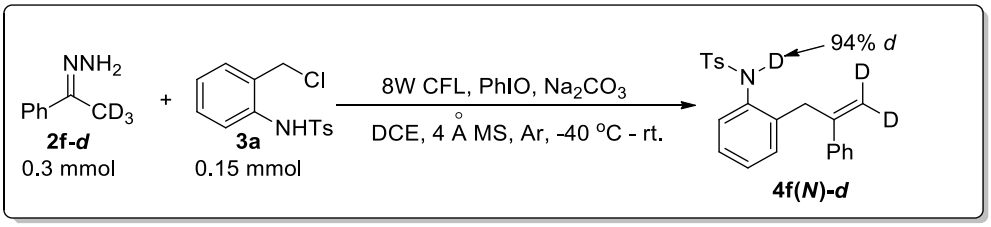

To a 10 mL oven-dried vial containing a magnetic stirring bar, hydrazone **2f-*d***(41.2 mg, 0.30 mmol), *N*-(2-chloromethylaryl) amide **3a** (44.4 mg, 0.15 mmol), Na_2CO_3 (31.8 mg, 2.0 equiv.), PhIO (66.0 mg, 0.30 mmol), and DCE (2.0 mL) were added in sequence under argon atmosphere at -40 °C under the irradiation of visible light (8 W CFL). The reaction was stirred for 10 h under these conditions and the reaction temperature warmed to room temperature

slowly in this period of time. When the reaction was completed (monitored by TLC), the solid was removed by filtering through a pad of Celite with Teflon filter (0.22 μm) at the bottom. And the filtrate was evaporated *in vacuo*. The resulting residue was directly subjected to proton NMR analysis with $CDCl_3$ as the solvent without any further purification (see fig. S115). According to this spectrum, 94% proton was transferred from methyl group to the *N*.

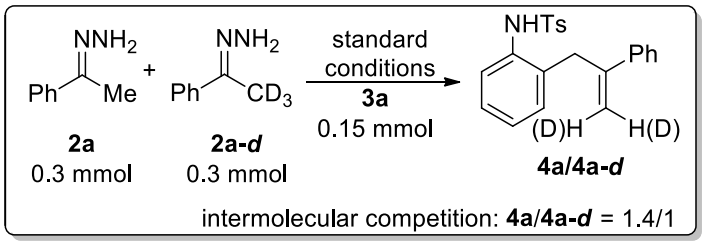

To a 10 mL oven-dried flask containing a magnetic stirring bar, hydrazone **2a** and **2a-*d*** (each on a 0.3 mmol scale in separated vial), anhydrous $MgSO_4$ (50 mg), MnO_2 (208.1 mg, 8.0 equiv), and 1,2-dichloroethane (3.0 mL) were added in sequence under argon atmosphere. Then the flask was wrapped in foil and the reaction mixture was allowed to stir for 45 min at 0 °C. After that, removing the solid by filtering through a pad of Celite with Teflon filter (0.22 μm) at the bottom, we could obtain the two pink solutions. Then two obtained pink solutions were mixed.

To a 10 mL oven-dried vial, which contains a magnetic stirring bar, *N*-(2-chloromethylaryl) amide **3a** (44.4 mg, 0.15 mmol), Cs_2CO_3 (97.7 mg, 2.0 equiv) under argon atmosphere, the above-mentioned mixed pink solution was added via syringe at -40 °C. The reaction was carried out by irradiation of visible light (8 W CFL) and warm to room temperature slowly. When the reaction was completed (monitored by TLC), the reaction mixture was quenched by saturated NH_4Cl (aq), extracted with ethyl acetate (15 X 3 mL), and washed with brine (50 mL). The organic phase was dried with Na_2SO_4 and evaporated *in vacuo*. The resulting residue was directly subjected to proton NMR analysis with $CDCl_3$ as the solvent without any further purification (see fig. S114). According to this spectrum, **4a**/**4a-*d*** = 1.4:1.

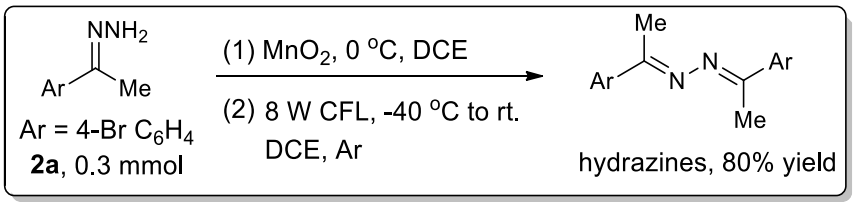

To a 10 mL oven-dried flask containing a magnetic stirring bar, hydrazone **2a** (63.9 mg, 0.3 mmol), anhydrous $MgSO_4$ (50 mg), MnO_2 (208.1 mg, 8.0 equiv), and 1,2-dichloroethane (3.0 mL) were added in sequence under argon atmosphere. Then the flask was wrapped in foil and the reaction mixture was allowed to stir for 45 min at 0 °C. After that, removing the solid by filtering through a pad of Celite with Teflon filter (0.22 μm) at the bottom, we could obtain the pink solution as the diazo compound **1a**.

Then to a 10 mL oven-dried vial, which contains a magnetic stirring bar, was added the obtained pink solutions at -40 °C under argon atmosphere. The reaction was carried out by irradiation of visible light (8 W CFL) and warm to room temperature slowly. When the reaction was completed (monitored by TLC), the reaction mixture was quenched by saturated NH_4Cl (aq), extracted with ethyl acetate (15 X 3 mL), and washed with brine (50 mL). The organic phase was dried with Na_2SO_4 and evaporated *in vacuo*. The resulting residue was purified by the flash column to afford the hydrazines product in 80% yield, and the data of NMR is consistence with the literature. ^{1}H NMR (400 MHz, $CDCl_3$) (δ, ppm) 7.78 (d, *J* = 7.8 Hz, 4H), 7.55 (d, *J* = 7.8 Hz, 4H), 2.29 (s, 6H); ^{13}C NMR (100 MHz, $CDCl_3$) (δ, ppm) 157.5, 137.3, 131.7, 128. 3, 124.3, 15.0.

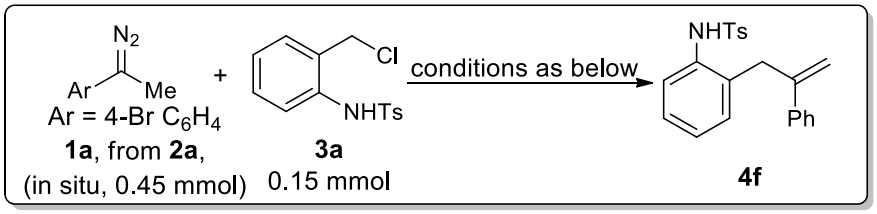

condition A	condition B (standard)	condition C
Cs_2CO_3 (2.0 equiv.), DCE, -40 °C to rt. Ar, **under dark** 55% yield	Cs_2CO_3 (2.0 equiv.), DCE, -40 °C to rt. Ar, **8 W CFL** 80% yield	Cs_2CO_3 (2.0 equiv.), DCE, -40 °C to rt. **TEMPO (2.0 equiv.)** Ar, **8 W CFL** 40% yield

To a 10 mL oven-dried flask containing a magnetic stirring bar, hydrazone **2a** (95.9 mg, 0.45 mmol), anhydrous $MgSO_4$ (60 mg), MnO_2 (312.0 mg, 8.0 equiv), and 1,2-dichloroethane (3.0 mL) were added in sequence under argon atmosphere. Then the flask was wrapped in foil and the reaction mixture was allowed to stir for 45 min at 0 °C. After that, removing the solid by filtering through a pad of Celite with Teflon filter (0.22 μm) at the bottom, we could obtain the pink solution as the diazo compound **1**.

To a 10 mL oven-dried vial, which contains a magnetic stirring bar, *N*-(2-chloromethylaryl) amide **3a** (44.4 mg, 0.15 mmol), Cs_2CO_3 (97.7 mg, 2.0 equiv) under argon atmosphere, the above-mentioned mixed pink solution was added via syringe at -40 °C. For the condition A: The reaction was carried out under the dark and warm to room temperature slowly. When the reaction was completed, When the reaction was completed (monitored by TLC), the reaction mixture was quenched by saturated NH_4Cl (aq), extracted with ethyl acetate (15 X 3 mL), and washed with brine (50 mL). The organic phase was dried with Na_2SO_4 and evaporated *in vacuo*. The resulting residue was purified by the flash column to afford **4f** in 55% yield. For the condition B: The reaction was the same to condition A except by irradiation of visible light (8 W CFL) rather than under the dark. And the isolated yield is 80%. For the condition C: The reaction was the same to condition B except adding 2.0 equiv. TEMPO, and the isolated yield is 40%.

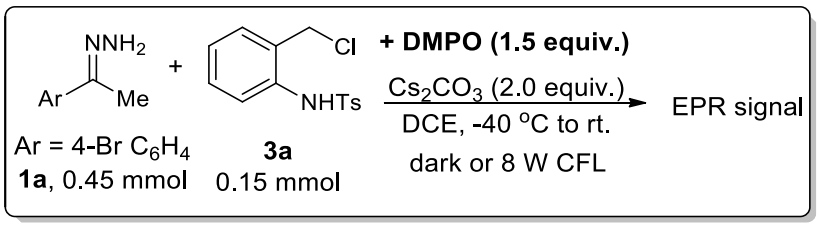

To a 10 mL oven-dried flask containing a magnetic stirring bar, hydrazone **2a** (95.9 mg, 0.45 mmol), anhydrous $MgSO_4$ (60 mg), MnO_2 (312.0 mg, 8.0 equiv), and 1,2-dichloroethane (3.0 mL) were added in sequence under argon atmosphere. Then the flask was wrapped in foil and the reaction mixture was allowed to stir for 45 min at 0 °C. After that, removing the solid by filtering through a pad of Celite with Teflon filter (0.22 μm) at the bottom, we could obtain the pink solution.

To a 10 mL oven-dried vial, which contains a magnetic stirring bar, *N*-(2-chloromethylaryl)

amide **3a** (44.4 mg, 0.15 mmol), Cs_2CO_3 (97.7 mg, 2.0 equiv) under argon atmosphere, the above-mentioned mixed pink solution was added via syringe at -40 °C. The reaction was carried out under the dark or by irradiation of visible light (8 W CFL) and warm to room temperature slowly. After 40 min, the solution of DMPO in 1,2-dichoroethane was added via syringe rapidly. Then after 5 min or 20 min, the reaction mixture was directly subjected to electron paramagnetic resonance (EPR) analysis (see fig. S5).

Computational Methods (related to Figure 4 and Figure 5)

All structures were optimized with the M06 (Zhao et al., 2008) density functional theory method combined with the 6-31G(d) (Hariharan et al., 1973) basis set for C, H, O, N, S atoms. Vibrational frequency analyses at the same level of theory were performed on all optimized structures to characterize stationary points as local minima or transition states. Further, intrinsic reaction coordinate (IRC) computations were carried out to confirm that transition states connect appropriate reactants and products. The gas-phase Gibbs free energies for all species were obtained at 298.15 K and 1 atm at their respective optimized structures. To consider solvation effects, single-point energy computations using the SMD model (Marenich et al., 2009) with dichloroethane as solvent were performed based on the optimized gas-phase geometries of all species. The basis sets, 6-311++G(d,p) for C, H, O, N, S atoms, were utilized for single-point energy calculations on stationary points. The solution-phase Gibbs free energy was determined by adding the solvation single-point energy and the gas-phase thermal correction to the Gibbs free energy obtained from the vibrational frequencies. Unless otherwise specified, the solution-phase Gibbs free energy was used in the present discussions. The Gaussian 09 suite of programs (Frisch et al., 2010) was used throughout.

Cartesian Coordinates and Energies

2f

Center Number	Atomic Number	Atomic Type	Coordinates (Angstroms) X	Y	Z
1	6	0	2.320160	1.009128	-0.000090
2	6	0	0.946468	1.218348	-0.000023
3	6	0	0.059470	0.133078	0.000087
4	6	0	0.594998	-1.164141	0.000101
5	6	0	1.966115	-1.364303	0.000053
6	6	0	2.840264	-0.279705	-0.000049
7	1	0	2.989005	1.868486	-0.000211
8	1	0	0.560263	2.236423	-0.000033
9	1	0	-0.071887	-2.026293	0.000178
10	1	0	2.357401	-2.380381	0.000103
11	1	0	3.916659	-0.439206	-0.000082

12	6	0	-1.380010	0.375632	0.000083
13	6	0	-2.003992	1.738239	0.000048
14	1	0	-3.096401	1.664520	0.000183
15	1	0	-1.707419	2.315036	0.887556
16	1	0	-1.707588	2.314922	-0.887596
17	7	0	-2.178542	-0.650695	-0.000058
18	7	0	-2.864440	-1.570900	-0.000135

Zero-point correction= 0.142956 (Hartree/Particle)
Thermal correction to Energy= 0.151745
Thermal correction to Enthalpy= 0.152690
Thermal correction to Gibbs Free Energy= 0.108903
Sum of electronic and zero-point Energies= -418.664951
Sum of electronic and thermal Energies= -418.656161
Sum of electronic and thermal Enthalpies= -418.655217
Sum of electronic and thermal Free Energies= -418.699004
M06/6-311++G(d,p)/SMD//M06/6-31G(d) energy= -418.91751654

3a'

Center Number	Atomic Number	Atomic Type	Coordinates (Angstroms) X	Y	Z
1	6	0	2.292961	-0.124163	-1.241462
2	6	0	1.952463	0.079209	0.155070
3	6	0	2.814149	-0.623172	1.153224
4	6	0	3.863011	-1.506991	0.682718
5	6	0	4.100836	-1.673347	-0.632977
6	6	0	3.298733	-0.959752	-1.593805
7	1	0	1.717260	0.404480	-1.993247
8	1	0	4.457514	-2.023003	1.436114
9	1	0	4.892380	-2.332314	-0.982091
10	1	0	3.513520	-1.102675	-2.652453
11	6	0	2.637209	-0.424938	2.473692
12	1	0	1.871903	0.253845	2.840995
13	1	0	3.263987	-0.937664	3.201189
14	7	0	0.973804	0.780072	0.650351
15	16	0	-0.141445	1.664619	-0.232149
16	8	0	-0.423925	2.840997	0.573003
17	8	0	0.197983	1.828828	-1.645702
18	6	0	-1.528083	0.561801	-0.131800
19	6	0	-2.360723	0.620949	0.980104
20	6	0	-1.743199	-0.363022	-1.147336
21	6	0	-3.428657	-0.260855	1.066795
22	1	0	-2.168638	1.362653	1.753048
23	6	0	-2.814492	-1.239275	-1.042748
24	1	0	-1.083095	-0.378308	-2.013061
25	6	0	-3.671939	-1.199029	0.059933
26	1	0	-4.091886	-0.223163	1.931233
27	1	0	-2.996464	-1.967285	-1.833588
28	6	0	-4.848672	-2.123159	0.145391
29	1	0	-5.740088	-1.670129	-0.310833
30	1	0	-4.660855	-3.066955	-0.380626
31	1	0	-5.103093	-2.358006	1.186053

Zero-point correction= 0.239970 (Hartree/Particle)
Thermal correction to Energy= 0.256243

Thermal correction to Enthalpy= 0.257187
Thermal correction to Gibbs Free Energy= 0.192787
Sum of electronic and zero-point Energies= -1143.808911
Sum of electronic and thermal Energies= -1143.792638
Sum of electronic and thermal Enthalpies= -1143.791694
Sum of electronic and thermal Free Energies= -1143.856094
M06/6-311++G(d,p)/SMD//M06/6-31G(d) energy= -1144.27268306

N_2

Center Number	Atomic Number	Atomic Type	Coordinates (Angstroms) X	Y	Z
1	7	0	0.000000	0.000000	0.552597
2	7	0	0.000000	0.000000	-0.552597

Zero-point correction= 0.005622 (Hartree/Particle)
Thermal correction to Energy= 0.007983
Thermal correction to Enthalpy= 0.008927
Thermal correction to Gibbs Free Energy= -0.012827
Sum of electronic and zero-point Energies= -109.453327
Sum of electronic and thermal Energies= -109.450967
Sum of electronic and thermal Enthalpies= -109.450023
Sum of electronic and thermal Free Energies= -109.471777
M06/6-311++G(d,p)/SMD//M06/6-31G(d) energy= -109.48474327

^{1}TS1

Center Number	Atomic Number	Atomic Type	Coordinates (Angstroms) X	Y	Z
1	6	0	-0.181548	3.571807	0.086311
2	6	0	-0.253712	2.199724	0.489423
3	6	0	-1.547221	1.716131	0.937601
4	6	0	-2.694752	2.553470	0.847378
5	6	0	-2.586765	3.847920	0.426449
6	6	0	-1.308536	4.346387	0.056664
7	1	0	0.779828	3.985233	-0.208928
8	1	0	-3.656520	2.139940	1.155684
9	1	0	-3.457399	4.498207	0.384838
10	1	0	-1.223823	5.382558	-0.269486
11	6	0	-1.650998	0.386152	1.343702
12	7	0	0.714174	1.285878	0.432221
13	16	0	2.118976	1.646191	-0.339455
14	8	0	1.862784	1.821618	-1.775079
15	8	0	2.906589	2.664511	0.356750
16	6	0	2.945415	0.082183	-0.140197
17	6	0	2.962142	-0.820480	-1.195334
18	6	0	3.546161	-0.226871	1.075737
19	6	0	3.590061	-2.049979	-1.027610
20	1	0	2.496240	-0.543656	-2.139935
21	6	0	4.163604	-1.459391	1.229637
22	1	0	3.528163	0.501234	1.884742
23	6	0	4.197499	-2.386079	0.182369
24	1	0	3.614102	-2.762776	-1.852445
25	1	0	4.637332	-1.712338	2.178791
26	6	0	4.900463	-3.699503	0.350620

27	1	0	4.550266	-4.440469	-0.377995
28	1	0	5.984842	-3.590255	0.208856
29	1	0	4.749228	-4.113368	1.355562
30	6	0	-5.244080	-1.648502	-0.644937
31	6	0	-4.021756	-1.010397	-0.819845
32	6	0	-2.856215	-1.556521	-0.273644
33	6	0	-2.943040	-2.744097	0.459826
34	6	0	-4.166392	-3.378869	0.626025
35	6	0	-5.322741	-2.835252	0.074635
36	1	0	-6.142083	-1.211440	-1.077749
37	1	0	-3.975464	-0.077004	-1.378264
38	1	0	-2.049678	-3.186025	0.901862
39	1	0	-4.214287	-4.307145	1.192278
40	1	0	-6.280646	-3.333870	0.207377
41	6	0	-1.587296	-0.797338	-0.417093
42	6	0	-1.386735	0.111235	-1.607171
43	1	0	-1.905432	1.064869	-1.430584
44	1	0	-0.328647	0.356085	-1.754628
45	1	0	-1.790446	-0.349442	-2.517397
46	1	0	-2.613812	0.027706	1.710524
47	1	0	-0.770079	-0.091795	1.772234
48	7	0	-0.482246	-1.509099	-0.107140
49	7	0	0.437840	-2.016022	0.313390

Zero-point correction= 0.385056 (Hartree/Particle)
Thermal correction to Energy= 0.410107
Thermal correction to Enthalpy= 0.411051
Thermal correction to Gibbs Free Energy= 0.329926
Sum of electronic and zero-point Energies= -1562.480026
Sum of electronic and thermal Energies= -1562.454975
Sum of electronic and thermal Enthalpies= -1562.454030
Sum of electronic and thermal Free Energies= -1562.535156
M06/6-311++G(d,p)/SMD//M06/6-31G(d) energy= -1563.20003768

[1]INT1

Center Number	Atomic Number	Atomic Type	Coordinates (Angstroms) X	Y	Z
1	6	0	0.437529	3.701445	-0.217475
2	6	0	0.627988	2.322856	-0.443910
3	6	0	1.929574	1.884488	-0.770258
4	6	0	2.975457	2.795249	-0.884899
5	6	0	2.771026	4.153919	-0.686269
6	6	0	1.493602	4.590360	-0.346646
7	1	0	-0.552800	4.071184	0.030802
8	1	0	3.971000	2.421593	-1.132260
9	1	0	3.593558	4.858942	-0.786049
10	1	0	1.308500	5.650531	-0.178337
11	6	0	2.190677	0.422976	-0.926726
12	7	0	-0.360714	1.340951	-0.397843
13	16	0	-1.694993	1.661232	0.513724
14	8	0	-1.380346	1.620386	1.948546
15	8	0	-2.431154	2.824028	0.009728
16	6	0	-2.674675	0.225111	0.146641
17	6	0	-3.228053	-0.494382	1.197740
18	6	0	-2.915967	-0.137988	-1.175927

19	6	0	-4.017281	-1.603964	0.918988
20	1	0	-3.014590	-0.189900	2.220431
21	6	0	-3.696860	-1.253400	-1.437239
22	1	0	-2.470409	0.441921	-1.982159
23	6	0	-4.259913	-2.000330	-0.396253
24	1	0	-4.449502	-2.179857	1.737600
25	1	0	-3.881206	-1.555650	-2.468770
26	6	0	-5.123863	-3.188214	-0.695188
27	1	0	-5.174617	-3.875203	0.157902
28	1	0	-6.153126	-2.881179	-0.928231
29	1	0	-4.753174	-3.749096	-1.562329
30	6	0	4.032670	-3.514320	0.932615
31	6	0	3.409348	-2.281600	1.102816
32	6	0	2.488322	-1.820359	0.162632
33	6	0	2.199773	-2.619916	-0.948408
34	6	0	2.814680	-3.852445	-1.111622
35	6	0	3.736024	-4.303634	-0.170442
36	1	0	4.751565	-3.857460	1.674011
37	1	0	3.660117	-1.680576	1.973471
38	1	0	1.475975	-2.283801	-1.691362
39	1	0	2.571468	-4.464240	-1.977990
40	1	0	4.218071	-5.270931	-0.297723
41	6	0	1.858157	-0.449438	0.294369
42	6	0	2.067452	0.249302	1.621867
43	1	0	3.098966	0.622022	1.660625
44	1	0	1.394072	1.105775	1.718499
45	1	0	1.889448	-0.427922	2.463910
46	1	0	3.261171	0.251412	-1.112749
47	1	0	1.659345	0.005935	-1.796526
48	7	0	0.324082	-0.705080	0.253908
49	7	0	-0.461361	-1.507705	0.342939

Zero-point correction= 0.387158 (Hartree/Particle)
Thermal correction to Energy= 0.412163
Thermal correction to Enthalpy= 0.413107
Thermal correction to Gibbs Free Energy= 0.331037
Sum of electronic and zero-point Energies= -1562.503468
Sum of electronic and thermal Energies= -1562.478464
Sum of electronic and thermal Enthalpies= -1562.477519
Sum of electronic and thermal Free Energies= -1562.559589
M06/6-311++G(d,p)/SMD//M06/6-31G(d) energy= -1563.22720443

^{1}TS2

Center Number	Atomic Number	Atomic Type	Coordinates (Angstroms) X	Y	Z
1	6	0	0.796750	3.370188	0.203587
2	6	0	0.622948	2.100471	-0.380000
3	6	0	1.732046	1.505727	-1.031599
4	6	0	2.942720	2.184543	-1.122237
5	6	0	3.094572	3.447353	-0.561094
6	6	0	2.013352	4.026163	0.102606
7	1	0	-0.034960	3.840003	0.724371
8	1	0	3.773984	1.716420	-1.654418
9	1	0	4.039753	3.978788	-0.650256
10	1	0	2.120611	5.013087	0.550795

11	6	0	1.521608	0.159420	-1.670644
12	7	0	-0.516973	1.325371	-0.375293
13	16	0	-1.786879	1.766849	0.556378
14	8	0	-2.478593	2.940159	0.020124
15	8	0	-1.437997	1.760509	1.982597
16	6	0	-2.806859	0.335867	0.254281
17	6	0	-3.432379	0.196078	-0.982169
18	6	0	-2.930544	-0.641618	1.231032
19	6	0	-4.168164	-0.949798	-1.242892
20	1	0	-3.330361	0.985178	-1.725675
21	6	0	-3.678258	-1.783608	0.957121
22	1	0	-2.448052	-0.494006	2.195876
23	6	0	-4.301396	-1.955995	-0.278389
24	1	0	-4.658936	-1.071063	-2.209613
25	1	0	-3.786877	-2.555233	1.720118
26	6	0	-5.123088	-3.175922	-0.569562
27	1	0	-4.972978	-3.955350	0.186895
28	1	0	-4.877676	-3.603083	-1.550776
29	1	0	-6.195487	-2.937267	-0.586552
30	6	0	3.569621	-3.826953	0.318097
31	6	0	2.446341	-3.155568	-0.147374
32	6	0	2.435327	-1.756974	-0.222448
33	6	0	3.566705	-1.046539	0.208903
34	6	0	4.678788	-1.719791	0.686764
35	6	0	4.685471	-3.112280	0.738724
36	1	0	3.569303	-4.914192	0.356596
37	1	0	1.584595	-3.731412	-0.476787
38	1	0	3.553793	0.042615	0.189846
39	1	0	5.545128	-1.155669	1.025641
40	1	0	5.560913	-3.639390	1.113060
41	6	0	1.263329	-1.036258	-0.757818
42	1	0	0.669434	0.229961	-2.360616
43	1	0	2.409042	-0.110729	-2.263122
44	7	0	0.583627	-0.314127	0.820261
45	7	0	0.562159	-0.391405	1.934309
46	6	0	0.038576	-1.809816	-1.133739
47	1	0	-0.235139	-2.582904	-0.408491
48	1	0	0.229995	-2.284425	-2.108009
49	1	0	-0.799772	-1.113262	-1.254550

Zero-point correction= 0.385962 (Hartree/Particle)
Thermal correction to Energy= 0.410700
Thermal correction to Enthalpy= 0.411644
Thermal correction to Gibbs Free Energy= 0.331499
Sum of electronic and zero-point Energies= -1562.505146
Sum of electronic and thermal Energies= -1562.480408
Sum of electronic and thermal Enthalpies= -1562.479463
Sum of electronic and thermal Free Energies= -1562.559609
M06/6-311++G(d,p)/SMD//M06/6-31G(d) energy= -1563.23075077

^{1}TS3

Center Number	Atomic Number	Atomic Type	Coordinates (Angstroms) X	Y	Z
1	6	0	2.371372	0.869472	-0.348909
2	6	0	1.033392	1.194983	-0.166024

3	6	0	0.100481	0.222317	0.238429
4	6	0	0.565785	-1.093425	0.434838
5	6	0	1.886301	-1.430210	0.197524
6	6	0	2.797105	-0.444436	-0.185884
7	1	0	3.083161	1.640767	-0.638928
8	1	0	0.708292	2.223447	-0.316934
9	1	0	-0.144703	-1.844006	0.780345
10	1	0	2.221077	-2.456732	0.335971
11	1	0	3.842495	-0.702041	-0.347880
12	6	0	-1.269510	0.553094	0.603330
13	6	0	-1.798480	1.862835	0.143065
14	1	0	-2.894418	1.889196	0.158757
15	1	0	-1.472611	2.574895	0.920382
16	1	0	-1.442226	2.256837	-0.825387
17	7	0	-2.373438	-0.703500	-0.437539
18	7	0	-3.057954	-1.580807	-0.357398

Zero-point correction= 0.138264 (Hartree/Particle)
Thermal correction to Energy= 0.147596
Thermal correction to Enthalpy= 0.148540
Thermal correction to Gibbs Free Energy= 0.103043
Sum of electronic and zero-point Energies= -418.610151
Sum of electronic and thermal Energies= -418.600819
Sum of electronic and thermal Enthalpies= -418.599875
Sum of electronic and thermal Free Energies= -418.645372
M06/6-311++G(d,p)/SMD//M06/6-31G(d) energy= -418.86170347

INT2

Center Number	Atomic Number	Atomic Type	Coordinates (Angstroms) X	Y	Z
1	6	0	0.685390	2.721698	0.276505
2	6	0	0.432037	1.395758	-0.246735
3	6	0	1.608606	0.660518	-0.775790
4	6	0	2.820101	1.431698	-1.046279
5	6	0	2.953257	2.709530	-0.643155
6	6	0	1.874740	3.337183	0.069033
7	1	0	-0.114525	3.238204	0.799559
8	1	0	3.634838	0.921295	-1.558632
9	1	0	3.866343	3.266037	-0.840158
10	1	0	2.014033	4.351165	0.442426
11	6	0	1.381158	-0.596370	-1.611108
12	7	0	-0.725414	0.793934	-0.300969
13	16	0	-2.081471	1.530253	0.342828
14	8	0	-1.899281	1.776258	1.773175
15	8	0	-2.512633	2.622348	-0.525845
16	6	0	-3.235316	0.194658	0.166702
17	6	0	-3.327084	-0.759928	1.172418
18	6	0	-4.027753	0.122337	-0.972176
19	6	0	-4.226456	-1.807361	1.025810
20	1	0	-2.704848	-0.667358	2.060937
21	6	0	-4.922906	-0.930817	-1.101783
22	1	0	-3.939286	0.893163	-1.735407
23	6	0	-5.036457	-1.906477	-0.108089
24	1	0	-4.310667	-2.562385	1.807774
25	1	0	-5.552336	-0.998332	-1.989527

26	6	0	-6.031753	-3.019077	-0.244332
27	1	0	-5.741449	-3.896318	0.346263
28	1	0	-7.025209	-2.705777	0.106114
29	1	0	-6.144072	-3.334271	-1.289028
30	6	0	5.322612	-1.021524	1.317584
31	6	0	4.012826	-0.640817	1.059478
32	6	0	3.313309	-1.188717	-0.018865
33	6	0	3.946824	-2.130986	-0.826896
34	6	0	5.258921	-2.517844	-0.566787
35	6	0	5.949375	-1.962896	0.503873
36	1	0	5.859598	-0.579305	2.155039
37	1	0	3.521222	0.105301	1.686060
38	1	0	3.402788	-2.571821	-1.662453
39	1	0	5.741325	-3.256377	-1.204854
40	1	0	6.976535	-2.261096	0.706270
41	6	0	1.878406	-0.823205	-0.247852
42	6	0	0.964348	-1.415029	0.798731
43	1	0	1.226635	-1.059889	1.803846
44	1	0	-0.088532	-1.192500	0.606740
45	1	0	1.099120	-2.505222	0.787414
46	1	0	2.057695	-0.717513	-2.456921
47	1	0	0.332413	-0.811424	-1.810306

Zero-point correction= 0.377442 (Hartree/Particle)
Thermal correction to Energy= 0.400618
Thermal correction to Enthalpy= 0.401563
Thermal correction to Gibbs Free Energy= 0.323335
Sum of electronic and zero-point Energies= -1453.110862
Sum of electronic and thermal Energies= -1453.087686
Sum of electronic and thermal Enthalpies= -1453.086741
Sum of electronic and thermal Free Energies= -1453.164969
M06/6-311++G(d,p)/SMD//M06/6-31G(d) energy= -1453.79032560

TS4

Center Number	Atomic Number	Atomic Type	Coordinates (Angstroms) X	Y	Z
1	6	0	0.982948	2.840123	0.457321
2	6	0	0.661644	1.693421	-0.314397
3	6	0	1.691552	1.111352	-1.111108
4	6	0	2.974223	1.680839	-1.104844
5	6	0	3.251584	2.817640	-0.377125
6	6	0	2.240331	3.394082	0.406724
7	1	0	0.219147	3.282756	1.091788
8	1	0	3.752893	1.223050	-1.715795
9	1	0	4.240671	3.269092	-0.418556
10	1	0	2.453563	4.287362	0.991677
11	6	0	1.450093	-0.157229	-1.897009
12	7	0	-0.558992	1.074341	-0.344245
13	16	0	-1.816040	1.642150	0.576859
14	8	0	-1.503883	1.630493	2.007935
15	8	0	-2.355328	2.863933	-0.015100
16	6	0	-2.945245	0.303470	0.264146
17	6	0	-3.182812	-0.638609	1.255034
18	6	0	-3.541438	0.196142	-0.989309
19	6	0	-4.027452	-1.709275	0.980115

20	1	0	-2.707116	-0.521706	2.226986
21	6	0	-4.378114	-0.878470	-1.248386
22	1	0	-3.344029	0.954710	-1.744980
23	6	0	-4.633615	-1.844989	-0.268650
24	1	0	-4.222316	-2.455614	1.750680
25	1	0	-4.849153	-0.975505	-2.227255
26	6	0	-5.560897	-2.987527	-0.554592
27	1	0	-5.454002	-3.788572	0.186333
28	1	0	-6.610060	-2.661297	-0.535335
29	1	0	-5.378970	-3.416914	-1.548167
30	6	0	3.987078	-2.351577	1.751272
31	6	0	2.799650	-1.913835	1.187925
32	6	0	2.732181	-1.562367	-0.170753
33	6	0	3.900376	-1.672849	-0.942387
34	6	0	5.082763	-2.132653	-0.381530
35	6	0	5.132340	-2.468757	0.967772
36	1	0	4.021314	-2.600531	2.809970
37	1	0	1.917596	-1.806221	1.816011
38	1	0	3.875280	-1.428603	-2.002740
39	1	0	5.972030	-2.226841	-1.001601
40	1	0	6.062984	-2.820868	1.408620
41	6	0	1.472073	-1.139747	-0.771865
42	6	0	0.211086	-1.474701	-0.219186
43	1	0	0.185020	-2.166426	0.623351
44	1	0	-0.254190	-0.369377	0.028494
45	1	0	-0.556030	-1.699100	-0.974279
46	1	0	2.240012	-0.304834	-2.641642
47	1	0	0.476526	-0.151652	-2.401281

Zero-point correction= 0.373250 (Hartree/Particle)
Thermal correction to Energy= 0.395790
Thermal correction to Enthalpy= 0.396734
Thermal correction to Gibbs Free Energy= 0.318832
Sum of electronic and zero-point Energies= -1453.090258
Sum of electronic and thermal Energies= -1453.067718
Sum of electronic and thermal Enthalpies= -1453.066773
Sum of electronic and thermal Free Energies= -1453.144676
M06/6-311++G(d,p)/SMD//M06/6-31G(d) energy= -1453.77308595

TS5

Center Number	Atomic Number	Atomic Type	Coordinates (Angstroms) X	Y	Z
1	6	0	-1.401630	-2.874825	0.608901
2	6	0	-1.010425	-1.704842	-0.108476
3	6	0	-1.959138	-1.166502	-1.030092
4	6	0	-3.237375	-1.713484	-1.135902
5	6	0	-3.600731	-2.829224	-0.401403
6	6	0	-2.663497	-3.402651	0.472187
7	1	0	-0.699779	-3.306968	1.319166
8	1	0	-3.940005	-1.291597	-1.857667
9	1	0	-4.584190	-3.276755	-0.528940
10	1	0	-2.938565	-4.279350	1.057086
11	6	0	-1.528523	-0.024873	-1.926396
12	7	0	0.160452	-1.047976	0.026401
13	16	0	1.445800	-1.799238	0.694510

14	8	0	1.823004	-3.016282	-0.029844
15	8	0	1.333485	-1.878300	2.155681
16	6	0	2.667042	-0.554971	0.327714
17	6	0	3.297603	-0.561781	-0.911328
18	6	0	2.930102	0.443828	1.256780
19	6	0	4.186894	0.457408	-1.225158
20	1	0	3.083943	-1.366255	-1.613153
21	6	0	3.824039	1.457592	0.929579
22	1	0	2.434818	0.408226	2.225821
23	6	0	4.460978	1.480855	-0.312957
24	1	0	4.686669	0.462122	-2.194660
25	1	0	4.038443	2.245485	1.652742
26	6	0	5.446831	2.559851	-0.648419
27	1	0	5.440903	2.795255	-1.720043
28	1	0	6.471484	2.255685	-0.392307
29	1	0	5.237389	3.484295	-0.096291
30	6	0	-4.491323	2.335127	0.218176
31	6	0	-3.554648	1.618861	-0.498749
32	6	0	-2.169069	1.826885	-0.300228
33	6	0	-1.780907	2.776311	0.672698
34	6	0	-2.723710	3.479247	1.401660
35	6	0	-4.080883	3.265586	1.174811
36	1	0	-5.551243	2.166823	0.040924
37	1	0	-3.893256	0.888945	-1.228224
38	1	0	-0.725436	2.942500	0.872280
39	1	0	-2.400771	4.194508	2.154834
40	1	0	-4.822626	3.819947	1.746457
41	6	0	-1.177638	1.147323	-1.086162
42	1	0	-2.354309	0.219269	-2.611653
43	1	0	-0.661266	-0.314176	-2.532612
44	6	0	0.216682	1.640325	-1.059622
45	1	0	0.841419	1.126719	-1.795440
46	1	0	0.679708	1.442879	-0.078549
47	1	0	0.244760	2.726480	-1.229126

Zero-point correction= 0.376684 (Hartree/Particle)
Thermal correction to Energy= 0.399062
Thermal correction to Enthalpy= 0.400006
Thermal correction to Gibbs Free Energy= 0.323959
Sum of electronic and zero-point Energies= -1453.077930
Sum of electronic and thermal Energies= -1453.055552
Sum of electronic and thermal Enthalpies= -1453.054608
Sum of electronic and thermal Free Energies= -1453.130655
M06/6-311++G(d,p)/SMD//M06/6-31G(d) energy= -1453.77275630

4f

Center Number	Atomic Number	Atomic Type	Coordinates (Angstroms) X	Y	Z
1	6	0	1.304447	2.911832	0.370488
2	6	0	0.949474	1.806467	-0.403909
3	6	0	1.884640	1.212755	-1.269153
4	6	0	3.166455	1.757230	-1.323858
5	6	0	3.533374	2.845166	-0.542621
6	6	0	2.595389	3.417369	0.307837
7	1	0	0.559426	3.371592	1.014659

8	1	0	3.895174	1.305800	-1.998431
9	1	0	4.543569	3.245034	-0.602740
10	1	0	2.862137	4.275156	0.922470
11	6	0	1.529967	0.023660	-2.133129
12	7	0	-0.387742	1.313452	-0.380035
13	16	0	-1.137424	1.025345	1.122611
14	8	0	-0.398502	0.035583	1.898118
15	8	0	-1.450276	2.316998	1.713127
16	6	0	-2.619972	0.270196	0.510022
17	6	0	-2.799286	-1.100391	0.646078
18	6	0	-3.581567	1.072636	-0.100392
19	6	0	-3.965976	-1.675556	0.155146
20	1	0	-2.034117	-1.698692	1.137209
21	6	0	-4.736212	0.480712	-0.585585
22	1	0	-3.414780	2.144868	-0.184588
23	6	0	-4.945599	-0.898096	-0.463406
24	1	0	-4.122697	-2.749129	0.257207
25	1	0	-5.498073	1.094226	-1.066813
26	6	0	-6.210030	-1.515041	-0.978691
27	1	0	-6.163591	-2.609742	-0.959611
28	1	0	-7.074503	-1.209128	-0.373857
29	1	0	-6.416527	-1.202234	-2.010335
30	6	0	2.839194	-2.613773	1.760090
31	6	0	1.876825	-2.123591	0.885854
32	6	0	2.227543	-1.729736	-0.408813
33	6	0	3.568629	-1.821678	-0.798322
34	6	0	4.527877	-2.321122	0.072424
35	6	0	4.165623	-2.719109	1.355526
36	1	0	2.551620	-2.900781	2.770035
37	1	0	0.848119	-1.994151	1.218926
38	1	0	3.862665	-1.520382	-1.803812
39	1	0	5.564480	-2.397623	-0.251730
40	1	0	4.918504	-3.101181	2.042923
41	6	0	1.199712	-1.227962	-1.348009
42	6	0	0.019396	-1.844660	-1.487896
43	1	0	-0.215790	-2.759213	-0.945292
44	1	0	-0.468882	0.435865	-0.895929
45	1	0	-0.741343	-1.475213	-2.178287
46	1	0	2.381789	-0.179568	-2.799464
47	1	0	0.686601	0.260308	-2.802107

Zero-point correction= 0.379313 (Hartree/Particle)
Thermal correction to Energy= 0.402134
Thermal correction to Enthalpy= 0.403078
Thermal correction to Gibbs Free Energy= 0.326109
Sum of electronic and zero-point Energies= -1453.137785
Sum of electronic and thermal Energies= -1453.114964
Sum of electronic and thermal Enthalpies= -1453.114020
Sum of electronic and thermal Free Energies= -1453.190989
M06/6-311++G(d,p)/SMD//M06/6-31G(d) energy= -1453.82364954

9

Center Number	Atomic Number	Atomic Type	Coordinates (Angstroms) X	Y	Z
1	6	0	-3.168939	-1.554166	0.622981

2	6	0	-2.393209	-0.743709	-0.200845
3	6	0	-2.984307	0.177940	-1.063374
4	6	0	-4.361223	0.308784	-1.116316
5	6	0	-5.153392	-0.487952	-0.291039
6	6	0	-4.553471	-1.406143	0.564355
7	1	0	-2.716913	-2.281605	1.290623
8	1	0	-4.814839	1.031290	-1.794587
9	1	0	-6.236874	-0.390664	-0.315910
10	1	0	-5.173244	-2.028426	1.207788
11	6	0	-1.928720	0.866824	-1.863918
12	7	0	-0.977063	-0.693237	-0.326102
13	16	0	-0.090710	-1.325787	0.986012
14	8	0	-0.415681	-2.745455	1.019272
15	8	0	-0.294452	-0.522849	2.184986
16	6	0	1.591630	-1.157024	0.474689
17	6	0	2.146973	-2.143966	-0.336337
18	6	0	2.340077	-0.075169	0.921707
19	6	0	3.467889	-2.015345	-0.735082
20	1	0	1.538700	-2.993394	-0.642652
21	6	0	3.660207	0.039947	0.504745
22	1	0	1.888330	0.662530	1.582325
23	6	0	4.239427	-0.920389	-0.326967
24	1	0	3.917079	-2.776005	-1.373682
25	1	0	4.253752	0.893391	0.832719
26	6	0	5.672689	-0.807671	-0.748374
27	1	0	5.816443	-1.144336	-1.782497
28	1	0	6.317583	-1.432782	-0.115158
29	1	0	6.038590	0.222570	-0.669534
30	6	0	-0.351748	3.166508	1.531684
31	6	0	-0.773446	2.073111	0.787282
32	6	0	-0.077195	1.673869	-0.358677
33	6	0	1.033410	2.423111	-0.750915
34	6	0	1.455587	3.522338	-0.008158
35	6	0	0.767668	3.895307	1.139430
36	1	0	-0.900954	3.446548	2.428701
37	1	0	-1.638247	1.504368	1.123126
38	1	0	1.600700	2.145572	-1.637119
39	1	0	2.329782	4.085775	-0.331198
40	1	0	1.098268	4.751080	1.725641
41	6	0	-0.576213	0.492533	-1.181901
42	1	0	-2.049929	1.957147	-1.909615
43	1	0	-1.931074	0.499954	-2.902273
44	6	0	0.401356	0.047681	-2.263142
45	1	0	0.033822	-0.882845	-2.712090
46	1	0	1.415881	-0.125592	-1.889750
47	1	0	0.454719	0.808602	-3.053392

Zero-point correction= 0.380433 (Hartree/Particle)
Thermal correction to Energy= 0.402575
Thermal correction to Enthalpy= 0.403519
Thermal correction to Gibbs Free Energy= 0.329139
Sum of electronic and zero-point Energies= -1453.158094
Sum of electronic and thermal Energies= -1453.135952
Sum of electronic and thermal Enthalpies= -1453.135008
Sum of electronic and thermal Free Energies= -1453.209388
M06/6-311++G(d,p)/SMD//M06/6-31G(d) energy= -1453.83772402

^{3}2f

Center Number	Atomic Number	Atomic Type	Coordinates (Angstroms) X	Y	Z
1	6	0	-2.239214	1.070377	0.000106
2	6	0	-0.866166	1.245765	0.000116
3	6	0	0.011911	0.138931	0.000099
4	6	0	-0.558393	-1.151964	0.000023
5	6	0	-1.933774	-1.317769	0.000019
6	6	0	-2.781965	-0.212928	0.000068
7	1	0	-2.892279	1.941226	0.000125
8	1	0	-0.462342	2.255953	0.000128
9	1	0	0.092953	-2.022683	-0.000038
10	1	0	-2.350357	-2.323275	-0.000030
11	1	0	-3.861797	-0.349888	0.000065
12	6	0	1.437901	0.370569	0.000087
13	6	0	2.010489	1.746892	0.000004
14	1	0	3.102279	1.682055	0.000308
15	1	0	1.697346	2.321094	-0.883807
16	1	0	1.696830	2.321415	0.883409
17	7	0	2.397815	-0.624524	-0.000156
18	7	0	2.243990	-1.827638	-0.000314

Zero-point correction= 0.140472 (Hartree/Particle)
Thermal correction to Energy= 0.149412
Thermal correction to Enthalpy= 0.150357
Thermal correction to Gibbs Free Energy= 0.105255
Sum of electronic and zero-point Energies= -418.627442
Sum of electronic and thermal Energies= -418.618502
Sum of electronic and thermal Enthalpies= -418.617558
Sum of electronic and thermal Free Energies= -418.662660
M06/6-311++G(d,p)/SMD//M06/6-31G(d) energy= -418.87644952

^{3}TS1b

Center Number	Atomic Number	Atomic Type	Coordinates (Angstroms) X	Y	Z
1	6	0	2.444647	0.981312	0.000028
2	6	0	1.083296	1.224653	0.000016
3	6	0	0.151780	0.150908	-0.000015
4	6	0	0.667094	-1.171046	-0.000028
5	6	0	2.030375	-1.395452	-0.000015
6	6	0	2.930429	-0.327006	0.000011
7	1	0	3.139316	1.819939	0.000053
8	1	0	0.711449	2.248759	0.000040
9	1	0	-0.029291	-2.005837	-0.000052
10	1	0	2.403877	-2.418177	-0.000026
11	1	0	4.002681	-0.513057	0.000019
12	6	0	-1.221082	0.427824	-0.000038
13	6	0	-1.992357	1.673163	-0.000024
14	1	0	-3.070515	1.457422	-0.000057
15	1	0	-1.777839	2.289664	0.887674
16	1	0	-1.777793	2.289698	-0.887687
17	7	0	-2.305969	-1.111419	0.000019
18	7	0	-3.432170	-0.967804	0.000043

Zero-point correction= 0.137614 (Hartree/Particle)
Thermal correction to Energy= 0.147105
Thermal correction to Enthalpy= 0.148049
Thermal correction to Gibbs Free Energy= 0.101499
Sum of electronic and zero-point Energies= -418.613392
Sum of electronic and thermal Energies= -418.603901
Sum of electronic and thermal Enthalpies= -418.602957
Sum of electronic and thermal Free Energies= -418.649507
M06/6-311++G(d,p)/SMD//M06/6-31G(d) energy= -418.85963934

^{3}INT1b

Center Number	Atomic Number	Atomic Type	Coordinates (Angstroms) X	Y	Z
1	6	0	-1.329097	1.349123	-0.000004
2	6	0	0.023181	1.057450	-0.000023
3	6	0	0.476992	-0.291159	-0.000024
4	6	0	-0.506717	-1.315898	-0.000001
5	6	0	-1.853439	-1.007154	0.000028
6	6	0	-2.277724	0.324460	0.000018
7	1	0	-1.653571	2.389006	-0.000013
8	1	0	0.758109	1.862524	-0.000033
9	1	0	-0.175419	-2.353431	0.000008
10	1	0	-2.589316	-1.809975	0.000066
11	1	0	-3.339849	0.561941	0.000009
12	6	0	1.838109	-0.596176	-0.000113
13	6	0	3.081079	0.175387	0.000060
14	1	0	3.160907	0.825115	0.888460
15	1	0	3.964121	-0.477189	-0.000292
16	1	0	3.160718	0.825815	-0.887848

Zero-point correction= 0.130151 (Hartree/Particle)
Thermal correction to Energy= 0.137487
Thermal correction to Enthalpy= 0.138431
Thermal correction to Gibbs Free Energy= 0.097479
Sum of electronic and zero-point Energies= -309.174191
Sum of electronic and thermal Energies= -309.166856
Sum of electronic and thermal Enthalpies= -309.165911
Sum of electronic and thermal Free Energies= -309.206863
M06/6-311++G(d,p)/SMD//M06/6-31G(d) energy= -309.38935151

^{3}TS2b

Center Number	Atomic Number	Atomic Type	Coordinates (Angstroms) X	Y	Z
1	6	0	1.424410	2.237839	0.172727
2	6	0	0.815814	1.168088	-0.579742
3	6	0	1.600292	0.605328	-1.700012
4	6	0	2.932470	1.096843	-1.935138
5	6	0	3.457729	2.094362	-1.184597
6	6	0	2.676709	2.670598	-0.130405
7	1	0	0.856861	2.697614	0.976477
8	1	0	3.503488	0.635799	-2.741028
9	1	0	4.465062	2.461100	-1.367677

10	1	0	3.109673	3.480449	0.455649
11	6	0	1.109076	-0.435706	-2.423525
12	7	0	-0.353730	0.609512	-0.364788
13	16	0	-1.254645	0.950978	0.982779
14	8	0	-0.777564	0.085639	2.067070
15	8	0	-1.406638	2.384009	1.234638
16	6	0	-2.830193	0.335858	0.442310
17	6	0	-3.615942	1.132516	-0.385573
18	6	0	-3.263909	-0.914473	0.858708
19	6	0	-4.845607	0.655066	-0.810491
20	1	0	-3.262836	2.119548	-0.678745
21	6	0	-4.502027	-1.377011	0.426102
22	1	0	-2.640005	-1.504622	1.527124
23	6	0	-5.304922	-0.605709	-0.413907
24	1	0	-5.471718	1.271849	-1.456053
25	1	0	-4.857808	-2.353945	0.753673
26	6	0	-6.632648	-1.110325	-0.892668
27	1	0	-7.417627	-0.353400	-0.767499
28	1	0	-6.600923	-1.363208	-1.961521
29	1	0	-6.942083	-2.010756	-0.349517
30	6	0	3.696479	-0.537042	1.818010
31	6	0	2.544422	-1.069726	1.261716
32	6	0	2.609357	-1.804586	0.050337
33	6	0	3.870715	-1.943249	-0.580020
34	6	0	5.011016	-1.407890	-0.009868
35	6	0	4.931990	-0.703335	1.193602
36	1	0	3.628393	0.025223	2.748228
37	1	0	1.578196	-0.911147	1.742176
38	1	0	3.923749	-2.491347	-1.521357
39	1	0	5.973848	-1.536610	-0.502388
40	1	0	5.831677	-0.283258	1.639994
41	6	0	1.451010	-2.330347	-0.543211
42	6	0	0.095198	-2.638340	-0.085675
43	1	0	-0.652526	-2.527662	-0.882747
44	1	0	0.028988	-3.676144	0.279250
45	1	0	-0.209967	-1.967702	0.736802
46	1	0	1.706781	-0.892782	-3.211016
47	1	0	0.084195	-0.770958	-2.296523

Zero-point correction= 0.372515 (Hartree/Particle)
Thermal correction to Energy= 0.396301
Thermal correction to Enthalpy= 0.397245
Thermal correction to Gibbs Free Energy= 0.317716
Sum of electronic and zero-point Energies= -1453.002377
Sum of electronic and thermal Energies= -1452.978590
Sum of electronic and thermal Enthalpies= -1452.977646
Sum of electronic and thermal Free Energies= -1453.057176
M06/6-311++G(d,p)/SMD//M06/6-31G(d) energy= -1453.67789656

^{3}TS2b′

Center Number	Atomic Number	Atomic Type	Coordinates (Angstroms) X	Y	Z
1	6	0	-1.549979	0.890501	-1.489936
2	6	0	-0.727353	1.210677	-0.345283
3	6	0	-1.382332	1.956386	0.760553

4	6	0	-2.724945	2.467821	0.540529
5	6	0	-3.416513	2.184101	-0.584623
6	6	0	-2.815289	1.366875	-1.599710
7	1	0	-1.118365	0.300574	-2.294303
8	1	0	-3.153494	3.090671	1.326053
9	1	0	-4.422876	2.569845	-0.733475
10	1	0	-3.393947	1.128318	-2.491207
11	6	0	-0.585184	2.590583	1.726535
12	7	0	0.539318	0.904717	-0.176122
13	16	0	1.240871	-0.205407	-1.195822
14	8	0	0.615662	-1.512409	-0.967388
15	8	0	1.349598	0.298498	-2.564068
16	6	0	2.873623	-0.256327	-0.505232
17	6	0	3.147621	-1.129674	0.542304
18	6	0	3.855136	0.575513	-1.025657
19	6	0	4.426276	-1.156345	1.077995
20	1	0	2.364704	-1.788762	0.913379
21	6	0	5.131586	0.536319	-0.476727
22	1	0	3.613585	1.231584	-1.859558
23	6	0	5.433992	-0.324388	0.578577
24	1	0	4.656962	-1.839353	1.896313
25	1	0	5.912216	1.182544	-0.878034
26	6	0	6.812002	-0.376083	1.166274
27	1	0	7.478597	0.358943	0.700754
28	1	0	6.793998	-0.176452	2.245984
29	1	0	7.264970	-1.368002	1.033885
30	6	0	-3.450462	-2.652084	-0.401921
31	6	0	-2.499096	-1.894943	0.259365
32	6	0	-2.878171	-0.731621	0.968096
33	6	0	-4.240027	-0.373735	0.991180
34	6	0	-5.186558	-1.144341	0.330115
35	6	0	-4.795581	-2.280594	-0.372261
36	1	0	-3.142097	-3.536347	-0.957012
37	1	0	-1.442800	-2.159097	0.193286
38	1	0	-4.542337	0.506853	1.555400
39	1	0	-6.236967	-0.859991	0.367458
40	1	0	-5.538543	-2.880222	-0.895431
41	6	0	-1.887172	0.052917	1.631082
42	6	0	-0.680320	-0.385609	2.340184
43	1	0	-0.717086	-1.468955	2.523659
44	1	0	0.234808	-0.169309	1.759830
45	1	0	-0.576644	0.121149	3.311362
46	1	0	-1.040195	3.243973	2.468362
47	1	0	0.486742	2.421111	1.762314

Zero-point correction= 0.370846 (Hartree/Particle)
Thermal correction to Energy= 0.394748
Thermal correction to Enthalpy= 0.395692
Thermal correction to Gibbs Free Energy= 0.315549
Sum of electronic and zero-point Energies= -1452.988857
Sum of electronic and thermal Energies= -1452.964955
Sum of electronic and thermal Enthalpies= -1452.964011
Sum of electronic and thermal Free Energies= -1453.044154
M06/6-311++G(d,p)/SMD//M06/6-31G(d) energy= -1453.66178869

^{3}INT2b

Center Number	Atomic Number	Atomic Type	Coordinates (Angstroms) X	Y	Z
1	6	0	0.141840	-3.198753	0.036720
2	6	0	-0.004380	-1.781528	-0.141421
3	6	0	-1.329198	-1.253052	-0.361913
4	6	0	-2.408788	-2.120619	-0.365237
5	6	0	-2.238002	-3.492789	-0.184701
6	6	0	-0.954303	-4.024292	0.013423
7	1	0	1.134103	-3.615281	0.188016
8	1	0	-3.409047	-1.709441	-0.507094
9	1	0	-3.104184	-4.151958	-0.195245
10	1	0	-0.825729	-5.095754	0.152018
11	6	0	-1.555694	0.225554	-0.570080
12	7	0	0.988850	-0.886818	-0.105262
13	16	0	2.557351	-1.400856	0.200517
14	8	0	2.639061	-1.829535	1.594179
15	8	0	3.009797	-2.293075	-0.863773
16	6	0	3.414501	0.139035	0.032104
17	6	0	4.090030	0.415796	-1.150555
18	6	0	3.410946	1.039430	1.091154
19	6	0	4.765738	1.622065	-1.270742
20	1	0	4.089946	-0.317685	-1.953640
21	6	0	4.089673	2.241964	0.951685
22	1	0	2.892351	0.789585	2.014985
23	6	0	4.771799	2.551401	-0.227525
24	1	0	5.306644	1.849308	-2.189689
25	1	0	4.100282	2.954925	1.775976
26	6	0	5.487420	3.859399	-0.380492
27	1	0	5.649235	4.346588	0.588101
28	1	0	6.464459	3.729470	-0.862687
29	1	0	4.910711	4.554701	-1.006151
30	6	0	-5.999953	2.131855	0.790054
31	6	0	-4.714945	1.719778	1.090594
32	6	0	-3.845024	1.203840	0.091285
33	6	0	-4.371579	1.129978	-1.226692
34	6	0	-5.658574	1.543957	-1.516927
35	6	0	-6.487684	2.050590	-0.514937
36	1	0	-6.635678	2.522344	1.583569
37	1	0	-4.363079	1.794020	2.117591
38	1	0	-3.757311	0.736008	-2.034525
39	1	0	-6.025144	1.470800	-2.539892
40	1	0	-7.499901	2.375260	-0.747810
41	6	0	-2.527264	0.785113	0.425942
42	6	0	-2.037817	0.830610	1.839333
43	1	0	-0.992639	0.503421	1.903490
44	1	0	-2.091979	1.844147	2.265416
45	1	0	-2.625985	0.179684	2.505766
46	1	0	-1.889810	0.385567	-1.603822
47	1	0	-0.590119	0.740625	-0.475482

Zero-point correction= 0.375322 (Hartree/Particle)
Thermal correction to Energy= 0.399081
Thermal correction to Enthalpy= 0.400025
Thermal correction to Gibbs Free Energy= 0.317882
Sum of electronic and zero-point Energies= -1453.085736
Sum of electronic and thermal Energies= -1453.061977

Sum of electronic and thermal Enthalpies= -1453.061033
Sum of electronic and thermal Free Energies= -1453.143176
M06/6-311++G(d,p)/SMD//M06/6-31G(d) energy= -1453.76144776

Supplemental References

Liu, G.-Q., Li, L., Duan, L., and Li, Y.-M. (2015). *m*CPBA-mediated metal-free intramolecular aminohydroxylation and dioxygenation of unfunctionalized olefins. RSC Adv. *5*, 61137–61143.

Ferrand, L., Tang, Y., Aubert, C., Fensterbank, L., Mouries-Mansuy, V., Petit, M., and Amatore, M. (2017). Niobium-catalyzed intramolecular addition of O–H and N–H bonds to alkenes: A tool for hydrofunctionalization. Org. Lett. *19*, 2062−2065.

Li, D., Mao, T., Huang, J., and Zhu, Q. (2017). Copper-catalyzed regioselective 1,2-thioamidation of alkenes. Chem. Commun. *53*, 3450−3453.

Yin, G., Wu, T., and Liu, G. (2012). Highly selective palladium‐catalyzed intramolecular chloroamination of unactivated alkenes by using hydrogen peroxide as an oxidant. Chem. Eur. J. *18*, 451−455.

Zhao, Y., and Truhlar, D. G. (2008). The M06 suite of density functionals for main group thermochemistry, thermochemical kinetics, noncovalent interactions, excited states, and transition elements: two new functionals and systematic testing of four M06-class functionals and 12 other functionals. Theor. Chem. Acc. *120*, 215–241.

Hariharan, P. C., and Pople, J. A. (1973). The influence of polarization functions on molecular orbital hydrogenation energies. Theor. Chim. Acta. *28*, 213–222.

Marenich, A. V., Cramer, C. J., and Truhlar, D. G. (2009). Universal solvation model based on solute electron density and on a continuum model of the solvent defined by the bulk dielectric constant and atomic surface tensions. J. Phys. Chem. B *113*, 6378–6396.

Frisch, M. J. et al., (2010). Gaussian 09, Revision C.01, Gaussian, Inc., Wallingford CT.